Impact of climate change effects on diversity and function of pelagic heterotrophic bacteria studied in large-scale mesocosm facilities

---

Thomas Hornick

geb. am 10.10.1986 in Rochlitz

Univ.-Diss.

(kumulative Ausführung)

zur Erlangung des akademischen Grades

"doctor rerum naturalium"

(Dr. rer. nat.)

in der Wissenschaftsdisziplin "Ökologie"

eingereicht an der

Mathematisch-Naturwissenschaftlichen Fakultät

Institut für Biochemie und Biologie

der Universität Potsdam

und

Institut für Gewässerökologie und Binnenfischerei (IGB) Berlin

Ort und Tag der Disputation:

Potsdam, den 11.03.2019

1. Gutachter (Hauptbetreuer): Prof. Dr. habil. Hans-Peter Großart
2. Gutachter: Prof. Dr. habil. Maren Voß
3. Gutachter: Prof. Dr. habil. Karlheinz Altendorf

Published online at the
Institutional Repository of the University of Potsdam:
https://doi.org/10.25932/publishup-42893
https://nbn-resolving.org/urn:nbn:de:kobv:517-opus4-428936

Preface

All parts of this work were conducted at the Leibniz-Institute of Freshwater Ecology and Inland Fisheries, Department of Experimental Limnology, Stechlin, Germany. Additionally, experimental work was partly performed at the Tvärminne Zoological Station (Hanko, Finland), The Sven Lovén Centre for Marine Sciences, Kristineberg (Fiskebäckskil, Sweden) and the Plataforma Oceánica de Canarias (PLOCAN) (Telde, Gran Canaria, Spain) during KOSMOS-mesocosm studies (Kiel Off-Shore Mesocosms for Ocean Simulations) on the effects of ocean acidification. This work was carried out within the framework of the following projects: SOPRAN (Surface Ocean Processes in the Anthropocene; BMBF), BIOACID II and III (Biological Impacts of Ocean Acidification; BMBF) and TemBi (Climate-driven changes in biodiversity of microbiota; Leibniz-SAW).

I. Table of contents

II. Key to abbreviations

BCC	Bacterial community composition
BGE	Bacterial growth efficiency
BIOACID	Biological Impacts of Ocean Acidification (project acronym)
BPP	Bacterial protein production
BR	Bacterial respiration
C	Carbon
CC	Climate change
CO_2	Carbon dioxide
Chl *a*	Chlorophyll *a*
DIC	Dissolved inorganic carbon
DOC	Dissolved organic carbon
DOM	Dissolved organic matter
ER	Ecosystem respiration
fCO_2	Fugacity of CO_2
FL	Free-living
FT-ICR-MS	Fourier-transform ion cyclotron resonance mass spectrometry
GPP	Gross primary production
$[H^+]$	Proton concentration
KOSMOS	Kiel off-shore mesocosms for future ocean simulations
NEP	Net ecosystem production
OA	Ocean acidification
OC	Organic carbon
OM	Organic matter
PA	Particle associated
PAR	Photosynthetically active radiation
pCO_2	Partial pressure of CO_2
POC	Particulate organic carbon
POM	Particulate organic matter
PP	Primary production
ppm	Parts per million
TemBi	Climate driven changes in biodiversity of microbiota (project acronym)
TEP	Transparent exopolymer particles
[ ]	Concentration

III. List of publications

The following four manuscripts were evaluated for this thesis. Thereby, manuscripts I-III have been published as articles in peer-reviewed journals.

My own contributions are indicated for each publication: ED – experimental design of study; DC – sampling and data collection; DA – data analysis; C – conceptualisation of manuscript; MS – writing of manuscript.

I. **Hornick, T.**, Bach, L. T., Crawfurd, K. J., Spilling, K., Achterberg, E. P., Woodhouse, J. N., Schulz, K. G., Brussaard, C. P. D., Riebesell, U., and Grossart, H.-P.: Ocean acidification impacts bacteria–phytoplankton coupling at low-nutrient conditions, *Biogeosciences*, 14, 1-15, https://doi.org/10.5194/bg-14-1-2017, 2017.
(ED, DC, DA, C, MS)

II. Spilling, K., Schulz, K. G., Paul, A. J., Boxhammer, T., Achterberg, E. P., **Hornick, T.**, Lischka, S., Stuhr, A., Bermúdez, R., Czerny, J., Crawfurd, K., Brussaard, C. P. D., Grossart, H.-P., and Riebesell, U.: Effects of ocean acidification on pelagic carbon fluxes in a mesocosm experiment, *Biogeosciences*, 13, 6081-6093, https://doi.org/10.5194/bg-13-6081-2016, 2016.
(ED, DC, DA, MS)

III. Zark, M., Broda, N. K., **Hornick, T.**, Grossart, H.-P., Riebesell, U. and Dittmar, T.: Ocean Acidification Experiments in Large-Scale Mesocosms Reveal Similar Dynamics of Dissolved Organic Matter Production and Biotransformation. *Front. Mar. Sci*. 4:271. doi: 10.3389/fmars.2017.00271, 2017.
(ED, DC, DA, MS)

IV. **Hornick, T.**, Ganzert, L., Berger, S. A., Gessner, M. O., Giling, D. P., Nejstgaard, J. C., Woodhouse, J. N., Grossart, H.-P.: Experimental summer storm induces changes in bacterial community structure with lasting biogeochemical consequences, in preparation for submission.
(ED, DC, DA, C, MS)

Further relevant publications for this thesis

Nausch, M., Bach, L. T., Czerny, J., Goldstein, J., Grossart, H.-P., Hellemann, D., **Hornick, T.**, Achterberg, E. P., Schulz, K.-G., and Riebesell, U.: Effects of CO_2 perturbation on phosphorus pool sizes and uptake in a mesocosm experiment during a low productive summer season in the northern Baltic Sea, *Biogeosciences*, 13, 3035-3050, https://doi.org/10.5194/bg-13-3035-2016, 2016.

Bach, L. T., Taucher, J., Boxhammer, T., Ludwig, A., The Kristineberg KOSMOS Consortium, Achterberg, E. P., Algueró-Muñiz, M., Anderson, L. G., Bellworthy, J., Büdenbender, J., Czerny, J., Ericson, Y., Esposito, M., Fischer, M., Haunost, M., Hellemann, D., Horn, H. G., **Hornick, T.**, Meyer, J., Sswat, M., Zark, M., Riebesell, U.: Influence of Ocean Acidification on a Natural Winter-to-Summer Plankton Succession: First Insights from a Long-Term Mesocosm Study Draw Attention to Periods of Low Nutrient Concentrations, *PLoS ONE* 11(8):e0159068, https://doi.org/10.1371/journal.pone.0159068, 2016.

Bach, L. T., Álvarez-Fernández, S., **Hornick, T**., Stuhr, A., Riebesell, U.: Simulated ocean acidification reveals winners and losers in coastal phytoplankton, *PLoS ONE* 12(11): e0188198, https://doi.org/10.1371/journal.pone.0188198, 2017.

Taucher, J., Bach, L. T., Boxhammer, T., Nauendorf, A., The Gran Canaria KOSMOS Consortium (**Hornick, T.** and 49 other members), Achterberg, E. P., Algueró-Muñiz, M., Arístegui, J., Czerny, J., Esposito, M., Guan, W., Haunost, M., Horn, H. G., Ludwig, A., Meyer, J., Spisla, C., Sswat, M., Stange, P., and Riebesell, U.: Influence of Ocean Acidification and Deep Water Upwelling on Oligotrophic Plankton Communities in the Subtropical North Atlantic: Insights from an *In situ* Mesocosm Study, *Front. Mar. Sci*. 4:85, https://doi.org/10.3389/fmars.2017.00085, 2017.

Further publications

Attermeyer, K., Premke, K., **Hornick, T.**, Hilt, S., and Grossart, H.-P.: Ecosystem-level studies of terrestrial carbon reveal contrasting bacterial metabolism in different aquatic habitats. *Ecology*, 94: 2754–2766, doi:10.1890/13-0420.1, 2013.

Attermeyer, K., **Hornick, T.**, Kayler, Z. E., Bahr, A., Zwirnmann, E., Grossart, H.-P., and Premke, K.: Enhanced bacterial decomposition with increasing addition of autochthonous to allochthonous carbon without any effect on bacterial community composition, *Biogeosciences*, 11, 1479-1489, https://doi.org/10.5194/bg-11-1479-2014, 2014.

Kolmakova, O. V., Gladyshev, M. I., Fonvielle, J. A., Ganzert, L., **Hornick, T.**, and Grossart, H.-P.: Effects of zooplankton carcasses degradation on freshwater bacterial community composition and implications for carbon cycling. *Environmental Microbiology*, doi:10.1111/1462-2920.14418, 2018.

Participation at conferences

Hornick, T., Berger, S., Nejstgaard, J. C., Giling, D. P., Gessner, M. O., Grossart, H.-P.: Bacterial responses to a heavy summer storm simulated in large-scale lake mesocosms, SAME 14th Symposium on Aquatic Microbial Ecology, Uppsala, Sweden, 2015. (poster presentation)

Hornick, T., Ganzert, L., Giling, D. P., Selmeczy, G. B., Berger, S. A., Nejstgaard, J. N., Grossart, H.-P.: Summer storm has lasting effects on composition and function of microbial communities in stratified lakes, SAME 15th Symposium on Aquatic Microbial Ecology, Zagreb, Croatia, 2017. (poster presentation)

Further contribution to conferences

Nejstgaard, J. C., Berger, S. A., Giling, S. A., Penske, A., Lenz, M., **Hornick, T.**, Grossart, H.-P., Kasprzak, P., Gessner, M. O.: Storm in a teapot: Simulating an extreme weather event in a large-scale mesocosm platform, Aquatic Sciences Meeting (ASLO), Granada, Spain, 22.-27 Feb. 2015. (oral presentation)

Published datasets

Hornick, T., Bach, L. T., Crawfurd, K. J., Spilling, K., Achterberg, E. P., Woodhouse, J. N., Schulz, K. G., Brussaard, C. P. D., Riebesell, U., Grossart, H.-P.: KOSMOS Finland 2012 mesocosm study: Size-fractionated bacterial protein production (BPP) of free-living and particle associated bacteria and abundance of particle associated heterotrophic prokaryotes. *PANGAEA*, https://doi.org/10.1594/PANGAEA.868621, 2016.

Contribution to data-driven project meetings and project reports

Hornick, T., Grossart, H.-P.: Climate-driven changes in diversity and function of pelagic bacteria, TemBi Final Meeting, Neuglobsow, 25.-26. Feb. 2014. (oral presentation)

Enke, G., **Hornick, T.**, Boxhammer, T., Bach, L. T., Czerny, J., Fischer, M., Riebesell, U., Grossart, H.-P.: Measurements of particle size and sinking velocity of sediment trap material, BIOACID Phase II Meeting, Kiel 10.-11. Sept. 2014. (poster presentation)

Hornick, T., Bach, L. T., Czerny, J., Riebesell, U., Grossart, H.-P.: Changes in bacterial community composition during the KOSMOS 2013 ocean acidification experiment, BIOACID Phase II Final Meeting, Kiel 06.-07. Oct. 2015. (poster presentation)

Bach, L. T., Boxhammer, T., Esposito, M., Achterberg, E. P., Meyer, J., Ludwig, A., Haunost, M., Fischer, M., Hellemann, D., Audritz, S., Büdenbender, J., Czerny, J., **Hornick, T.**, Grossart, H.-P., Sswat, M., Clemmesen, C., Scheinin, M., Wohlrab, S., Eberlein, T., John,

U., van de Waal, D., Algueró-Muñiz, M., Lange, J., Horn, H., Boersma, M., Zark, M., Dittmar, T., Abrahamson, K., Anderson, L. G., Ericson, Y., Lundve, B., and Riebesell, U.: Effects of ocean acidification on a winter-to-summer phytoplankton succession, BIOACID Phase II Final Meeting, Kiel 06.-07. Oct. 2015. (oral presentation)

Hornick, T., The Tvärminne KOSMOS Consortium, The Kristineberg KOSMOS Consortium, The Gran Canaria KOSMOS Consortium, Riebesell, U., Grossart, H.-P.: Will ocean acidification affect microbial life? – Conclusions from several KOSMOS experiments, BIOACID final meeting and synthesis workshop, Kiel, 29.-31. May 2017. (poster presentation)

Zark, M., **Hornick, T.**, Grossart, H.-P., Dittmar, T.: Carbon turnover related to organic substrate quality and functioning of microbial communities, BIOACID final meeting and synthesis workshop, Kiel, 29.-31. May 2017. (poster presentation)

Grossart, H.-P., **Hornick, T.**, Abschlussbericht zum Leibniz-Wettbewerb geförderten Vorhaben SAW-2011-IGB-2.22 "Klimagetriebene Veränderungen der Biodiversität von Mikrobiota – TemBi": Teilprojekt III – Diversität und Funktion pelagischer heterotropher Bakterien.

Grossart, H.-P., **Hornick, T.**, BIOACID III Zwischenbericht für Berichtszeitraum 01.10-2015 – 31.12.2016, WP 1.3.: „Biogeochemische Funktion von Mikroorganismen". Bundesministerium für Bildung und Forschung (BMBF)-gefördertes Forschungsvorhaben 03F0728C.

Grossart, H.-P., **Hornick, T.**, BIOACID III Abschlussbericht WP 1.3.: „Biogeochemische Funktion von Mikroorganismen". Bundesministerium für Bildung und Forschung (BMBF)-gefördertes Forschungsvorhaben 03F0728C.

IV. Summary

The unprecedented increase in atmospheric concentrations of carbon dioxide (CO_2) and other greenhouse gases (GHG) by anthropogenic activities since the Industrial Revolution impacts on various earth system processes, commonly referred to as `climate change´ (CC). CC faces aquatic ecosystems with extreme abiotic perturbations that potentially alter the interrelations between functional autotrophic and heterotrophic plankton groups. These relations, however, modulate biogeochemical cycling and mediate the functioning of aquatic ecosystems as C sources or sinks to the atmosphere. The aim of this thesis was therefore to investigate how different aspects of CC influence community composition and functioning of pelagic heterotrophic bacteria. These organisms constitute a major component of biogeochemical cycling and largely determine the balance between autotrophic and heterotrophic processes.

Due to the vast amount of potential CC impacts, this thesis focuses on the following two aspects: (1) Increased exchange of CO_2 across the atmosphere-water interface and reaction of CO_2 with seawater leads to profound shifts in seawater carbonate chemistry, commonly termed as `ocean acidification´ (OA), with consequences for organism physiology and the availability of dissolved inorganic carbon (DIC) in seawater. (2) The increase in atmospheric GHG concentration impacts on the efficiency with which the earth cools to space, affecting global surface temperature and climate. With ongoing CC, shifts in frequency and severity of episodic weather events, such as storms, are expected that in particular might affect lake ecosystems by disrupting thermal summer stratification. Both aspects of CC were studied at the ecosystem-level in large-volume mesocosm experiments by using the Kiel Off-shore Mesocosms for Future Ocean Simulations (KOSMOS) deployed at different coastal marine locations, and the LakeLab facility in Lake Stechlin.

We evaluated the impact of OA on heterotrophic bacterial metabolism in a brackish coastal ecosystem during low-nutrient summer months in the Baltic Sea. There are several in situ experiments that already assessed potential OA-induced changes in natural plankton communities at diverse spatial and seasonal conditions. However, most studies were performed at high phytoplankton biomass conditions, partly provoked by nutrient amendments. Our study highlights potential OA effects at low-nutrient conditions that are representative for most parts of the ocean and of particular interest in current OA research. The results suggest that during extended periods at low-nutrient concentrations, increasing pCO_2 levels indirectly impact the growth balance of heterotrophic bacteria via trophic bacteria-phytoplankton interactions and shift the ecosystem to a more autotrophic system.

Further work investigated how OA affects heterotrophic bacterial dissolved organic matter (DOM) transformation in two mesocosm studies, performed at different nutrient conditions. We observed similar succession patterns for individual compound pools during a phytoplankton bloom and subsequent accumulation of these compounds irrespective of the pCO_2 treatment. Our results indicate that OA-induced changes in the dynamics of

bacterial DOM transformation and potential impacts on DOM quality are unlikely. In addition, there have been no indications that in dependence of nutrient conditions, different amounts of photosynthetic organic matter are channelled into the more recalcitrant DOM pool. This provides novel insights into the general dynamics of the marine DOM pool.

A fourth enclosure experiment in oligo-mesotrophic Lake Stechlin assessed the impact of a severe summer storm on lake bacterial communities during thermal stratification by artificial mixing. Mixing disrupted and lowered the thermocline, increasing the upper mixed layer and substantially changed water physical-chemical variables. Deep water entrainment and associated changes in water physical-chemical variables significantly affected relative bacterial abundances for about one week. Afterwards, a pronounced cyanobacterial bloom developed in response to mixing which affected community assembly of heterotrophic bacteria. Colonization and mineralization of senescent phytoplankton cells by heterotrophic bacteria largely determined C-sequestration to the sediment. About six weeks after mixing, bacterial communities and measured activity parameters converged to control conditions. As such, summer storms have the potential to affect bacterial communities for a prolonged period during summer stratification. The results highlight effects on community assembly and heterotrophic bacterial metabolism that are associated to entrainment of deep water into the mixed water layer and assess consequences of an episodic disturbance event for the coupling between bacterial metabolism and autochthonous DOM production in large volume clear-water lakes.

Altogether, this doctoral thesis revealed substantial sensitivities of heterotrophic bacterial metabolism and community structure in response to OA and a simulated summer storm event, which should be considered when assessing the impact of climate change on marine and lake ecosystems.

V. Zusammenfassung

Seit der Industriellen Revolution steigen die Konzentrationen von Kohlenstoffdioxid (CO_2) und anderen Treibhausgasen in der Erdatmosphäre stetig an. Dieser Anstieg beeinflusst wesentliche Prozesse im Erdsystem was mit dem Begriff „climate change“ oder „Klimawandel“ umschrieben wird. Ebenso aquatische Ökosysteme sind davon betroffen und werden mit erheblichen Veränderungen ihrer abiotischen Umwelt konfrontiert. Mögliche Veränderungen in der Organismenzusammensetzung und in biologischen Prozessen könnten die Folge sein, welche maßgeblich die regulierende Funktion von Gewässern im Klimasystem beeinflussen könnte. Insbesondere eine Verschiebung des Verhältnisses zwischen autotrophen und heterotrophen Prozessen ist dabei von Bedeutung. Dieses bestimmt grundlegend, ob Gewässer CO_2 binden oder emittieren. Heterotrophe Bakterien nehmen dabei eine zentrale Rolle ein. Ziel dieser Doktorarbeit war daher zu bestimmen, wie verschiedene Auswirkungen des Klimawandels die Gemeinschaftsstruktur und Aktivität von heterotrophen Bakterien in Gewässern verändert.

Diese Arbeit konzentriert sich auf zwei Aspekte des Klimawandels: (1) Zum einen bewirkt der atmosphärische Anstieg der CO_2-Konzentration, dass gleichermaßen mehr CO_2 in Gewässern gelöst wird. Ozeane nehmen dabei einen Großteil des CO_2 auf, welches im Meerwasser das chemische Gleichgewicht des Karbonatsystems verschiebt („Ozeanversauerung“). Die damit verbundene Senkung des pH-Wertes als auch der Anstieg gelösten anorganischen Kohlenstoffs kann zu physiologischen Anpassungen von Organismen führen. (2) Zum anderen beeinflussen Treibhausgase die Absorption von Wärmeenergie der Sonne, was sich in einem kontinuierlichen Anstieg der Erdoberflächentemperatur äußert. Dadurch bedingt werden Veränderungen im Klimasystem der Erde vorhergesagt, welche unter anderem die Häufigkeit und Heftigkeit von episodischen Wetterereignissen (z.B. Stürme) verstärken werden. Insbesondere Sommer-Stürme sind dabei in der Lage die sommerliche thermische Stratifizierung der Wassersäule geschichteter Seen zu zerstören, was weitreichende Auswirkungen auf die Wasserchemie/-physik und die Verteilung von Organismen haben kann. Beide Aspekte des Klimawandels wurden mittels Mesokosmen simuliert, welche größere Wasservolumina einschließen und aufgrund ihrer Größe (ca. 55 m^3-1200 m^3) erlauben, dass komplexe Ökosysteme mit trophischen Interaktionen untersucht werden können.

Dabei untersuchten wir den Einfluss der Ozeanversauerung auf heterotrophe bakterielle Prozesse in einem Brackwassersystem der Ostsee, in welchem während der Sommermonate geringe Konzentrationen an gelösten Nährstoffen vorherrschen. Im Gegensatz zu zahlreichen anderen Studien, welche bereits Ozeanversauerungseffekte bei hoher Phytoplankton-Biomasse oder nach Zugabe von Nährstoffen untersuchten, fokussiert diese Studie speziell auf Zeiträume unter Nährstofflimitation. Unsere Ergebnisse zeigen, dass während solcher Phasen, Ozeanversauerungseffekte indirekt das Wachstum von

heterotrophen Bakterien durch veränderte trophische Interaktionen beeinflussen und potentiell zu einer Erhöhung der Autotrophie des Ökosystems führen können.

In einer weiteren vergleichenden Studie zweier Mesokosmenexperimente bei unterschiedlichen Nährstoffbedingungen untersuchten wir, wie Ozeanversauerung die Umsetzung gelösten organischen Materials (DOM) durch heterotrophe Bakterien beeinflusst. Wir beobachteten vergleichbare zeitliche Verläufe ausgewählter DOM-Verbindungen während und nach einer Phytoplankton-Blüte in beiden Experimenten, sowie vergleichbare Akkumulation dieser Verbindungen unabhängig vom pCO_2. Diese Ergebnisse deuten darauf hin, dass Änderungen in der DOM-Qualität durch heterotrophe bakterielle Prozesse mit zunehmender Ozeanversauerung unwahrscheinlich sind. Unsere Studie verdeutlicht somit vorherrschende generelle Dynamiken des marinen DOM-Pools.

In einer vierten Mesokosmenstudie im oligotroph-mesotrophen Stechlinsee wurde der Einfluss eines starken Sommer-Sturmes auf See-Ökosysteme während der sommerlichen Stratifizierung untersucht. Mittels oberflächlicher Durchmischung wurde die bestehende Thermokline zerstört und die durchmischte Oberflächenwasserschicht vergrößert. Dies änderte physikalische und chemische Gradienten innerhalb der stratifizierten Wassersäule. Effekte der Einmischung von Tiefenwasser änderten daraufhin die Zusammensetzung der bakteriellen Gemeinschaftsstruktur für ca. eine Woche und stimulierten das Wachstum filamentöser Cyanobakterien (hauptsächlich *Dolichospermum* sp.). Daraufhin entwickelte sich in durchmischten Mesokosmen eine Cyanobakterien-Blüte, welche entscheidend die Entwicklung heterotropher bakterieller Gemeinschaften und Prozesse bestimmte. Nach ca. sechs Wochen konnte in den meisten beprobten Parametern kein Unterschied mehr zu den Kontrollbedingungen detektiert werden. Unsere Studie gibt ein mechanistisches Verständnis, wie Sommer-Stürme nachhaltig bakterielle Gemeinschaften und Prozesse für längere Zeit während der sommerlichen Stratifizierung beeinflussen können.

Die in dieser Arbeit präsentierten Ergebnisse zeigen Veränderungen bakterieller Gemeinschaften und Prozesse in aquatischen Ökosystemen, welche mit dem einhergehenden Klimawandel erwartet werden können. Diese sollten bei Beurteilung klimarelevanter Fragen hinsichtlich eines zukünftigen Gewässermanagements Berücksichtigung finden.

1. Chapter 1 - General Introduction

Earth ecosystem processes have become dominated by anthropogenic activities, necessitating a new socio-ecological view of ecosystem processes that incorporates human activities into ecology (Ducklow, 2008). The term `climate change´ is commonly used to describe this issue, however, originally refers to the process `[…] that alters the composition of the global atmosphere and which is in addition to natural climate variability observed over comparable time periods', as defined by The Framework Convention on Climate Change in its Article 1 (UNFCCC, 1992).

Since the Industrial Revolution, human activities have increased concentrations of atmospheric carbon dioxide (CO_2) and other greenhouse gases (e.g. methane (CH_4), nitrous oxide (N_2O)) to levels exceeding by far the natural range observed over the last 800,000 years (Siegenthaler, 2005; Lüthi et al., 2008; Ciais et al., 2013). About 40 % of these emissions have remained in the atmosphere which impacts on the efficiency with which the Earth cools to space, influencing global surface temperature and climate (IPCC, 2013a). Of the 60 % of emissions removed from the atmosphere roughly half was stored on land and inland waters, and half in the oceans (IPCC, 2013a). As such, aquatic ecosystems are faced with extreme abiotic perturbations in the Earth system, that might impact essential ecosystem services provided to human wellbeing and society in large (IPCC, 2013b, 2014). While future changes of the abiotic environment (e.g. temperature, concentration of CO_2) can be reasonably well projected by climate models within a relatively small range of uncertainty, their effects on organismic physiology, community composition and biological processes are much less understood (Walther et al., 2002; Sarmiento et al., 2004; Goldman et al., 2012; IPCC, 2013b).

The majority of organisms in aquatic ecosystems comprise functional groups of free drifting microorganisms that live in the `pelagic zone´ - the open water column. The so called `plankton´ tightly interacts with one another in the pelagic food-web (e.g. Strickland, 1960; Kirchman, 2008). Here, the interrelations within and between process-relevant functional groups of plankton (e.g. primary producers, consumers, decomposers) and their abiotic environment determine biogeochemical cycles, ecosystem processes and thus invariably link to ecosystem services. In particular, the balance between autotrophic and heterotrophic processes determines net productivity and carbon sequestration. Thereby, pelagic biogeochemical cycling generates important feedbacks in the climate system and mediates the functioning of aquatic systems as C sources or sinks to the atmosphere. Heterotrophic processes are primarily mediated by bacteria which represent a major component in biogeochemical cycling (e.g. Kirchman, 2008). Hence, obtaining scientific data on potential impacts of climate change on bacterial processes is of utmost importance in order to make valid projections of how ecosystem services provided by aquatic environments might be impacted in the future.

1.1 Aquatic ecosystems in the carbon cycle

1.1.1 Oceans in the global carbon cycle

The global carbon (C) cycle describes a series of C reservoirs, which are connected by exchange fluxes of C in the Earth system. After the lithosphere (≈75,000,000 PgC) the oceans constitute the second largest pool of C on Earth, containing about 38,000 PgC, followed by the terrestrial biosphere (≈2,000 PgC) and the atmosphere (≈830 PgC) (Falkowski, 2000; Ciais et al., 2013) **(Fig. 1)**. The world oceans cover about 70 % of the Earth's surface and are an important driver of Earth´s climate by exchanging approximately 100 PgC per year, including CO_2 and other greenhouse gases (e.g. CH_4), across the atmosphere-water interface (Raven and Falkowski, 1999).

Most of the C in the oceans is present in the form of dissolved inorganic carbon (DIC, ≈98 %), which represents about 50 times more soluble inorganic C than contained in the atmosphere (Raven and Falkowski, 1999). About 2 % contributes to the pool of dissolved organic carbon (DOC) and only a negligible amount consists of particulate organic carbon (POC), which comprises also the living biomass (Falkowski, 2000; Hansell et al., 2009; Sarmiento and Gruber, 2002). Although the photosynthetic biomass in the world's oceans approximates only to about 0.2 % relative to terrestrial ecosystems, marine net primary production (NPP) is estimated to equal roughly the total terrestrial NPP (Field, 1998; Falkowski and Raven, 2007). The huge discrepancy between NPP and biomass points to a high turnover of autotrophic biomass, which is performed due to interactions between autotrophic and heterotrophic parts of the marine food-web. Thereby, interactions within the marine food-web generate important feedbacks in the climate system which impact on the greenhouse gas exchange between oceans and the atmosphere and thus, largely determine the sequestration of atmospheric CO_2 in the deep ocean. In marine systems all these processes are summarized in the concept of the `biological C pump´ which is the sum of processes that transport biogenic C from the euphotic zone at the surface to the oceans interior where the material is mineralized (Hansell et al., 2009).

1.1.2 Inland waters in the global carbon cycle

Because inland aquatic systems cover only a small fraction of the Earth´s surface area (ca. 3.7 %) (Verpoorter et al., 2014) they have rarely been considered as potentially important quantitative components of the C cycle (Cole et al., 2007; Battin et al., 2009; Raymond et al., 2013). Mostly due to methodological limitations, they were regarded as part of terrestrial ecosystems, functioning solely as `pipes´ which transport C from terrestrial ecosystems to the oceans (Cole et al., 2007; Battin et al., 2009). However, inland waters are extremely active sites for transport, transformation, and storage of C from the terrestrial environment and therefore may have an effect that is disproportional to their spatial extent (Dean and Gorham, 1998; Cole et al., 2007; Battin et al., 2008; Tranvik et al., 2009; Biddanda,

2017; Tranvik et al., 2018). Cole et al. (2007) proposed that roughly twice as much C (≈1.9 PgC yr^{-1}) enters inland aquatic systems from land as is exported from land to the sea (≈0.9 PgC yr^{-1}). More recent estimates suggest that inland waters transport, mineralize and bury about 2.7-2.9 PgC yr^{-1}, which is in the range of NEP of the terrestrial biosphere (≈1-4 PgC yr^{-1}) or corresponds to the size of the terrestrial C sink for anthropogenic emissions (≈2.8 Pg yr^{-1}) (Randerson et al., 2002; Tranvik et al., 2009; Battin et al., 2009). Most of the terrestrial C entering inland waters is respired by heterotrophic biota (≈1.2 PgC) and released as CO_2 to the atmosphere (Battin et al., 2009; Raymond et al., 2013). However, inland waters have also been recognized to affect the global land greenhouse gas sink estimates substantially via the release of methane (CH_4) (Bastviken et al., 2004, 2011). On the other hand, inland waters function as important sites for C sequestration, giving a negative climate feedback. Thus, Tranvik et al. (2009) estimated that the rate of OC burial in inland water sediments may exceed OC sequestration on the ocean floor.

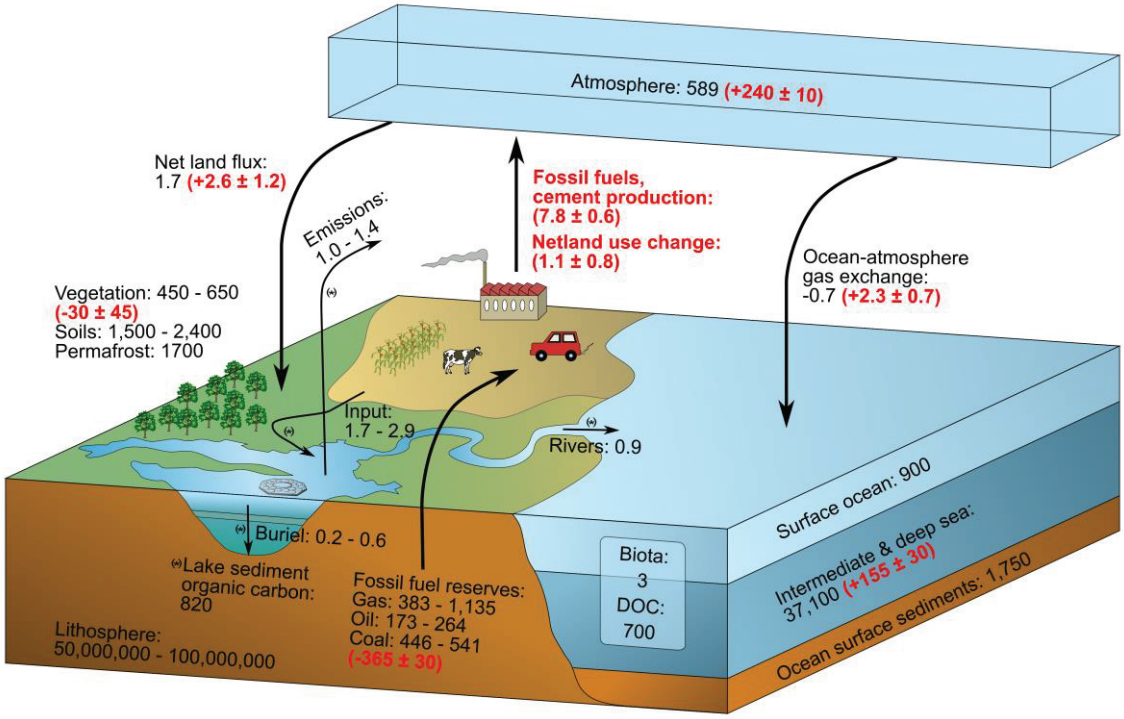

Figure 1: Overview of the global carbon cycle. Numbers represent reservoir masses in PgC and annual C exchange fluxes in PgC yr^{-1}. Black numbers and arrows indicate reservoir masses and exchange fluxes estimated for the time prior to the Industrial Era. The red numbers and arrows indicate annual anthropogenic fluxes averaged over the 2000-2009 time period and refer to the perturbation of the C cycle during the Industrial Era post 1750. Masses and fluxes without asterisks (*) are estimates from Ciais et al. (2013). Thereby, uncertainties are reported as 90 % confidence intervals. Reservoir sizes and fluxes marked with asterisks (*) are estimates for inland waters and denote minimum and maximum values derived from Cole et al. (2007), Tranvik et al. (2009) and Ciais et al. (2013), respectively. Please note: Only estimates for the most important reservoir masses and fluxes with focus on inland waters and oceans are given. The scheme does not represent a closed budget of the carbon cycle.

1.2 Role of heterotrophic bacteria for carbon cycling in the planktonic food web

Functional groups of plankton interact within the pelagic food web, channelling C, additional macronutrients (e.g. phosphorus (P), nitrogen (N)) and other chemical elements between inorganic forms, the living biomass and dead organic matter (OM). They comprise the main drivers of biogeochemical cycling and form the base of the aquatic food-web (e.g. Kirchman, 2008).

In the euphotic zone, photoautotrophic phytoplankton perform primary production, transforming carbon dioxide (CO_2) and inorganic nutrients into organic compounds and oxygen using sunlight energy and water as the electron donor (e.g. Strickland, 1960, 1965). Primary production directly (e.g. production, exudation, death) or indirectly via trophic interrelations (e.g. consumption, remineralization, aggregation) adds to the pool of dissolved (DOM) and particulate organic matter (POM) (summarized, e.g. in Dittmar and Stubbins (2014)). Heterotrophic bacteria catalyze dominant reactions which affect OM. Approximately one-half of the C that is fixed by marine autotrophs is directly processed by bacteria (Cole et al., 1988; Ducklow et al., 1993; Buchan et al., 2014).

Since bacteria are limited to the uptake of sufficiently small DOM of up to ca. 600 Da, they release extracellular enzymes to catalyze the initial step in converting high-molecular-weight (HMW) organic matter to smaller substrates, which can be transported across the bacterial cell membrane (Weiss et al., 1991; Arnosti, 2011). Thereby, hydrolytic enzymes mediate a biochemical mechanism for large-scale transfer of organic matter from POM (i.e. sinking particles, detritus, etc.) to the dissolved phase affecting nutrient recycling in surface waters and finally the sequestration of OM to the sediment (Smith et al., 1992). Subsequently, heterotrophic bacteria mineralize DOM back to inorganic forms (e.g. CO_2) or excrete metabolically transformed products. Another fraction of DOM is used for biomass production which can have possible consequences for trophic interrelations by channelling DOM via ingestion to higher trophic levels (e.g. Pomeroy, 1974; Williams, 1981; Azam et al., 1983; Azam, 1998; Hessen and Tranvik, 1998; Carpenter et al., 2005). The recognition that much of energy is transferred through a DOM-bacteria-protozoan pathway by e.g. Pomeroy (1974), Williams (1981) or Sieburth and Davis (1982), later termed as `microbial loop´ (Azam et al., 1983), marks an important change in the understanding of the bacteria´s role in pelagic C cycling (e.g. Tranvik, 1992; Kirchman, 2008). Thereby, heterotrophic bacteria are regarded not only as mineralizers, responsible for the recycling of nutrients for the primary producers, but also exhibit a relevant trophic role as producers (analogous to phytoplankton), which are consumed by other organisms (e.g. Ducklow, 1983; Azam and Malfatti, 2007) **(Fig. 2)**. As a consequence, about one fourth of the total net primary production is channelled through DOM and the `microbial loop´ to higher trophic levels, which would otherwise be unavailable for larger secondary consumers (Azam et al., 1983). Generally, the concept of the `microbial loop´ can be applied for both marine as well as

freshwater systems (Hobbie, 1988; Tranvik, 1992). However, macrozooplankton (Cladocera) may be efficient grazers of bacterioplankton only in freshwaters, short-circuiting the `microbial loop´ by a direct bacteria-macrozooplankton transfer (Bosselmann and Riemann, 1986; Hobbie, 1988).

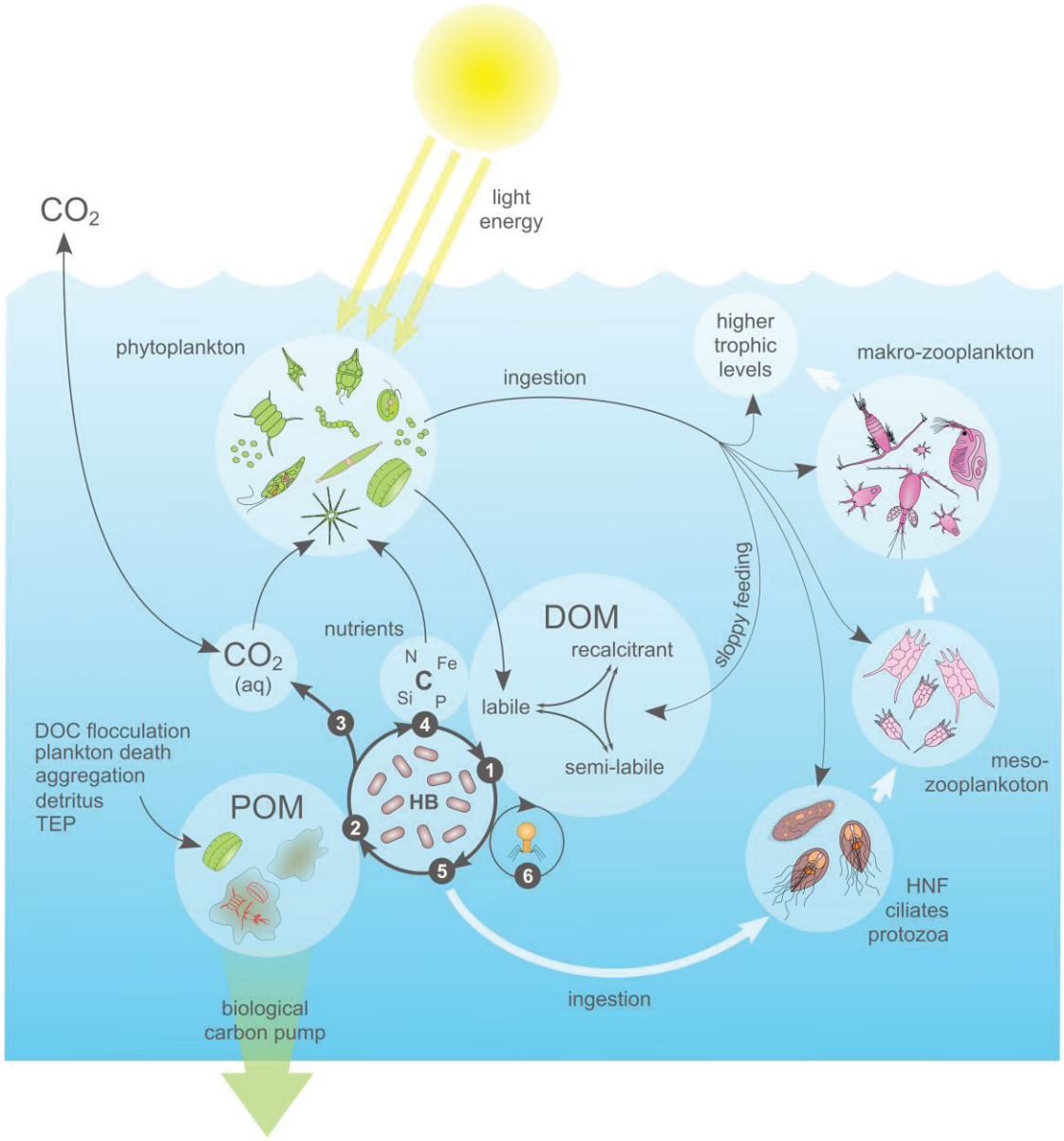

Figure 2: Heterotrophic bacteria (HB) in the aquatic food web. A large fraction of organic matter that is synthesized by primary producers (phytoplankton) becomes dissolved (DOM) or particulate organic matter (POM). HB mediate important biogeochemical processes such as the decomposition and transformation of DOM (1) and POM (2). Thereby, organic matter is transformed by the release of extracellular enzymes, respired to CO_2 (3) or assimilated into HB biomass. The decomposition of DOM by HB regenerates nutrients that are used by primary producers and other organisms in the aquatic food web (4). Grazing of HB channels HB biomass via the `microbial loop´ (white arrows) to higher trophic levels (5). Vial lysis of HB releases DOM (`viral loop´) (6). OM transformations by HB influence air-sea exchange of CO_2 and carbon storage through POM sinking flux (`biological carbon pump´), thus, playing a major role in C cycling (e.g. Azam and Malfatti, 2007).

1.2.1 DOM in the aquatic environment

DOM comprises the largest pool of organic carbon (OC) and one of the largest reactive carbon pools in the biosphere (Druffel et al., 1992; Hedges, 1992). About 90 % of this organic matter occurs as non-living DOM (Cauwet, 1978), the vast majority of which is still uncharacterized and their cycling largely unknown (Druffel et al., 1992; Ogawa and Tanoue, 2003; Dittmar and Stubbins, 2014). Depending on size or molecular weight, extraction procedure, reactivity, elemental composition or other molecular characterizations, DOM comprises different fractions, which contribute to the DOM pool (Druffel et al., 1992; Amon and Benner, 1994; Ogawa and Tanoue, 2003; Dittmar and Stubbins, 2014).

A conceptual framework regularly used in global models on DOM turnover divides the bulk of DOM into distinct fractions with different microbial reactivity based on fate, transformation and accumulation in the water column (Hansell et al., 2009; Dittmar and Stubbins, 2014; Moran et al., 2016). The biologically labile fraction represents a large C flux, but with rapid turnover it constitutes a very small fraction (<1 %) of DOM (Hansell et al., 2009). Labile DOM comprises, e.g. free amino acids, sugars and organic acids which turn over in minutes to days through rapid bacterial uptake and mineralization (e.g. Hansell and Carlson, 2002). A more biologically resistant fraction is not immediately mineralized and accumulates as biologically semi-labile DOM with an annual to multi-decadal time scale of removal (e.g. Carlson, 2002). Ocean models indicate that especially the semi-labile fraction is the most reactive fraction during biogeochemical cycling, accounting for net export to depths > 100 m at 1.8 PgC yr^{-1}, or about 20 % of the global export production (Hansell et al., 2009). The vast amount of DOM, however, is composed of refractory/recalcitrant C, highly resistant to microbial oxidation, with average turnover times of hundreds to thousands of years (Hansell and Carlson, 2002; Ogawa and Tanoue, 2003; Dittmar and Stubbins, 2014).

Primary production by phytoplankton is the ultimate source of marine DOM (e.g. Ogawa and Tanoue, 2003). In coastal environments and especially inland waters, DOM might to a higher degree also originate from allochthonous DOM introduced into the aquatic environment from the terrestrial catchment site (i.e. soil, stream runoff). Terrestrial DOM quality and quantity are largely dependent on site-specific properties, (Tranvik, 1992). For instance, large clear-water lakes are less influenced by such compounds in contrast to small or more humic inland waters (Tranvik, 1988).

Photosynthetic cells passively or actively excrete excess photosynthates when C fixation exceeds incorporation into new cell material; an overflow metabolism of carbon during nutrient limitation (Fogg, 1983; Bjørnsen, 1988). Additionally, phyto- and bacterioplankton actively release DOM for the engineering of microenvironments through the excretion of transparent exopolymeric compounds, mainly consisting of polysaccharides (TEP) (Bjørnsen, 1988; Logan et al., 1995; Gogou and Repeta, 2010; Passow and Alldredge, 1994; Passow, 2000; Passow et al., 2001; Passow, 2002; De La Rocha and Passow, 2007). Such compounds affect the buoyancy of unicellular organisms (Mari, 2008), facilitate chemical

communication among cells (Guan and Kamino, 2001; Skindersoe et al., 2008), create an envelope that surrounds plankton (in which large parts of the cell's ectoenzymes are embedded to scavenge DOM from the water) (Heissenberger et al., 1996; Stoderegger and Herndl, 1998; Carlson et al., 2007), or largely influence the aggregation of cells in plankton blooms (Mari et al., 2005; Passow and Alldredge, 1994; Logan et al., 1995). Further loss of valuable organics to the water column is largely determined by sloppy feeding through heterotrophic consumers (i.e. macrozooplankton) (Banse, 1995; Møller et al., 2003) and cell death caused by viral lyses (Gobler et al., 1997; Middelboe and Jørgensen, 2006; Noble and Fuhrman, 1999). Thus, up to 30 % of DOM originate from protistan grazing on phytoplankton and bacteria (Sherr and Sherr, 1994). In addition, about 20-50 % of the microbial biomass is turned over daily by viral infection, releasing intracellular OM into the surrounding water (Suttle, 2007).

1.2.2 Factors impacting DOM transformation and bacterial dynamics

Historically, environmental conditions such as temperature, pH, salinity, oxygen concentration or the availability of light and nutrients have been mainly considered to impact bacterial dynamics in activity and biomass (Pomeroy and Deibel, 1986; Nedwell, 1999; Kirchman et al., 2005; Shiah and Ducklow, 1994; Wijtes et al., 1993; Berggren et al., 2010; Sulzberger and Durisch-Kaiser, 2009). Also trophic interrelations were recognized to account for bacterial losses due to viral mortality and grazing, but also to stimulate bacterial production by increases in phytoplankton- and bacteria-derived DOM availability, substrate regeneration through the viral shunt (Fuhrman and Suttle, 1993; Fuhrman, 1999; Suttle, 2007) and sloppy feeding by grazers (Pomeroy, 1974; Porter et al., 1985). Several comparative studies of a wide range of natural aquatic systems demonstrated that bacterial production is correlated with and averages about 30 % of net primary production (Ducklow and Carlson, 1992; Cole et al., 1988; del Giorgio and Cole, 1998).

More recently, the development of high-resolution methods to characterize biogeochemical substrate pools and the bacterial community composition (BCC) by, e.g. Fourier transform ion cyclotron mass spectroscopy (FTICR-MS) or Sequencing-Techniques (e.g. 454 pyrosequencing, Ilumina MiSeq), in combination with advances in bioinformatics, allow for a more detailed studying of the biogeochemical complexity and bacterial diversity (Grossart, 2010). It is thus not surprising that the recognized spatio-temporal variability in bacterial activity and biomass towards environmental conditions and food-web characteristics is also mirrored to a certain extent in changes in the BCC and chemical diversity of mainly DOM.

A recent publication that evaluates structure and function of the global ocean microbiome reveals temperature to be the major environmental factor shaping taxonomic and functional microbial community composition in the photic open ocean (Sunagawa et al., 2015). However, defining determinants of community structure in the global plankton interactome by also taking into account food-web interactions suggests that abiotic factors have a more limited effect on community structure and biotic factors (i.e. selective grazing,

infection, etc.) should be considered as more important (Lima-Mendez et al., 2015; Verity and Smetacek, 1996).

A considerable parameter in the selection process for specific bacterial populations is the substrate and nutrient availability by phytoplankton-derived OM (Grossart and Simon, 2007; Allgaier et al., 2008). Thereby, the availability and subsequent bacterial usage of DOM is largely determined by both DOM quality and quantity (e.g. Marcarelli et al., 2011; Roiha et al., 2012; Nelson and Wear, 2014; Attermeyer et al., 2014; Sarmento et al., 2016). It has been suggested, that the quantity of C defines productivity while its quality defines the BCC (Roiha et al., 2012; Attermeyer et al., 2014). Quantity and chemical composition of phytoplankton-released compounds varies with phytoplankton species and the physiological status of the phytoplankton, influencing both the stoichiometry (C to N to P ratio) and bioreactivity of phytoplankton-derived POM and DOM (Bjørnsen, 1988; Biddanda and Benner, 1997; Azam and Malfatti, 2007). The bacterioplankton community structure can change rapidly in response to growth and decay of different phytoplankton, indicating that DOM from different algae select for specific metabolic degradation pathways and thus differential bacterial communities (Covert and Moran, 2001; Pinhassi and Berman, 2003; Pinhassi et al., 2004; Grossart and Simon, 2007). How differences in structure and C turnover of microbial communities subsequently translate into differences in the functioning of whole aquatic ecosystems is currently subject of intense research (Graham et al., 2016; Giling et al., 2017a).

1.3 Mesocosms as a tool for studying complex food web interactions

Mesocosm experiments provide an important bridge between smaller, more tightly controlled microcosm experiments and the biological complexity of natural systems. Whilst laboratory microcosm experiments have been regularly used to test for mechanistic relationships at the cellular or organismic level (i.e. to relate changes in environmental conditions to physiological properties or population growth rate) their limited realism can make extrapolations to natural systems difficult to justify (Riebesell et al., 2010). Mesocosms can include a more biological complexity at larger scales to test for community- and ecosystem-level responses, especially for taxa that cannot be housed in microcosms but may be important for community responses to climate change (Stewart et al., 2013). Thereby, mesocosm experiments can help to disentangle direct effects of environmental variables (e.g. temperature, pH) from indirect effects which only evolve during complex food-web interactions (i.e. impact on food availability to higher trophic levels). An important strength of mesocosm experiments is that they allow for the manipulation of replicate enclosed populations in combination with key properties of natural systems. Thus, they have the predictive power to test statistically for causal relationships at larger scales. This is of great importance, since modelling the impact of climate change effects on complex plankton communities is often hampered by the lack of predictive ability of ecological data

and mechanistic insights into trophic interrelations at larger temporal and spatial scales (Evans, 2012; Stewart et al., 2013).

1.3.1 Mesocosm systems

All data evaluated in this thesis were collected from large-volume mesocosm experiments, 1.5 to 5 months in duration, conducted in two different mesocosm facilities to study climate change impacts on marine and lake ecosystems.

(1) The Kiel Off-shore Mesocosms for Future Ocean Simulations (KOSMOS) facility consists of sea-going mesocosm units made of flexible-wall polyurethane bags with an attached floating frame (Riebesell et al., 2013). Bags are 2 m in diameter and reach a depth of 15-19 m (ca. 35-55 m^3 volume) with a sediment trap attached to the bottom in order to allow the study of carbon export (Boxhammer et al., 2016) **(Fig. 3B)**. Although the system is open to the atmosphere, the facility has been used for making C and nutrient budgets (Czerny et al., 2013a; Spilling et al., 2016b; Boxhammer et al., 2018) based on the determination of air-sea gas exchange (Czerny et al., 2013c) and enclosed volumes (Czerny et al., 2013b).

(2) The LakeLab (www.lake-lab.de) installed in Lake Stechlin, an oligo-mesotrophic, dimictic hardwater lake in northeastern Germany (53°08’36" N, 13°01’41" E), consists of 24 mesocosm units. Each unit has a diameter of 9 m, reaches a depth of 14-21 m and consists of flexible, light-impermeable walls which are moored in the sediment, thus, enclosing about 1.2 million liters of water and the upper sediment layer **(Fig. 3C)**. Thermal stratification patterns and patterns in plankton distribution within the water column, including the occurrence of a deep chlorophyll maximum (DCM), can be mimicked realistically in the LakeLab, allowing for climate change research in deep lakes.

1.4 Impact of climate change on aquatic ecosystems

During the 420,000 years prior to the industrial period, the Earth’s climate system settled into a persistent pattern of glacial-interglacial cycles, with atmospheric CO_2 concentrations oscillating between 180 ppm in glacial and 280 ppm in interglacial times (Petit et al., 1999). Since the Industrial Revolution, the Earth´s atmosphere C content exhibited an increase from about 590 PgC to about 830 PgC, exceeding natural variability as a consequence of anthropogenic fossil fuel CO_2 emissions, cement production and land-use changes (Ciais et al., 2013). This increase corresponds to a current atmospheric CO_2 concentration of about 410 ppm that was reached at the Mauna Loa observatory (Tans and Keeling, 2015). How the atmospheric CO_2 level will develop in future will largely depend on the release of emissions and intergovernmental agreements on the mitigation of climate change (e.g. Schellnhuber et al., 2016). Under business-as-usual conditions, however, projections reach about 1000 ppm CO_2 at the end of the century (representative concentration pathway (RCP) 8.5; (Riahi et al., 2007; Meinshausen et al., 2011; Collins et al., 2013). Although the changes in atmospheric C concentration is considerably less compared to other Earth system C pools,

the atmospheric C content is of critical importance due to its effects on the Earth´s climate and exchange of CO_2 across the water-atmosphere interface (Raven and Falkowski, 1999; Rahmstorf et al., 2007; Rhein et al., 2013; Trenberth et al., 2015b).

1.4.1 Impact of ocean acidification

Oceans have taken up approximately 155 Pg (±20 %) of anthropogenic C across the water-atmosphere interface (Rhein et al., 2013). Thereby, the oceans' uptake of anthropogenic CO_2 limited atmospheric CO_2 levels, thus, playing a central role in regulating Earth´s climate, but at the same time changed the ocean´s carbonate chemistry (Raven and Falkowski, 1999). The majority of CO_2 that dissolved in seawater reacted with water (H_2O), forming carbonic acid (H_2CO_3), which then dissociated by losing hydrogen ions (H^+) to form bicarbonate (HCO_3^-) and carbonate (CO_3^{2-}) ions (Doney et al., 2009). The process decreased pH and increased the concentration of dissolved inorganic carbon species (DIC) (Raven et al., 2005). Even though surface waters will remain alkaline, the corresponding increase in ocean acidity termed the process `ocean acidification´ (OA). Surface seawater pH has already decreased by 0.1 pH units since preindustrial times and might further decrease about 0.3-0.4 pH units until the end of the century (Wolf-Gladrow et al., 1999; Caldeira and Wickett, 2005). In contrast to freshwater systems, which can experience fluctuations up to several pH units even on a daily bases, the surface-ocean pH has been relatively stable between 8.3 and 8.2 over the last 2 million years until the industrial revolution with changes happening on time scales of glacial cycles (Zeebe, 2012). The current increase in ocean acidity is about 100 times faster than any previous natural change, causing a perturbation on marine ecosystems on a time scale which might not allow organisms to adapt (Raven et al., 2005; Pörtner, 2008).

1.4.2 Impact on weather patterns – episodic extreme events

According to different Representative Concentration Pathways (RCP) scenarios for the development of future emissions that are considered by the Intergovernmental Panel on Climate Change (IPCC), the removal of human-emitted GHG from the atmosphere by natural processes will take a few hundred thousand years (Ciais et al., 2013). The long time required to remove anthropogenic GHG makes climate to change (Ciais et al., 2013). GHG impact on the redistribution of energy within the atmosphere and between the atmosphere, land and the ocean, thus, is altering the radiative balance of the Earth (Hartmann et al., 2013; Rhein et al., 2013). As a consequence, temperatures are expected to rise which also impacts associated circulation and weather patterns. It is projected, that the already recorded increase in sea surface temperature and atmospheric moisture will provide a warmer and wetter weather, increasing the occurrence and severity of global weather extremes (Trenberth, 2012; IPCC, 2013b). This is expected to result in more heavy and frequent episodic weather-related events, such as storms, even in the presence of large natural variability and thus high uncertainty of predictions (Easterling, 2000; Rahmstorf et al., 2007;

Rahmstorf and Coumou, 2011; Coumou and Rahmstorf, 2012; Trenberth, 2012; Trenberth et al., 2015a; Trenberth et al., 2015b; Wang et al., 2017a). In particular, summer storms can act as major disturbances on lake ecosystems, perturbating the thermal summer stratification and changing the physical or chemical environment that may affect local plankton communities (Glasby and Underwood, 1996; Shade et al., 2012b). Ecological consequences of such episodic events, however, are challenging to study at the ecosystem scale. As there is an inverse relationship between disturbance frequency and magnitude, extreme events occure infrequently and are hard to predict (Sousa, 1984; Romme et al., 1998; Turner et al., 1998; Turner and Dale, 1998; White and Jentsch, 2001). In addition, harsh environmenal conditions associated with exteme events often hinder a targeted sampling and the lack of true replication of natural observations does often not allow to gain a basic knowledge on underlying mechanisms that cause specific post-disturbance responses in plankton communities and ecosystem functioning. Experimental ecosystem-scale approaches, such as the LakeLab facility, to assess how such events alter activity, compostion, resilience and function of plankton communities, thus, represent a method of choice to circumvent conditional difficulties related to studying natural episodic events.

1.4.3 Potential impact of OA on heterotrophic bacteria within marine plankton communities

The oceanic uptake of CO_2 is accompanied by complex changes in seawater carbonate chemistry which are considered as stressors for marine organism physiology (Doney et al., 2009; Kroeker et al., 2010, 2013). Physiological responses to, e.g. a decrease in pH, $[CO_3^{2-}]$ and carbonate saturation (Ω) or an increase in pCO_2/fCO_2, $[H^+]$, $[CO_2]_{(aq)}$, $[H_2CO_3]$ and $[HCO_3^-]$ have been reported across various groups of organisms during single species laboratory studies up to ecosystem-level experiments. However, the responses are diverse and non-uniform across organisms, physiological processes and experimental scales (reviewed in e.g. Fabry et al., 2008; Kroeker et al., 2013; Riebesell and Tortell, 2011). One reason for the inconsistency of results, especially between experimental scales, might be that physiological responses to OA comprise simultaneously effects of `acidification´ and `carbonation´, which are inevitable linked through contemporary changes in carbonate chemistry. Thereby, `acidification´ refers to an increase in hydrogen ion concentration that is mainly considered to impact organism homeostasis and calcification processes, whereas `carbonation´ describes an increase in DIC and thus implies a potential `fertilisation´ of autotrophic carbon fixation (Riebesell et al., 2009; Bach et al., 2011, 2013). Both aspects of OA are expected to cause changes in the competitive fitness between different plankton species that impact on the balance between autotrophic and heterotrophic processes.

Although a shift away from the study of individual organisms to complex communities has been observed that allow for studying of autotrophic and heterotrophic processes simultaneously, there is still an imbalance of considerably more studies reporting on a few prominent physiological processes (e.g. calcification) and taxonomic groups mainly related

to phytoplankton (Yang et al., 2016). In particular, potential OA impacts on heterotrophic bacterial processes are not well represented, either in single/multi-species laboratory studies nor community-level experiments (Yang et al., 2016). Little is known on OA effects at the subcellular level, demonstrating differential gene expression patterns in heterotrophic bacteria as a physiological response to elevated pCO_2 (Bunse et al., 2016). Some studies even argue that bacterial metabolism will be impacted generally under future higher CO_2/lower pH conditions (Joint et al., 2011). However, the few ecosystem-level studies on the effects of OA imply that differences in the activity of heterotrophic bacteria result indirectly from concurrent differences in other OA-sensitive variables that represent more important impacts on the bacterial metabolism, rather than being a direct consequence of changes in pH or pCO_2 (Grossart et al., 2006a; Allgaier et al., 2008; Piontek et al., 2010; Liu et al., 2010). Diverse responses of bacterial production in response to pCO_2 are reported, partly depending on the community considered (attached versus free-living bacteria) and the normalisation used (e.g. cell-specific rates) (reviewed in Liu et al., 2010). Endres et al. (2014) reported a stimulated bacterial growth at elevated pCO_2, studying microbial production and removal processes in the surface ocean during research cruises at low and high latitudes as well as during CO_2-manipulation studies simulating future ocean conditions. The authors conclude that the ongoing OA has the potential to facilitate the microbial recycling of freshly produced organic matter, thus strengthening the role of the microbial production of climate-active gases in the surface ocean (Endres et al., 2014). Grossart et al. (2006a) observed significant higher bacterial protein production (BPP), cell-specific protein production (csBPP) and biomass, but only of attached bacteria at elevated pCO_2. Allgaier et al. (2008) suggested that there was no difference in bacterial production in response to pCO_2, but observed an significant impact of pCO_2 levels on linear regressions between BPP of free-living bacteria, BPP of attached bacteria or csBPP of attached bacteria and C:N ratios of suspended matter. There are also indications that the extra-cellular activity of particular enzymes might increase due to lower pH as reported for protease as well as α- and β-glucosidase (Grossart et al., 2006a; Piontek et al., 2010), whereas other studies could not reveal any effect of pH/CO_2 on enzyme activities (Tanaka et al., 2008). In studies that distinguish between different bacterial life-styles, there is a preferential stimulation of activity and abundance of attached bacteria with elevated pCO_2. Generally, attached bacteria experience a higher nutrient-availability in the presence of aggregates, but may also respond to increased production of TEP at increasing pCO_2 (Engel, 2002; Engel et al., 2004; Mari, 2008). Although there are several indications of a direct positive effect of OA-conditions on polysaccharide exudation, e.g. Egge et al. (2009) could not find any significant effect of elevated pCO_2 on TEP concentration which stresses the fact that at present-day pCO_2 TEP production should already be saturated (Engel et al., 2004; Liu et al., 2010). In most studies, little or no effects of pCO_2 could be detected on bacterial abundances and biomass (e.g. Grossart et al., 2006a; Allgaier et al., 2008; Yamada et al., 2008; reviewed in Liu et al., 2010). It is questionable that potential impacts could have been masked by trophic transfer of bacterial biomass to higher trophic levels via the microbial loop. Such complex trophic

interrelations were mostly not assessed in the scope of the above mentioned studies. Recently, a mass balance approach reports such an enhanced transfer of organic matter to higher trophic levels caused by OA, however not resolving the particular role of heterotrophic bacteria (Boxhammer et al., 2018). Also, a promoted herring larvae survival (Sswat et al., 2018) and a benefitting of copepods (Taucher et al., 2017b) at OA conditions suggest that potential OA-effects on the bacterial biomass could be masked by complex trophic interrelations.

When CO_2-effects could be detected, bacterial activity and/or abundance changed primarily in dependence on the available quantity and quality of phytoplankton-derived organic matter, which both are considered to be impacted by OA (Sambrotto et al., 1993; Hein and Sand-Jensen, 1997; Riebesell, 2004; Riebesell et al., 2007; Engel et al., 2013; Schulz et al., 2017). An enhancement of primary production has been described as one of the most consistent OA responses, however, a potential impact on phytoplankton production is largely dependent on the prevailing nutrient conditions and phytoplankton community composition (Gruber et al., 2009; Riebesell and Tortell, 2011; Kroeker et al., 2013; Schulz et al., 2017; Alvarez-Fernandez et al., 2018). Thereby, differences in CO_2 related physiology between phytoplankton taxa can lead to differences in their ability to utilize CO_2, influencing the competitive fitness between phytoplankton and impacting on population growth and phytoplankton community composition (Riebesell, 2004; Kroeker et al., 2013; Dutkiewicz et al., 2015; Pardew et al., 2018). Yet the precise mechanism are unresolved, changes in carbon concentrating mechanisms (CCM) or photorespiration are potential mechanisms suggested to cause impacts on phytoplankton energy fluxes (Hennon et al., 2017). In general, dinoflagellates and prymnesiophytes including calcifying coccolithophores have been suggested to respond negatively to OA, whereas diatoms, diazotrophic cyanobacteria and small-sized picoeukaryotes are usually favoured (e.g Kroeker et al., 2013; Dutkiewicz et al., 2015; Hennon et al., 2017; Schulz et al., 2017). However, responses across taxa within phytoplankton groups and especially the response in growth and N_2-fixation rate of diazotrophs does not seem to be uniform (Eichner et al., 2014). Although there are still uncertainties about metabolic phytoplankton responses to OA, it is expected that the impact of OA on the metabolic rates of primary producers will also impact their chemical composition. Thus, OA effects on the chlorophyll *a* content per cell, the phytoplankton fatty acid content and composition or the partitioning of C:N:P have been reported to potentially alter POM/DOM stoichiometry and food-availability for primary and secondary heterotrophic consumers (Hutchins et al., 2009; Riebesell and Tortell, 2011; Hennon et al., 2017; Wang et al., 2017b). Although a comparison of OA studies on natural plankton assemblages by Hutchins et al. (2009) found no general response pattern of POM, C:N or N:P stoichiometry with pCO_2, single studies reveal large potential shifts in future global C:N or N:P export stoichiometry (Engel et al., 2005; Riebesell et al., 2007).

All mentioned impacts of OA on marine plankton will likely change community structure and functional behaviour of different plankton in the pelagic food-web. Potential impacts on

production and growth balance of heterotrophic bacteria are expected (e.g. Motegi et al., 2013). The inconsistency in reported results at different levels of complexity and environmental settings, however, imply that indirect chemical effects on bacterial processes can result in apparently different consequences of acidification. Although it has been recognized that, in particular, different aspects of OA might change in response to nutrient conditions, surprisingly little is known how OA affects the structure of the microbial food chain when nutrient concentrations are low or even limiting for plankton production. However, this is an important factor that has to be considered in predictions on effects of OA, since large parts of the oceans are oligotrophic or experience extended periods of time at low nutrient conditions.

1.4.4 Potential impact of summer storm events on heterotrophic bacteria within lake plankton communities

During the summer and winter stratification period the simultanious change in temperature and freshwater density with depth separates typical temperate, dimictic lakes in two to three distinct thermal strata that usually do not mix (e.g. Imberger, 1985; Schwoerbel, 1999). As the temperature of maximum density for freshwater is 4°C, mixing typically occurs only twice a year during the spring and fall when the water temperature throughout the water column is about 4°C. In the absence of any temperature or density difference, wind energy is sufficient to overturn the lake water mass. During winter such lakes are usually covered by ice, forming a warmer bottom water of about 4°C (hypolimnion) which is separated from colder surface waters (epilimnion) by temperature-derived density differences. After the spring overturn and with increasing water temperatures, a warmer epilimnion forms on top of the colder hypolimnion, separated by the metalimnion, a layer with a strong temperature and density gradient (Monismith and MacIntyre, 2009; Read et al., 2011). Mostly synonymously used to the term metalimnion, the thermocline specifies the depth of the mixed layer (z_{mix}) and is defined as the depth with the maximal temperature gradient (Hutchinson, 1975). During summer stagnation wind forcing is usually only sufficient to cause a circulation and transport of thermal energy within the upper well-mixed epilimnic region. Thereby, the resistance to mechanical mixing (described, e.g. by buoyancy, Schmidt stability, Brunt-Väisälä frequency or Wedderburn Number) and on the contrary wind stress and convection as destratifying forces determine the epilimnion thickness (Schmidt, 1928; Hutchinson, 1975; Idso, 1973; Thompson and Imberger, 1980; Gorham and Boyce, 1989; Imberger and Patternson, 1990; Schwoerbel, 1999; Read et al., 2011; Winslow et al., 2016). The latter depends mainly on lake surface area, lake orientation, the relationship between lake length and width or specific catchment properties (e.g. forestation, relief) (Patalas, 1984; Gorham and Boyce, 1989; Schwoerbel, 1999). With increasing surface water temperature the resistance to mechanical mixing increases, preventing vertical transfer between bottom and surface waters, thus controling in-lake vertical fluxes of dissolved and particulate material (Robertson and Imberger, 1994;

Aeschbach-Hertig et al., 2007). Consequently, the vertical partitioning of the water colum and its resulting consequences for the availability of nutrients, light and substrates has important implications for the vertical distribution, community composition, activity, migration, and feeding of different autotrophic and heterotrophic plankton (Read et al., 2011). With increasing duration of the stratification period, this often results in a nutrient rich but light-limited meta-/hypolimnion, and a rich in light but nutrient-poor epilimnion (MacIntyre et al., 1999). Further, the decline in PAR with depth increases the contribution of heterotrophic to autotrophic processes, thus increasing meta-/hypolimnic concentration of CO_2 and changing redox conditions.

Summer storms have the potential to perturb this thermal stratification, disrupting the thermocline and deepening the mixed layer (Tsai et al., 2008; Jennings et al., 2012; Klug et al., 2012; Kuha et al., 2016; Kasprzak et al., 2017; Giling et al., 2017a; Perga et al., 2018). Additional mixing during summer thus acts as an unusual extreme ecosystem disturbance for summer communities that happens on comparable short time scales compared to the seasonal mixing with gradual cooling of the epilimnion and periodic entrainment of these waters into the hypolimnion (Shade et al., 2012b). Especially, when meta- and hypolimnic water masses are eroded by the mixing event, communities that are separated over several months and adapted to respective conditions in the hypo-, meta- or epilimnion are eventually mixed together and experience new vertical gradients of environmental conditions that are created by mixing. Mixing by summer storms often leads to an intrusion of colder metalimnic and eventually hypolimnic water into the surface layer, which (i) decreases the surface layer water temperature and increases the thickness of the mixed layer, (ii) redistributes meta-/hypolimnic organisms throughout the whole mixed layer, and (iii) adds nutrient- (P,N) and CO_2-rich meta-/hypolimnic water to the upper mixed layer. Physical and chemical properties of the water column can be changed for several days with potential long-term effects on spatial distribution, composition and functionality of organisms (e.g. Jennings et al., 2012; Kasprzak et al., 2017). However, possible biological responses are also largely dependent on the terrestrial-aquatic coupling between lake and the catchment (i.e. surface runoff, flood pulse) and a potential resuspention of sediment material into the water column (Battoe, 1985; Weyhenmeyer et al., 2004; Arvola et al., 2006; Jennings et al., 2012; Sadro and Melack, 2012; de Eyto et al., 2016). The additional input of DOM might be an important factor controlling organism physiology when considering lakes with a small volume or a short residence time (Rantakari and Kortelainen, 2005; Ojala et al., 2011; Vachon and del Giorgio, 2014). Small lakes usually experience a reduction in PAR due to the terrestrial DOC input or sediment resuspension (Chrost and Riemann, 1994; Carpenter et al., 1998; Cole et al., 2000; Houser, 2006; Tsai et al., 2008; Blottière et al., 2017). In combination with the increased disturbance, summer storms have the capacity to shift small lakes towards an increased degree of heterotrophy by negatively impacting autotrophic organisms (Battoe, 1985; Jennings et al., 2012). In contrast, large volume, deep, clear-water lakes, like Lake Stechlin, are usually internally regulated even after intense precipitation events (Rantakari and Kortelainen, 2005; Ojala et al., 2011;

Vachon and del Giorgio, 2014). Here, mixing might expose organisms from deeper thermal strata to higher levels of PAR (Giling et al., 2017a). In combination with an increase in inorganic carbon and nutrient availability, thus, mixing has been shown to usually fuel phytoplankton production in the phototrophic zone by releasing organisms from nutrient and light limitation (Weithoff et al., 2000; Jennings et al., 2012; Giling et al., 2017a).

Especially, when a deep chlorophyll maximum (DCM) is eroded by deeper mixing, large amoungt of biomass can be allocated to the mixed layer, stimulating phytoplankton blooms (Kasprzak et al., 2017). Frequently, deep chlorophyll maxima (DCM) are associated to the thermocline in deep lakes, a situation also occurring regularly in Lake Stechlin during the summer stratfication period (Fee, 1976; Moll and Stoermer, 1981; Gervais et al., 1997; Leach et al., 2017). DCM contain high amounts of biomass, concentrated in a certain depth depending on the availability of light and the vertical nutrient gradients between epi- and hypolimnion that establish with thermal stratification, and may contribute substantially to whole-lake metabolism making up to 50 % of GPP and 60 % of ER (Giling et al., 2017b). DCM are typically dominated by diatoms, dinoflagelletes, cryptophytes or less frequently cyanobacteria, but can also contain large amounts of mixotrophs, heterotrophic protozoans and up to 10-times higher bacterial biomass compared to the surrounding water (Leach et al., 2017). In July 2011, such a phytoplankton bloom development was observed subsequent the exceptional summer storm `Otto´ after disrupting a DCM and distributing the organisms into the mixed layer (Kasprzak et al., 2017). The storm caused a pronounced cyanobacterial bloom of *Dolichospermum* sp. in clear Lake Stechlin, triggering a cascade of processes towards extreme turbidity never observed before within three decades of lake monitoring (Kasprzak et al., 2017). Also in the Irish deep Lake Leane such a cyanobacteria bloom development of *Dolichospermum flos-aquae* (sensu *Anabaena flos-aquae*) could be observed (Jennings et al., 2012), but also biomass increases and bloom formations of green algae, in particular chlorophytes and cryptophytes, or diatoms have been reported to follow thermocline deepening, lake mixing or storm events (Huisman et al., 2004; Cantin et al., 2011; Jennings et al., 2012).

Changes in the turbulence structure and vertical physical-chemical gradients of lakes by storm events may not only impact phytoplankton productivity, but also induce major shifts in the species composition of phytoplankton communities (Klausmeier and Litchman, 2001; Huisman et al., 2004; Giling et al., 2017a). Models of mixed water columns suggest that the light-to-nutrient ratio is an important determinant of phytoplankton dynamics (Huisman and Weissing, 1995; Diehl, 2002). Also, the plankton sinking velocity, capability in nutrient uptake and storage, or mechanisms for grazing defence are important traits, determining phytoplankton species competition that can be altered directly, or indirectly through food-web interrelations by effects of mixing (Sommer, 1988; van Donk and Hessen, 1993; Huisman and Weissing, 1995; Huisman et al., 1999; Klausmeier and Litchman, 2001; Ptacnik et al., 2003; Jäger et al., 2010; Huisman et al., 2004; Cantin et al., 2011; Sarnelle, 2005). Huisman et al. (2004) suggest that species with the lowest critical light intensity should

competitively exclude all other species during mixing (Huisman and Weissing, 1994; Weissing and Huisman, 1994). Here, in particular cryptophytes and chrysophytes might benefit from a deeper thermocline because of their low light-to-nutrient needs (Ptacnik et al., 2003; Cantin et al., 2011). Further, Arvola et al. (2006) reports on a wash-out of the smallest fraction of plankton during high turbulence.

Although episodic weather-related events have long been recognised to impact vertical physico-chemical gradients and phytoplankton development in lakes, there are only a few studies that specifically address also impacts on heterotrophic bacterial processes, biomass development, and community assembly (Weithoff et al., 2000; Jones et al., 2008; Shade et al., 2010a; b, 2011, 2012b; Jones et al., 2013; Blottière et al., 2017) or focus on metabolic community responses that give an indication on heterotrophic bacterial activity (Vachon and del Giorgio, 2014; Giling et al., 2017a; Perga et al., 2018). In particular, for large and deep clear-water lakes possible consequences for the development of heterotrophic bacteria in response to mixing and to potential mixing-related alterations in phytoplankton development are largely unknown.

Shade et al. (2010a) investigated the influence of post-mixing environmental condtions and biotic interactions on BCC and incubated waters from the epilimnion, hypolimnion and a mixture of both within the epi- and hypolimnion. The authors wanted to know how robust lake bacteria from each thermal strata are to lake mixing (Shade et al., 2010a). Usually, in temperate lakes, bacterial communities follow a seasonal trajectory with distinct communities that are present during summer stratification in each thermal strata and communities occurring during regular spring or fall mixing (Yannarell et al., 2003; Allgaier and Grossart, 2006; Shade et al., 2007, 2008, 2010b; Rösel et al., 2012). In particular, temperature and oxygen concentration, but also the availability of nutrients and the quantity and quality of phytoplankton-derived DOM/POM have been described as key drivers of vertical distribution of bacterial activity and community composition across seasons (Shade et al., 2007, 2008; Rösel et al., 2012; Rösel and Grossart, 2012). Thus, during the stratification period, communities adapted to lower temperatures and oxygen concentrations are present in the hypolimnion, separated from epilimnic communities that experience higher temperatures and oxygen concentrations but may also preferentially be associated to specific phytoplankton (Shade et al., 2007, 2008; Rösel et al., 2012; Rösel and Grossart, 2012). However, the transplant experiment performed by Shade et al. (2010a) revealed, that approximately 30 % of all bacterial operational taxonomic units (OTU) are generalists that can occure in both the epi- as well as hypolimnic layer and only 6 % of epilimnic and 4 % of hypolimnic OTUs were specialists, that could only survive in their respective straification layer. Additional 9 % and 15 % of OTUs had a preference for either the epilimnion or hypolimnion, respectively (Shade et al., 2010a). Although there was a high contribution of generalist OTUs and a strong influence of the inocula composition in a community´s response to transplant, Shade et al. (2010a) observed responses in both epilimnic and hypolimnic communities to mixing that were modulated by the local water

conditions in epi- and hypolimnion. Thus, hypolimnion communities incubated in the epilimnion changed more than those incubated in their ambient hypolimnion and epilimnion-incubated communities were generally more different than hypolimnion-incubated ones (Shade et al., 2010a). Also, the high number of generalist OTUs imply that no matter where the generalist OTUs are transported during mixing, some may be serving as pioneer species during the post-mixing re-stratification (Shade et al., 2010a). To determine the stability of microbial communitities after a large summer mixing disturbance event, Shade et al. (2012b) conducted a follow-up whole-ecosystem manipulation during peak summer thermal stratification in a shallow humic lake. Thereby, stability describes the general capacity to return to equilibrium after a perturbation, and includes components of resistance, recovery and resilience (Pimm, 1984; Shade et al., 2011, 2012a; Allison and Martiny, 2008). Resistance is the degree to which the community composition remains unchanged in the face of a disturbance, recovery is the community´s ability to return to its pre-disturbance composition or function, and resilience describes the rate at which the microbial composition returns to its original composition after being disturbed (Pimm, 1984; Shade et al., 2011, 2012a; Allison and Martiny, 2008). In their experiment, Shade et al. (2012b) observed that environmental bacterial communities were not resistant to summer mixing, but were highly resilient. A similar pattern was also observed after different episodic mixing events, including typhoons and huricanes (Yannarell et al., 2007; Jones et al., 2008; Shade et al., 2010b).

Irrespective of changes in community assembly and stability of bacterial communities after water column mixing the question arises how such disturbance events might also impact the activity and biomass of heterotrophic bacteria. Given the central role of bacteria in ecosystem processes, alterations in bacterial production, respiration or enzymatic capacity to degrade substrates have the potential to impact the balance of autotrophic to heterotrophic processes and might consequently change the functioning of a lake as C source or sink to the atmosphere. In a coastal marine ecosystem Chrost and Riemann (1994) observed a short-term increase of aminopeptidase and β-glucosidase activities and bacterial secondary production following a simulated storm in enclosures, however, a perturbation and resuspension of sediments strongly affected the kinetic parameters of both enzymes. Weithoff et al. (2000) and Blottière et al. (2017) monitored onlythe bacterial abundance development after artificial mixing in mesocosm facilities deployed in shallow to medium shallow eutrophic systems. Whereas Blottière et al. (2017) observed no change in bacterial abundance, the experiment performed by Weithoff et al. (2000) revealed an increase of bacterial abundance following mixing. During the typhoon season, Tsai et al. (2008) report a decrease of gross primary production and ecosystem respiration by approximately 50 % and 25 %, respectively, for a shallow subtropical humic lake. Also, de Eyto et al. (2016) and Perga et al. (2018) observed a decrease in primary production and an associated increase in heterotrophy in a humic Irish lake after an extreme precipitation event as well as an alpine lake after storm events, respectively. However, all observations are related to studies in eutrophic, humic, or shallow systems or associated with high turbidity input from the

watershed. So far, only Kasprzak et al. (2017) and Giling et al. (2017a) report on metabolic consequences of summer storms in deep, clear-water lakes, but with focus on phytoplankton production. Both studies observed an increase in primary production as a result of increased PAR and nutrients associated to storm events, however, conseqences for heterotrophic bacterial activity and biomass development remain unresolved (Kasprzak et al., 2017; Giling et al., 2017a).

1.5 Objectives and hypotheses

Human impact on the environment has initialized a new epoch, termed `Anthropocene´, with mankind being the major environmental force in creating impacts in the Earth System that are summarized as `climate change´ (Crutzen, 2002; Lewis and Maslin, 2015). While the impact on the abiotic environment can reasonable been projected, potential consequences for organisms and their functioning in aquatic ecosystems are largely unknown. Especially processes maintained by heterotrophic bacteria are often neglected, although they possess a vital ecological role in maintaining nutrient cycles or channelling energy to higher trophic levels. The main objectives of this dissertation are therefore to assess ***(1) how and to what extent heterotrophic bacterial processes might be impacted with ongoing climate change*** and ***(2) how potential climate change-driven alterations in bacterial C processing might affect carbon cycling in aquatic ecosystems***. Due to the vast amount of potential climate change impacts on diverse aquatic ecosystems, this thesis focuses on the impacts of (1) ocean acidification and (2) severe storm events, which are expected to shift in frequency, severity or timing with ongoing climate change, based on results from four large-volume mesocosm experiments that were performed in marine and lake ecosystems. The evaluation of scientific knowledge on both research topics identified existing knowledge-gaps and generated so far unresolved research questions and deduced hypotheses which are subsequent pointed out in detail.

I) Assessing the impact of OA on DOM processing by marine heterotrophic bacteria

Previous studies on the impact of OA on single plankton species and plankton assemblages have given a first insight into how phytoplankton C production and subsequent bacterial C transformation might be affected. In principal, autotrophs should be fertilised by an enhanced CO_2 availability, increasing the production of POM and DOM (Hein and Sand-Jensen, 1997; Riebesell et al., 2007) and subsequently enhancing bacterial C transformation (Grossart et al., 2006a; Piontek et al., 2010). However, previous experiments assessed mostly the impact of OA at nutrient replete conditions, i.e. during productive phases or following nutrient additions, to stimulate plankton production. Surprisingly little is known about how OA affects the physiology of heterotrophic bacteria or the coupling of heterotrophic bacteria to phytoplankton when nutrient concentrations are low or even limiting for plankton production.

We wanted to fill this knowledge gap and assessed the impact of OA on a Baltic Sea coastal plankton community in July-August after the nominal spring bloom during low-nutrient conditions using pelagic mesocosms which were manipulated with a gradient of CO_2 concentrations extending from present to future conditions. **Chapter 2** presents bacterial production and biovolume dynamics and evaluates consequences of OA for the bacteria-phytoplankton coupling at low-nutrient conditions. **Chapter 3** gives an overview of the biogeochemical pools and fluxes during this mesocosm study and estimates the heterotrophic bacterial contribution to changes in C pool and C flux sizes in respect to increasing concentrations of CO_2. Thereby the following research questions (RQ) and hypotheses (H) have been addressed:

RQ1: *Does OA affect heterotrophic bacterial production when phytoplankton production is low or even limited by nutrients?*

H1: *OA will not stimulate heterotrophic bacterial production at low-nutrient concentrations.* **(Chapter 2)**

RQ2: *Does OA impact the C budget of a coastal summer plankton community by affecting the size of heterotrophic bacterial pools and fluxes? Thus, has OA the potential to stimulate C-export by reducing bacterial mineralization processes at low nutrient concentrations?*

H2: *OA will not affect the C-budget due to a stimulation of heterotrophic bacterial processes, thus potentially increasing C-export, at low-nutrient concentrations.* **(Chapter 3)**

After evaluating quantitative consequences of OA for bacterial C cycling at low-nutrient conditions, **Chapter 4** analyses how potential OA-induced changes in bacterial activity relate to qualitative changes in DOM at different nutrient conditions. The production and transport of recalcitrant and semi-labile organic matter maintain the biological carbon pump and determine C export from the surface ocean to the ocean interior (Volk and Hoffert, 1985). Why these molecules resist degradation in the surface ocean where heterotrophic microbes are often limited by substrate and nutrient availability remains unresolved so far (e.g. reviewed in Dittmar and Stubbins, 2014). However, as a substantial and temporally stable component of DOM, semi-labile DOM affects the overall rate of C turnover in the oceans, thus illuminating its composition and identifying impacts on metabolic pathways that can degrade it are important for predictive understanding of carbon sequestration (Moran et al., 2016). So far, OA experiments monitored mainly bulk DOC concentrations by neglecting the quality of the DOM pool or only resolved POM/DOM stoichiometry (Czerny et al., 2013a; Engel et al., 2013). Reasons might be that experiments seeking to measure changes in DOM quality are hampered by inherently low rates of net C turnover and analytical techniques that provide limited structural resolution of resistant molecules. Therefore, we compared two mesocosm studies performed at oligotrophic (Gando Bay, Gran Canaria, Spain) and eutrophic (Gullmarfjord, Sweden) nutrient conditions and related cumulative BPP rates to qualitative changes in DOM by using FT-ICR-MS data. We intended to examine the effect of

OA on how bacterial activity determines the accumulation of semi-labile DOM in the surface ocean.

RQ3: *Do the effects of OA translate differently in the transformation of semi-labile/refractory DOM by heterotrophic bacteria depending on the nutrient conditions?*

H3: *Under oligotrophic compared to eutrophic conditions OA effects channel more of primary production via the microbial loop into the more recalcitrant DOM pool.* **(Chapter 4)**

II) Assessing the impact of severe storm events on heterotrophic bacteria in stratified lake ecosystems

Future shifts in frequency, severity or timing of storms are an important component of climate change. Observations in lakes indicate that water-column mixing by storms can have pronounced ecosystem-scale consequences impacting plankton dynamics, community assembly and thus C and nutrient cycling. Changes in physical and chemical environmental conditions and a potential increase in phytoplankton production can be expected, as observed for the exceptional summer storm "Otto" that impacted Lake Stechlin in July 2011 (Kasprzak et al., 2017). However, the underlying mechanisms that change community assembly and activity of heterotrophic bacteria have not been rigorously assessed in ecosystem-level experiments. To better understand the ecological mechanisms of storm-induced short-term disturbances in stratified lakes, we experimentally assessed the following research questions and hypotheses related to water-column mixing in summer 2014 by using the LakeLab mesocosm-facility in oligo-mesotrophic Lake Stechlin (www.lake-lab.de) **(Chapter 5)**:

RQ4: *Does water-column mixing change bacterial community composition and activity? How do environmental conditions and biotic interactions drive post-mixing compositional changes and activity of heterotrophic bacteria?*

H4: *Artificial mixing does change heterotrophic bacterial community composition and increases metabolic heterotrophic processes due to enhanced autotrophic productivity.* **(Chapter 5)**

RQ5: *How resistant/resilient are the bacterial community composition and activity to artificial water-column mixing? How long will a potential recovery of the bacterial community composition and activity to control-conditions take? Are the control-conditions after the potential recovery comparable to pre-mixing conditions?*

H5: *The bacterial community is not resistant, but resilient to artificial water-column mixing.* **(Chapter 5)**

RQ6: *Do changes in the activity of heterotrophic bacteria relate to changes in C export?*

H6: *Changes in heterotrophic bacterial activity alter C export*. **(Chapter 5)**

The following chapters present results of two lead author manuscripts (Chapters 2 and 5) and two co-author manuscripts (Chapters 3 and 4) which address the topic-specific hypotheses, however, this thesis also refers to several co-author publications (listed in the publication record) that are particularly relevant. The thesis concludes with a comprehensive synthesis, which discusses the results of the different chapters and embeds them into current knowledge on climate change.

Figure 3: Graphical summary. →

A) The increase in atmospheric GHG concentrations, commonly referred to as `climate change´ (CC), impacts on various Earth system processes (IPCC, 2013b). As such, the change in atmospheric GHG concentrations decreases the radiation back to space affecting Earth surface temperature and climate. Hence, more frequent and intense extreme weather events are expected (Trenberth, 2012; IPCC, 2013b). Further, the increase in atmospheric CO_2 concentration causes ocean acidification via enhanced ocean-atmosphere gas exchange and associated dissolution of CO_2 into the surface ocean (Raven et al., 2005). Both aspects of CC were studied in ecosystem-level, large-volume mesocosm experiments by using **B)** the Kiel Off-shore Mesocosms for Future Ocean Simulations (KOSMOS) at different coastal marine locations and **C)** the LakeLab in Lake Stechlin (www.lake-lab.de). This doctoral thesis evaluates, how **D)** ocean acidification in coastal marine ecosystems and **E)** artificial mixing (i.e., simulation of an episodic summer storm event) in lake ecosystems impact community composition and function of pelagic heterotrophic bacteria in both ecosystems. `Purple´ arrows and boxes refer to bacterial processes and food web interactions which were studied in detail. Roman numerals II-IV highlight the chapters of this thesis. H1-H6 refer to specific hypothesis (see section 1.5). ENV-environmental variables (e.g. water chemistry, temperature, PAR); DOM-dissolved organic matter; HB-heterotrophic bacteria; HTL-higher trophic levels (e.g. zooplankton); PP-phytoplankton.

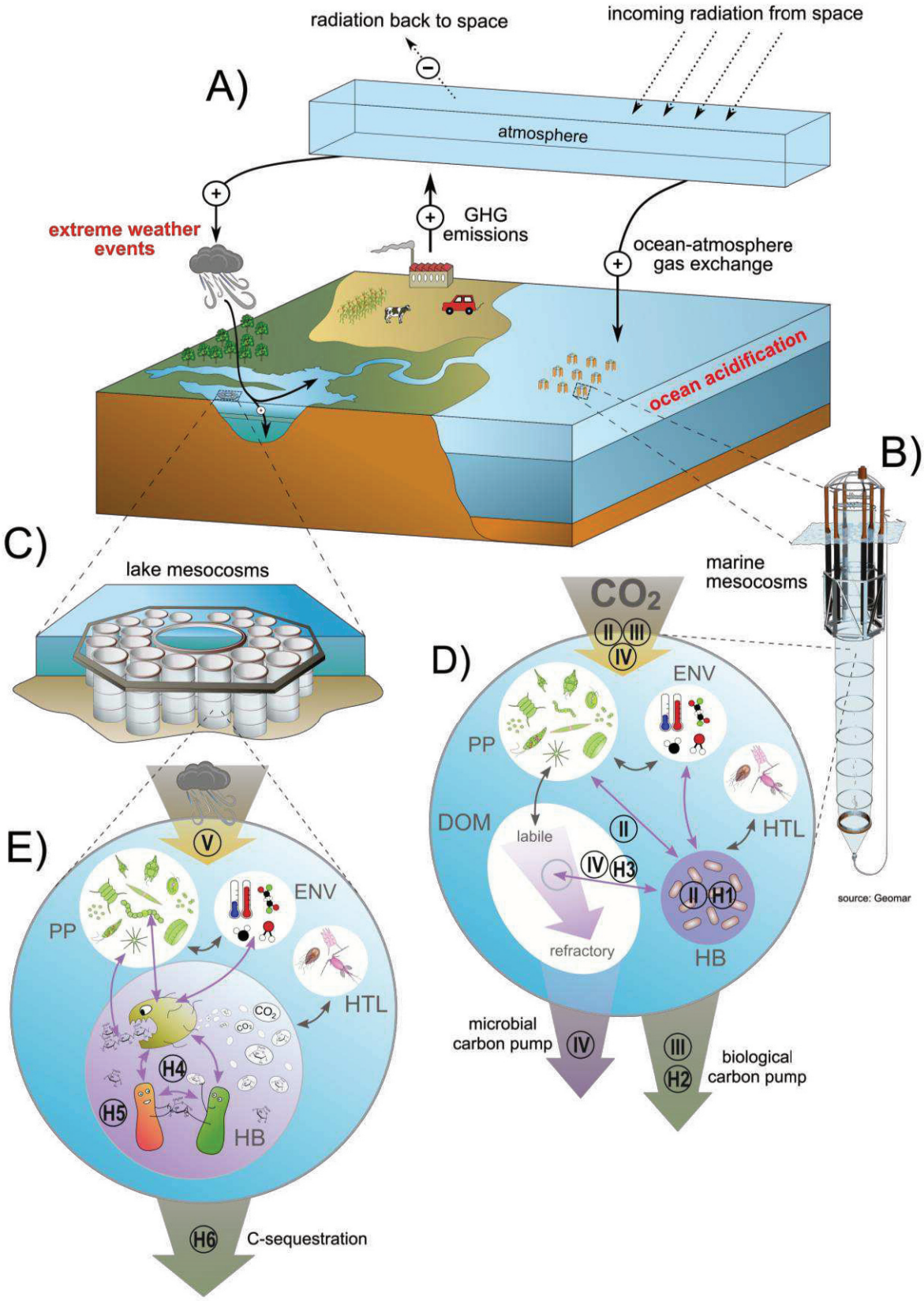
A)
radiation back to space
incoming radiation from space
atmosphere
GHG emissions
extreme weather events
ocean-atmosphere gas exchange
ocean acidification
B)
marine mesocosms
source: Geomar
C)
lake mesocosms
D)
CO2
II III IV
ENV
PP
DOM
labile
refractory
HTL
II H1
HB
IV H3
microbial carbon pump
IV
III H2
biological carbon pump
E)
V
ENV
PP
HTL
H4
H5
HB
H6
C-sequestration

2. Chapter 2 - Manuscript 1

Ocean acidification impacts bacteria–phytoplankton coupling at low-nutrient conditions

---

Thomas Hornick[1]*, Lennart T. Bach[2], Katharine J. Crawfurd[3], Kristian Spilling[4,5], Eric P. Achterberg[2,6], Jason N. Woodhouse[1], Kai G. Schulz[2,7], Corina P. D. Brussaard[3,8], Ulf Riebesell[2], and Hans-Peter Grossart[1,9]

Published in *Biogeosciences***

[1] Leibniz Institute of Freshwater Ecology and Inland Fisheries (IGB), Experimental Limnology, 16775 Stechlin, Germany

[2] GEOMAR Helmholtz Centre for Ocean Research Kiel, Düsternbrooker Weg 20, 24105 Kiel, Germany

[3] NIOZ Royal Netherlands Institute for Sea Research, Department of Marine Microbiology and Biogeochemistry, and Utrecht University, P.O. Box 59, 1790 AB Den Burg, Texel, the Netherlands

[4] Marine Research Centre, Finnish Environment Institute, P.O. Box 140, 00251 Helsinki, Finland

[5] Tvärminne Zoological Station, University of Helsinki, J. A. Palménin tie 260, 10900 Hanko, Finland

[6] National Oceanography Centre Southampton, European Way, University of Southampton, Southampton, SO14 3ZH, UK

[7] Southern Cross University, P.O. Box 157, Lismore, NSW 2480, Australia

[8] Aquatic Microbiology, Institute for Biodiversity and Ecosystem Dynamics, University of Amsterdam, P.O. Box 94248, 1090 GE Amsterdam, the Netherlands

[9] Potsdam University, Institute for Biochemistry and Biology, Maulbeerallee 2, 14469 Potsdam, Germany

*corresponding author: hornick@igb-berlin.de (T. Hornick)

** manuscript formatted in style of *Biogeosciences*

Biogeosciences, 14, 1–15, 2017
www.biogeosciences.net/14/1/2017/
doi:10.5194/bg-14-1-2017

Biogeosciences Open Access EGU

Ocean acidification impacts bacteria–phytoplankton coupling at low-nutrient conditions

Thomas Hornick[1], Lennart T. Bach[2], Katharine J. Crawfurd[3], Kristian Spilling[4,5], Eric P. Achterberg[2,6], Jason N. Woodhouse[1], Kai G. Schulz[2,7], Corina P. D. Brussaard[3,8], Ulf Riebesell[2], and Hans-Peter Grossart[1,9]

[1]Leibniz Institute of Freshwater Ecology and Inland Fisheries (IGB), Experimental Limnology, 16775 Stechlin, Germany
[2]GEOMAR Helmholtz Centre for Ocean Research Kiel, Düsternbrooker Weg 20, 24105 Kiel, Germany
[3]NIOZ Royal Netherlands Institute for Sea Research, Department of Marine Microbiology and Biogeochemistry, and Utrecht University, P.O. Box 59, 1790 AB Den Burg, Texel, the Netherlands
[4]Marine Research Centre, Finnish Environment Institute, P.O. Box 140, 00251 Helsinki, Finland
[5]Tvärminne Zoological Station, University of Helsinki, J. A. Palménin tie 260, 10900 Hanko, Finland
[6]National Oceanography Centre Southampton, European Way, University of Southampton, Southampton, SO14 3ZH, UK
[7]Southern Cross University, P.O. Box 157, Lismore, NSW 2480, Australia
[8]Aquatic Microbiology, Institute for Biodiversity and Ecosystem Dynamics, University of Amsterdam, P.O. Box 94248, 1090 GE Amsterdam, the Netherlands
[9]Potsdam University, Institute for Biochemistry and Biology, Maulbeerallee 2, 14469 Potsdam, Germany

Correspondence to: Thomas Hornick (hornick@igb-berlin.de)

Received: 19 February 2016 – Published in Biogeosciences Discuss.: 10 March 2016
Revised: 23 September 2016 – Accepted: 9 October 2016 – Published: 2 January 2017

Abstract. The oceans absorb about a quarter of the annually produced anthropogenic atmospheric carbon dioxide (CO_2), resulting in a decrease in surface water pH, a process termed ocean acidification (OA). Surprisingly little is known about how OA affects the physiology of heterotrophic bacteria or the coupling of heterotrophic bacteria to phytoplankton when nutrients are limited. Previous experiments were, for the most part, undertaken during productive phases or following nutrient additions designed to stimulate algal blooms. Therefore, we performed an in situ large-volume mesocosm ($\sim 55\,m^3$) experiment in the Baltic Sea by simulating different fugacities of CO_2 (fCO_2) extending from present to future conditions. The study was conducted in July–August after the nominal spring bloom, in order to maintain low-nutrient conditions throughout the experiment. This resulted in phytoplankton communities dominated by small-sized functional groups (picophytoplankton). There was no consistent fCO_2-induced effect on bacterial protein production (BPP), cell-specific BPP (csBPP) or biovolumes (BVs) of either free-living (FL) or particle-associated (PA) heterotrophic bacteria, when considered as individual components (univariate analyses). Permutational Multivariate Analysis of Variance (PERMANOVA) revealed a significant effect of the fCO_2 treatment on entire assemblages of dissolved and particulate nutrients, metabolic parameters and the bacteria–phytoplankton community. However, distance-based linear modelling only identified fCO_2 as a factor explaining the variability observed amongst the microbial community composition, but not for explaining variability within the metabolic parameters. This suggests that fCO_2 impacts on microbial metabolic parameters occurred indirectly through varying physicochemical parameters and microbial species composition. Cluster analyses examining the co-occurrence of different functional groups of bacteria and phytoplankton further revealed a separation of the four fCO_2-treated mesocosms from both control mesocosms, indicating that complex trophic interactions might be altered in a future acidified ocean. Possible consequences for nutrient cycling and carbon export are still largely unknown, in particular in a nutrient-limited ocean.

Published by Copernicus Publications on behalf of the European Geosciences Union.

1 Introduction

Since the industrial revolution the oceans have absorbed ca. one half of anthropogenic carbon dioxide (CO_2). This has resulted in a shift in carbonate equilibria and pH (e.g. Caldeira and Wickett, 2003) with potential consequences for organismal physiology (Taylor et al., 2012). In principal, autotrophs should be fertilised by an enhanced CO_2 availability, increasing the production of particulate (POM) and dissolved organic matter (DOM; Hein and Sand-Jensen, 1997; Riebesell et al., 2007). However, most CO_2 enrichment experiments studying natural plankton assemblages under variable nutrient conditions do not reveal a consistent response of primary production to elevated CO_2 (e.g. Engel et al., 2005; Riebesell et al., 2007; Bach et al., 2016). Both amount and stoichiometric composition of algal DOM and POM can be affected by changes in fCO_2. For example, Riebesell et al. (2007) and Maat et al. (2014) reported an increased stoichiometric drawdown of inorganic carbon (C) to nitrogen (N) at higher levels of fCO_2, most likely as a result from C overconsumption (Toggweiler, 1993).

Heterotrophic bacteria, in oligotrophic systems, are largely dependent on phytoplankton-derived organic carbon (e.g. Azam, 1998), and as such respond to alterations in both the quantity and quality of phytoplankton-derived DOM and POM (e.g. Allgaier et al., 2008; Grossart et al., 2006a). Availability and competition for nutrients, however, can substantially impact fCO_2-induced changes in activity and biomass of phytoplankton and subsequently of heterotrophic bacteria. In nutrient-depleted or nutrient-limited systems, bacteria are restricted in their utilization of phytoplankton-derived organic carbon (Hoikkala et al., 2009; Lignell et al., 2008). Consequently, fCO_2-dependent increases in inorganic C availability for autotrophs may not stimulate heterotrophic activity, causing a decoupling of heterotrophic and autotrophic processes (Thingstad et al., 2008). The accumulation of bioavailable dissolved organic carbon (DOC) and particulate organic carbon (POC), as a consequence of this decoupling in nutrient-limited oceanic surface waters, may have profound consequences for nutrient cycling and the nature of the oceanic carbon pump (e.g. Thingstad et al., 1997). Given that various studies have reported on limitation of bacterial growth by inorganic nutrients in several parts of the Baltic Sea (e.g. Hoikkala et al., 2009; Kuparinen and Heinänen, 1993), we sought to evaluate the effects of enhanced fCO_2 on activity and biomass of free-living (FL) as well as particle-associated (PA) bacteria during a period characterized by low nutrients and low productivity.

2 Methods

2.1 Experimental setup, CO_2 manipulation and sampling

Nine floating, pelagic KOSMOS (Kiel Off-Shore Mesocosms for future Ocean Simulations) mesocosms (cylindrical, 2 m diameter, 17 m long with conical sediment trap extending to 19 m depth) were moored (day $-10 = t - 10$; 10 days before CO_2 manipulation) at 59°51.5′ N, 23°15.5′ E, in the Baltic Sea at Tvärminne Storfjärden on the southwestern coast of Finland on 12 June 2012. Mesocosm bags were rinsed for a period of 5 days, covered on the top and bottom with a 3 mm net to exclude larger organisms. Thereby, the containing water was fully exchanged with the surrounding water masses. Sediment traps were attached to the bottom of each mesocosm at 17 m depth 5 days prior the start of the experiment ($t - 5$). In addition, submerged mesocosm bags were drawn 1.5 m above the water surface, enclosing and separating $\sim 55\ m^3$ of water from the surrounding Baltic Sea, and meshes were removed. Mesocosms were covered by a photosynthetic active radiation (PAR) transparent roof to prevent nutrient addition from birds and freshwater input from rain. Additionally, existing haloclines were removed in each mesocosm as described in Paul et al. (2015), thereby creating a fully homogeneous water body.

The experiment was conducted between 17 June ($t-5$) and 4 August ($t43$) 2012. To minimize environmental stress on enclosed organisms, CO_2 addition was performed stepwise over 3 days commencing on day $t0$. CO_2 addition was repeated on $t15$ in the upper mixed 7 m of water to compensate for outgassing. Different fCO_2 treatments were achieved by equally distributing filtered (50 µm), CO_2-saturated seawater into the treated mesocosms with a water distributor as described by Paul et al. (2015). Control mesocosms were also manipulated with the water distributor and 50 µM pre-filtered water without CO_2. CO_2 amendments resulted in ca. 0.04–0.35 % increases in the total water volume across mesocosms (Paul et al., 2015). Integrated water samples (0–17 m) were collected from each mesocosm and the surrounding seawater using depth-integrated water samplers (IWS, HYDRO-BIOS, Kiel). Samples for activity measurements were directly subsampled from the IWS on the sampling boat without headspace to maintain in situ fCO_2 levels during incubation.

Unfortunately, three mesocosms failed during the experiment as a consequence of welding faults, resulting in unquantifiable water exchanges with the surrounding waters. Therefore, with reference to the six remaining mesocosms, CO_2 concentrations defining each treatment are reported as the mean fCO_2 determined over the initial 43 days ($t1-t43$) as described in Paul et al. (2015). The control mesocosms (two replicates) had 365 and 368 µatm fCO_2. The four treatment mesocosms each had 497, 821, 1007 and 1231 µatm fCO_2. Detailed descriptions on the study site, mesocosm

deployment, system performance of the mesocosm facility throughout the experiment, CO_2 addition, carbonate chemistry, cleaning of the mesocosm bags, as well as sampling frequencies of single parameters are given in Paul et al. (2015).

2.2 Physical and chemical parameters

Temperature and salinity were measured using a CTC60M memory probe (Sea and Sun Technology GmbH, Trappenkamp, Germany) and are calculated as the mean integrated over the total depth. Photosynthetic active radiation (PAR) was measured with a PAR sensor (LI-COR LI-192) on the roof of Tvärminne Zoological Station.

Samples for dissolved inorganic carbon (DIC) and total pH were gently pressure-filtered (Sarstedt Filtropur PES, 0.2 µm pore size) using a membrane pump (Stepdos). As described in Dickson et al. (2007), total pH was determined on a Cary 100 (Varian) spectrophotometer in a temperature-controlled 10 cm cuvette using *m*-cresol indicator dye. DIC concentrations were determined by infrared absorption using a LI-COR LI-7000 on an AIRICA system (MARIANDA e.K., Kiel). Total pH and DIC were used to calculate carbonate chemistry speciation using the stoichiometric equilibrium constants for carbonic acid of Mehrbach et al. (1973) as refitted by Lueker et al. (2000).

Samples for dissolved organic carbon (DOC), total dissolved nitrogen (TDN), dissolved silica (DSi) and dissolved inorganic phosphate (DIP) were filtered through precombusted (450 °C, 6 h) GF/F filters (Whatman, nominal pore size of 0.7 µm). Concentrations of DOC and TDN were determined using a high-temperature catalytic combustion technique with a Shimadzu TOC-TN V analyser following Badr et al. (2003). DSi concentrations were determined using standard colorimetric techniques (Grasshoff et al., 1983) at the micromolar level with a nutrient autoanalyser (Seal Analytical, QuAAtro). DIP concentrations were determined with a colorimetric method using a 2 m liquid waveguide capillary cell (Patey et al., 2008) with a miniaturized detector (Ocean Optics Ltd).

Total particulate carbon (TPC), particulate organic nitrogen (PON) and total particulate phosphorus (TPP) samples were collected onto pre-combusted (450 °C, 6 h) GF/F filters (Whatman, nominal pore size of 0.7 µm) using gentle vacuum filtration and stored in glass Petri dishes at −20 °C. Biogenic silica (BSi) samples were collected on cellulose acetate filters (0.65 µm, Whatman) using gentle vacuum filtration (< 200 mbar) and stored in glass Petri dishes at −20 °C. Filters for TPC/PON analyses were dried at 60 °C, packed into tin capsules and measured on an elemental analyser (EuroEA) according to Sharp (1974), coupled by either a Conflo II to a Finnigan Delta^{Plus} isotope ratio mass spectrometer or a Conflo III to a Thermo Finnigan Delta^{Plus} XP isotope ratio mass spectrometer. Filters for TPP were treated with oxidizing decomposition reagent (MERCK, catalogue no. 112936) to oxidize organic phosphorus to orthophosphate. Particulate silica was leached from filtered material. Concentrations of dissolved inorganic phosphate as well as dissolved silica were determined spectrophotometrically according to Hansen and Koroleff (1999).

Samples for chlorophyll *a* (Chl *a*) were filtered on GF/F filters (Whatman, nominal pore size of 0.7 µm) and stored at −20 °C. Chl *a* was extracted in acetone (90 %) and samples were homogenized. After centrifugation (10 min, 800 × *g*, 4 °C) the supernatant was analysed on a fluorometer (TURNER 10-AU) to determine concentrations of Chl *a* (Welschmeyer, 1994).

Further details on the determination of physical parameters, concentration of Chl *a*, as well as dissolved and particulate nutrients can be obtained from Paul et al. (2015).

2.3 Microbial standing stock

Abundance of free-living (FL) heterotrophic prokaryotes (HP) and photoautotrophic prokaryotic (*Synechococcus* spp.) as well as eukaryotic cells (< 20 µm) were determined by flow cytometry (Crawfurd et al., 2016). Briefly, phytoplankton were discriminated based on their chlorophyll red and/or phycoerythrin orange autofluorescence (Marie et al., 1999). In combination with their side scatter signal and size fractionation, the phytoplankton community could be divided into six clusters, varying in size from 1 to 8.8 µm average cell diameter (Crawfurd et al., 2016). Three groups of picoeukaryotic phytoplankton (Pico I-III), 1 picoprokaryotic photoautotroph (*Synechococcus* spp., SYN) and 2 nanoeukaryotic phytoplankton groups (Nano I–II) were detected. Biovolume (BV) estimations were based on cell abundance and average cell diameters by assuming a spherical cell shape. The BV sum of *Synechococcus* and Pico I-III is expressed as BV_{Pico}. The BV sum of Nano I and II will be referred to as BV_{Nano}.

Abundances of FL prokaryotes were determined from 0.5 % glutaraldehyde fixed samples after staining with the nucleic acid-specific dye SYBR green I (Crawfurd et al., 2016). Unicellular cyanobacteria (*Synechococcus* spp.) contributed at maximum 10 % of total counts. Two additional groups were identified based on their low (LDNA) and high (HDNA) fluorescence. This identification was based on gating of SYBR green I fluorescence against the side scatter signal (Crawfurd et al., 2016). Particle-associated (PA) prokaryotes were enumerated by epifluorescence-microscopy on a Leica Leitz DMRB fluorescence microscope with UV- and blue light excitation filters (Leica Microsystems, Wetzlar, Germany). Fresh samples were gently mixed to prevent particle settling and a 15 mL subsample was filtered on a 0.1 % Irgalan Black coloured 5.0 µm polycarbonate filter (Whatman, Maidstone, UK; Hobbie et al., 1977). Filters were fixed with glutaraldehyde (Carl Roth, Karlsruhe, Germany; final conc. 2 %) and stained for 15 min with 4-6-diamidino-2-phenylindole (DAPI, final conc. 1 µg mL^{-1}; Porter and Feig, 1980) directly on the filtration device and rinsed twice with

sterile filtered habitat water before air-drying and embedding in Citifluor AF1 (Citifluor Ltd, London, UK) on a microscopic slide (Rieck et al., 2015). Counts were made based on 15 random unique squares as observed at a magnification of 1000×. The total number of heterotrophic PA prokaryotes was enumerated by subtracting Chl *a* autofluorescent cells from DAPI-stained cells (Rieck et al., 2015).

BV of FL and PA prokaryotes was calculated separately. For FL prokaryotes we estimated BVs on the basis of an average cell volume of 0.06 µm^3 (Hagström et al., 1979). BV of PA prokaryotes was calculated from measurements of 1600 cells across three different mesocosms (346, 868, 1333 µatm) and three time points ($t0$, $t20$, $t39$) throughout the experiment (Massana et al., 1997). A resulting average BV of 0.16 µm^3 per cell was used to calculate BV of PA prokaryotes derived from cell abundances. We subsequently adopted the term "heterotrophic bacteria", since bacteria account for the majority of non-photosynthetic prokaryotes in surface waters (Kirchman et al., 2007).

2.4 Metabolic parameters

Rates of bacterial protein production (BPP) were determined by incorporation of ^{14}[C]-leucine (^{14}C-Leu; Simon and Azam, 1989) according to Grossart et al. (2006a). Triplicates and a formalin-killed control were incubated with ^{14}C-Leu (213 mCi mmol^{-1}; Hartmann Analytic GmbH, Germany) at a final concentration of 165 nM, which ensured saturation of the uptake systems of both FL and PA bacteria. Incubation was performed in the dark at in situ temperature (between 7.8 and 15.8 °C) for 1.5 h. After fixation with 2 % formalin, samples were filtered onto 5.0 µm (PA bacteria) nitrocellulose filters (Sartorius, Germany) and extracted with ice-cold 5 % trichloroacetic acid (TCA) for 5 min. Thereafter, filters were rinsed twice with ice-cold 5 % TCA, once with ethanol (50 % v/v) and dissolved in ethyl acetate for measurement by liquid scintillation counting (Wallac 1414, Perkin Elmer). Afterwards, the collected filtrate was filtered on 0.2 µm (FL bacteria) nitrocellulose filters (Sartorius, Germany) and processed in the same way as the 5.0 µm filters. Standard deviation of triplicate measurements was usually < 15 %. The amount of incorporated ^{14}C-Leu was converted into BPP by using an intracellular isotope dilution factor of 2. A conversion factor of 0.86 was used to convert the produced protein into carbon (Simon and Azam, 1989). Cell-specific BPP rates (csBPP) were calculated by dividing BPP rates by abundances of FL prokaryotes and PA HP.

Community respiration (CR) rates were calculated from oxygen consumption during an incubation period of 48 h at in situ temperature in the dark by assuming a respiratory quotient of 1 (Berggren et al., 2012). Thereby, oxygen concentrations were measured in triplicate in 120 mL O_2 bottles without headspace, using a fiber optical dipping probe (PreSens, Fibox 3), which was calibrated against anoxic and air saturated water.

Primary production (PP) was measured using radiolabelled $NaH^{14}CO_3$ (Steeman-Nielsen, 1952) in 0–10 m depth-integrated samples. After incubation of duplicate samples with 10 µL of ^{14}C bicarbonate solution (DHI Lab, 20 µCi mL^{-1}) in 8 mL vials at 2, 4, 6, 8 and 10 m for 24 h, samples were acidified with 1 M HCl to remove remaining inorganic ^{14}C. Radioactivity was determined by using a scintillation counter (Wallac 1414, Perkin Elmer). PP was calculated knowing the dark-control corrected ^{14}C incorporation and the fraction of the ^{14}C addition to the total inorganic carbon pool according to Gargas (1975). Further details on the measurement of CR and PP are given by Spilling et al. (2016a).

2.5 Statistical analyses

Permutational multivariate analysis of variance – PERMANOVA (Anderson, 2001) was used to determine associations between physical/chemical variables and biotic variables. PERMANOVA (perm = 9999) was performed to test for significant differences in variance over time and between fCO_2-treated mesocosms (Anderson et al., 2008). Environmental data were normalized according to Clarke and Gorley (2006). Biotic abundance data were $\log(x+1)$ transformed (Clarke and Gorley, 2006). PERMANOVA partitions the total sum of squares based on the experimental design and calculates a distance-based pseudo-F statistic for each term in the model. Distance-based linear modelling (DistLM) was implemented to relate physical/chemical predictor variables and the multivariate assemblage of biotic variables (Supplement Table S1; Legendre and Anderson, 1999; Anderson et al., 2008). The DistLM routine was based on the AIC model selection criterion (see Anderson et al., 2008) using a stepwise selection procedure. In case of equally AIC-ranked models (difference < 1), a model with fewer parameters was preferred. A Principal Component Analysis (PCA) was performed on normalized chemical data to identify chemical gradients and patterns between the differently fCO_2-treated mesocosms over time (Clarke and Gorley, 2006). Distance-based redundancy analysis (dbRDA) was used for visual interpretation of the DistLM in multidimensional space (Anderson et al., 2008). Multivariate analyses of physicochemical, metabolic and community data were performed on a reduced data set comprising 10 time points ($t5 - t29$, every 3 days; $t31$), containing all measured activity variables (BPP, areal PP and CR). Missing values of nutrient data or abundance data (based on every-other-day measurements) were estimated as means of the preceding and following measurement day. In general, no activity data were interpolated or extrapolated.

Cluster analyses were performed based on Spearman's rank correlation coefficient calculated for each mesocosm between all possible combinations of LDNA, HDNA, pico- and nanophytoplankton abundances as well as total Chl *a*. Thereafter, p values were corrected for multiple testing ac-

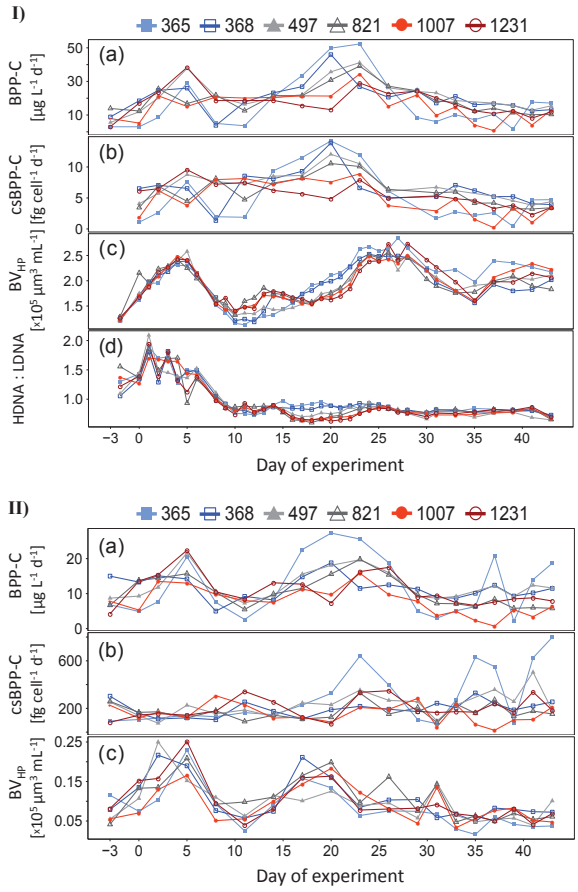

Figure 1. I: Free-living (0.2–5.0 µm) and II: particle-associated (> 5.0 µm), size-fractionated rates of **(a)** bacterial protein production (BPP) [µg C L^{-1} d^{-1}] as well as **(b)** cell-specific bacterial protein production (csBPP) [fg C $cell^{-1}$ d^{-1}] and **(c)** heterotrophic prokaryotic biovolume (BV_{HP}) [$\times 10^5$ µm^3 mL^{-1}] during the course of the experiment. I: **(d)** Ratio of high vs. low nucleic acid-stained prokaryotic heterotrophs (HDNA : LDNA). Colours and symbols indicate average fCO_2 [µatm] between $t1 - t43$.

cording to Benjamini and Hochberg (1995). The R package pvclust was used to assess the uncertainty in hierarchical cluster analysis (Suzuki and Shimodeira, 2015). For each cluster, AU (approximately unbiased) p values (between 0 and 1) were calculated via multiscale bootstrap resampling (Suzuki and Shimodaira, 2015).

PERMANOVA, distLM and dbRDA were carried out using Primer 6.0 and PERMANOVA + for PRIMER software (Clarke and Gorley, 2006; Anderson et al., 2008). All other analyses and the visualization of results were performed with R 3.2.5 (R Core Team, 2016) using packages Hmisc (Harrell et al., 2016), vegan (Oksanen et al., 2016), pvclust (Suzuki and Shimodeira, 2015), gplots (Warnes et al., 2016) and ggplot2 (Wickham, 2009).

3 Results

3.1 Bacterial dynamics

Heterotrophic bacterial BV was predominantly comprised of FL bacteria. PA bacteria contributed at maximum 2 ± 0.7–10 ± 0.7 % (mean 4.8 ± 0.6 %) of total bacterial BV. PA bacteria, however, accounted for a substantial fraction of overall BPP (27 ± 1–59 ± 7 %, mean 39 ± 4 %). There was no significant effect of fCO_2 on BPP, csBPP or BV of neither FL nor PA heterotrophic bacteria ($p_{perm} > 0.05$); however, a significant temporal effect was observed ($p_{perm} < 0.05$). Both bacterial size-fractions had distinct dynamics in abundance, BPP and csBPP during the course of the experiment (Fig. 1). BPP and bacterial abundances were closely related to Chl a and BV of nano- and picophytoplankton, trending along with Chl a until $t10$ and then continuing to increase with BVs of nano- and photoautotrophs and Chl a. The period between $t16$ and $t26$, following a sharp decrease in Chl a at $t16$, revealed the highest BPP rates across the experiment with lower rates at higher fCO_2 for PA as well as FL bacteria. CsBPP rates were lower at elevated fCO_2 for only the FL bacteria during this period. Additionally, BVs of FL and PA bacteria revealed contrasting dynamics (Figs. 1, S1 in the Supplement). PA bacterial BVs declined with the decay of Chl a, whereas FL bacterial BVs increased strongly associated with an increase in BV of picophotoautotrophs during this period. The ratio of HDNA : LDNA prokaryotes, which both make up FL bacteria, also showed differences between the experimental treatments. Between $t14 - t25$ the ratio of HDNA : LDNA was lower at higher fCO_2.

3.2 Phytoplankton dynamics

Chl a concentration exhibited distinct maxima at two time periods ($t5$ and $t16$). The second maximum was associated with an increase in the BV of nanophotoautotrophs (BV_{Nano}, Fig. 2). This increase was reduced in mesocosms containing higher levels of fCO_2 between $t13 - t17$. The differences in BV_{Nano} between the treatments were reflected in lower concentrations of Chl a in the three highest fCO_2-treated mesocosm at $t16$. Chl a and BV_{Nano} concentrations declined after $t16$. In contrast, BV of picophotoautotrophs (BV_{Pico}) increased after $t11$, associated with an increase in BV of *Synechococcus* spp., which accounted for 31 ± 2 to 59 ± 2 % of BV_{Pico} across the period of this study (Fig. S2). All four groups of picoautotrophs distinguished by flow cytometry, exhibited time-dependent positive or negative relationships with fCO_2 (Figs. 3, S2, S3). The Pico I (~ 1 µm) and Pico II taxa infrequently exhibited strong fertilization effects in response to the fCO_2 treatment. In contrast, *Synechococcus*

Table 1. Results of two-factor permutational multivariate analysis of variance (PERMANOVA)[a] on a resemblance matrix (Euclidian distance) of normalized chemical variables (Phosphate, DOC, TDN, DSi, TPC, PON, POP, BSi). Degrees of freedom (df); sum of squares (SS); mean square (MS).

Source of variation	df	SS	MS	Pseudo-F	p (perm)	Unique perms
Time	9	309.93	34.436	11.118	0.0001	9920
$f\mathrm{CO_2}$[b]	4	31.974	7.9936	2.5808	0.0246	9936
Time x $f\mathrm{CO_2}$	36	80.177	2.2271	0.71906	0.8794	9904
Residuals	10	30.973	3.0973			
Total	59	472				

[a] Permutation was performed with unrestricted permutation of raw data. [b] Pairwise test could only be performed for control mesocosms ($n = 2$) with each $f\mathrm{CO_2}$ treatment ($n = 1$), due to missing replication for each $f\mathrm{CO_2}$ treatment. Pairwise comparison was only significant between controls and the highest $f\mathrm{CO_2}$ treatment ($p_{\mathrm{perm}} = 0.029$).

Table 2. Eigenvectors and explained variation of the first four axes of a PCA on normalized variables of dissolved and particulate nutrients. Ordination of the PCA is visualized in Fig. 6.

	Variable	PC1	PC2	PC3	PC4
	DOC	−0.4	−0.23	0.04	0.68
	TDN	0.39	0.21	0.21	0.47
	Phosphate	−0.1	0.48	−0.74	0.35
	DSi	0.3	0.52	−0.03	−0.24
	TPC	0.48	−0.06	0.03	0.13
	PON	0.46	−0.05	−0.05	0.16
	POP	0.36	−0.39	−0.04	0.21
	BSi	0.17	−0.51	−0.63	−0.22
% variation		49.2	19.7	11.4	7.2
cum. % variation		49.2	68.9	80.4	87.6

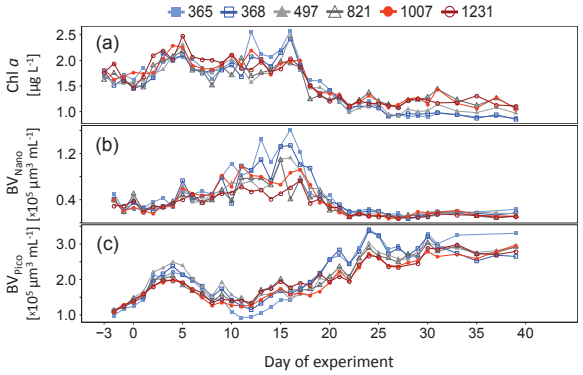

Figure 2. **(a)** Concentration of chlorophyll a [µg $\mathrm{L^{-1}}$], **(b)** biovolume of nanophytoplankton (Nano I and Nano II) [$\times 10^5$ µm^3 $\mathrm{mL^{-1}}$] and **(c)** biovolume of picophytoplankton (*Synechococcus* spp., Pico I-III) [$\times 10^5$ µm^3 $\mathrm{mL^{-1}}$] during the course of the experiment. Colours and symbols indicate average $f\mathrm{CO_2}$ [µatm] between $t1$ and $t43$.

spp. and Pico III were infrequently negatively affected by the $f\mathrm{CO_2}$ treatment.

3.3 Relation between functional heterotrophic and autotrophic groups

A cluster analysis of pairwise Spearman correlations between functional bacterial and phytoplankton groups revealed a separation based on $f\mathrm{CO_2}$ treatment. Specifically the four $\mathrm{CO_2}$-amended mesocosms were readily distinguishable from the control treatments. Multiple bootstrap resampling (Suzuki and Shimodaira, 2015) supported this, but only significantly for the three highest $f\mathrm{CO_2}$-treated mesocosms. The two highest $f\mathrm{CO_2}$ treatments revealed a positive correlation between LDNA bacteria and Pico I, which could not be observed in any other experimental treatment. In all $\mathrm{CO_2}$-treated mesocosms we observed positive correlations between *Synechococcus* spp. and Pico III as well as *Synechococcus* spp. and Pico I, which were not present in both control mesocosms. In contrast, positive correlations between LDNA and HDNA were not detected in any $f\mathrm{CO_2}$ treatment. Additionally, positive correlations between Pico I and Nano II as well as HDNA and Cyanobacteria were only present in both controls and the lowest $f\mathrm{CO_2}$ treatment (Fig. 4).

After $t10$, the ratio between heterotrophic prokaryotic BV and Chl a varied between the $f\mathrm{CO_2}$ treatments, but did not show a consistent pattern. After $t17$, however, the control mesocosms revealed a higher ratio compared to all $f\mathrm{CO_2}$-treated mesocosms (Fig. 5).

3.4 Multivariate physicochemical characterization

Integrated water temperature and PAR ranged between 8.0–15.9 °C and 11.2–66.8 mol $\mathrm{m^{-2}}$ $\mathrm{day^{-1}}$ during the experiment respectively. Integrated water temperature reached the maximum at $t15$ and dropped again to 8.2 °C at $t31$.

PERMANOVA results (Table 1) on a multivariate assemblage of dissolved (DOC, TDN, Phosphate, BSi) and particulate (TPC, PON, POP, BSi) nutrients showed significant temporal (Time-$F_{9,10} = 11.1$, $p = 0.0001$) and spa-

Table 3. Results of two-factor permutational multivariate analysis of variance (PERMANOVA)[a] on a resemblance matrix (Euclidian distance) based on normalized metabolic variables (bacterial protein production (BPP), areal primary production (PP) and community respiration (CR)). Degrees of freedom (df); sum of squares (SS); mean square (MS).

Source of variation	df	SS	MS	Pseudo-F	p (perm)	Unique perms
Time	9	92.128	10.236	6.73	0.001	9931
$f\mathrm{CO}_2$[b]	4	16.044	4.011	2.637	0.023	9944
Time x $f\mathrm{CO}_2$	36	42.721	1.1867	0.78018	0.792	9904
Residuals	10	15.21	1.521			
Total	59	182.46				

[a] Permutation was performed with unrestricted permutation of raw data. [b] Pairwise test could only be performed for control mesocosms ($n = 2$) with each $f\mathrm{CO}_2$ treatment ($n = 1$), due to missing replication for each $f\mathrm{CO}_2$ treatment. Pairwise comparisons were significant between control and all $f\mathrm{CO}_2$ treatments ($p_{\mathrm{perm}} < 0.04$).

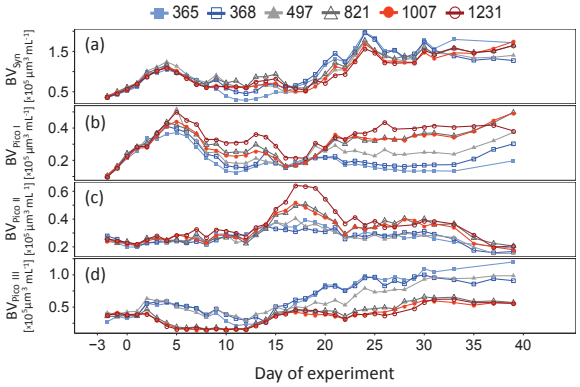

Figure 3. (a) Biovolume of *Synechococcus* spp. [$\times 10^5$ µm^3 mL^{-1}] and **(b–d)** biovolume of picoeukaryote groups I–III (Pico I-III) [$\times 10^5$ µm^3 mL^{-1}] during the course of the experiment. Colours and symbols indicate average $f\mathrm{CO}_2$ [µatm] between $t1$ and $t43$.

tial variations along the $f\mathrm{CO}_2$ gradient ($f\mathrm{CO}_2$-$F_{4,10} = 2.6$, $p = 0.02$). PCA ordination of the same chemical dataset strongly reflects the temporal pattern, separating the initial time points before $t11$ from other time points of the experiment along the first PCA axis (Fig. 6). Thereby, eigenvectors of TPC and PON were highest on PCA axis 1 (Table 2). PCA axis two was mainly characterized by high eigenvectors of dissolved phosphate as well as dissolved and particulate silica. The first two PCA axes explained 69 % of variation, and cumulatively 80 % including axis three (Table 2).

3.5 Multivariate characterization of metabolic parameters

PERMANOVA on the resemblance matrix of normalized metabolic variables (BPP, areal PP, CR) revealed significant temporal (Time-$F_{9,10} = 6.7$, $p = 0.0002$) and spatial variations along the $f\mathrm{CO}_2$-gradient ($f\mathrm{CO}_2$-$F_{4,10} = 2.64$, $p < 0.03$) (Table 3). DistLM identified significant effects of temperature ($p < 0.03$), phosphate ($p < 0.02$), DOC

Table 4. Summary of a DistLM procedure for modelling the relationship between physicochemical variables and a resemblance matrix based on a multivariate assemblage comprising normalized data of bacterial protein production (BPP), areal primary production (PP) and community respiration (CR). Redundant physicochemical variables were removed prior to analysis. Therefore, PON and pH were excluded from the subsequent analysis due to high correlations ($r_s > 0.9$) to TPC and $f\mathrm{CO}_2$ respectively.

Variable	SS (trace)	Pseudo-F	p	Prop.
$f\mathrm{CO}_2$	5.0551	1.6527	0.1759	0.03
Temp*	10.209	3.4376	0.0229	0.055
PAR*	6.2466	2.056	0.1067	0.034
DOC*	8.6228	2.8769	0.0474	0.047
TDN	4.7628	1.5545	0.1984	0.026
Phosphate*	12.319	4.1994	0.0111	0.068
DSi	0.26167	0.083	0.9648	0.001
TPC	7.7827	2.5842	0.0613	0.004
POP	5.0171	1.6399	0.1818	0.027
BSi	11.688	3.9696	0.0111	0.064

* Variables selected in stepwise procedure based on AIC.

($p < 0.05$) and BSi ($p < 0.02$) on the multivariate assemblage of metabolic variables (Table 4). The stepwise procedure selects PAR, temperature, DOC and phosphate as determining factors (AIC = 59.6, $R^2 = 0.26$, number of variables = 4). The dbRDA ordination separates the temporal development. Thereby, 92 % of the variability in the fitted model and 24 % of the total variation is explained by the first two dbRDA axes (Fig. 6).

3.6 Multivariate characterization of the bacterioplankton and phytoplankton community

PERMANOVA on the resemblance matrix of a multivariate assemblage comprising variables of bacterial and phytoplankton communities (abundances of Pico I-III, Nano I-II, FL bacteria (HDNA, LDNA), PA bacteria, *Synechococcus* spp. and Chl *a*) revealed significant tempo-

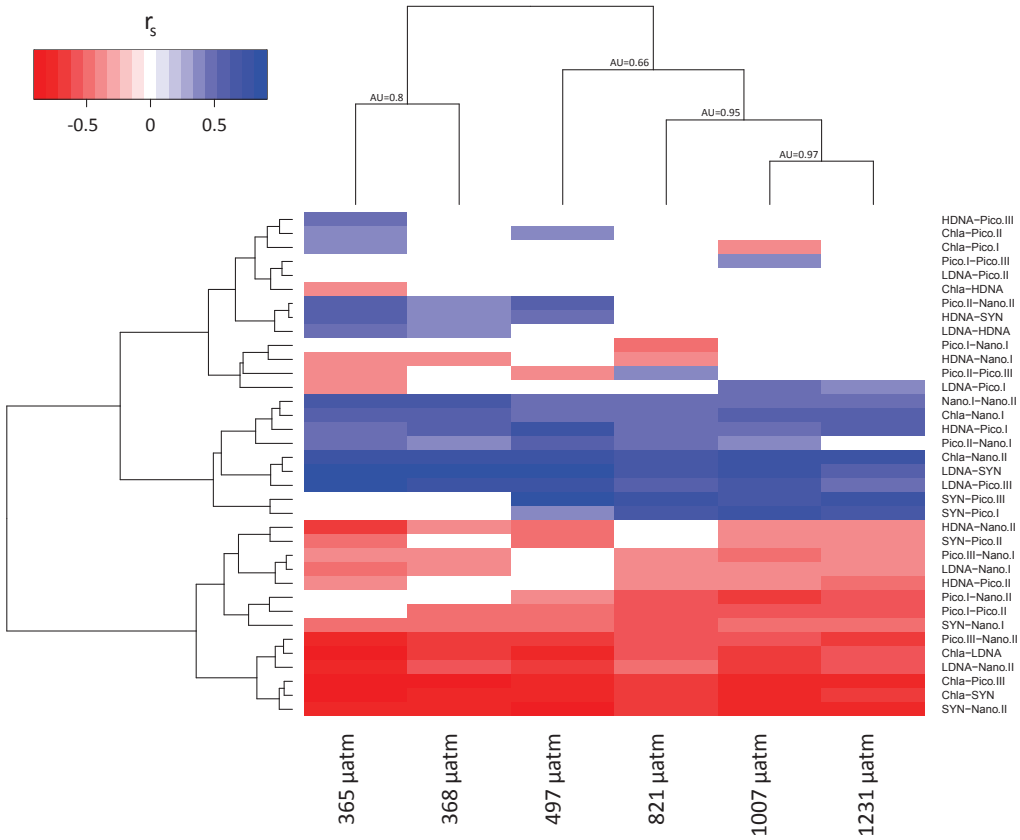

Figure 4. Heatmap and cluster analysis based on significant Spearman's rank correlation coefficients calculated for each mesocosm between all possible combinations of abundances between different functional heterotrophic prokaryotic and phytoplanktonic groups (high and low nucleic acid-stained prokaryotic heterotrophs (HDNA : LDNA), *Synechococcus* spp. (SYN), picoeukaryotes I-III (Pico I-III), nanophytoplankton I-II (Nano I-II)) and Chl *a* based on daily measurements between $t1$ and $t39$. Colours indicate the Spearman'r rank coefficient (r_S) between two variables. P values of correlations were corrected for multiple testing according to Benjamini and Hochberg (1995). Uncertainty in hierarchical clustering was assessed with multiscale bootstrap resampling using approximately unbiased (AU) p values (between 0 and 1; Suzuki and Shimodeira, 2015). Clusters of the three highest fCO_2 treatments are significantly different at the 0.05 level. Numbers indicate the fCO_2 treatment with average fCO_2 [µatm] between $t1$ and $t43$.

ral (Time-$F_{9,10} = 56.8$, $p = 0.0001$) and spatial variations along the fCO_2-gradient (fCO_2-$F_{4,10} = 14.9$, $p = 0.0001$) (Table 5). DistLM identified significant effects of fCO_2 ($p < 0.02$), temperature ($p < 0.001$), phosphate ($p < 0.003$), TPC ($p < 0.001$), BSi ($p < 0.001$) and POP ($p < 0.001$) on the multivariate assemblage of bacterial and phytoplankton communities (Table 6). The stepwise procedure selects fCO_2, temperature, TPC and phosphate as determining factors (AIC= 67.2; $R^2 = 0.44$; number of variables = 4). The dbRDA reveals a separation along the gradient of fCO_2 on the second dbRDA axis. The first dbRDA axis represents the overall temporal development. Thereby, the first two dbRDA axes capture 74 % of the variability in the fitted model and 32 % of the total variation.

4 Discussion

Although OA and its ecological consequences have received growing recognition during the last decade (Riebesell and Gattuso, 2015), surprisingly little is known about the ecological effects on heterotrophic bacterial biomass or the production and coupling of bacterio- and phytoplankton at nutrient-limited conditions. Previous experiments were, for the most part, conducted during productive phases of the year (e.g. phytoplankton blooms), under eutrophic conditions (e.g. coastal areas) or with nutrient additions (e.g. Grossart et al., 2006a; Allgaier et al., 2008; Brussaard et al., 2013; Bach et al., 2016). However, large parts of the oceans are nutrient limited or experience extended nutrient-limited periods during the year (Moore et al., 2013). Thus, we conducted our

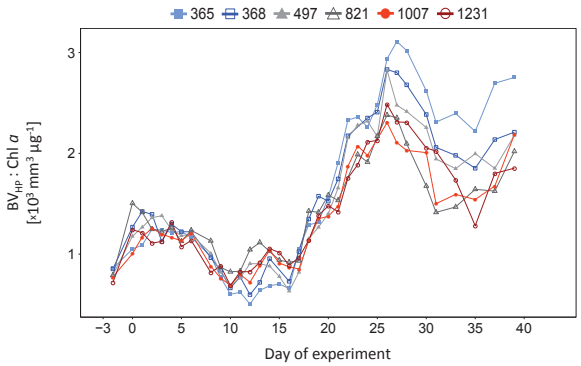

Figure 5. Ratio of heterotrophic prokaryotic biovolume and Chl *a* (BV_{HP} : Chl *a*) during the course of the experiment. PA BV_{HP} was interpolated using splines with software R (R Core Team, 2016) for time-points, where no data were available. Colours and symbols indicate average fCO_2 [µatm] between $t1$ and $t43$.

experiment in July–August, when nutrients and phytoplankton production were relatively low in the northeastern Baltic Sea (Hoikkala et al., 2009; Lignell et al., 2008), and exposed a natural plankton community to different levels of CO_2.

4.1 Phytoplankton–bacterioplankton coupling at low nutrient conditions

Heterotrophic bacteria are important recyclers of autochthonous DOM in aquatic systems and play an important role in nutrient remineralization in natural plankton assemblages (Kirchman, 1994). BV and production of heterotrophic bacteria are highly dependent on quantity and quality of phytoplankton-derived organic carbon and are usually tightly related to phytoplankton development (e.g. Grossart et al., 2006b; Allgaier et al., 2008). During this study, low nitrogen availability limited overall autotrophic production (Paul et al., 2015; Nausch et al., 2016). This resulted in a post spring bloom phytoplankton community, dominated by picophytoplankton (Paul et al., 2015). This is consistent with previous reports of picophytoplankton accounting for a large fraction of total phytoplankton biomass in oligotrophic, nutrient-poor systems (e.g. Agawin et al., 2000). Chl *a* dynamics indicated two minor blooms of larger phytoplankton during the first half of the experiment, although picophytoplankton still accounted for mostly > 50 % of the total Chl *a* during this period (Paul et al., 2015; Spilling et al., 2016b). The phytoplankton development was also reflected in the PCA ordination of dissolved and particulate nutrients, clearly separating the preceding period before $t11$, including the first peak of Chl *a*, from the other observations during the experiment (Fig. 6). The separation was primarily driven by concentrations of particulate matter (Table 2), which decreased until $t11$ and subsequently sank out of the water column (Paul et al., 2015).

Bacterial BV and BPP paralleled phytoplankton development during this period. With the decay of the initial phytoplankton bloom, a second bloom event resulted, comprised primarily of nanophytoplankton and picophytoplankton (Crawfurd et al., 2016). A decrease in nanophytoplankton BV and Chl *a* concentrations after $t16/t17$ benefitted both FL heterotrophic bacteria and picophotoautotrophs. The increased availability of DOM, resulting from cell lysis and remineralization of POM, was associated with increases in the BV of both groups and bacterial production levels (Figs. 1, S1). We attributed these increases to the cells of Picoplankton, which, due to their high volume-to-surface ratio as well as a small boundary layer surrounding these cells, are generally favoured compared to larger cells in terms of resource acquisition at low nutrient conditions (Raven, 1998; Moore et al., 2013). If cell size is the major factor determining the access to dissolved nitrogen and phosphorous, bacteria should be able to compete equally or better with picophytoplankton at low concentrations (Suttle et al., 1990; Drakare et al., 2003). However, when phytoplankton is restricted in growth due to the lack of mineral nutrients, a strong commensalistic relationship between phytoplanktonic DOM production and bacterioplanktonic DOM utilization may evolve (Azam et al., 1983; Bratbak and Thingstad, 1985; Joint et al., 2002). Although heterotrophic microbes may indirectly limit primary production by depriving phytoplankton of nutrients, they would not be able to outcompete autotrophs completely since this would remove their source of substrates for carbon and energy (Bratbak and Thingstad, 1985; Joint et al., 2002). Such a relationship might explain the paralleled increase in FL bacterial and picophytoplankton BV.

PA bacteria are typically impacted to a lesser extent by nutrient limitation due to consistently higher nutrient availability at particle surfaces (e.g. Grossart and Simon, 1993). This was reflected in this study by the maintenance of high csBPP rates associated with PA heterotrophic bacteria throughout the experiment. Overall, PA bacteria contributed only a minor fraction (at maximum 10 ± 0.7 %) to the overall bacterial BV, which is typical for oligotrophic or mesotrophic ecosystems (Lapoussière et al., 2011). Nevertheless, their substantial contribution to overall BPP emphasizes their importance, especially during such low productive periods (e.g. Grossart, 2010). PA heterotrophic bacteria are essential for the remineralization of nutrients from autotrophic biomass, which would otherwise sink down from surface waters (Grossart, 2010). Leakage of hydrolysis products and the attachment and detachment of bacteria to and from particles stimulate production amongst free-living bacteria (Smith et al., 1992; Grossart, 2010) and picophytoplankton.

Table 5. Results of two-factor permutational multivariate analysis of variance (PERMANOVA)[a] on a resemblance matrix (Bray–Curtis similarity coefficient) based on $\log(X+1)$ transformed abundances of Pico I-III, Nano I-II, FL bacteria (HDNA, LDNA), PA bacteria, SYN and Chl *a*. Degrees of freedom (d*f*); sum of squares (SS); mean square (MS).

Source of variation	d*f*	SS	MS	Pseudo-*F*	*p* (perm)	Unique perms
Time	9	201.83	22.426	56.754	0.0001	9923
fCO_2[b]	4	23.631	5.9077	14.951	0.0001	9940
Time *x* fCO_2	36	19.859	0.55164	1.396	0.151	9915
Residuals	10	3.9515	0.39515			
Total	59	271.01				

[a] Permutation was performed with unrestricted permutation of raw data. [b] Pairwise test could only be performed for control mesocosms ($n=2$) with each fCO_2 treatment ($n=1$), due to missing replication for each fCO_2 treatment. Pairwise comparisons were significant between control and all fCO_2 treatments ($p_{perm}<0.01$).

Table 6. Summary of a DistLM procedure for modelling the relationship between physicochemical variables and a multivariate assemblage, comprising variables of the bacterial and phytoplankton community. The resemblance matrix (Bray–Curtis similarity coefficient) was based on $\log(X+1)$ transformed abundances of Pico I-III, Nano I-II, FL bacteria (HDNA, LDNA), PA bacteria, *Synechococcus* spp. and Chl *a*. Redundant physicochemical variables were removed prior analysis. Therefore, PON and pH were excluded from the subsequent analysis due to high correlations ($r_s>0.9$) to TPC and fCO_2 respectively.

Variable	SS (trace)	Pseudo-*F*	*p*	Prop.
fCO_2*	20.469	4.7386	0.0119	0.075
Temp*	51.838	13.718	0.0001	0.191
PAR	10.791	2.4051	0.0813	0.039
DOC	11.14	2.4864	0.0769	0.041
TDN	9.4456	2.0945	0.1078	0.034
Phosphate*	25.649	6.063	0.0029	0.095
DSi	9.5766	2.1246	0.103	0.035
TPC*	36.038	8.8955	0.0002	0.133
POP	52.171	13.827	0.0001	0.193
BSi	36.439	9.01	0.0005	0.134

* Variables selected in stepwise procedure based on AIC.

4.2 Effects of fCO_2/pH on phytoplankton–bacterioplankton coupling at low nutrient conditions

The response of heterotrophic bacteria to changes in fCO_2 has been previously shown to be related to phytoplankton rather than being a direct effect of pH or CO_2 (e.g. Allgaier et al., 2008; Grossart et al., 2006a). Here, neither BPP nor BV of neither FL nor PA bacteria suggested a direct effect of CO_2 on these variables (PERMANOVA). Differences in FL bacterial BV, BPP and the ratio of HDNA : LDNA occurred along the gradient of fCO_2, but were limited to short time periods. Furthermore, these changes were not consistent with fCO_2, resulting in both increases and decreases of a particular variable at specific times (Fig. 1). Periods where fCO_2-related effects were apparent comprised periods with high organic matter turnover (e.g. breakdown of Chl *a* maximum). However, Paul et al. (2015) could not reveal any effect of fCO_2 on the export of carbon, neither across the study period nor at individual time points. Thus, it is reasonable to assume that these small fCO_2-related differences in bacterial variables are a consequence of other altered components of the aquatic food web, and do not necessarily manifest as changes in carbon export.

Given the inability to relate individual aspects of microbial metabolism or community composition to fCO_2 concentrations, we sought to determine whether an impact was evident using a multivariate approach. Chemical, metabolic and community matrices exhibited large variations in relation to a strong temporal effect throughout the whole sampling period ($p<0.01$; Tables 1, 3, 5). In addition, an effect of the fCO_2 treatment was also evident in all three multivariate assemblages, albeit explaining far less of the observed variability in chemical and metabolic variables ($p<0.03$; Tables 1, 3, 5). However, when relating physicochemical to metabolic variables (DistLM, Table 4), neither fCO_2 nor pH were suitable to explaining the observed variability. In contrast, fCO_2 contributed to explaining the variability amongst the bacterioplankton–phytoplankton community dynamics (DistLM, Table 6). Taken together, this suggests that effects of fCO_2 treatments manifest indirectly, through either altering physicochemical parameters or more likely the composition of the microbial community with possible but so far hidden consequences for microbial metabolism.

4.3 fCO_2/pH effects on phytoplankton indirectly alter phytoplankton–bacterioplankton coupling at low-nutrient conditions

Autotrophic organisms can be fertilized by an enhanced CO_2 availability, altering growth conditions of phytoplankton and increasing the production of particulate (POM) and dissolved organic matter (DOM; Hein and Sand-Jensen, 1997; Riebesell et al., 2007). As a consequence of this increased photosynthetic fixation rate, both quantity and quality of dis-

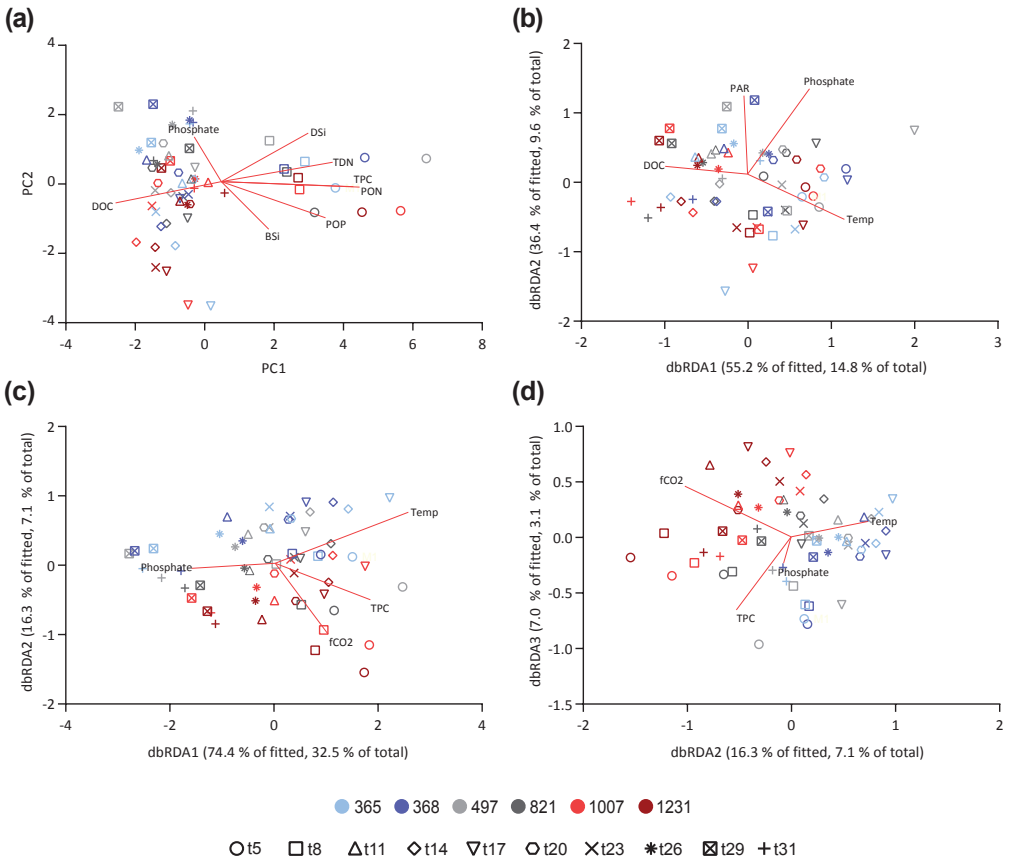

Figure 6. (a) First and second axis of a principal component analysis (PCA) calculated on normalized variables of dissolved and particulate nutrients ($n = 60$). The set of variables and the eigenvectors of the first four axes can be derived from Table 2. **(b)** Ordination of a distance-based redundancy analysis (dbRDA) for visual interpretation of distance-based linear modelling (DistLM) between physical/chemical predictor variables and metabolic variables as well as **(c–d)** abundances of functional bacterial and phytoplankton groups. A table comprising the set of variables used for DistLM can be derived from the Supplement (Table S1).

solved organic matter (DOM) available for heterotrophic bacteria are impacted, with potential implications for the nature of coupling between phytoplankton and bacterioplankton at low-nutrient conditions (Azam et al., 1983; Bratbak and Thingstad, 1985). So far, CO_2 enrichment experiments examining natural plankton assemblages (e.g. Engel et al., 2005; Riebesell et al., 2007; Bach et al., 2016) have not revealed a consistent pattern of species response or primary production to elevated CO_2. During this experiment, Spilling et al. (2016a) could not detect any effect of increased CO_2 on total primary production, even though Crawfurd et al. (2016) reported effects of CO_2 on several groups of picophytoplankton. Although one larger picoeukaryote (Pico III) was negatively impacted by fCO_2 during our study, two small picoeukaryotes (Pico I, Pico II) benefitted from the CO_2 addition, yielding significantly higher growth rates and BVs at higher fCO_2 (Crawfurd et al., 2016). This is consistent with recent evidence suggesting a positive impact of enhanced fCO_2 on the abundance of small picoeukaryotic phytoplankton (Brussaard et al., 2013; Newbold et al., 2012; Sala et al., 2015). Both picoeukaryotic groups were identified as variables explaining the separation along the fCO_2 gradient on the second and third dbRDA axes in the DistLM ordination of the bacteria–phytoplankton community. Specifically, Pico I was highly negatively correlated ($r_s = -0.67$) to dbRDA axis two. However, dbRDA also indicated opposing effects of fCO_2 on Pico II ($r_s = 0.54$) and HDNA prokaryotes ($r_s = -0.31$), being positively or negatively correlated with axis three. Indeed, sharp increases in $BV_{Pico\,II}$ at high fCO_2 between $t14$ and $t17$ were associated with decreases in BV_{HDNA}.

Although we are not able to draw solid conclusions on the interaction of these two particular groups of organisms, a cluster analysis of pairwise Spearman correlations between

functional groups of bacteria and phytoplankton revealed a distinct clustering with mesocosms based on fCO_2 levels (Fig. 4). We also detected a change in the ratio of heterotrophic bacterial BV to Chl *a* between the different fCO_2 treatments, though this change was not visible for the entire study duration and not consistent with fCO_2. These results strongly suggest that trophic interactions between functional groups of bacteria and phytoplankton might be changing in a future acidified ocean.

In nutrient-poor systems, variable growth rates of phytoplankton, DOM quality and quantity, and also loss of phyto- and bacterioplankton due to grazing or viral lysis may potentially contribute to this observed decoupling of phytoplankton and bacterioplankton at high fCO_2 (Azam et al., 1983; Bratbak and Thingstad, 1985; Sheik et al., 2014). The viral shunt or bacterivory may release phytoplankton from competition with bacteria for limited nutrients (e.g. Bratbak and Thingstad, 1985; Caron and Goldman, 1990). How increased fCO_2 will affect these processes (e.g. viral lysis and bacterial grazing) under nutrient-limited conditions remains uncertain so far. Bacterial grazing by mixotrophs, which would also directly benefit from increased CO_2 availability (Rose et al., 2009), may provide a mechanism for recycling of inorganic nutrients, otherwise bound in bacterial biomass, as a means for supporting phytoplankton growth (e.g. Mitra et al., 2014). However, other studies examining bacterial grazing under different nutrient conditions reported conflicting positive and negative results of increased fCO_2 (e.g. Brussaard et al., 2013; Rose et al., 2009). Although we are unable to draw defined conclusions on how this myriad of complex biological processes are impacted by fCO_2, it is very likely that there is an impact on trophic interactions which may account for the portion of unexplained variance we observed in our multivariate analyses.

5 Conclusions

The use of large-volume mesocosms allowed us to test for multiple fCO_2-related effects on dynamics of heterotrophic bacterial activity and their biovolume in a near-realistic ecosystem by including trophic interactions from microorganisms up to zooplankton. Complex interactions between various trophic levels, which can only be properly addressed at the scale of whole ecosystems, are important for understanding and predicting fCO_2-induced effects on aquatic food webs and biogeochemistry in a future, acidified ocean. We examined these impacts in a nutrient-depleted system, which is representative for large parts of the oceans (Moore et al., 2013). Heterotrophic bacterial productivity was, for the most part, tightly coupled to the availability of phytoplankton-derived organic matter. When accounting for temporal development and taking into account trophic interactions using multivariate statistics, changes in nutrient composition, metabolic parameters and bacteria–phytoplankton communities revealed a significant effect of the fCO_2 treatment. Although not consistent throughout the experiment, differences in the ratio of heterotrophic bacterial BV to Chl *a* during the last half of the experiment suggest that a future ocean will become more autotrophic during low productive periods as a result of altered trophic interactions between functional groups of bacteria and phytoplankton. There is additional support for this conclusion from examining the atmospheric exchange of CO_2 (Spilling et al., 2016b). During the limited timescale of this study, the observed effects of fCO_2 did not manifest as altered carbon export (Paul et al., 2015). However, over several years, maintained changes in nutrient cycling, as a consequence of a permanent decoupling between bacteria and phytoplankton, are likely to arise and impact the nature of the carbon pump.

6 Data availability

Data of primary production and respiration can be obtained from Spilling et al. (2016c). Other variables from the experiment (e.g. total particulate and dissolved nutrients) can be found in Paul et al. (2016). Flow cytometry data can be obtained from Crawfurd et al. (2016). Bacterial protein production rates and abundances of particle-associated bacteria can be obtained from Hornick et al. (2016).

The Supplement related to this article is available online at doi:10.5194/bg-14-1-2017-supplement.

Acknowledgements. We thank the KOSMOS team and all of the participants in the mesocosm campaign for organization, maintenance and support during the experiment. In particular, we would like to thank Andrea Ludwig for coordinating the campaign logistics and assistance with CTD operations, the diving team and Allanah Paul for her help in data acquisition. Furthermore, we thank the Tvärminne Zoological Station for the opportunity to carry out such a big mesocosm experiment at their research station and for technical support on site. Additionally, we acknowledge the captain and crew of R/V *ALKOR* for their work transporting, deploying (AL394) and recovering (AL397) the mesocosms. We also thank the two reviewers for their comments to improve this article. The collaborative mesocosm campaign was funded by BMBF projects BIOACID II (FKZ 03F06550) and SOPRAN Phase II (FKZ 03F0611). Thomas Hornick was further financially supported by DFG grant GR 1540/23-1, given to Hans-Peter Grossart. Corina P. D. Brussaard was financially supported by the Darwin project, the Royal Netherlands Institute for Sea Research (NIOZ) and the EU project MESOAQUA (grant agreement number 228224).

Edited by: J. Engström-Öst
Reviewed by: L. Rhodes and one anonymous referee

References

Agawin, N. S. R., Duarte, C. M., and Agusti, S.: Nutrient and temperature control of the contribution of picoplankton to phytoplankton biomass and production, Limnol. Oceanogr., 45, 591–600, 2000.

Allgaier, M., Riebesell, U., Vogt, M., Thyrhaug, R., and Grossart, H.-P.: Coupling of heterotrophic bacteria to phytoplankton bloom development at different pCO_2 levels: a mesocosm study, Biogeosciences, 5, 1007–1022, doi:10.5194/bg-5-1007-2008, 2008.

Anderson, M. J.: A new method for non-parametric multivariate analysis of variance, Aust. Ecol., 35, 32–46, 2001.

Anderson, M. J., Gorley, R. N., and Clarke, K. R.: PERMANOVA+ for PRIMER: Guide to Software and Statistical Methods, PRIMER-E, Plymouth, UK, 214 pp., 2008.

Azam, F.: Microbial Control of Oceanic Carbon Flux: The Plot Thickens, Science, 280, 694–696, doi:10.1126/science.280.5364.694, 1998.

Azam, F., Fenchel, T., Field, J. G., Gray, J. S., Meyer-Reil, L. A., and Thingstad, F.: The Ecological Role of Water-Column Microbes in the Sea, Mar. Ecol.-Prog. Ser., 10, 257–263, 1983.

Bach, L. T., Taucher, J., Boxhammer, T., Ludwig, A., The Kristineberg KOSMOS Consortium, Achterberg, E. P., Algueró-Muizñiz, M., Anderson, L. G., Bellworthy, J., Büdenbender, J., Czerny, J., Ericson, Y., Esposito, M., Fischer, M., Haunost, M., Hellemann, D., Horn, H. G., Hornick, T., Meyer, J., Sswat, M., Zark, M., and Riebesell, U.: Influence of Ocean Acidification on a Natural Winter-to-Summer Plankton Succession: First Insights from a Long-Term Mesocosm Study Draw Attention to Periods of Low Nutrient Concentrations, PLoS ONE, 11, e0159068, doi:10.1371/journal.pone.0159068, 2016.

Badr, E.-S. A., Achterberg, E. P., Tappin, A. D., Hill, S. J., and Braungardt, C. B.: Determination of dissolved organic nitrogen in natural waters using high-temperature catalytic oxidation, TrAC-Trend, Anal. Chem., 22, 819–827, doi:10.1016/S0165-9936(03)01202-0, 2003.

Benjamini, Y. and Hochberg, Y.: Controlling the false discovery rate: a practical and powerful approach to multiple testing, J. Roy. Stat. Soc. B, 57, 289–300, 1995.

Berggren, M., Lapierre, J.-F., and del Giorgio, P. A.: Magnitude and regulation of bacterioplankton respiratory quotient across freshwater environmental gradients, ISME J., 6, 984–993, 2012.

Bratbak, G. and Thingstad, T. F.: Phytoplankton-bacteria interactions: an apparent paradox? Analysis of a model system with both competition and commensalism, Mar. Ecol.-Prog. Ser., 25, 23–30, 1985.

Brussaard, C. P. D., Noordeloos, A. A. M., Witte, H., Collenteur, M. C. J., Schulz, K., Ludwig, A., and Riebesell, U.: Arctic microbial community dynamics influenced by elevated CO_2 levels, Biogeosciences, 10, 719–731, doi:10.5194/bg-10-719-2013, 2013.

Caldeira, K. and Wickett, M. E.: Anthropogenic carbon and ocean pH, Nature, 425, 365–365, 2003.

Caron, D. A. and Goldman, J. C.: Protozoan nutrient regeneration, in: Ecology of marine protozoa, edited by: Capriulo, G. M., Oxford University Press, New York, 283–306, 1990.

Clarke, K. R. and Gorley, R. N.: PRIMER v6: User manual/tutorial, PRIMER-E, Plymouth, UK, 115 pp., 2006.

Crawfurd, K. J., Brussaard, C. P. D., and Riebesell, U.: Shifts in the microbial community in the Baltic Sea with increasing CO_2, Biogeosciences Discuss., doi:10.5194/bg-2015-606, in review, 2016.

Dickson, A. G., Sabine, C., and Christian, J. (Eds.): Guide to best practices for ocean CO_2 measurements, PICES Special Publication 3, 191 pp., http://aquaticcommons.org/1443/ (last access: 16 October 2012), 2007.

Drakare, S., Blomqvist, P., Bergström, A.-K., and Jansson, M.: Relationships between picophytoplankton and environmental variables in lakes along a gradient of water colour and nutrient content, Freshwater Biol., 48, 729–740, 2003.

Engel, A., Zondervan, I., Aerts, K., Beaufort, L., Benthien, A., Chou, L., Delille, B., Gattuso, J.-P., Harlay, J., and Heemann, C.: Testing the direct effect of CO_2 concentration on a bloom of the coccolithophorid Emiliania huxleyi in mesocosm experiments, Limnol. Oceanogr., 50, 493–507, doi:10.4319/lo.2005.50.2.0493, 2005.

Gargas, E.: A manual for phytoplankton primary production studies in the Baltic, The Baltic Marine Biologist, Hørsholm, Denmark, 88 pp., 1975.

Grasshoff, K., Ehrhardt, M., Kremling, K., and Almgren, T.: Methods of seawater analysis, Wiley Verlag Chemie GmbH, Weinheim, Germany, 1983.

Grossart, H.-P.: Ecological consequences of bacterioplankton lifestyles: changes in concepts are needed, Environ. Microbiol. Rep., 2, 706–714, doi:10.1111/j.1758-2229.2010.00179.x, 2010.

Grossart, H.-P. and Simon, M.: Limnetic macroscopic organic aggregates (lake snow): Occurrence, characteristics, and microbial dynamics in Lake Constance, Limnol. Oceanogr., 38, 532–546, 1993.

Grossart, H.-P., Allgaier, M., Passow, U., and Riebesell, U.: Testing the effect of CO_2 concentration on the dynamics of marine heterotrophic bacterioplankton, Limnol. Oceanogr., 51, 1–11, 2006a.

Grossart, H.-P., Czub, G., and Simon, M.: Specific interactions of planktonic algae and bacteria: Implications for aggregation and organic matter cycling in the sea, Environ. Microbiol., 8, 1074–1084, 2006b.

Hagström, Å., Larsson, U., Hörstedt, P., and Normark, S.: Frequency of Dividing Cells, a New Approach to the Determination of Bacterial Growth Rates in Aquatic Environments, Appl. Environ. Microbiol., 37, 805–812, 1979.

Hansen, H. P. and Koroleff, F.: Determination of nutrients, in: Methods of Seawater Analysis, edited by: Grasshoff, K., Kremling, K., and Ehrhardt, M., Wiley Verlag Chemie GmbH, Zeinheim, Germany, 159–228, 1999.

Harrell Jr., F. E., Dupont, C. and many others: Hmisc: Harrell Miscellaneous, R package version 3.17-4, http://CRAN.R-project.org/package=Hmisc, last access: 2 September 2016.

Hein, M. and Sand-Jensen, K.: CO_2 increases oceanic primary production, Nature, 388, 526–527, doi:10.1038/41457, 1997.

Hobbie, J. E., Daley, R. J., and Jasper, S.: Use of nuclepore filters for counting bacteria by fluorescence microscopy, Appl. Environ. Microbiol., 33, 1225–1228, 1977.

Hoikkala, L., Aarnos, H., and Lignell, R.: Changes in Nutrient and Carbon Availability and Temperature as Factors Controlling Bacterial Growth in the Northern Baltic Sea., Estuar. Coast., 32, 720–733, doi:10.1007/s12237-009-9154-z, 2009.

Hornick, T., Bach, L. T., Crawfurd, K. J., Spilling, K., Achterberg, E. P., Woodhouse, J. N., Schulz, K. G., Brussaard, C. P. D., Riebesell, U., and Grossart, H.-P.: KOSMOS Finland 2012 mesocosm study: Size-fractionated bacterial protein production (BPP) of free-living and particle associated bacteria and abundance of particle associated heterotrophic prokaryotes, doi:10.1594/PANGAEA.868621, 2016.

Joint, I., Henriksen, P., Fonnes, G. A., Bourne, D., Thingstad, T. F., and Riemann, B.: Competition for inorganic nutrients between phytoplankton and bacterioplankton in nutrient manipulated mesocosms, Aqut. Microb. Ecol., 29, 145–159, 2002.

Kirchman, D. L.: The Uptake of Inorganic Nutrients by Heterotrophic Bacteria, Microb. Ecol., 28, 255–271, 1994

Kirchman, D. L., Elifantz, H., Dittel, A. I., Malmstrom, R. R., and Cottrell, M. T.: Standing stocks and activity of Archaea and Bacteria in the western Arctic Ocean, Limnol. Oceanogr., 52, 495–507, 2007.

Kuparinen, J. and Heinänen, A.: Inorganic Nutrient and Carbon Controlled Bacterioplankton Growth in the Baltic Sea, Estuar. Coast. Shelf Sci., 37, 271–285, 1993.

Lapoussière, A., Michel, C., Starr, M., Gosselin, M., and Poulin, M.: Role of free-living and particle-attached bacteria in the recycling and export of organic material in the Hudson Bay system, J. Mar. Syst., 88, 434–445, 2011.

Legendre, P. and Anderson, M. J.: Distance-based redundancy analysis: testing multispecies responses in multifactorial ecological experiments, Ecol. Monogr., 69, 1–24, 1999.

Lignell, R., Hoikkala, L., and Lahtinen, T.: Effects of inorganic nutrients, glucose and solar radiation treatments on bacterial growth and exploitation of dissolved organic carbon and nitrogen in the northern Baltic Sea, Aquat. Microb. Ecol., 51, 209–221, 2008.

Lueker, T. J., Dickson, A. G., and Keeling, C. D.: Ocean pCO_2 calculated from dissolved inorganic carbon, alkalinity, and equations for K1 and K2: validation based on laboratory measurements of CO_2 in gas and seawater at equilibrium, Mar. Chem., 70, 105–119, doi:10.1016/S0304-4203(00)00022-0, 2000.

Maat, D. S., Crawfurd, K. J., Timmermans, K. R., and Brussaard, C. P. D.: Elevated CO_2 and Phosphate Limitation Favor *Micromonas pusilla* through Stimulated Growth and Reduced Viral Impact, Appl. Environ. Microbiol., 80, 3119–3127, doi:10.1128/AEM.03639-13, 2014.

Marie, D., Brussaard, C. P. D., Thyrhaug, R., Bratbak, G., and Vaulot, D.: Enumeration of marine viruses in culture and natural samples by flow cytometry, Appl. Environ. Microbiol., 65, 45–52, 1999.

Massana, R., Gasol, J. M., Bjørnsen, P. K., Blackburn, N., Hagström, Å., Hietanen, S., Hygum, B. H., Kuparinen, J. and Pedrós-Alió, C.: Measurement of bacterial size via image analysis of epifluorescence preparations: description of an inexpensive system and solutions to some of the most common problems, Sci. Mar., 61, 397–407, 1997.

Mehrbach, C., Culberson, C. H., Hawley, J. E., and Pytkowicz, R. M.: Measurement of apparent dissociation constants of carbonic acid in seawater at atmospheric pressure, Limnol. Oceanogr., 18, 897–807, 1973.

Mitra, A., Flynn, K. J., Burkholder, J. M., Berge, T., Calbet, A., Raven, J. A., Granéli, E., Glibert, P. M., Hansen, P. J., Stoecker, D. K., Thingstad, F., Tillmann, U., Våge, S., Wilken, S., and Zubkov, M. V.: The role of mixotrophic protists in the biological carbon pump, Biogeosciences, 11, 995–1005, doi:10.5194/bg-11-995-2014, 2014.

Moore, C. M., Mills, M. M., Arrigo, K. R., Berman-Frank, I, Bopp, L., Boyd, P. W., Galbraith, E. D., Geider, R. J., Guieu, C., Jaccard, S. L., Jickells, T. D., La Roche, J., Lenton, T. M., Mahowald, N. M., Marañón, E., Marinov, I., Moore, J. K., Nakatsuka, T., Oschlies, A., Sito, M. A., Thingstad, T. F., Tsuda, A., and Ulloa, O.: Processes and patterns of oceanic nutrient limitation, Nat. Geosci., 6, 701–710, doi:10.1038/NGEO1765, 2013.

Nausch, M., Bach, L. T., Czerny, J., Goldstein, J., Grossart, H.-P., Hellemann, D., Hornick, T., Achterberg, E. P., Schulz, K.-G., and Riebesell, U.: Effects of CO_2 perturbation on phosphorus pool sizes and uptake in a mesocosm experiment during a low productive summer season in the northern Baltic Sea, Biogeosciences, 13, 3035–3050, doi:10.5194/bg-13-3035-2016, 2016.

Newbold, L., Oliver, A. E., Booth, T., Tiwari, B., DeSantis, T., Maguire, M., Andersen, G., van der Gast, C. J., and Whiteley, A. S.: The response of marine picoplankton to ocean acidification, Environ. Microbiol., 14, 2293–2307, 2012.

Oksanen, J., Blanchet, F. G., Friendly, M., Kindt, R., Legendre, P., McGlinn, D., Minchin, P. R., O'Hara, R. B., Simpson, G. L., Solymos, P., Stevens, M. H. H., Szoecs, E., and Wagner, H.: vegan: Community Ecology Package, R package version 2.4-0, https://CRAN.R-project.org/package=vegan, last access: 2 September 2016.

Patey, M. D., Rijkenberg, M. J. A., Statham, P. J., Stinchcombe, M. C., Achterberg, E. P., and Mowlem, M.: Determination of nitrate and phosphate in seawater at nanomolar concentrations, TrAC-Trend, Anal. Chem., 27, 169–182, doi:10.1016/j.trac.2007.12.006, 2008.

Paul, A. J., Bach, L. T., Schulz, K.-G., Boxhammer, T., Czerny, J., Achterberg, E. P., Hellemann, D., Trense, Y., Nausch, M., Sswat, M., and Riebesell, U.: Effect of elevated CO_2 on organic matter pools and fluxes in a summer Baltic Sea plankton community, Biogeosciences, 12, 6181–6203, doi:10.5194/bg-12-6181-2015, 2015.

Paul, A., Schulz, K. G., Achterberg, E. P., Hellemann, D., Nausch, M., Boxhammer, T., Bach, L. T., and Trense, Y.: KOSMOS Finland 2012 mesocosm study: carbonate chemistry, particulate and dissolved matter pools, and phytoplankton community composition using marker pigments (CHEMTAX), doi:10.1594/PANGAEA.863032, 2016.

Porter, K. G. and Feig, Y. S.: Dapi for identifying and counting aquatic microflora, Limnol. Oceanogr., 25, 943–948, 1980.

Raven, J. A.: The twelfth Tansley Lecture. Small is beautiful: the picophytoplankton, Funct. Ecol., 12, 503–513, 1998.

R Core Team R: A language and environment for statistical computing. R Foundation for Statistical Computing, Vienna, Austria, URL http://www.R-project.org/, last access: 2 September 2016.

Riebesell, U. and Gattuso, J.-P.: Lessons learned from ocean acidification research, Reflection on the rapidly growing field of ocean acidification research highlights priorities for future research on the changing ocean, Nature Climate Change, 5, 12–14, doi:10.1038/nclimate2456, 2015.

Riebesell, U., Schulz, K. G., Bellerby, R. G. J., Botros, M., Fritsche, P., Meyerhöfer, M., Neill, C., Nondal, G., Oschlies, A., Wohlers, J., and Zöllner, E.: Enhanced biological carbon consumption in a high CO_2 ocean, Nat. Lett., 450, 545–548, doi:10.1038/nature06267, 2007.

Rieck, A., Herlemann, D. P. R., Jürgens, K., and Grossart, H.-P.: Particle-Associated Differ from Free-Living Bacteria in Surface Waters of the Baltic Sea, Front. Microbiol., 6, doi:10.3389/fmicb.2015.01297, 2015.

Rose, J. M., Feng, Y., Gobler, C. J., Gutierrez, R., Hare, C. E., Leblanc, K., and Hutchins, D. A.: Effects of increased pCO_2 and temperature on the North Atlantic spring bloom, II. Microzooplankton abundance and grazing, Mar. Ecol.-Prog. Ser., 388, 27–40, 2009.

Sala, M. M., Aparicio, F. L., Balagué, V., Boras, J. A., Borrull, E., Cardelús, C., Cros, L., Gomes, A., López-Sanz, A., Malits, A., Martinez, R. A., Mestre, M., Movilla, J., Sarmento, H., Vázquez-Dominguez, E., Vaqué, D., Pinhassi, J., Calbet, A., Calvo, E., Gasol, J. M., Pelejero, C., and Marrasé, C.: Contrasting effects of ocean acidification on the microbial food web under different trophic conditions, ICES J. Mar. Sci., 73, 670–679, doi:10.1093/icesjms/fsv130, 2015.

Sharp, J.: Improved analysis for particulate organic carbon and nitrogen from seawater, Limnol. Oceanogr., 19, 984–989, 1974.

Sheik, A. R., Brussaard, C. P. D., Lavik, G., Lam, P., Musat, N., Krupke, A., Littmann, S., Strous, M., and Kuypers M. M. M.: Responses of the coastal bacterial community to viral infection of the algae Phaeocystic globosa, ISME J., 8, 212–225, doi:10.1038/ismej.2013.135, 2014.

Simon, M. and Azam, F.: Protein content and protein synthesis rates of planktonic marine bacteria, Mar. Ecol.-Prog. Ser., 51, 201–213, 1989.

Smith, D. C., Simon, M., Alldredge, A. L., and Azam, F.: Intense hydrolytic enzyme activity on marine aggregates and implications for rapid particle dissolution, Nature, 359, 139–142, 1992.

Spilling, K., Paul, A. J., Virkkala, N., Hastings, T., Lischka, S., Stuhr, A., Bermúdez, R., Czerny, J., Boxhammer, T., Schulz, K. G., Ludwig, A., and Riebesell, U.: Ocean acidification decreases plankton respiration: evidence from a mesocosm experiment, Biogeosciences, 13, 4707–4719, doi:10.5194/bg-13-4707-2016, 2016a.

Spilling, K., Schulz, K. G., Paul, A. J., Boxhammer, T., Achterberg, E. P., Hornick, T., Lischka, S., Stuhr, A., Bermúdez, R., Czerny, J., Crawfurd, K., Brussaard, C. P. D., Grossart, H.-P., and Riebesell, U.: Effects of ocean acidification on pelagic carbon fluxes in a mesocosm experiment, Biogeosciences, 13, 6081–6093, doi:10.5194/bg-13-6081-2016, 2016b.

Spilling, K., Paul, A., Virkkala, N., Hastings, T., Lischka, S., Stuhr, A., Bermúdez, R., Czerny, J., Boxhammer, T., Schulz, K. G., Ludwig, A., and Riebesell, U.: KOSMOS Finland 2012 mesocosm study: primary production and respiration, doi:10.1594/PANGAEA.863933, 2016c.

Steeman-Nielsen, E.: The use of radioactive carbon for measuring organic production in the sea, J. Cons. Int. Explor. Mer., 18, 117–140, 1952.

Suttle, C. A., Fuhrman, J. A., and Capone, D. G.: Rapid ammonium cycling and concentration-dependent partitioning of ammonium and phosphate: Implications for carbon transfer in planktonic communities, Limnol. Oceanogr., 35, 424–433, 1990.

Suzuki, R. and Shimodaira, H.: pvclust: Hierarchical Clustering with p-values via Multiscale Bootstrap Resampling, R package version 2.0-0., https://CRAN.R-project.org/package=pvclust (last access: 2 September 2016), 2015.

Taylor, A. R., Brownlee, C., and Wheeler, G. L.: Proton channels in algae: reasons to be excited, Trends Plant Sci., 17, 675–684, doi:10.1016/j.tplants.2012.06.009, 2012.

Thingstad, T. F., Hagström, Å., and Rassoulzadegan, F.: Accumulation of degradable DOC in surface waters: Is it caused by a malfunctioning microbial loop?, Limnol. Oceanogr., 42, 398–404, 1997.

Thingstad, T. F., Bellerby, R. G. J., Bratbak, G., Borsheim, K. Y., Egge, J. K., Heldal, M., Larsen, A., Neill, C., Nejstgaard, J., Norland, S., Sandaa, R.-A., Skjoldal, E. F., Tanaka, T., Thyrhaug, R., and Töpper, B.: Counterintuitive carbon-to-nutrient coupling in an Arctic pelagic ecosystem, Nat. Lett., 455, 387–391, doi:10.1038/nature07235, 2008.

Toggweiler, J. R.: Carbon overconsumption, Nature, 363, 210–211, 1993.

Warnes, G. R., Bolker, B., Bonebakker, L., Gentleman, R., Liaw, W. H. A., Lumley, T., Maechler, M., Magnusson, A., Moeller, S., Schwartz, M., and Venables, B.: gplots: Various R Programming Tools for Plotting Data, R package version 3.0.1, https://CRAN.R-project.org/package=gplots, last access: 2 September 2016.

Welschmeyer, N. A.: Fluorometric analysis of chlorophyll a in the presence of chlorophyll b and pheopigments, Limnol. Oceanogr., 39, 1985–1992, doi:10.4319/lo.1994.39.8.1985, 1994.

Wickham, H.: ggplot2: Elegant graphics for data analysis, Springer-Verlag New York, 2009.

Supplement of Biogeosciences, 14, 1–15, 2017
http://www.biogeosciences.net/14/1/2017/
doi:10.5194/bg-14-1-2017-supplement

Biogeosciences Open Access EGU

Supplement of

Ocean acidification impacts bacteria–phytoplankton coupling at low-nutrient conditions

Thomas Hornick et al.

Correspondence to: Thomas Hornick (hornick@igb-berlin.de)

Supplementary

Table S1: Summary of I) Physical/chemical predictor variables and A) metabolic variables and C) abundances of functional bacterial and phytoplankton groups used for distance-based modelling (DistLM) and II) A) Chemical, B) metabolic and C) abundances of functional bacterial and phytoplankton groups used for permutational multivariate analysis of variance (PERMANOVA). Fugacity of CO_2 (fCO_2), temperature (Temp), photosynthetically active radiation (PAR), dissolved organic carbon (DOC), total dissolved nitrogen (TDN), dissolved silica (DSi), total particulate carbon (TPC), particulate organic phosphorus (POP), particulate biogenic silica (BSi), bacterial protein production (BPP), areal primary production (PP), community respiration (CR), chlorophyll *a* (Chl *a*), particle-associated (PA) prokaryotes; flow-cytometric determined: low SYBR green I fluorescent prokaryotes (LDNA), high SYBR green I fluorescent prokaryotes (HDNA), *Synechococcus* spp. (SYN), picophytoplankton I-III (Pico I-III), naophytoplankton I-II (Nano I-II)

I)	A)	predictor variables:	fCO_2, Temp, PAR, DOC, TDN, Phosphate, DSi, TPC, POP, BSi
		metabolic variables:	BPP, PP, CR
	B)	predictor variables:	fCO_2, Temp, PAR, DOC, TDN, Phosphate, DSi, TPC, POP, BSi
		functional groups:	LDNA, HDNA, PA prokaryotes, SYN, Pico I, Pico II, Pico III, Nano I, Nano II, Chl *a*
II)	A)	chemical variables:	DOC, TDN, Phosphate, DSi, TPC, TPN, POP, BSi
	B)	metabolic variables:	BPP, PP, CR
	C)	functional groups:	LDNA, HDNA, SYN, Pico I, Pico II, Pico III, Nano I, Nano II, Chl *a*

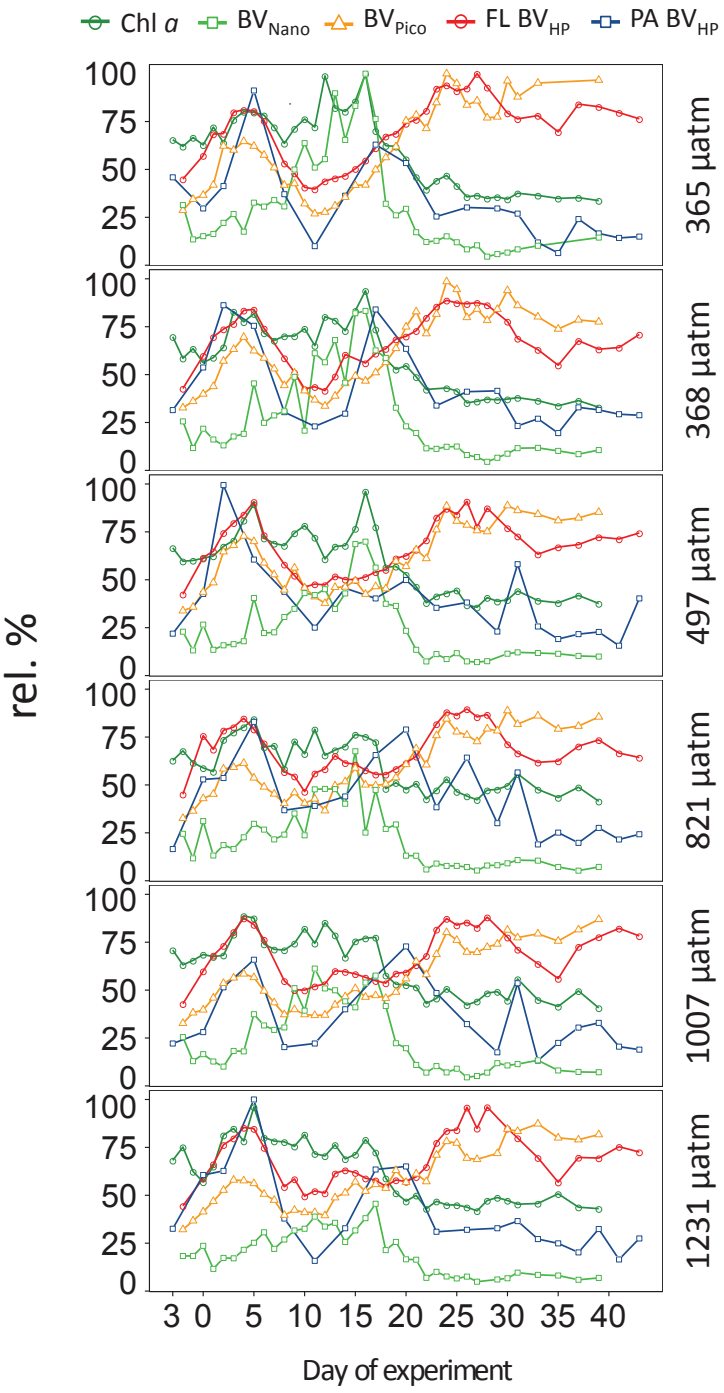

Figure S1. Concentration of Chl *a*, biovolumes of picophotoautotrophs (BV_{Pico}; sum of *Synechococcus* spp. and Pico I-III) and nanophotoautotrophs (BV_{Nano}; sum of Nano I and II) as well as biovolumes of free-living (FL BV_{HP}) and particle-associated (PA BV_{HP}) heterotrophic prokaryotes during the course of the experiment in the respective mesocosms labelled with the average fCO_2 [µatm] between t1-t43. Biovolumes are standardized to the highest observed value for each parameter and expressed as relative percentage.

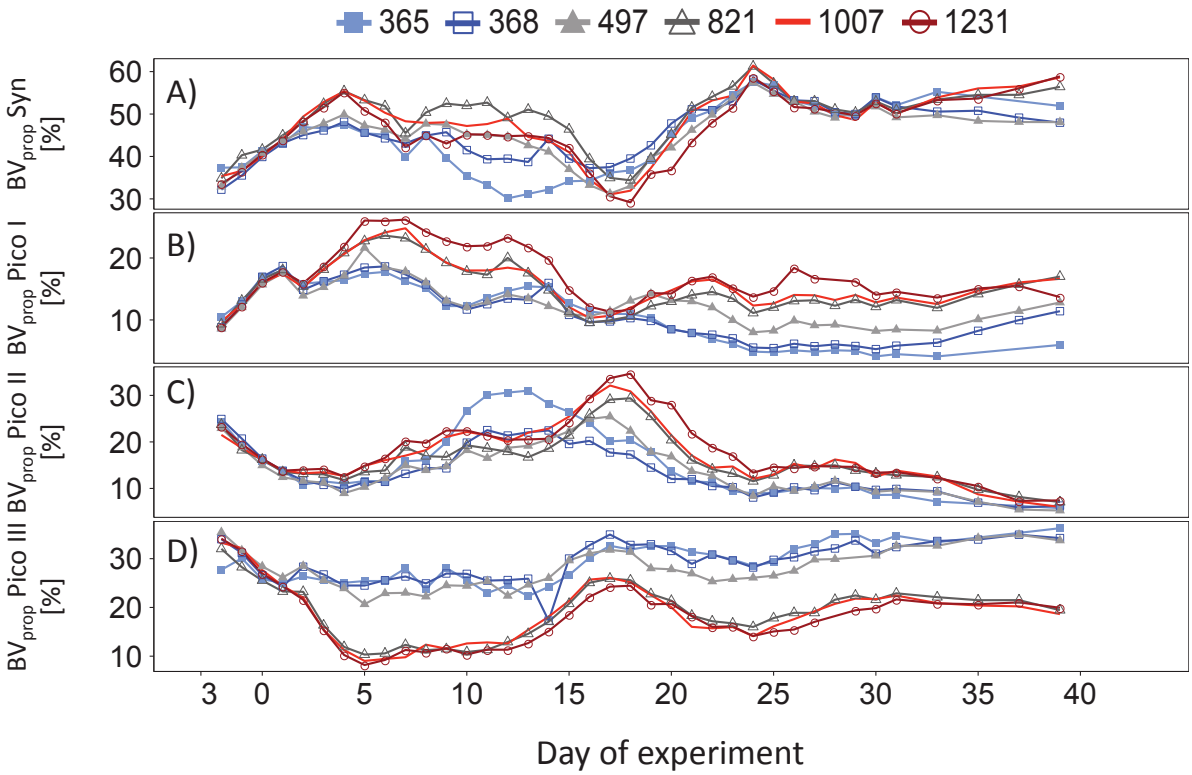

Figure S2. Relative biovolume (BV) contribution of A) BV of *Synechococcus* spp. [x10^5 µm^3 ml^{-1}] and B-D) BV of picoeukaryote groups I-III (Pico I-III) [x10^5 µm^3 ml^{-1}] to total BV of picophotoautotrophs (sum of *Synechococcus* spp. and Pico I-III) revealed by flow-cytometry during the course of the experiment. Colours and symbols indicate average fCO_2 [µatm] between t1-t43.

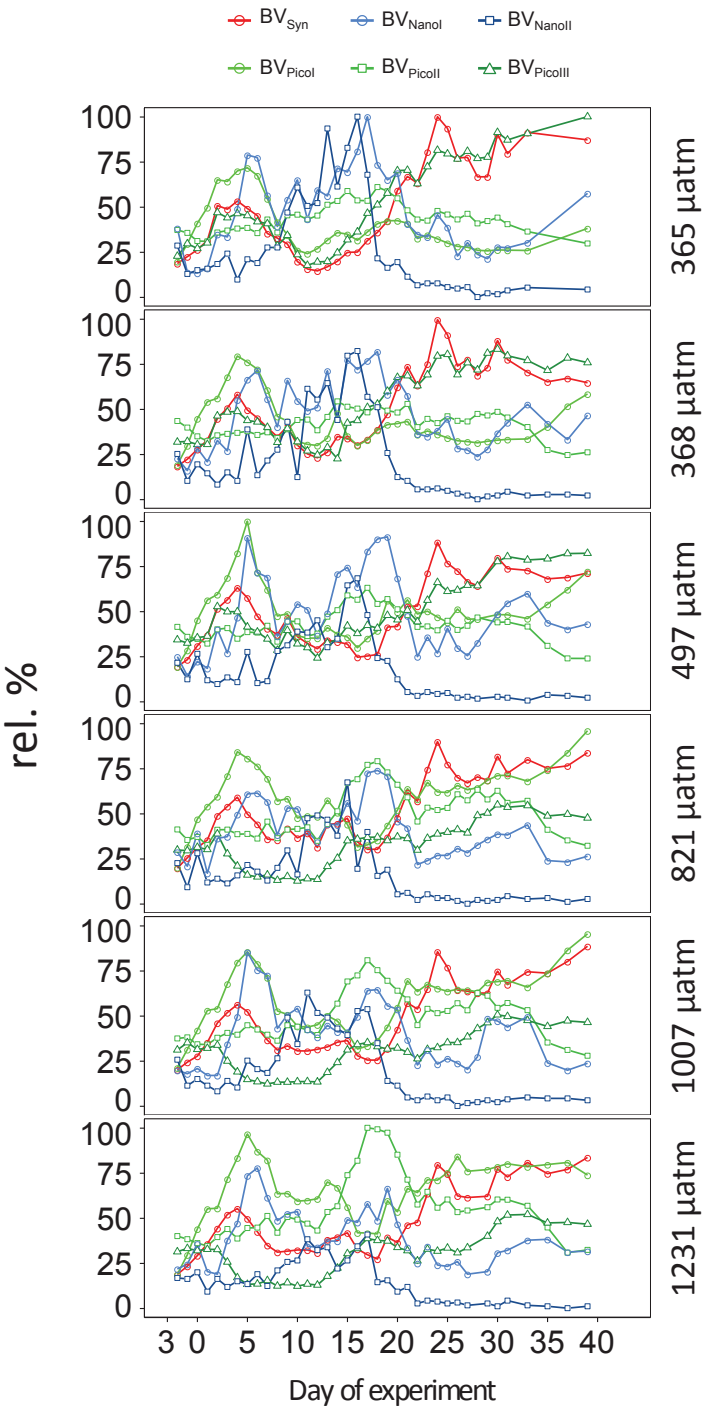

Figure S3. Biovolumes of *Synechococcus* spp., picoeukaryote groups I-III and nanophytoplankton groups I-II during the course of the experiment in the respective mesocosms labelled with the average fCO_2 [µatm] between t1-t43. Biovolumes are standardized to the highest observed value for each organism group and expressed as relative percentage.

3. Chapter 3 - Manuscript 2

Effects of ocean acidification on pelagic carbon fluxes in a mesocosm experiment

Kristian Spilling[1,2*,] Kai G. Schulz[3], Allanah J. Paul[4], Tim Boxhammer[4], Eric P. Achterberg[4,5], **Thomas Hornick[6]**, Silke Lischka[4], Annegret Stuhr[4], Rafael Bermúdez[4,7], Jan Czerny[4], Kate Crawfurd[8], Corina P. D. Brussaard[8,9], Hans-Peter Grossart[6,10], and Ulf Riebesell[4]

Published in *Biogeosciences***

[1] Marine Research Centre, Finnish Environment Institute, P.O. Box 140, 00251 Helsinki, Finland

[2] Tvärminne Zoological Station, University of Helsinki, J. A. Palménin tie 260, 10900 Hanko, Finland

[3] Centre for Coastal Biogeochemistry, Southern Cross University, Military Road, East Lismore, NSW 2480, Australia

[4] GEOMAR Helmholtz Centre for Ocean Research Kiel, Düsternbrooker Weg 20, 24105 Kiel, Germany

[5] National Oceanography Centre Southampton, European Way, University of Southampton, Southampton, SO14 3ZH, UK

[6] Leibniz Institute of Freshwater Ecology and Inland Fisheries (IGB), Experimental Limnology, 16775 Stechlin, Germany

[7] Facultad de Ingeniería Marítima, Ciencias Biológicas, Oceánicas y Recursos Naturales. ESPOL, Escuela Superior Politécnica del Litoral, Guayaquil, Ecuador

[8] NIOZ Royal Netherlands Institute for Sea Research, Department of Marine Microbiology and Biogeochemistry, and Utrecht University, P.O. Box 59, 1790 AB Den Burg, Texel, the Netherlands

[9] Department of Aquatic Microbiology, Institute for Biodiversity and Ecosystem Dynamics (IBED), University of Amsterdam, Amsterdam, the Netherlands

[10] Institute for Biochemistry and Biology, Potsdam University, 14469 Potsdam, Germany

*corresponding author: kristian.spilling@environment.fi (K. Spilling)

** manuscript formatted in style of *Biogeosciences*

Biogeosciences, 13, 6081–6093, 2016
www.biogeosciences.net/13/6081/2016/
doi:10.5194/bg-13-6081-2016

Biogeosciences Open Access EGU

Effects of ocean acidification on pelagic carbon fluxes in a mesocosm experiment

Kristian Spilling[1,2], Kai G. Schulz[3], Allanah J. Paul[4], Tim Boxhammer[4], Eric P. Achterberg[4,5], Thomas Hornick[6], Silke Lischka[4], Annegret Stuhr[4], Rafael Bermúdez[4,7], Jan Czerny[4], Kate Crawfurd[8], Corina P. D. Brussaard[8,9], Hans-Peter Grossart[6,10], and Ulf Riebesell[4]

[1]Marine Research Centre, Finnish Environment Institute, P.O. Box 140, 00251 Helsinki, Finland
[2]Tvärminne Zoological Station, University of Helsinki, J. A. Palménin tie 260, 10900 Hanko, Finland
[3]Centre for Coastal Biogeochemistry, Southern Cross University, Military Road, East Lismore, NSW 2480, Australia
[4]GEOMAR Helmholtz Centre for Ocean Research Kiel, Düsternbrooker Weg 20, 24105 Kiel, Germany
[5]National Oceanography Centre Southampton, European Way, University of Southampton, Southampton, SO14 3ZH, UK
[6]Leibniz Institute of Freshwater Ecology and Inland Fisheries (IGB), Experimental Limnology, 16775 Stechlin, Germany
[7]Facultad de Ingeniería Marítima, Ciencias Biológicas, Oceánicas y Recursos Naturales. ESPOL, Escuela Superior Politécnica del Litoral, Guayaquil, Ecuador
[8]NIOZ Royal Netherlands Institute for Sea Research, Department of Marine Microbiology and Biogeochemistry, and Utrecht University, P.O. Box 59, 1790 AB Den Burg, Texel, the Netherlands
[9]Department of Aquatic Microbiology, Institute for Biodiversity and Ecosystem Dynamics (IBED), University of Amsterdam, Amsterdam, the Netherlands
[10]Institute for Biochemistry and Biology, Potsdam University, 14469 Potsdam, Germany

Correspondence to: Kristian Spilling (kristian.spilling@environment.fi)

Received: 17 February 2016 – Published in Biogeosciences Discuss.: 7 March 2016
Revised: 21 September 2016 – Accepted: 22 September 2016 – Published: 4 November 2016

Abstract. About a quarter of anthropogenic CO_2 emissions are currently taken up by the oceans, decreasing seawater pH. We performed a mesocosm experiment in the Baltic Sea in order to investigate the consequences of increasing CO_2 levels on pelagic carbon fluxes. A gradient of different CO_2 scenarios, ranging from ambient ($\sim$ 370 µatm) to high ($\sim$ 1200 µatm), were set up in mesocosm bags ($\sim$ 55 m^3). We determined standing stocks and temporal changes of total particulate carbon (TPC), dissolved organic carbon (DOC), dissolved inorganic carbon (DIC), and particulate organic carbon (POC) of specific plankton groups. We also measured carbon flux via CO_2 exchange with the atmosphere and sedimentation (export), and biological rate measurements of primary production, bacterial production, and total respiration. The experiment lasted for 44 days and was divided into three different phases (I: *t0–t16*; II: *t17–t30*; III: *t31–t43*). Pools of TPC, DOC, and DIC were approximately 420, 7200, and 25 200 mmol C m^{-2} at the start of the experiment, and the initial CO_2 additions increased the DIC pool by $\sim$ 7 % in the highest CO_2 treatment. Overall, there was a decrease in TPC and increase of DOC over the course of the experiment. The decrease in TPC was lower, and increase in DOC higher, in treatments with added CO_2. During phase I the estimated gross primary production (GPP) was $\sim$ 100 mmol C m^{-2} day^{-1}, from which 75–95 % was respired, $\sim$ 1 % ended up in the TPC (including export), and 5–25 % was added to the DOC pool. During phase II, the respiration loss increased to $\sim$ 100 % of GPP at the ambient CO_2 concentration, whereas respiration was lower (85–95 % of GPP) in the highest CO_2 treatment. Bacterial production was $\sim$ 30 % lower, on average, at the highest CO_2 concentration than in the controls during phases II and III. This resulted in a higher accumulation of DOC and lower reduction in the TPC pool in the elevated CO_2 treatments at the end of phase II extending throughout phase III. The "extra" organic carbon at high CO_2 remained fixed in an increasing biomass of small-sized plankton and in the DOC pool, and did not transfer into large, sinking aggregates. Our re-

Published by Copernicus Publications on behalf of the European Geosciences Union.

sults revealed a clear effect of increasing CO_2 on the carbon budget and mineralization, in particular under nutrient limited conditions. Lower carbon loss processes (respiration and bacterial remineralization) at elevated CO_2 levels resulted in higher TPC and DOC pools than ambient CO_2 concentration. These results highlight the importance of addressing not only net changes in carbon standing stocks but also carbon fluxes and budgets to better disentangle the effects of ocean acidification.

1 Introduction

Combustion of fossil fuels and change in land use have caused increasing atmospheric concentrations of carbon dioxide (CO_2). Ca. 25 % of the anthropogenic CO_2 is absorbed by the oceans, thereby decreasing surface water pH, a process termed ocean acidification (Le Quéré et al., 2009). Ocean acidification and its alterations of aquatic ecosystems have received considerable attention during the past decade, but there are many open questions, in particular related to consequences for plankton-mediated carbon fluxes.

Some studies on ocean acidification have reported increased carbon fixation (Egge et al., 2009; Engel et al., 2013), bacterial production (BP; Grossart et al., 2006), and bacterial degradation of polysaccharides (Piontek et al., 2010) at enhanced CO_2 levels, with potential consequences for carbon fluxes within pelagic ecosystems and export to the deep ocean, i.e., the biological carbon pump. Increasing carbon fixation in a high-CO_2 environment can translate into an enhanced sequestration of carbon (Riebesell et al., 2007), but this depends on numerous environmental factors, including phytoplankton community composition, aggregate formation, and nutrient availability. For example, if the community shifts towards smaller cell sizes and/or enhanced cycling of organic matter carbon, export from the upper water layers may decrease (Czerny et al., 2013a).

The effect of ocean acidification has mostly been studied in marine ecosystems under high phytoplankton biomass. Brackish water has lower buffering capacity than ocean water, and the pH fluctuates more. The limited number of studies of ocean acidification in brackish water and indications that ocean acidification effects are greatest under nutrient limitation (De Kluijver et al., 2010) motivated this mesocosm study in the Baltic Sea during low-nutrient summer months.

The Baltic Sea is functionally much like a large estuary, with a salinity gradient ranging from approximately 20 in the southwest to < 3 in the northernmost Bothnian Bay. It is an almost-landlocked body of water with a large population in its vicinity (∼ 80 million). Human activities (e.g., agriculture, shipping, and fishing) cause a number of environmental problems such as eutrophication and pollution. As a coastal sea projected to change rapidly due to interaction of direct and indirect anthropogenic pressures, the Baltic Sea can be seen as a model ecosystem for studying global change scenarios (Niiranen et al., 2013).

Most primary data from this experiment are published in several papers of this special issue (Riebesell et al., 2015). The aim of the present paper is to provide an overarching synthesis of all information related to carbon standing stocks and fluxes. This enabled us to calculate carbon budgets in relation to different CO_2 levels.

2 Materials and methods

2.1 Experimental setup

Six Kiel Off-Shore Mesocosms for Ocean Simulations (KOSMOS; with a volume of ca. 55 m^3) were moored at Storfjärden, on the south west coast of Finland (59°51.5′ N; 23°15.5′ E) on 12 June 2012 (nine KOSMOS units were originally deployed, but three were lost due to leaks). A more detailed description of the setup can be found in Paul et al. (2015). The mesocosms extended from the surface down to 19 m depth and had a conical bottom end, which enabled quantitative collection of the settling material. Different CO_2 levels in the bags were achieved by adding filtered (50 µm), CO_2-saturated seawater. The CO_2-enriched water was evenly distributed over the upper 17 m of the water columns and added in four consecutive time steps (*t0–t3*). Two controls and four treatments were used, and for the controls, filtered seawater (without additional CO_2 enrichment) was added. The CO_2 fugacity gradient after all additions ranged from ambient (average throughout the experiment: ∼ 370 µatm fCO_2) in the two control mesocosms (M1 and M5) up to ∼ 1200 µatm fCO_2 in the highest treatment (M8). We used the average fCO_2 throughout this experiment (*t1–t43*) to denote the different treatments: 365 (M1), 368 (M5), 497 (M7), 821 (M6), 1007 (M3), and 1231 (M8) µatm fCO_2. On *t15*, additional CO_2-saturated seawater was added to the upper 7 m in the same manner as the initial enrichment, to counteract outgassing of CO_2.

We sampled the mesocosms every morning, but some variables were determined only every second day. Depth-integrated water samples (0–17 m) were taken by using integrating water samplers (IWS, HYDRO-BIOS, Kiel). The water was collected into plastic carboys (10 L) and transferred to the laboratory for sub-sampling and subsequent determination of carbon stocks.

2.2 Primary variables

For more detailed descriptions of the primary variables and the different methods used during this CO_2 mesocosm campaign, we refer to other papers in this joint volume: i.e., total particulate carbon (TPC), dissolved organic carbon (DOC), and dissolved inorganic carbon (DIC) are described by Paul et al. (2015); micro- and nanophytoplankton enumeration by Bermúdez et al. (2016); picophytoplankton, heterotrophic

prokaryotes, and viruses by Crawfurd et al. (2016); zooplankton community by Lischka et al. (2015); primary production and respiration by Spilling et al. (2016a); BP by Hornick et al. (2016); and sedimentation by Boxhammer et al. (2016) and Paul et al. (2015).

Briefly, samples for TPC (500 mL) were GF/F-filtered and determined using an elemental analyzer (EuroAE). DOC was measured using the high-temperature combustion method (Shimadzu TOC–VCPN) following Badr et al. (2003). DIC was determined by infrared absorption (LI-COR LI-7000 on an AIRICA system). The DIC concentrations were converted from µmol kg^{-1} to µmol L^{-1} using the average seawater density of 1.0038 kg L^{-1} throughout the experiment. Settling particles were quantitatively collected every other day from sediment traps at the bottom of the mesocosm units, and the TPC was determined from the processed samples (Boxhammer et al., 2016) as described above.

Mesozooplankton was collected by net hauls (100 µm mesh size), fixed (ethanol), and counted in a stereomicroscope. Zooplankton carbon biomass (CB) was calculated using the displacement volume (DV) and the equation of Wiebe (1988): $(\log \mathrm{DV} + 1.429) / 0.82 = \log \mathrm{CB}$. Micro- and nanoplankton (zoo- and phytoplankton) CB was determined from microscopic counts of fixed (acidic Lugol's iodine solution) samples, and the cellular bio-volumes were determined according to Olenina et al. (2006) and converted to particulate organic carbon (POC) by the equations provided by Menden-Deuer and Lessard (2000).

Picophytoplankton were counted using flow cytometry and converted to CB by size fractionation (Veldhuis and Kraay, 2004) and cellular carbon conversion factors (0.2 pg C µ m^{-3}; Waterbury et al., 1986). Prokaryotes and viruses were determined according to Marie et al. (1999) and Brussaard (2004), respectively. All heterotrophic prokaryotes, hereafter termed bacteria, and viruses were converted to CB assuming 12.5 fg C $cell^{-1}$ (Heinänen and Kuparinen, 1991) and 0.055 fg C $virus^{-1}$ (Steward et al., 2007), respectively.

The respiration rate was calculated from the difference between the O_2 concentration (measured with a Fibox 3, PreSens) before and after a 48 h incubation period in a dark climate-controlled room set to the average temperature observed in the mesocosms.

BP was determined by ^{14}C-leucine (^{14}C-Leu) incorporation (Simon and Azam, 1989) according to Grossart et al. (2006). The amount of incorporated ^{14}C-Leu was converted into BP by using an intracellular isotope dilution factor of 2. A conversion factor of 0.86 was used to convert the produced protein into carbon (Simon and Azam, 1989).

Net primary production (NPP) was measured using radiolabeled $NaH^{14}CO_3$ (Steeman-Nielsen, 1952). Samples were incubated for 24 h in duplicate 8 mL vials moored on small incubation platforms at 2, 4, 6, 8, and 10 m depth next to the mesocosms. The areal primary production was calculated based on a simple linear model of the production measurements from the different depths (Spilling et al., 2016a).

2.3 Gas exchange

In order to calculate the CO_2 gas exchange with the atmosphere ($CO_{2\mathrm{flux}}$), we used N_2O as a tracer gas, added to mesocosm M5 and M8 (control and high CO_2 treatment) according to Czerny et al. (2013b). The N_2O concentration was determined every second day using gas chromatography. Using the N_2O measurements, the fluxes across the water surface (F_{N_2O}) were calculated according to

$$F_{\mathrm{N_2O}} = I_{t_1} - I_{t_2}/(A \times \Delta t), \quad (1)$$

where I_{t_1} andI_{t_2} are the bulk N_2O concentration at time t_1 and t_2, respectively; A is the surface area; and Δt is the time difference between t_1 and t_2.

The flux velocity was then calculated by

$$K_{\mathrm{N_2O}} = F_{\mathrm{N_2O}} / \left(C_{\mathrm{N_2O\,w}} - \left(C_{\mathrm{N_2O\,aw}}\right)\right), \quad (2)$$

where $C_{\mathrm{N_2O\,w}}$ is the bulk N_2O concentration in the water at a given point in time and $C_{\mathrm{N_2O\,aw}}$ is the equilibrium concentration for N_2O (Weiss and Price, 1980).

The flux velocity for CO_2 was calculated from the flux velocity of N_2O according to

$$k_{\mathrm{CO_2}} = k_{\mathrm{N_2O}} / \left(Sc_{\mathrm{CO_2}} / Sc_{\mathrm{N_2O}}\right)^{0.5}, \quad (3)$$

where Sc_{CO_2} and Sc_{N_2O} are the Schmidt numbers for CO_2 and N_2O, respectively. The CO_2flux across the water surface was calculated according to

$$F_{\mathrm{CO_2}} = k_{\mathrm{CO_2}} \left(C_{\mathrm{CO_2w}} - C_{\mathrm{CO_2aw}}\right), \quad (4)$$

where C_{CO_2w} is the water concentration of CO_2 and C_{CO_2aw} is the equilibrium concentration of CO_2. CO_2 is preferentially taken up by phytoplankton at the surface, where also the atmospheric exchange takes place. For this reason, we used the calculated CO_2 concentration (based on the integrated CO_2 concentration and pH in the surface) from the upper 5 m as the input for Eq. (5).

In contrast to N_2O, the CO_2 flux can be chemically enhanced by hydration reactions of CO_2 with hydroxide ions and water molecules in the boundary layer (Wanninkhof and Knox, 1996). Using the method outlined in Czerny et al. (2013b), we found an enhancement of up to 12 % on warm days, and this was included into our flux calculations.

2.4 Data treatment

The primary data generated in this study comprise carbon standing stock measurements of TPC, DOC, and DIC, as well as carbon estimates of meso- and microzooplankton, micro-, nano- and picophytoplankton, bacteria, and viruses.

Flux measurements of atmospheric CO_2 exchange and sedimentation of TPC as well as the biological rates of net primary production ($NPP_{^{14}C}$), BP, and total respiration (TR) enabled us to make carbon budget.

Based on the primary variables (chlorophyll *a* (Chl *a*) and temperature), the experiment where divided into three distinct phases: phase I: *t0–t16*; phase II: *t17–t30*; and phase III: *t31–t43*, where, e.g., Chl *a* concentration was relatively high during phase I, decreased during phase II, and remained low during phase III (Paul et al., 2015). Measurements of pools and rates were averaged for the two first sampling points of each experimental phase ($n = 2$) and were normalized to square meters (m^2) knowing the total depth (17 m, excluding the sedimentation funnel) of the mesocosms. For phase III we used the average of the last two measurements as the end point ($n = 2$).

For fluxes and biological rates we used the average for the whole periods normalized to days (day^{-1}). The same was done for rates of change (ΔTPC, ΔDOC, and ΔDIC), which accounted for the difference between the start and end of each phase for all carbon pools (TPC_{pool}, DOC_{pool}, DIC_{pool}). All error estimates were calculated as standard error (SE), and this was calculated using all measurements within each phase (e.g., calculating the ΔTPC SE using the difference between each TPC measurement). The three different phases of the experiments were of different length, and each variable had a slightly different sampling regime (every 1–3 days, with some measurements missing due to technical problems). The exact sample number (n) for each SE is presented in the Table legends 1–3. The SE for estimated rates was calculated from the square root of the sum of variance for all the variables (Eq. 5–10 below). The primary papers mentioned above (Sect. 2.2.) present detailed statistical analyses, and we only refer to those here.

NPP was measured directly, and we additionally estimated the net community production (NCP). This was done in two different ways, from the organic (NCP_o) and the inorganic (NCP_i) fractions of carbon. NCP_o was calculated from changes in the organic fraction plus the exported TPC (EXP_{TPC}) according to

$$NCP_o = EXP_{TPC} + \Delta TPC + \Delta DOC. \quad (5)$$

Direct measurements using ^{14}C isotope incubations should in principal provide a higher value than summing up the difference in overall carbon balance (our NCP_o), as the latter would incorporate total respiration and not only autotrophic respiration. NCP_i was calculated through changes in the dissolved inorganic carbon pool, corrected for CO_2 gas exchange with the atmosphere (CO_{2flux}) according to

$$NCP_i = CO_{2flux} - \Delta DIC. \quad (6)$$

In order to close the budget, we estimated GPP and DOC production (DOC_{prod}). GPP is defined as the photosynthetically fixed carbon without any loss processes (i.e., NPP + autotrophic respiration). GPP can be estimated based on changes in organic (GPP_o) or inorganic (GPP_i) carbon pools, and we used these two different approaches providing a GPP range:

$$GPP_o = NCP_o + TR, \quad (7)$$

$$GPP_i = TR + CO_{2flux} - \Delta DIC. \quad (8)$$

During phase III, TR was not measured, and we estimated TR based on the ratios between NCP_o and BP to TR during phase II. The minimum production of DOC (DOC_{minp}) in the system was calculated assuming bacterial carbon uptake was taken from the DOC pool according to

$$DOC_{minp} = \Delta DOC + BP. \quad (9)$$

However, this could underestimate DOC_{prod} as a fraction of bacterial DOC uptake is respired. Without direct measurement of (heterotrophic prokaryote) bacterial respiration (BR), we estimated BR from TR. The share of active bacteria contributing to bacterial production is typically in the range of 10–30 % of the total bacterial community (Lignell et al., 2013). We used the fraction of bacterial biomass (BB) of total biomass (TB) as the maximum limit of BR ($BR \leq BB / TB$) and hence calculated max DOC production (DOC_{maxp}) according to

$$DOC_{maxp} = \Delta DOC + BP + (BB \times TR/TB). \quad (10)$$

We assumed that carbon synthesized by bacteria was added to the TPC pool.

There are a number of uncertainties in these calculations, but this budgeting exercise provides an order-of-magnitude estimate of the flow of carbon within the system and enables comparison between the treatments. The average of the two controls (M1 and M5) and the two highest CO_2 treatments (M3 and M8) were used to illustrate CO_2 effects.

3 Results and discussion

3.1 Change in plankton community, from large to small forms over time

The overall size structure of the plankton community decreased over the course of the experiment. Figure 1 illustrates the carbon content in different plankton groups in the control mesocosms. During phase I, the phytoplankton abundances increased at first in all treatments before starting to decrease at the end of phase I (Paul et al., 2015). At the start of phase II (*t17*), the phytoplankton biomass was higher than at the start of the experiment ($\sim 130\,mmol\,C\,m^{-2}$ in the controls) but decreased throughout phases II and III. The fraction of picophytoplankton increased in all treatments, but some groups of picophytoplankton increased more in the high CO_2 treatments (Crawfurd et al., 2016).

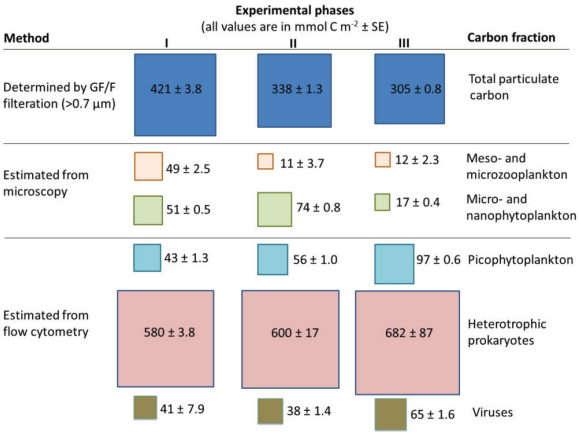

Figure 1. The different fractions of carbon in the control mesocosms (M1 and M5) at the start of phases I (*t0*), II (*t17*), and III (*t31*), in mmol C $m^{-2} \pm$ SE ($n = 2$). The differences between the controls and elevated CO_2 concentration are discussed in the text. The size of the boxes indicates the relative size of the carbon standing stocks.

Nitrogen was the limiting nutrient throughout the entire experiment (Paul et al., 2015), and primary producers are generally N-limited in the main sub-basins of the Baltic Sea (Tamminen and Andersen, 2007). The surface-to-volume ratio increases with decreasing cell size, and consequently small cells have higher nutrient affinity and are better competitors for scarce nutrient sources than large cells (Reynolds, 2006). The prevailing N limitation was likely the reason for the decreasing size structure of the phytoplankton community.

Micro- and mesozooplankton standing stock was approximately half of the phytoplankton biomass initially but decreased rapidly in the control treatments during phase I (Fig. 1). In the CO_2-enriched treatments, the zooplankton biomass also decreased but not to the same extent as in the control treatments (Spilling et al., 2016a). Overall, smaller species benefitted from the extra CO_2 addition, but there was no significant negative effect of high CO_2 on the mesozooplankton community (Lischka et al., 2015).

Bacterial biomass was the main fraction of the plankton carbon throughout the experiment. The bacterial numbers largely followed the phytoplankton biomass with an initial increase then decrease during phase I, increase during phase II, and slight decrease during phase III (Crawfurd et al., 2016). The bacterial community was controlled by mineral nutrient limitation, bacterial grazing, and viral lysis (Crawfurd et al., 2016), and bacterial growth is typically limited by N or a combination of N and C in the study area (Lignell et al., 2008, 2013).

The bacterial carbon pool was higher than the measured TPC. Part of the bacteria must have passed the GF/F filters (0.7 µm), and assuming pico- to mesoplankton was part of the TPC, >50 % of the bacterial carbon was not contributing to the measured TPC. The conversion factor from cells to carbon is positively correlated to cell size, and there is consequently uncertainty related to the absolute carbon content of the bacterial pool (we used a constant conversion factor). However, bacteria are known to be the dominating carbon share in the Baltic Sea during the N-limited summer months (Lignell et al., 2013), and their relative dominance is in line with this.

Although there is some uncertainty in the carbon estimate (Jover et al., 2014), viruses make up (due to their numerical dominance) a significant fraction of the pelagic carbon pool. Of the different plankton fractions the virioplankton have been the least studied, but their role in the pelagic ecosystem is ecologically important (Suttle, 2007; Brussaard et al., 2008; Mojica et al., 2016). Viral lysis rates were equivalent to the grazing rates for phytoplankton and for bacteria in the current study (Crawfurd et al., 2016). As mortality agents, viruses are key drivers of the regenerative microbial food web (Suttle, 2007; Brussaard et al., 2008). Overall, the structure of the plankton community reflected the nutrient status of the system: the increasing N limitation favored development of smaller cells and increased dependence of the primary producers on regenerated nutrients.

3.2 The DIC pool and atmospheric exchange of CO_2

The DIC pool was the largest carbon pool: three–four-fold higher than the DOC pool and roughly 60-fold higher than the TPC pool (Tables 1–3). After the addition of CO_2, the DIC pool was ∼7 % higher in the highest CO_2 treatment than in the control mesocosms (Table 1). The gas exchange with the atmosphere was the most apparent flux affected by CO_2 addition (Tables 1–3). Seawater in the mesocosms with added CO_2 was supersaturated; hence CO_2 outgassed throughout the experiment. The control mesocosms were initially undersaturated; hence ingassing occurred during phases I and II (Fig. 2). In the first part of phase III, the control mesocosms reached equilibrium with the atmospheric fCO_2 (Fig. 2). The gas exchange had direct effects on the DIC concentration in the mesocosms (Fig. 3). From the measured gas exchange and change in DIC it is possible to calculate the biologically mediated carbon flux. In the mesocosms with ambient CO_2 concentration, the flux measurements indicated net heterotrophy throughout the experiment. The opposite pattern, net autotrophy, was indicated in the two mesocosms with the highest CO_2 addition (Fig. 3; see also Sect. 3.7.).

3.3 The DOC pool, DOC production, and remineralization

The DOC pool increased throughout the experiment in all mesocosm bags, albeit more in the treatments with elevated

Table 1. The standing stock of total particulate carbon (TPC_{pool}), dissolved organic carbon (DOC_{pool}), and dissolved inorganic carbon (DIC_{pool}) at the start of phase I in mmol C $m^{-2} \pm$ SE ($n = 2$). The DOC_{pool} was missing some initial measurements and is the average for all mesocosms assuming that the DOC concentration was similar at the onset of the experiment. The net changes in TPC (ΔTPC), DOC (ΔDOC), and DIC (ΔDIC) are average changes in the standing stocks during phase I in mmol C m^{-2} $day^{-1} \pm$ SE ($n = 8$). Flux measurements of atmospheric gas exchange (CO_{2flux}) and exported carbon (EXP_{TPC}) plus biological rates – total respiration (TR), bacterial production (BP), and net primary production ($NPP_{^{14}C}$) – and net community production estimated based on organic carbon pools' (NCP_o) net primary production are all averages for the whole of phase I in mmol C m^{-2} $day^{-1} \pm$ SE ($n = 13$, 9, 16, 7, and 11 for CO_{2flux}, EXP_{TCP}, TR, BP, and $NPP_{^{14}C}$, respectively). SE for NCP_o was calculated from the square root of the sum of variance of the three variables used in Eq. (6). The NCP_o was calculated from the net change in carbon pools plus carbon export, whereas $NPP_{^{14}C}$ was measured carbon fixation using radio-labeled ^{14}C over a 24 h incubation period in situ. TR was measured as O_2 consumption, and for comparison with carbon fixation we used a respiratory quotient (RQ) of 1. CO_{2flux} was only calculated for the period after full addition of CO_2 (*t4–t16*). A total budget of carbon fluxes for ambient and high CO_2 treatments is presented in Fig. 5.

Phase I (*t0–t16*)						
CO_2 treatment (µatm fCO_2)	365	368	497	821	1007	1231
Mesocosm number	M1	M5	M7	M6	M3	M8
TPC_{pool}	417 ± 38	425 ± 39	472 ± 48	458 ± 38	431 ± 48	446 ± 57
DOC_{pool}	7172 ± 87	7172 ± 87	7172 ± 87	7172 ± 87	7172 ± 87	7172 ± 87
DIC_{pool}	25 158 ± 9	25 182 ± 10	25 628 ± 8	26 295 ± 22	26 637 ± 36	26 953 ± 48
ΔTPC	−4.6 ± 15	−5.2 ± 13	−8.3 ± 13	−8.2 ± 17	−7.0 ± 13	−6.3 ± 20
ΔDOC	15.5 ± 58	18.3 ± 30	18.5 ± 33	25.0 ± 36	18.5 ± 73	18.1 ± 63
ΔDIC	5.5 ± 5.2	6.9 ± 9.2	−6.1 ± 11	−24 ± 14	−32 ± 20	−49 ± 42
CO_{2flux}	4.4 ± 0.2	4.8 ± 0.3	−0.8 ± 0.5	−11 ± 1.0	−17 ± 1.4	−23 ± 2.0
EXP_{TPC}	6.6 ± 0.10	5.6 ± 0.04	5.4 ± 0.07	6.0 ± 0.07	5.6 ± 0.06	6.0 ± 0.05
TR	107 ± 9	82 ± 7	81 ± 6	80 ± 8	75 ± 8	74 ± 8
BP	27 ± 8	41 ± 6	43 ± 8	41 ± 4	36 ± 5	46 ± 9
$NPP_{^{14}C}$	4.8 ± 0.8	11.4 ± 2.1	14.9 ± 3.6	12.3 ± 2.3	11.3 ± 2.4	14.5 ± 2.7
NCP_o	17.4 ± 33	18.7 ± 20	15.6 ± 30	22.8 ± 28	17.1 ± 25	17.8 ± 28

Table 2. The standing stock of total particulate carbon (TPC_{pool}), dissolved organic carbon (DOC_{pool}), and dissolved inorganic carbon (DIC_{pool}) at the start of phase II in mmol C $m^{-2} \pm$ SE ($n = 2$). The net changes in TPC (ΔTPC), DOC (ΔDOC), and DIC (ΔDIC) are average changes in the standing stocks during phase II in mmol C m^{-2} $day^{-1} \pm$ SE ($n = 7$). Flux measurements of atmospheric gas exchange (CO_{2flux}) and exported carbon (EXP_{TPC}) plus biological rates – TR, BP, and measured ($NPP_{^{14}C}$) – and net community production estimated based on organic carbon pools (NCP_o) are all averages for phase II in mmol C m^{-2} $day^{-1} \pm$ SE ($n = 8$, 7, 14, 5, and 14 for CO_{2flux}, EXP_{TCP}, TR, BP, and $NPP_{^{14}C}$, respectively). See Table 1 legend for further details.

Phase II (*t17–t30*)						
CO_2 treatment (µatm fCO_2)	365	368	497	821	1007	1231
Mesocosm number	M1	M5	M7	M6	M3	M8
TPC_{pool}	339 ± 14	337 ± 20	331 ± 22	318 ± 9	312 ± 12	339 ± 23
DOC_{pool}	7435 ± 38	7483 ± 37	7487 ± 43	7597 ± 37	7487 ± 61	7479 ± 37
DIC_{pool}	25 247 ± 34	25 269 ± 34	25 639 ± 8	26 177 ± 25	26 413 ± 28	26 757 ± 45
ΔTPC	−2.4 ± 5	−2.3 ± 8	−1.6 ± 14	0.3 ± 6	2.8 ± 4	3.2 ± 8
ΔDOC	−0.6 ± 39	2.4 ± 30	3.6 ± 40	8.4 ± 31	11.3 ± 58	9.1 ± 36
ΔDIC	22.4 ± 12	17.6 ± 8.1	−0.4 ± 4.5	−10.5 ± 16	−14.2 ± 10	−23.1 ± 13
CO_{2flux}	1.7 ± 0.3	1.2 ± 0.3	−2.6 ± 0.3	−10 ± 0.5	−14 ± 0.6	−19 ± 1.0
EXP_{TPC}	3.3 ± 0.08	2.6 ± 0.06	2.5 ± 0.08	2.6 ± 0.06	2.8 ± 0.07	2.9 ± 0.06
TR	140 ± 7	127 ± 5	103 ± 3	103 ± 4	101 ± 5	86 ± 4
BP	66 ± 17	57 ± 8	61 ± 7	57 ± 7	43 ± 6	47 ± 6
$NPP_{^{14}C}$	3.8 ± 0.6	11.2 ± 1.9	10.8 ± 2.0	14.3 ± 2.8	10.4 ± 2.1	12.0 ± 2.5
NCP_o	0.3 ± 20	2.7 ± 15	4.5 ± 22	11.4 ± 16	16.9 ± 19	15.2 ± 16

Table 3. The standing stock of total particulate carbon (TPC_{pool}), dissolved organic carbon (DOC_{pool}), and dissolved inorganic carbon (DIC_{pool}) at the start of phase III in mmol C $m^{-2} \pm$ SE ($n = 2$). The net change in TPC (ΔTPC), DOC (ΔDOC), and DIC (ΔDIC) are average changes in the standing stocks during phase III in mmol C m^{-2} $day^{-1} \pm$ SE ($n = 6$), using the average of the last two sampling days as the end point. Flux measurements of atmospheric gas exchange (CO_{2flux}) and exported carbon (EXP_{TPC}) plus biological rates – BP and net community production estimated based on organic carbon pools (NCP_o) – are all averages for phase III in mmol C m^{-2} $day^{-1} \pm$ SE ($n = 7$, 6, and 7 for CO_{2flux}, EXP_{TCP}, and BP, respectively). See Table 1 legend for further details. During phase III we did not have direct measurements of net primary production ($NPP_{^{14}C}$) or TR.

Phase III (*t31–t43*)						
CO_2 treatment (µatm fCO_2)	365	368	497	821	1007	1231
Mesocosm number	M1	M5	M7	M6	M3	M8
TPC_{pool}	306 ± 12	304 ± 20	309 ± 20	323 ± 2	351 ± 13	384 ± 16
DOC_{pool}	7426 ± 16	7469 ± 20	7485 ± 92	7553 ± 20	7593 ± 30	7562 ± 38
DIC_{pool}	25 557 ± 9	25 545 ± 10	25 648 ± 13	26 030 ± 19	26 197 ± 31	26 371 ± 32
ΔTPC	−3.8 ± 10	0.3 ± 7	3.3 ± 14	3.3 ± 10	−1.4 ± 8	−4.8 ± 8
ΔDOC	9.8 ± 5	8.8 ± 7	8.9 ± 43	9.2 ± 10	5.7 ± 17	16.3 ± 20
ΔDIC	4.3 ± 3.9	5.5 ± 8.7	6.2 ± 11	−12.3 ± 7.2	−16.3 ± 14	−20.1 ± 14
CO_{2flux}	−0.3 ± 0.7	−0.8 ± 0.6	−3.0 ± 0.5	−7.3 ± 0.5	−9.4 ± 0.6	−13 ± 0.6
EXP_{TPC}	1.5 ± 0.07	1.4 ± 0.05	0.4 ± 0.07	1.9 ± 0.05	1.6 ± 0.04	1.7 ± 0.05
BP	31 ± 6.8	37 ± 1.4	38 ± 1.4	27 ± 2.1	17 ± 3.8	28 ± 2.3
NCP_o	7.6 ± 16	10.5 ± 13	12.7 ± 20	14.3 ± 13	6.0 ± 10	13.2 ± 14

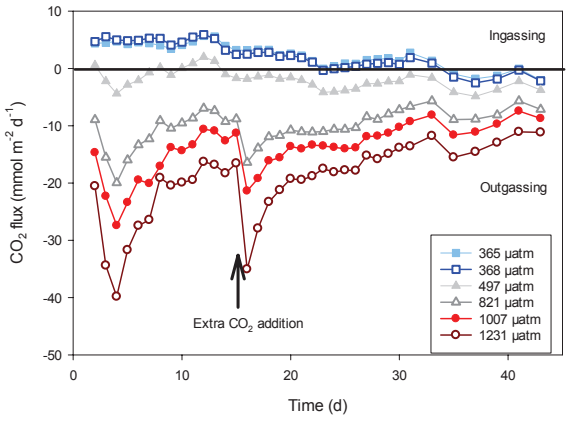

Figure 2. The calculated exchange of CO_2 between the mesocosms and the atmosphere. Positive values indicate net influx (ingassing), and negative values net outflux (outgassing) from the mesocosms. The flux was based on measurements of N_2O as a tracer gas and calculated using Eqs. (2)–(5).

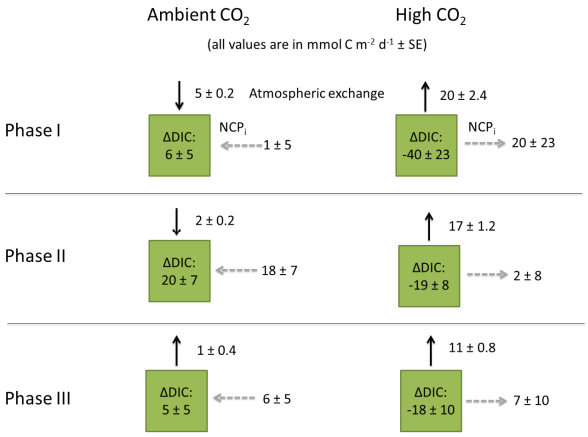

Figure 3. Change in DIC pool and the atmospheric CO_2 exchange (Fig. 2). All values are average mmol C m^{-2} $day^{-1} \pm$ SE for the three different phases ($n = 13$, 8, and 7 for phases I, II, and III, respectively) in the control mesocosms (M1 + M5) and high-CO_2 mesocosms (M3 + M8). Solid black arrows indicate measured fluxes. Dashed grey arrows are estimated by closing the budget and indicate the net community production based on inorganic carbon budget (NCP_i), which equals biological uptake or release of CO_2.

CO_2 concentration. The initial DOC standing stock in all treatments was approximately 7200 mmol C m^{-2}. At the end of the experiment, the DOC pool was ∼2 % higher in the two highest CO_2 treatments than in the controls (Fig. 4), and there is statistical support for this difference between CO_2 treatments (phase III, $p = 0.05$) (Paul et al., 2015). Interestingly, the data do not point to a substantially higher release of DOC at high CO_2 (Figs. 4 and 5). The bacterial production was notably lower during phase II in the high CO_2 treatments (Hornick et al., 2016) and of similar magnitude to the rate of change in DOC pool (Tables 2 and 3), indicating reduced bacterial uptake and remineralization of DOC. The combined results suggest that the increase in the DOC pool at high CO_2 was related to reduced DOC loss (uptake by bacteria), rather than increased release of DOC by the plankton community, at elevated CO_2 concentration.

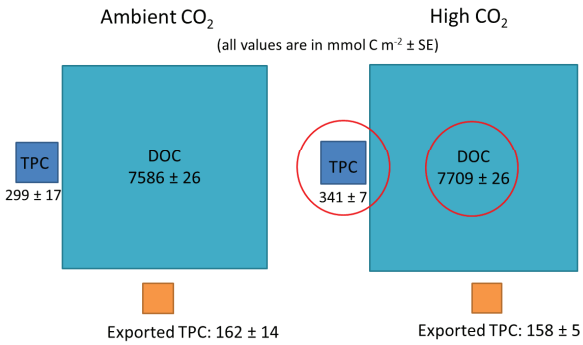

Figure 4. Standing stocks of total particulate carbon (TPC) and dissolved organic carbon (DOC) at the last day of the experiment (*t43*), plus the sum of exported TPC throughout the experiment; all values are in mmol C m^{-2} ± SE ($n = 2$). The values are averages of the two controls (M1 and M5) and the two highest CO_2 treatments (M3 and M8). Red circles indicate statistically significant higher standing stocks in the high CO_2 treatments (further details in text). The size of the boxes indicates the relative size of the carbon standing stocks and export.

The Baltic Sea is affected by large inflow of freshwater containing high concentrations of refractory DOC, such as humic substances, and the concentration in the Gulf of Finland is typically 400–500 µmol C L^{-1} (Hoikkala et al., 2015). The large pool of DOC and turnover times of ~200 days (Tables 1–3) are most likely a reflection of the relatively low fraction of labile DOC, but bacterial limitation of mineral nutrients can also increase turnover times (Thingstad et al., 1997).

The DOC pool has been demonstrated to aggregate into transparent exopolymeric particles (TEPs) under certain circumstances, which can increase sedimentation at high CO_2 levels (Riebesell et al., 2007). We did not have any direct measurements of TEP, but any CO_2 effect on its formation is highly dependent on the plankton community and its physiological status (MacGilchrist et al., 2014). No observed effect of CO_2 treatment on carbon export suggests that we did not have a community where the TEP production was any different between the treatments used.

3.4 The TPC pool and export of carbon

There was a positive effect of elevated CO_2 on TPC relative to the controls. At the start of the experiment, the measured TPC concentration in the enclosed water columns was 400–500 mmol C m^{-2} (Table 1). The TPC pool decreased over time, albeit less in the high CO_2 treatment, and at the end of the experiment the standing stock of TPC was ~6 % higher (phase III, $p = 0.01$; Paul et al., 2015) in the high CO_2 treatment (Fig. 4).

The export of TPC was not dependent on the CO_2 concentration but varied temporally. The largest flux of TPC out of the mesocosms occurred during phase I with ~6 mmol C m^{-2} day^{-1}. It decreased to ~3 mmol C m^{-2} day^{-1} during phase II and was ~2 mmol C m^{-2} day^{-1} during phase III (Tables 1–3). The exported carbon as the percent of average TPC standing stock similarly decreased from ~1.3 % during phase I to 0.3–0.5 % during phase III. The initial increase in the autotrophic biomass was likely the reason for relatively more of the carbon settling in the mesocosms in the beginning of the experiment, whereas the decreasing carbon export was most likely caused by the shift towards a plankton community depending on recycled nitrogen. The relatively high initial sedimentation reduced the overall suspended TPC and also the average plankton size in the community.

3.5 Biological rates: respiration

TR was always lower in the CO_2-enriched treatments (Tables 1–2). The average TR was 83 mmol C m^{-2} day^{-1} during phase I, and initially without any detectable treatment effect. The respiration rate started to be lower in the high CO_2 treatments than in the controls in the beginning of phase II. At the end of phase II there was a significant difference ($p = 0.02$; Spilling et al., 2016a) between the treatments (Table 2) and 40 % lower respiration rate in the highest CO_2 treatment than in the controls (Spilling et al., 2016a).

Cytosol pH is close to neutral in most organisms, and reduced energetic cost for internal pH regulation (e.g., transport of H^+) and at lower external pH levels could be one factor reducing respiration (Smith and Raven, 1979). Hopkinson et al. (2010) found indirect evidence of decreased respiration and also proposed that increased CO_2 concentration (i.e., decreased pH) reduced metabolic cost of remaining intracellular homeostasis. Mitochondrial respiration in plant foliage decreases in high-CO_2 environments, possibly affected by respiratory enzymes or other metabolic processes (Amthor, 1991; Puhe and Ulrich, 2012). Most inorganic carbon in water is in the form of bicarbonate (HCO_3^-) at relevant pH, and many aquatic autotrophs have developed carbon-concentrating mechanisms (CCMs) (e.g., Singh et al., 2014) that could reduce the cost of growth (Raven, 1991). There are some studies that have pointed to savings of metabolic energy due to downregulation of carbon-concentrating mechanisms (Hopkinson et al., 2010) or overall photosynthetic apparatus (Sobrino et al., 2014) in phytoplankton at high CO_2 concentrations. Yet other studies of the total plankton community have pointed to no effect or increased respiration at elevated CO_2 concentration (Li and Gao, 2012; Tanaka et al., 2013), and the metabolic changes behind reduced respiration remain an open question. Membrane transport of H^+ is sensitive to changes in external pH, but the physiological impacts of increasing H^+ need further study to better address effects of ocean acidification (Taylor et al., 2012). An important aspect is also to consider the microenvironment surrounding plankton; exchange of nutrients and gases takes

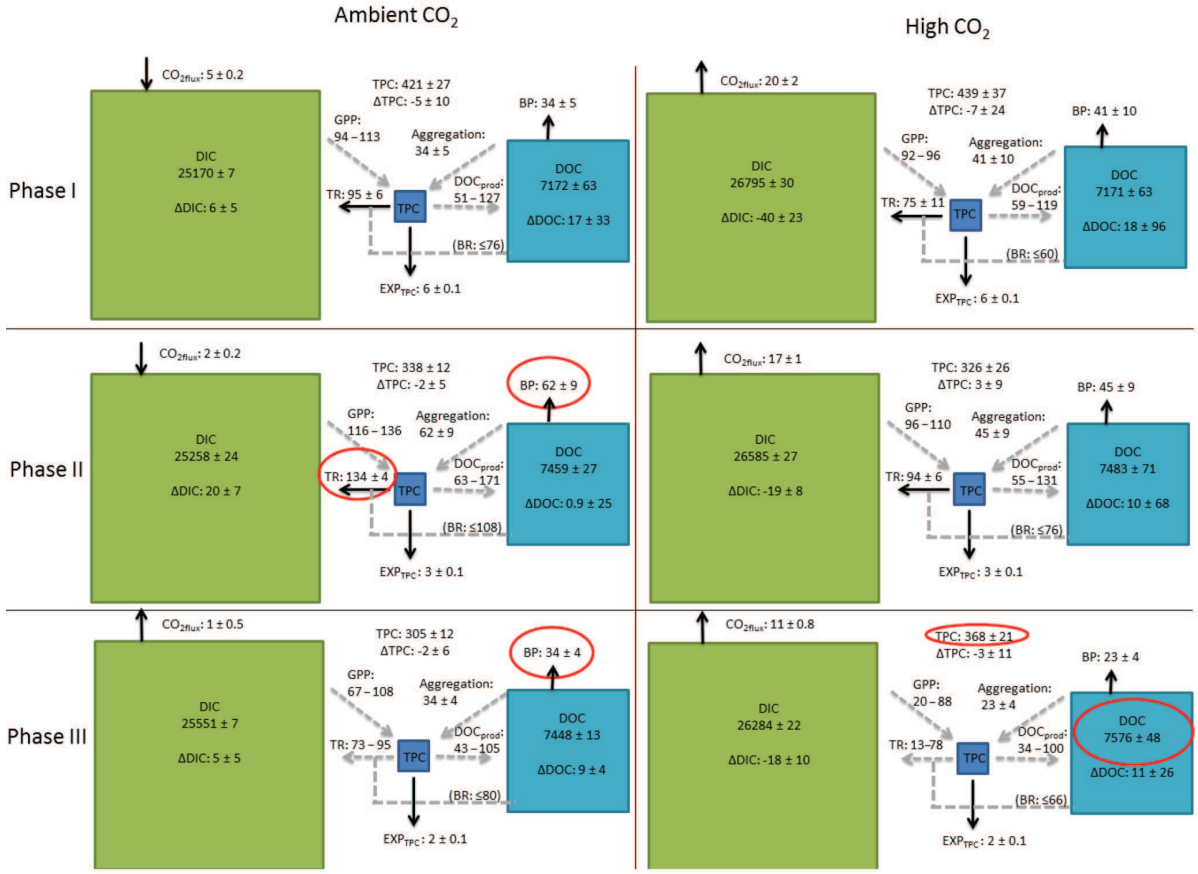

Figure 5. Average carbon standing stocks and flow in the control mesocosms (M1 + M5) and high-CO_2 mesocosms (M3 + M8) during the three phases of the experiment. All carbon stocks (squares) – dissolved inorganic carbon (DIC), total particulate carbon (TPC), and dissolved organic carbon (DOC) – are averages from the start of the period in mmol C m^{-2} ± SE ($n = 2$). Fluxes (arrows) and net changes (Δ) are averages for the whole phase in mmol C m^{-2} day^{-1} ± SE (n presented in Table legends 1–3). Solid black arrows indicate measured fluxes (Tables 1–3): TR, BP, and exported TPC (EXP_{TPC}). Dashed grey arrows are estimated by closing the budget: gross primary production (GPP) using Eqs. (7) and (8), and DOC production (DOC_{prod}) using Eqs. (9) and (10). Bacterial respiration was calculated using Eq. (10) and is a share of TR (indicated by the parenthesis). Aggregation was assumed to equal BP. Red circles indicate statistically significant higher values ($p < 0.05$, tests presented in the primary papers described in Sect. 2.2.). The size of the boxes indicates the relative size of the carbon standing stocks.

place through the boundary layer, which might have very different pH properties than bulk water measurements (Flynn et al., 2012).

3.6 Biological rates: bacterial production

BP became lower in the high CO_2 treatment in the latter part of the experiment. During phase I, BP ranged from 27 to 46 mmol C m^{-2} day^{-1} (Table 1). The difference in BP between treatments became apparent in phases II and III of the experiment. The average BP was 18 and 24 % higher in the controls than in the highest CO_2 treatments during phases II and III, respectively (Tables 2 and 3).

The lower bacterial production accounted for ∼ 40 % of the reduced respiration during phase II, and the reduced respiration described above could at least partly be explained by the lower bacterial activity. This raises an interesting question: what was the mechanism behind the reduced bacterial production/respiration in the high CO_2 treatment? There are examples of decreased bacterial production (Motegi et al., 2013) and respiration (Teira et al., 2012) at elevated CO_2 concentration. However, most previous studies have reported no change (Allgaier et al., 2008) or a higher bacterial production at elevated CO_2 concentration (Grossart et al., 2006; Piontek et al., 2010; Endres et al., 2014). The latter was also supported by the recent study of Bunse et al. (2016), de-

scribing upregulation of bacterial genes related to respiration, membrane transport, and protein metabolism at elevated CO_2 concentration; however, this effect was not evident when inorganic nutrients had been added (high Chl *a* treatment).

In this study, the lower bacterial activity in the high CO_2 treatments could either be due to limitation and/or inhibition of bacterial growth or driven by difference in loss processes. Bacterial grazing and viral lysis were higher in the high CO_2 treatments during periods of the experiment (Crawfurd et al., 2016) and would at least partly be the reason for the reduced bacterial production at high CO_2 concentration.

N limitation increased during the experiment (Paul et al., 2015), and mineral nutrient limitation of bacteria can lead to accumulation of DOC, i.e., reduced bacterial uptake (Thingstad et al., 1997), similar to our results. Bacterial N limitation is common in the area during summer (Lignell et al., 2013), however, this N limitation was not apparently different in the controls (Paul et al., 2015), and CO_2 did not affect N fixation (Paul et al., 2016a). In a scenario where the competition for N is fierce, the balance between bacteria and similar sized picophytoplankton could be tilted in favor of phytoplankton if they gain an advantage by having easier access to carbon, i.e., CO_2 (Hornick et al., 2016). We have not found evidence in the literature that bacterial production will be suppressed in the observed pH range inside the mesocosms, varying from approximately pH 8.1 in the control to pH 7.6 in the highest fCO_2 treatment (Paul et al., 2015), although enzyme activity seems to be affected even by moderate pH changes. For example, some studies report on an increase in protein-degrading enzyme leucine aminopeptidase activities at reduced pH (Grossart et al., 2006; Piontek et al., 2010; Endres et al., 2014), whereas others indicate a reduced activity of this enzyme (Yamada and Suzumura, 2010). A range of other factors affect this enzyme, for example the nitrogen source and salinity (Stepanauskas et al., 1999), and any potential interaction effects with decreasing pH are not yet resolved. Any pH-induced changes in bacterial enzymatic activity could potentially affect bacterial production.

3.7 Biological rates: primary production

There was an effect of CO_2 concentration on the net community production based on the organic carbon fraction (NCP_o). NCP_o was higher during phase I than during the rest of the experiments and during this initial phase without any apparent CO_2 effect. There was no consistent difference between CO_2 treatments for $NPP_{^{14}C}$ ($p > 0.1$), but NCP_o increased with increasing CO_2 enrichment during phase II (phase II; linear regression $p = 0.003$; $R^2 = 0.91$). This was caused by the different development in the TPC and DOC pools. The pattern of GPP was similar to NCP_o during phases I and II. During phase III there was no respiration or $NPP_{^{14}C}$ measurements, and the estimated GPP is more uncertain. The NCP_o and GPP indicated a smaller difference between treatments during phase III than phase II.

The measures of $NPP_{^{14}C}$ and NCP_o were of a similar magnitude (Tables 1–3). During phase I, $NPP_{^{14}C} < NCP_o$ (Table 1); this relationship reversed for most treatments during phase II, with the exception of the highest CO_2 levels (Table 2). The difference between $NPP_{^{14}C}$ and NCP_o suggests that observed reduction in respiration at elevated CO_2 could be mainly heterotrophic respiration. However, in terms of the $NPP_{^{14}C} < NCP_o$, the uncertainty seems to be higher than the potential signal of heterotrophic respiration. This would also indicate that the $NPP_{^{14}C}$ during phase I have been underestimated, in particular for the control mesocosm M1. During phase II, the $NPP_{^{14}C}$ was higher than NCP_o, except for the two highest CO_2 treatments, more in line with our assumption of $NPP_{^{14}C} > NCP_o$. The systematic offset in $NPP_{^{14}C}$ during phase I could be due to changed parameterization during incubation in small volumes (8 mL; Spilling et al., 2016a), for example increased loss due to grazing.

The results of the DIC pool and atmospheric exchange of CO_2 provide another way of estimating the net community production based on inorganic carbon (NCP_i). There was some discrepancy between the NCP_o and NCP_i as the latter suggested net heterotrophy in the ambient CO_2 treatments, whereas the high CO_2 treatments were net autotrophic during all three phases of the experiment (Fig. 3). For the NCP_o there was no indication of net heterotrophy at ambient CO_2 concentration. In terms of the absolute numbers, the NCP_i estimate is probably more uncertain than NCP_o. Calculating the CO_2 atmospheric exchange from the measurements of a tracer gas involves several calculation steps (Eq. 1–4), each adding uncertainty to the calculation. However, both estimations (NCP_i and NCP_o) indicate that increased CO_2 concentrations lead to higher overall community production, supporting our overall conclusion.

3.8 Budget

A carbon budget for the two control mesocosms and two highest CO_2 additions is presented in Fig. 5. During phase I the estimated GPP was ~ 100 mmol C fixed m^{-2} day^{-1}, from which 75–95 % was respired, ~ 1 % ended up in the TPC (including export), and 5–25 % added to the DOC pool. The main difference between CO_2 treatments became apparent during phase II when the NCP_o was higher in the elevated CO_2 treatments. The respiration loss increased to ~ 100 % of GPP at the ambient CO_2 concentration, whereas respiration was lower (85–95 % of GPP) in the highest CO_2 treatment. Bacterial production was ~ 30 % lower, on average, at the highest CO_2 concentration than in the controls during phase II. The share of NCP_o of GPP ranged from 2 to 20 %, and the minimum flux to the DOC pool was 11 to 18 % of TPC.

The overall budget was calculated by using the direct measurements of changes in standing stocks and fluxes of export, respiration, and bacterial production rates. The most robust data are the direct measurements of carbon standing stocks

and their development (e.g., ΔTPC). These are based on well-established analytical methods with relatively low SE of the carbon pools. However, the dynamic nature of these pools made the relative SE for the rate of change much higher, reflecting that the rate of change varied considerably within the different phases.

The rate variables, calculated based on conversion factors, have greater uncertainty, although their SEs were relatively low, caused by uncertainty in the conversion steps. For example, the RQ was set to 1, which is a good estimate for carbohydrate oxidation. For lipids and proteins the RQ is close to 0.7, but in a natural environment RQ is often > 1 (Berggren et al., 2012) and is affected by physiological state, e.g., nutrient limitation (Romero-Kutzner et al., 2015). Any temporal variability in the conversion factors would directly change the overall budget calculations, e.g., RQ affecting total respiration and gross primary production estimates. However, the budget provides an order-of-magnitude estimate of the carbon flow within the system. Some of the variables such as GPP were estimated using different approaches, providing a more robust comparison of the different treatments.

The primary effect of increasing CO_2 concentration was the higher standing stocks of TPC and DOC compared with ambient CO_2 concentration. The increasing DOC pool and relatively higher TPC pool were driven by reduced respiration and bacterial production at elevated CO_2 concentration. Decreasing respiration rate reduced the recycling of organic carbon back to the DIC pool. The lower respiration and bacterial production also indicate reduced remineralization of DOC. These two effects caused the higher TPC and DOC pools in the elevated CO_2 treatments. The results highlight the importance of looking beyond net changes in carbon standing stocks to understand how carbon fluxes are affected under increasing ocean acidification.

4 Data availability

The data presented in this paper can be found in Paul et al. (2016b) and Spilling et al. (2016b).

Acknowledgements. We would like to thank all of the staff at Tvärminne Zoological Station, for great help during this experiment, and Michael Sswat for carrying out the TPC filtrations. We also gratefully acknowledge the captain and crew of R/V *ALKOR* (AL394 and AL397) for their work transporting, deploying, and recovering the mesocosms. The collaborative mesocosm campaign was funded by BMBF projects BIOACID II (FKZ 03F06550) and SOPRAN phase II (FKZ 03F0611). Additional financial support for this study came from the Academy of Finland (KS – Decisions nos. 259164 and 263862) and Walter and Andrée de Nottbeck Foundation (KS). Thomas Hornick and Hans-Peter Grossart were financially supported by the SAW project TemBi of the Leibniz Foundation. Corina P. D. Brussaard was financially supported by the Darwin project, the Royal Netherlands Institute for Sea Research (NIOZ), and the EU project MESOAQUA (grant agreement number 228224).

Edited by: J.-P. Gattuso
Reviewed by: F. Gazeau and one anonymous referee

References

Allgaier, M., Riebesell, U., Vogt, M., Thyrhaug, R., and Grossart, H.-P.: Coupling of heterotrophic bacteria to phytoplankton bloom development at different pCO_2 levels: a mesocosm study, Biogeosciences, 5, 1007–1022, doi:10.5194/bg-5-1007-2008, 2008.

Amthor, J.: Respiration in a future, higher-CO_2 world, Plant Cell Environ., 14, 13–20, 1991.

Badr, E.-S. A., Achterberg, E. P., Tappin, A. D., Hill, S. J., and Braungardt, C. B.: Determination of dissolved organic nitrogen in natural waters using high temperature catalytic oxidation, Trend. Anal. Chem., 22, 819–827, 2003.

Berggren, M., Lapierre, J.-F., and del Giorgio, P. A.: Magnitude and regulation of bacterioplankton respiratory quotient across freshwater environmental gradients, ISME J., 6, 984–993, 2012.

Bermúdez, J. R., Winder, M., Stuhr, A., Almén, A. K., Engström-Öst, J., and Riebesell, U.: Effect of ocean acidification on the structure and fatty acid composition of a natural plankton community in the Baltic Sea, Biogeosciences Discuss., doi:10.5194/bg-2015-669, in review, 2016.

Boxhammer, T., Bach, L. T., Czerny, J., and Riebesell, U.: Technical note: Sampling and processing of mesocosm sediment trap material for quantitative biogeochemical analysis, Biogeosciences, 13, 2849–2858, doi:10.5194/bg-13-2849-2016, 2016.

Brussaard, C. P. D.: Optimization of procedures for counting viruses by flow cytometry, Appl. Environ. Microb., 70, 1506–1513, 2004.

Brussaard, C. P. D., Wilhelm, S. W., Thingstad, F., Weinbauer, M. G., Bratbak, G., Heldal, M., Kimmance, S. A., Middelboe, M., Nagasaki, K., Paul, J. H., Schroeder, D. C., Suttle, C. A., Vaqué, D., and Wommack, K. E.: Global-scale processes with a nanoscale drive: the role of marine viruses, ISME J., 2, 575–578, 2008.

Bunse, C., Lundin, D., Karlsson, C. M., Vila-Costa, M., Palovaara, J., Akram, N., Svensson, L., Holmfeldt, K., González, J. M., Calvo, E., Pelejero, C., Marrasé, C., Dopson, M., Gasol, J. M., and Pinhassi J.: Response of marine bacterioplankton pH homeostasis gene expression to elevated CO_2, Nature Clim. Change, 6, 483–487, 2016.

Crawfurd, K. J., Brussaard, C. P. D., and Riebesell, U.: Shifts in the microbial community in the Baltic Sea with increasing CO_2, Biogeosciences Discuss., doi:10.5194/bg-2015-606, in review, 2016.

Czerny, J., Schulz, K. G., Boxhammer, T., Bellerby, R. G. J., Büdenbender, J., Engel, A., Krug, S. A., Ludwig, A., Nachtigall, K., Nondal, G., Niehoff, B., Silyakova, A., and Riebesell, U.: Implications of elevated CO_2 on pelagic carbon fluxes in an Arctic mesocosm study – an elemental mass balance approach, Biogeosciences, 10, 3109–3125, doi:10.5194/bg-10-3109-2013, 2013a.

Czerny, J., Schulz, K. G., Ludwig, A., and Riebesell, U.: Technical Note: A simple method for air–sea gas exchange measurements

in mesocosms and its application in carbon budgeting, Biogeosciences, 10, 1379–1390, doi:10.5194/bg-10-1379-2013, 2013b.

de Kluijver, A., Soetaert, K., Schulz, K. G., Riebesell, U., Bellerby, R. G. J., and Middelburg, J. J.: Phytoplankton-bacteria coupling under elevated CO_2 levels: a stable isotope labelling study, Biogeosciences, 7, 3783–3797, doi:10.5194/bg-7-3783-2010, 2010.

Egge, J. K., Thingstad, T. F., Larsen, A., Engel, A., Wohlers, J., Bellerby, R. G. J., and Riebesell, U.: Primary production during nutrient-induced blooms at elevated CO_2 concentrations, Biogeosciences, 6, 877–885, doi:10.5194/bg-6-877-2009, 2009.

Endres, S., Galgani, L., Riebesell, U., Schulz, K.-G., and Engel, A.: Stimulated bacterial growth under elevated pCO_2: results from an off-shore mesocosm study, Plos One, 9, e99228, doi:10.1371/journal.pone.0099228, 2014.

Engel, A., Borchard, C., Piontek, J., Schulz, K. G., Riebesell, U., and Bellerby, R.: CO_2 increases ^{14}C primary production in an Arctic plankton community, Biogeosciences, 10, 1291–1308, doi:10.5194/bg-10-1291-2013, 2013.

Flynn, K. J., Blackford, J. C., Baird, M. E., Raven, J. A., Clark, D. R., Beardall, J., Brownlee, C., Fabian, H., and Wheeler, G. L.: Changes in pH at the exterior surface of plankton with ocean acidification, Nature Clim. Change, 2, 510–513, 2012.

Grossart, H.-P., Allgaier, M., Passow, U., and Riebesell, U.: Testing the effect of CO_2 concentration on the dynamics of marine heterotrophic bacterioplankton, Limnol. Oceanogr., 51, 1–11, 2006.

Heinänen, A. and Kuparinen, J.: Horizontal variation of bacterioplankton in the Baltic Sea, Appl. Environ. Microb., 57, 3150–3155, 1991.

Hoikkala, L., Kortelainen, P., Soinne, H., and Kuosa, H.: Dissolved organic matter in the Baltic Sea, J. Marine Syst., 142, 47–61, 2015.

Hopkinson, B. M., Xu, Y., Shi, D., McGinn, P. J., and Morel, F. M.: The effect of CO_2 on the photosynthetic physiology of phytoplankton in the Gulf of Alaska, Limnol. Oceanogr., 55, 2011–2024, 2010.

Hornick, T., Bach, L. T., Crawfurd, K. J., Spilling, K., Achterberg, E. P., Woodhouse, J. N., Schultz, K. G., Brussaard, C. P. D., Riebesell, U., and Grossart, H.-P.: Ocean acidification impacts bacteria-phytoplankton coupling at low nutrient-conditions, Biogeosciences Discuss., doi:10.5194/bg-2016-61, in review, 2016.

Jover, L. F., Effler, T. C., Buchan, A., Wilhelm, S. W., and Weitz, J. S.: The elemental composition of virus particles: implications for marine biogeochemical cycles, Nat. Rev. Microbiol., 12, 519–528, 2014.

Le Quéré, C., Raupach, M. R., Canadell, J. G., Marland, G., Bopp, L., Ciais, P., Conway, T. J., Doney, S. C., Feely, R. A., and Foster, P.: Trends in the sources and sinks of carbon dioxide, Nat. Geosci., 2, 831–836, 2009.

Li, W. and Gao, K.: A marine secondary producer respires and feeds more in a high CO_2 ocean, Mar. Pollut. Bull., 64, 699–703, 2012.

Lignell, R., Hoikkala, L., and Lahtinen, T.: Effects of inorganic nutrients, glucose and solar radiation on bacterial growth and exploitation of dissolved organic carbon and nitrogen in the northern Baltic Sea, Aquat. Microb. Ecol., 51, 209–221, 2008.

Lignell, R., Haario, H., Laine, M., and Thingstad, T. F.: Getting the "right" parameter values for models of the pelagic microbial food web, Limnol. Oceanogr., 58, 301–313, 2013.

Lischka, S., Bach, L. T., Schulz, K.-G., and Riebesell, U.: Micro- and mesozooplankton community response to increasing CO_2 levels in the Baltic Sea: insights from a large-scale mesocosm experiment, Biogeosciences Discuss., 12, 20025–20070, doi:10.5194/bgd-12-20025-2015, 2015.

MacGilchrist, G. A., Shi, T., Tyrrell, T., Richier, S., Moore, C. M., Dumousseaud, C., and Achterberg, E. P.: Effect of enhanced pCO_2 levels on the production of dissolved organic carbon and transparent exopolymer particles in short-term bioassay experiments, Biogeosciences, 11, 3695–3706, doi:10.5194/bg-11-3695-2014, 2014.

Marie, D., Brussaard, C. P. D., Thyrhaug, R., Bratbak, G., and Vaulot, D.: Enumeration of marine viruses in culture and natural samples by flow cytometry, Appl. Environ. Microb., 65, 45–52, 1999.

Menden-Deuer, S. and Lessard, E. J.: Carbon to volume relationships for dinoflagellates, diatoms, and other protist plankton, Limnol. Oceanogr., 45, 569–579, 2000.

Mojica, K. D., Huisman, J., Wilhelm, S. W., and Brussaard, C. P. D.: Latitudinal variation in virus-induced mortality of phytoplankton across the North Atlantic Ocean, ISME J., 10, 500–513, 2016.

Motegi, C., Tanaka, T., Piontek, J., Brussaard, C. P. D., Gattuso, J.-P., and Weinbauer, M. G.: Effect of CO_2 enrichment on bacterial metabolism in an Arctic fjord, Biogeosciences, 10, 3285–3296, doi:10.5194/bg-10-3285-2013, 2013.

Niiranen, S., Yletyinen, J., Tomczak, M. T., Blenckner, T., Hjerne, O., MacKenzie, B. R., Müller-Karulis, B., Neumann, T., and Meier, H.: Combined effects of global climate change and regional ecosystem drivers on an exploited marine food web, Glob. Change Biol., 19, 3327–3342, 2013.

Olenina, I., Hajdu, S., Edler, L., Andersson, A., Wasmund, N., Busch, S., Göbel, J., Gromisz, S., Huseby, S., Huttunen, M., Jaanus, A., Kokkonen, P., Ledaine, I., and Niemkiewicz, E.: Biovolumes and size-classes of phytoplankton in the Baltic Sea, HELCOM, Balt. Sea Environ. Proc., No. 106, 144 pp., 2006.

Paul, A. J., Bach, L. T., Schulz, K.-G., Boxhammer, T., Czerny, J., Achterberg, E. P., Hellemann, D., Trense, Y., Nausch, M., Sswat, M., and Riebesell, U.: Effect of elevated CO_2 on organic matter pools and fluxes in a summer Baltic Sea plankton community, Biogeosciences, 12, 6181–6203, doi:10.5194/bg-12-6181-2015, 2015.

Paul, A. J., Achterberg, E. P., Bach, L. T., Boxhammer, T., Czerny, J., Haunost, M., Schulz, K.-G., Stuhr, A., and Riebesell, U.: No observed effect of ocean acidification on nitrogen biogeochemistry in a summer Baltic Sea plankton community, Biogeosciences, 13, 3901–3913, doi:10.5194/bg-13-3901-2016, 2016a.

Paul, A., Schulz, K. G., Achterberg, E. P., Hellemann, D., Nausch, M., Boxhammer, T., Bach, L. T., and Trense, Y.: KOSMOS Finland 2012 mesocosm study: carbonate chemistry, particulate and dissolved matter pools, and phytoplankton community composition using marker pigments (CHEMTAX), doi:10.1594/PANGAEA.863032, 2016b.

Piontek, J., Lunau, M., Händel, N., Borchard, C., Wurst, M., and Engel, A.: Acidification increases microbial polysaccharide degradation in the ocean, Biogeosciences, 7, 1615–1624, doi:10.5194/bg-7-1615-2010, 2010.

Puhe, J. and Ulrich, B.: Global climate change and human impacts on forest ecosystems: postglacial development, present situation and future trends in Central Europe, Ecological studies – analysis and synthesis, Springer, Berlin, Germany, 476 pp., 2012.

Raven, J. A.: Physiology of inorganic C acquisition and implications for resource use efficiency by marine phytoplankton: relation to increased CO_2 and temperature, Plant Cell Environ., 14, 779–794, 1991.

Reynolds, C. S.: Ecology of phytoplankton, Cambridge University Press, Cambridge, UK, 535 pp., 2006.

Riebesell, U., Schulz, K. G., Bellerby, R., Botros, M., Fritsche, P., Meyerhöfer, M., Neill, C., Nondal, G., Oschlies, A., and Wohlers, J.: Enhanced biological carbon consumption in a high CO_2 ocean, Nature, 450, 545–548, 2007.

Riebesell, U., Achterberg, E. P., Brussaard, C. P. D., Engström-Öst, J., Gattuso, J.-P., Grossart, H.-P., and Schulz, K. G. (Eds): Effects of rising CO_2 on a Baltic Sea plankton community: ecological and biogeochemical impacts, Biogeosciences, http://www.biogeosciences.net/special_issue204.html, 2015.

Romero-Kutzner, V., Packard, T., Berdalet, E., Roy, S., Gagné, J., and Gómez, M.: Respiration quotient variability: bacterial evidence, Mar. Ecol.-Prog. Ser., 519, 47–59, 2015.

Simon, M. and Azam, F.: Protein content and protein synthesis rates of planktonic marine bacteria, Mar. Ecol.-Prog. Ser., 51, 201–213, 1989.

Singh, S. K., Sundaram, S., and Kishor, K.: Photosynthetic microorganisms: Mechanism for carbon concentration, Springer, Berlin, Germany, 131 pp., 2014.

Smith, F. and Raven, J. A.: Intracellular pH and its regulation, Ann. Rev. Plant Physio., 30, 289–311, 1979.

Sobrino, C., Segovia, M., Neale, P., Mercado, J., García-Gómez, C., Kulk, G., Lorenzo, M., Camarena, T., van de Poll, W., Spilling, K., and Ruan, Z.: Effect of CO_2, nutrients and light on coastal plankton. IV. Physiological responses, Aquat. Biol., 22, 77–93, 2014.

Spilling, K., Paul, A. J., Virkkala, N., Hastings, T., Lischka, S., Stuhr, A., Bermúdez, R., Czerny, J., Boxhammer, T., Schulz, K. G., Ludwig, A., and Riebesell, U.: Ocean acidification decreases plankton respiration: evidence from a mesocosm experiment, Biogeosciences, 13, 4707–4719, doi:10.5194/bg-13-4707-2016, 2016a.

Spilling, K., Paul, A., Virkkala, N., Hastings, T., Lischka, S., Stuhr, A., Bermúdez, R., Czerny, J., Boxhammer, T., Schulz, K. G., Ludwig, A., and Riebesell, U.: KOSMOS Finland 2012 mesocosm study: primary production and respiration, doi:10.1594/PANGAEA.863933, 2016b.

Steeman-Nielsen, E.: The use of radioactive carbon for measuring organic production in the sea, J. Cons. Int. Explor. Mer., 18, 117–140, 1952.

Stepanauskas, R., Edling, H., and Tranvik, L. J.: Differential dissolved organic nitrogen availability and bacterial aminopeptidase activity in limnic and marine waters, Microb. Ecol., 38, 264–272, 1999.

Steward, G. F., Fandino, L. B., Hollibaugh, J. T., Whitledge, T. E., and Azam, F.: Microbial biomass and viral infections of heterotrophic prokaryotes in the sub-surface layer of the central Arctic Ocean, Deep-Sea Res. Pt. I, 54, 1744–1757, 2007.

Suttle, C. A.: Marine viruses – major players in the global ecosystem, Nat. Rev. Microbiol., 5, 801–812, 2007.

Tamminen, T. and Andersen, T.: Seasonal phytoplankton nutrient limitation patterns as revealed by bioassays over Baltic Sea gradients of salinity and eutrophication, Mar. Ecol.-Prog. Ser., 340, 121–138, 2007.

Tanaka, T., Alliouane, S., Bellerby, R. G. B., Czerny, J., de Kluijver, A., Riebesell, U., Schulz, K. G., Silyakova, A., and Gattuso, J.-P.: Effect of increased pCO_2 on the planktonic metabolic balance during a mesocosm experiment in an Arctic fjord, Biogeosciences, 10, 315–325, doi:10.5194/bg-10-315-2013, 2013.

Taylor, A. R., Brownlee, C., and Wheeler, G. L.: Proton channels in algae: reasons to be excited, Trends Plant Sci., 17, 675–684, 2012.

Teira, E., Fernández, A., Álvarez-Salgado, X. A., García-Martín, E. E., Serret, P., and Sobrino, C.: Response of two marine bacterial isolates to high CO_2 concentration, Mar. Ecol.-Prog. Ser., 453, 27–36, 2012.

Thingstad, T. F., Hagström, Å., and Rassoulzadegan, F.: Accumulation of degradable DOC in surface waters: Is it caused by a malfunctioning microbialloop?, Limnol. Oceanogr., 42, 398–404, 1997.

Veldhuis, M. J. and Kraay, G. W.: Phytoplankton in the subtropical Atlantic Ocean: towards a better assessment of biomass and composition, Deep-Sea Res. Pt. I, 51, 507–530, 2004.

Wanninkhof, R. and Knox, M.: Chemical enhancement of CO_2 exchange in natural waters, Limnol. Oceanogr., 41, 689–697, 1996.

Waterbury, J. B., Watson, S. W., Valois, F. W., and Franks, D. G.: Biological and ecological characterization of the marine unicellular cyanobacterium Synechococcus, Can. B. Fish. Aquat. Sci., 214, 71–120, 1986.

Weiss, R. and Price, B.: Nitrous oxide solubility in water and seawater, Mar. Chem., 8, 347–359, 1980.

Wiebe, P. H.: Functional regression equations for zooplankton displacement volume, wet weight, dry weight, and carbon: a correction, Fish. B., 86, 833–835, 1988.

Yamada, N. and Suzumura, M.: Effects of seawater acidification on hydrolytic enzyme activities, J. Oceanogr., 66, 233–241, 2010.

4. Chapter 4 - Manuscript 3

Ocean Acidification Experiments in Large-Scale Mesocosms Reveal Similar Dynamics of Dissolved Organic Matter Production and Biotransformation

---

Maren Zark[1]*, Nadine K. Broda[1], **Thomas Hornick[2]**, Hans-Peter Grossart[2,3], Ulf Riebesell[4] and Thorsten Dittmar[1]

Published in *Frontiers in Marine Science***

[1] Research Group for Marine Geochemistry (ICBM-MPI Bridging Group), Institute for Chemistry and Biology of the Marine Environment, Carl von Ossietzky University of Oldenburg, Oldenburg, Germany,

[2] Experimental Limnology, Leibniz-Institute of Freshwater Ecology and Inland Fisheries, Stechlin, Germany

[3] Institute for Biochemistry and Biology, University of Potsdam, Potsdam, Germany

[4] GEOMAR Helmholtz Centre for Ocean Research Kiel, Kiel, Germany

*corresponding author: maren.zark@uni-oldenburg.de (M. Zark)

** manuscript formatted in style of *Frontiers in Marine Science*

frontiers in Marine Science

ORIGINAL RESEARCH
published: 05 September 2017
doi: 10.3389/fmars.2017.00271

Ocean Acidification Experiments in Large-Scale Mesocosms Reveal Similar Dynamics of Dissolved Organic Matter Production and Biotransformation

Maren Zark[1], Nadine K. Broda[1], Thomas Hornick[2], Hans-Peter Grossart[2,3], Ulf Riebesell[4] and Thorsten Dittmar[1]*

[1] *Research Group for Marine Geochemistry (ICBM-MPI Bridging Group), Institute for Chemistry and Biology of the Marine Environment, Carl von Ossietzky University of Oldenburg, Oldenburg, Germany,* [2] *Experimental Limnology, Leibniz-Institute of Freshwater Ecology and Inland Fisheries, Stechlin, Germany,* [3] *Institute for Biochemistry and Biology, University of Potsdam, Potsdam, Germany,* [4] *GEOMAR Helmholtz Centre for Ocean Research Kiel, Kiel, Germany*

OPEN ACCESS

Edited by:
Christel Hassler, Université de Genève, Switzerland

Reviewed by:
Wei-dong Zhai, Shandong University, China
Elvira Pulido-Villena, Mediterranean Institute of Oceanography - MIO, France

****Correspondence:***
Maren Zark
maren.zark@uni-oldenburg.de

Specialty section:
This article was submitted to Marine Biogeochemistry, a section of the journal Frontiers in Marine Science

Received: *22 March 2017*
Accepted: *07 August 2017*
Published: *05 September 2017*

Citation:
Zark M, Broda NK, Hornick T, Grossart H-P, Riebesell U and Dittmar T (2017) Ocean Acidification Experiments in Large-Scale Mesocosms Reveal Similar Dynamics of Dissolved Organic Matter Production and Biotransformation. Front. Mar. Sci. 4:271. doi: 10.3389/fmars.2017.00271

Dissolved organic matter (DOM) represents a major reservoir of carbon in the oceans. Environmental stressors such as ocean acidification (OA) potentially affect DOM production and degradation processes, e.g., phytoplankton exudation or microbial uptake and biotransformation of molecules. Resulting changes in carbon storage capacity of the ocean, thus, may cause feedbacks on the global carbon cycle. Previous experiments studying OA effects on the DOM pool under natural conditions, however, were mostly conducted in temperate and coastal eutrophic areas. Here, we report on OA effects on the existing and newly produced DOM pool during an experiment in the subtropical North Atlantic Ocean at the Canary Islands during an (1) oligotrophic phase and (2) after simulated deep water upwelling. The last is a frequently occurring event in this region controlling nutrient and phytoplankton dynamics. We manipulated nine large-scale mesocosms with a gradient of pCO_2 ranging from ∼350 up to ∼1,030 μatm and monitored the DOM molecular composition using ultrahigh-resolution mass spectrometry via Fourier-transform ion cyclotron resonance mass spectrometry (FT-ICR-MS). An increase of 37 μmol L^{-1} DOC was observed in all mesocosms during a phytoplankton bloom induced by simulated upwelling. Indications for enhanced DOC accumulation under elevated CO_2 became apparent during a phase of nutrient recycling toward the end of the experiment. The production of DOM was reflected in changes of the molecular DOM composition. Out of the 7,212 molecular formulae, which were detected throughout the experiment, ∼50% correlated significantly in mass spectrometric signal intensity with cumulative bacterial protein production (BPP) and are likely a product of microbial transformation. However, no differences in the produced compounds were found with respect to CO_2 levels. Comparing the results of this experiment with a comparable OA experiment in the Swedish Gullmar Fjord, reveals similar succession patterns for individual compound pools during a phytoplankton bloom

and subsequent accumulation of these compounds were observed. The similar behavior of DOM production and biotransformation during and following a phytoplankton bloom irrespective of plankton community composition and CO_2 treatment provides novel insights into general dynamics of the marine DOM pool.

Keywords: dissolved organic matter, ocean acidification, ultrahigh resolution mass spectrometry, FT-ICR-MS, molecular composition, subtropical North Atlantic, mesocosm experiment

INTRODUCTION

The global ocean currently takes up about 25% of all annually emitted anthropogenic CO_2 (Le Queré et al., 2013). Once dissolved in seawater, most of the CO_2 is transported into deep waters via thermohaline circulation and the biological pump. A smaller fraction of the CO_2, however, forms carbonic acid and causes a decline in pH in the surface ocean (Zhai and Zhao, 2016). This process is commonly referred to as ocean acidification (OA). Under a business-as-usual climate scenario, surface ocean pH could be reduced by 0.4 units until the end of the century compared to pre-industrial levels (IPCC, 2014). OA may impact physiology of marine organisms, structure of phytoplankton communities, and the biogeochemical cycling of elements (Riebesell et al., 2007, 2017; Kroeker et al., 2010; Dutkiewicz et al., 2015).

One important pool in the marine carbon cycle that may be affected by OA is dissolved organic matter (DOM). It holds a similar amount of carbon as all living biomass on Earth (Hedges, 1992). This huge carbon pool is mainly produced by marine primary producers and consumed and biotransformed within the microbial loop at the bottom of the marine food web (Azam et al., 1983; Carlson et al., 2007). A stimulation of marine primary production by OA (Riebesell, 2000; Engel et al., 2013; Eberlein et al., 2017) may consequently lead to enhanced production of DOM and subsequently stimulate microbial mineralization (Grossart et al., 2006; Piontek et al., 2010). Thus, concurrent OA-induced changes in degradation and transformation processes affect DOM quantity and quality and have the potential to impact the biogeochemical carbon cycle (Moran et al., 2016).

The surface ocean contains a large fraction of labile DOM that is readily respired to CO_2. Only a smaller fraction of marine primary production is channeled into more recalcitrant DOM fractions (Hansell et al., 2012). This recalcitrant DOM is of importance in terms of oceanic carbon storage and may be altered in a more acidified ocean. So far, OA experiments monitored mainly bulk dissolved organic carbon (DOC) concentrations by neglecting the quality of DOM pools. Thereby, the effect of elevated CO_2 on bulk DOC concentrations in seawater was reported to be positive in large-scale mesocosm and incubation experiments (e.g., Czerny et al., 2013; Engel et al., 2013). However, other studies report no or even negative effects (Yoshimura et al., 2010; Engel et al., 2014; MacGilchrist et al., 2014; Zark et al., 2015a). In contrast, monitoring the molecular DOM composition via FT-ICR-MS may reveal changes in the quality of the accumulating DOM fraction. FT-ICR-MS is to date the only available analytical technique that holds the power to resolve the molecular masses of more than 60% of intact molecules in DOM (Mopper et al., 2007; Dittmar et al., 2008). In a previous long-term mesocosm experiment in the Swedish Gullmar Fjord, OA effects on DOM molecular composition were analyzed for the first time in an ultrahigh resolution by using Fourier-transform ion cyclotron resonance mass spectrometry (FT-ICR-MS). This study revealed no effects of elevated pCO_2 as projected for the end of this century on the DOM pool size and molecular composition in this eutrophic temperate system (Zark et al., 2015a). To what extent these findings can be extrapolated to other regions, in particular less eutrophic open waters, is presently unknown. Microbial communities in surface waters of oligotrophic areas experience less variability in pH than in coastal regions (Hofmann et al., 2011) and are hence less adapted to rapid changes in pH (Salisbury et al., 2008; Joint et al., 2011).

In this study, we tested the effects of OA on the DOM molecular composition in a subtropical system under oligotrophic conditions and in response to simulated upwelling of nutrient-rich deep water. Oligotrophic areas comprise ∼30% of the global oceanic primary production and changes in DOM accumulation in these areas may have significant impacts on the marine carbon cycle (Longhurst et al., 1995). So far, effects of OA in oligotrophic environments remain largely unknown, since most community-level field experiments were conducted under nutrient replete conditions. To bridge this knowledge gap, we performed a large-scale pelagic mesocosm experiment in the subtropical North Atlantic Ocean off the coast of Gran Canaria. This area is part of the Canary Current system, where upwelling of nutrient-rich deep water seasonally induces phytoplankton blooms (Aristeguí et al., 2009) and controls net production of DOC by input of additional nutrients (Romera-Castillo et al., 2016). Nine sea-going mesocosm systems were deployed, two of them served as controls with ambient pCO_2 levels and seven others were artificially enriched with CO_2. A gradient design with a range of pCO_2 levels from ∼350 to ∼1,030 µatm was chosen to test for the presence of a threshold for detecting pCO_2 induced effects. After ∼3 weeks, we added ∼8,000 L of nutrient-rich deep-sea water to each mesocosm to simulate an upwelling event and monitored responses for another ∼5 weeks (Taucher et al., 2017). DOC and dissolved organic nitrogen (DON) concentrations were measured as well as the changes in molecular DOM composition via FT-ICR-MS over the course of the oligotrophic phase and an upwelling-induced phytoplankton bloom. Specifically, we aimed for DOM that accumulates on timescales of weeks or longer, because it represents the non-labile fraction of DOM and is most important for carbon storage. We hypothesize that the effect of increased pCO_2 on the amount of primary production channeled

via the microbial loop into the more recalcitrant DOM pool is more pronounced under oligotrophic compared to eutrophic conditions.

MATERIALS AND METHODS

Experimental Set-Up

The mesocosm experiment was performed from September to November 2014 at the Plataforma Oceánica de Canarias (PLOCAN) on Gran Canaria, Spain. A technical description of the Kiel Off-Shore Mesocosms for Ocean Simulations (KOSMOS) facility and the experimental design is given in Riebesell et al. (2013) and Schulz et al. (2013). In brief, nine cylindrical mesocosms of ∼35 m^3 volume were deployed in the Bay of Gando (**Figure 1**) and filled at the same time with seawater from the Atlantic. The mesocosms were manipulated with CO_2 to reach average pCO_2 levels of 450 (M5), 560 (M3), 670 (M7), 720 (M4), 890 (M2), and 1,030 µatm (M8) between day 1 and day 55 (rounded values). The remaining two mesocosms were used as controls at ambient pCO_2-values of 350 (M9) to 370 µatm (M1). Initial manipulations with CO_2 were done by stepwise addition of CO_2 saturated seawater (days 0, 2, 4, and 6). All mesocosms were open to the atmosphere and CO_2 enriched water had to be added at several time points to keep the pCO_2 level close to the target (days 21 and 38). After CO_2 manipulation, the pH was on average 0.26 units lower in the enriched mesocosms compared to the controls. To simulate a naturally occurring upwelling event we added about 8,000 L deep-sea water (62 µmol L^{-1} DOC, 17 µmol L^{-1} combined NO_3^- and NO_2^-) to each of the mesocosms on day 23. It has to be noted that one of the mesocosms with moderate pCO_2 treatment (M6) was damaged on day 26 and had to be excluded from all statistical and graphical analyses. Comprehensive information about experiment design and basic parameters is provided in an overview by Taucher et al. (2017).

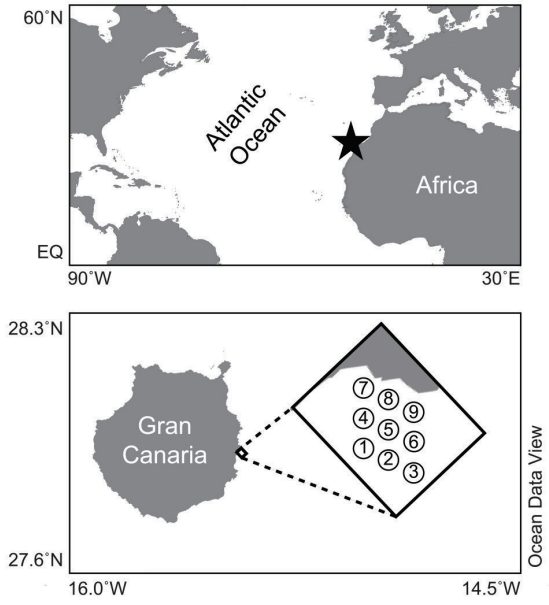

FIGURE 1 | Map of study site in the Atlantic Ocean. Mesocosms were moored in the Bay of Gando, off the coast of Gran Canaria (Spain).

Sample Preparation and Bulk Analysis

Representative samples were collected for both, the mesocosms and the surrounding Atlantic water, every other day from boats between 09:00 a.m. and 12:00 a.m. local time, starting from the day after the mesocosm bags were closed (day -3). We used 5 L integrating water samplers (IWS, Hydrobios) collecting a representative sample for the upper 13 m of the water column. Carbonate chemistry parameters such as pH and pCO_2 were calculated from total alkalinity (TA) and dissolved inorganic carbon (DIC) using CO_2SYS (Pierrot et al., 2006) and dissociation constants of Lueker et al. (2000) as described in Taucher et al. (2017). In brief, TA analyses were carried out via potentiometric titration (Metrohm 862 Titrosampler) after Dickson et al. (2003) and DIC concentrations were determined by infrared absorption of CO_2 purged from an acidified sample (MARIANDA AIRICA system with LI-COR LI-7000). Concentrations of chlorophyll *a* (Chl *a*) and other phytoplankton pigments were analyzed by high performance liquid chromatography (HPLC). Therefore, samples (500–1,000 mL) were collected by filtration onto glass fiber filters (GF/F Whatman, nominal pore size of 0.7 µm) and stored in cryovials at −80°C. For the HPLC analyses, samples were extracted in acetone (100%) in plastic vials by homogenization of the filters using glass beads in a cell mill. After centrifugation (10 min, 5,200 rpm, 4°C) the supernatant was filtered through 0.2 µm PTFE filters (VWR International). From this, phytoplankton pigment concentrations were determined using a Thermo Scientific HPLC Ultimate 3000 with Eclipse XDB-C8 3.5u 4.6 × 150 column.

For dissolved organic carbon (DOC) and total dissolved nitrogen (TDN) analysis, samples were collected into pre-rinsed 250 mL polycarbonate bottles (Nalgene) in triplicate. The samples were then filtered through a syringe with 0.7 µm GF/F pre-combusted (400°C, 4 h) glass microfiber filters (Whatman) into pre-combusted 20 mL glass vials (400°C, 4 h) with acid-rinsed Teflon caps (Wheaton). Directly after filtration, we acidified samples with HCl (25%, analysis grade, Carl Roth) to pH 2. The analysis of DOC and TDN concentrations was done via a high-temperature catalytic oxidation method (Qian and Mopper, 1996) using a Shimadzu TOC-VCPH/CPN Total Organic Carbon Analyzer, equipped with ASI V auto sampler and TNM-1 module for the determination of TDN. The accuracy of the measurement was controlled with Florida Strait Water reference material (D.A. Hansell, University of Miami, Florida) for every run. The error for DOC and TDN analysis was on average 4 and 10%, respectively. Average concentrations were calculated for each mesocosm and time point from triplicates. We calculated dissolved organic nitrogen (DON) concentrations from TDN by subtracting the concentration of all dissolved inorganic nitrogen species (DIN). DIN is the sum of nitrate,

nitrite and ammonium concentrations that were measured using a segmented flow analyzer (SEAL QuAAtro).

Molecular Characterization

Samples for molecular DOM characterization were collected from the IWS sampler into 2 L acid-rinsed polycarbonate bottles (Nalgene). The samples were transported to shore and stored at *in situ* water temperatures in the dark until processing on the same day. After filtration through 0.7 µm GF/F glass microfiber filters (Whatman) using manual vacuum pumps (<200 mbar) we acidified samples with HCl (25%, analysis grade, Carl Roth) to pH 2. Samples were stored at 4°C in the dark until subsequent solid phase extraction (SPE) according to Dittmar et al. (2008). We used a commercially available modified styrene divinyl benzene polymer resin (PPL, 1 g, Agilent). Prior to use, cartridges were soaked in methanol (HPLC grade, Sigma-Aldrich) overnight, and rinsed sequentially with methanol and 0.01 mol L^{-1} HCl in ultrapure water. After loading the samples onto the cartridges they were rinsed with 0.01 mol L^{-1} HCl to remove all remaining salts and dried with nitrogen gas (analysis grade, Air Liquide). The extracted DOM was eluted with 6 mL methanol and stored in pre-combusted glass vials at 20°C. Extraction efficiencies for this method are typically >60% on a carbon basis (Stubbins and Dittmar, 2012; Green et al., 2014). Especially colloidal matter and small ionic compounds may escape extraction and are likely lost from our analytical window. For this study the average extraction efficiency was 34 ± 4% across all mesocosms. Despite the relatively low recovery, SPE-DOC concentrations followed the general succession of DOC concentrations and can hence be considered as representative. Procedural blanks were prepared by processing ultrapure water the same way as DOM samples. The detection limit for solid phase extractable DOC (SPE-DOC) was lower than the detection limit for regular DOC samples (Stubbins and Dittmar, 2012) due to concentration by a factor of hundred. SPE-DOC concentrations in the resulting blank extracts were slightly above detection limit but did not exceed a concentration level of 12.3 µmol L^{-1}.

We used FT-ICR mass spectrometry for molecular characterization of the DOM pool. Thereby, individual compounds can be resolved from the complex mixture and due to the high mass accuracy, molecular formulae can be assigned. Molecular formulae may be grouped into categories according to indices derived from elemental composition ("Aliphatics" H/C ≥ 1.5, "CRAM O-poor" H/C < 1.5 & AI_{mod} ≤ 0.5 & O/C ≤ 5, "CRAM O-rich" H/C < 1.5 & AI_{mod} ≤ 0.5 & O/C > 0.5, "Polyphenols" 0.5 < AI_{mod} ≤ 0.66, "Polycyclic aromatics" AI_{mod} > 0.66) (Koch and Dittmar, 2006; Riedel et al., 2016). This is not meant to be an unambiguous identification of molecular structures.

Mass spectra were obtained on a 15 Tesla Solarix FT-ICR-MS system (Bruker Daltonics) equipped with an electrospray ionization source (ESI, Bruker Apollo II) applied in negative ionization mode. Methanol extracts were diluted with ultrapure water and methanol to give a final concentration of 15 mg C L^{-1} in a 1:1 mixture (v/v) of methanol (HPLC grade, Sigma-Aldrich) and ultra-pure water. For each measurement we accumulated 500 scans in the mass window of 150–2,000 Da. We calibrated spectra internally with a reference mass list using the Bruker Daltonics Data Analysis software package. The mass error of the calibration was <0.06 ppm for all samples. To remove noise a method detection limit following the guidelines of Riedel and Dittmar (2014) was applied. Compounds detected in procedural blanks were removed. We further found a group of likely contaminants (n = 50), which continuously increased in all mesocosms. These compounds were excluded from statistical analysis, as some of them correspond to known constituents of detergents. During previous mesocosm experiments using the identical setup, however, no such contamination could be observed (Zark et al., 2015a).

All 89 samples from a total of 10 time points (79 samples from mesocosms and 10 from the Atlantic) were analyzed via FT-ICR-MS in random order. To test the reproducibility and stability of the FT-ICR-MS analysis, we analyzed DOM extract of North Equatorial Pacific Intermediate Water (NEqPIW) twice per day (Green et al., 2014). MATLAB routines developed by our working group were applied for molecular formula assignment and further data processing. All molecules were detected as singly-charged ions and molecular formulae were assigned based on the criteria by Koch et al. (2007) and Rossel et al. (2013), under consideration of the elements C, H, O, N, S, and P.

Bacterial Protein Production

Rates of bacterial protein production (BPP) were determined by incorporation of ^{14}C-leucine (Simon and Azam, 1989) modified after Grossart et al. (2006) and Allgaier et al. (2008). Triplicates and a formol-killed control were incubated *in situ* with ^{14}C-Leu (318 mCi $mmol^{-1}$; Hartmann Analytic) at a concentration, which ensured saturation of the bacterial uptake systems. Incubation was performed for 1 h in dark at *in situ* temperature and gentle moving of closed containers in a water bath to prevent settling of particles. After fixation with 2% formalin, samples were filtered onto 5.0 µm nitrocellulose filters (Sartorius AG) for the particle associated bacteria fraction and extracted with ice-cold 5% trichloracetic acid (TCA) for 5 min. Thereafter, filters were rinsed twice with ice-cold 5% TCA, once with ethanol (50% v/v) and mixed with liquid scintillation cocktail (Ultima Gold™, Perkin Elmer). For the free-living bacteria the filtrate was filtered on 0.2 µm nitrocellulose filters (Sartorius) and processed in the same way. The incorporated leucine was measured as disintegrations per minute (dpm) on a liquid scintillation analyzer (TriCarb 2810 TR, Perkin Elmer). The sum of incorporated ^{14}C-leucine of both size-fractions was converted into BPP by using an intracellular isotope dilution factor of 2 (Kirchman, 1993). A factor of 0.86 was used to convert the produced protein in carbon (Simon and Azam, 1989). Standard deviation of triplicate measurements was usually <15%. Cumulative BPP was determined by summing up the average rates per day of experiment.

Statistical Analysis of FT-ICR-MS Data

All statistical analyses were based on normalized peak magnitudes of FT-ICR-MS signals. Variations in the molecular

DOM composition were characterized by principal components analysis (PCA). Additionally, a Bray-Curtis based distance matrix was calculated. This method from ecology aims at quantification of the dissimilarity of different ecological sites based on the counts of individual species (Bray and Curtis, 1957). In analogy, we calculated the dissimilarity of all mesocosms at each time point throughout the experiment based on normalized peak magnitudes of the individual DOM compounds. The dissimilarity may reach values between 0 (the two mesocosms share all molecular formulae in similar abundances) and 1 (the mesocosms share no molecular formulae). Thereby, a general comparison of the molecular diversity between samples can be obtained. We further calculated Pearson product-moment correlation coefficients (r) for the co-correlation of individual relative signal intensities of each detected molecular formula with cumulative BPP over time (**Figure 4C**). This statistical approach results in Pearson correlation coefficients (r) for all molecular formulae of each individual mesocosm (**Figure 4B**). Pearson correlation coefficients can range from −1 (negative linear relationship) to 1 (positive linear relation). We then used the obtained correlation coefficients for a follow-up Pearson correlation between the mesocosm units that aimed at revealing similar temporal dynamics of DOM molecular formulae (**Figure 4A**). All statistical analyses were performed with the software package R (Version 3.0.2, package "vegan," Oksanen et al., 2013).

RESULTS

DOC Production after a Phytoplankton Bloom Induced by Artificial Upwelling

Prior to the addition of CO_2, mesocosms showed similar conditions after a short equilibration period (**Figures 2A–D**). After CO_2 addition, pCO_2 inside the mesocosms showed temporal fluctuations throughout the experiment due to outgassing and repeated additions of CO_2 that were done to readjust the gradient. An overview on the temporal succession of pCO_2 in the experiment is provided by Taucher et al. (2017). The temporal succession of phytoplankton biomass was similar for all mesocosms and can be divided into three phases that were driven by different processes. The first phase of the experiment was characterized by oligotrophic conditions (phase I) with stable and low chlorophyll *a* concentrations (**Figure 2A**). During this phase, an increase in DOC concentration was observed (**Figure 2B**) from 80 ± 5 µmol L^{-1} on day 3 to 112 ± 5 µmol L^{-1} on day 23 (mean ± *SD*), while BPP remained stable (**Figure 2D**). A similar trend was not observed for the samples from the Atlantic. Immediately after the start of phase II, with addition of nutrient-rich deep water, chlorophyll *a* rapidly increased in all mesocosms (**Figure 2A**). A maximum of 3.5 µg L^{-1} was reached on day 28 which is within the range of chlorophyll *a* (Chl *a*) maxima in winter months and is typical for the subtropical oligotrophic Atlantic after upwelling events at this time of the year (Neuer

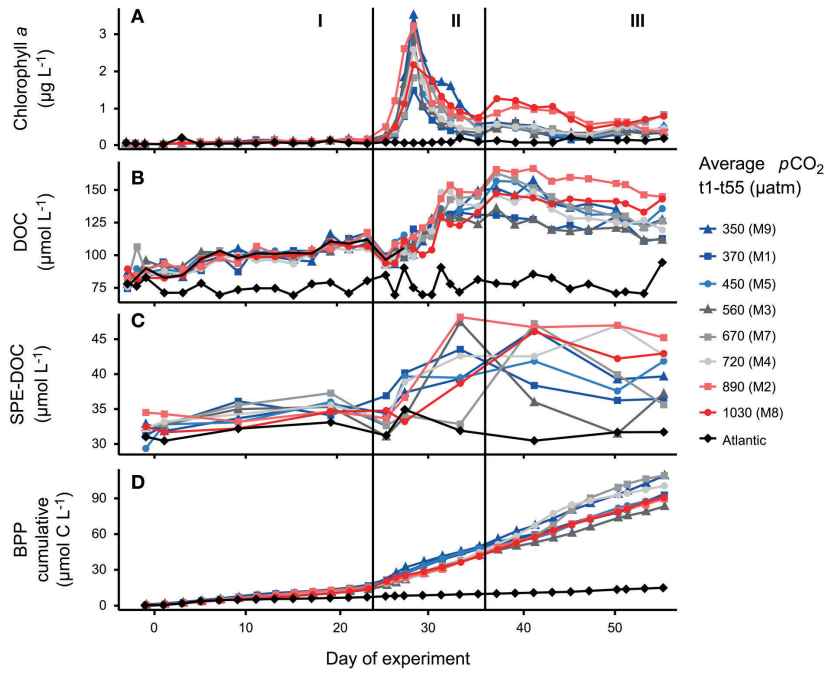

FIGURE 2 | Time series data from the mesocosm units and surrounding Atlantic water. Colors display the average pCO_2 value from day 1 to day 55. Concentration of **(A)** chlorophyll *a*, **(B)** dissolved organic carbon (DOC), **(C)** SPE-DOC as measure of the solid-phase extractable component in dissolved organic matter, and (**D**) cumulative bacterial protein production over experiment time.

et al., 2007). The bloom was dominated by diatoms (~70% of Chl *a*) as the most abundant group, but also included other groups such as dinoflagellates, prymnesiophytes (*Phaeocystis*) and cyanobacteria (e.g., *Synechococcus*) (Taucher et al., 2017). A sharp decrease of DOC from day 23 to day 25 occurred due to dilution by the injected deep water. At the same time, cumulative BPP increased from 41.8 ± 3.1 to 54.5 ± 4.4 μmol C L^{-1} (**Figure 2D**). DOC concentrations increased to a maximum of 149 ± 12 μmol L^{-1} after the decay of the bloom on day 37 (**Figure 2B**). Inorganic nutrients were again depleted from day 30 until the end of the experiment. At the beginning of phase III, a second phytoplankton bloom developed in mesocosms M2 and M8, sustained from recycled production with a low Chl *a* concentration (0.7 μg L^{-1} on day 37, **Figure 2A**). Cumulative BPP increased constantly during phase III and bacterial activity remained on a high level during the post-bloom (**Figure 2D**).

Apart from these general trends, the two mesocosms with the highest pCO_2 treatments (1,030 and 890 μatm pCO_2) showed higher Chl *a* and DOC concentrations during recycled production in post-bloom phase III. This trend is significant in a linear regression of both, DOC and Chl *a* with phase-averages of pCO_2 ($p < 0.05$) (Supplementary Materials Figure 1). It has to be noted that the plankton community composition in both high CO_2 treatments was clearly different from the other treatments and may have accounted for the differences in both, DOC and Chl *a* (Taucher et al., 2017). There were no differences with CO_2 between treatments for phases I and II.

The Succession of Molecular DOM Composition

Taken together, a total of 7,212 intact compounds with assigned molecular formulae were identified across all mesocosm samples after removal of contaminant signals. For further statistical analysis, the 5,205 molecular formulae with highest signal intensities were selected from each sample. This number was chosen because it was the lowest number in a single sample across the entire sample set. SPE-DOC concentrations in the collected DOM extracts reflect the same general trends as DOC concentration (**Figure 2C**) and our analysis can thus be considered representative for the fraction in DOM that showed variability during the experiment. FT-ICR-MS signal intensities followed an overall similar pattern with a bell-shaped distribution along the mass axis and an intensity weighted maximum at 372 Da. Using PCA, we could summarize 60% of the total variability of the complex molecular information in a single component (PC1). This component correlated significantly in a Pearson's product-moment correlation with DOC and showed a highly reproducible trend among all independent mesocosm units over time (Pearson, $r = 0.60$, $p < 0.0001$, $n = 79$). Thus, it represents the accumulating molecular signature (Supplementary materials Figure 2). A positive correlation was observed for PC3 with CO_2 (Pearson, $r = 0.20$, $p < 0.05$, $n = 79$). This component, however, explains only 6% of the total observed variability. In agreement to the results from PCA, the dissimilarity on a Bray-Curtis level from on average 8.7% in phase I and phase II, which is within our analytical error, increased to 14.4% in phase III (Supplementary materials Figure 3), but without indications for a trend associated to pCO_2 levels and the same amount of variability was observed for comparing control to control mesocosms and control to high CO_2 mesocosms.

To compare the succession of DOM on a molecular level between individual mesocosm units in more detail, we performed targeted statistical analysis on specific compound groups using cumulative BPP as proxy. We assume that molecular formulae showing close coupling to cumulative BPP in their succession of signal intensities represent the DOM that is a product of bacterial transformation of freshly produced carbon. This fraction of the marine DOM pool accumulates over timescales of weeks to months and is most important in terms of carbon storage. A Pearson correlation of the normalized signal intensities with cumulative BPP for the individual mesocosms revealed that 50% of all detected molecular formulae ($n = 3{,}583$) were showing significant correlations with cumulative BPP (Pearson, $p < 0.05$) (**Figure 3**). This is in good agreement to the results from Bray-Curtis based dissimilarity analysis. No differences were observed

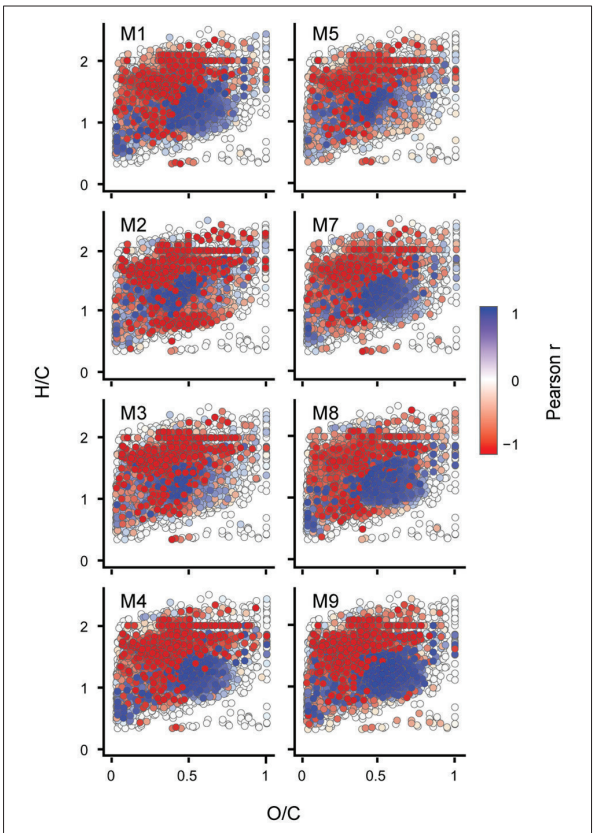

FIGURE 3 | Trends of individual molecular compounds displayed in van Krevelen space. Each dot represents one molecular formula ($n = 7{,}212$). Pearson's product-moment correlation of cumulative bacterial protein production (BPP) with relative signal intensities for the individual mesocosm units. The color displays the Pearson correlation coefficient (*r*) with values between −1 (negative linear relation) and 1 (positive linear relation).

in the type of accumulating molecular formulae between CO_2 levels.

To test for generality of these results, we applied the same proxy approach to published molecular DOM data from a mesocosm experiment performed in a eutrophic and temperate environment in the Swedish Gullmar Fjord (Zark et al., 2015a,b). For the fraction of common molecular formulae present in both studies (n = 3,972), we searched for molecular formulae showing co-correlation with cumulative BPP (**Figure 4C**) by calculating Pearson's product-moment correlation coefficients (r) for each individual molecular formula (**Figure 4B**). In a second step, Pearson's product-moment correlation coefficients between individual mesocosms were calculated to test whether molecular formulae show the same co-correlation patterns in the two experiments contrasting in location and habitat features (**Figure 4A**). The result was highly significant with average Pearson correlation coefficients of r = 0.71 for this study and r = 0.68 for the eutrophic study in the Swedish Fjord (Pearson, $p < 0.0001$). The average of the Pearson correlation coefficients between both experiments was lower, but also highly significant (r = 0.46, $p < 0.0001$). Grouping the molecular formulae into molecular categories confirmed this finding (**Figure 5**). While aliphatic compounds were not produced over the course of both experiments (**Figures 5A,B**), highly unsaturated compounds, also known as carboxyl-rich alicyclic molecules (CRAM) (Hertkorn et al., 2006) decreased in relative intensity (**Figures 5C,D,E,F**). It should be mentioned that these molecular categories are deduced from elemental compositions only, without further structural information (Šantl-Temkiv et al., 2013). The overall percentages of the individual compound groups varied with trophy, i.e., between the eutrophic and oligotrophic systems (**Figure 5**). Most importantly, however, there were no major differences in the most abundant compound groups.

DISCUSSION

CO_2 Effects on the Marine DOM Pool

No differences were observed between the mesocosms during DOC production in phases I and II with respect to bulk parameters and DOM molecular composition. The increase in DOC concentration in phase I was presumably caused by several factors. In the beginning of phase I a bloom of unicellular picocyanobacteria occurred, followed by a dust event from day 16 to day 22 which induced an increase of diatom biomass (Taucher et al., 2017). Concentrations of DOC and SPE-DOC started to diverge between treatments with the onset of recycled production in phase III, after inorganic nutrients added by the deep water injection had been consumed. DOC concentrations were highest in the two mesocosms with highest pCO_2 (890 and 1,030 µatm) during this period. This is likely an indirect effect of differences in plankton community structure, which were induced by elevated pCO_2 and remained apparent in all three phases of the experiment (Taucher et al., 2017). Our findings provide evidence for the existence of a threshold for indirect pCO_2-effects on DOC concentrations above ~890 µatm pCO_2. Doubtlessly, this estimate is very coarse considering the chosen pCO_2 levels, spatial limitations of the mesocosms, the

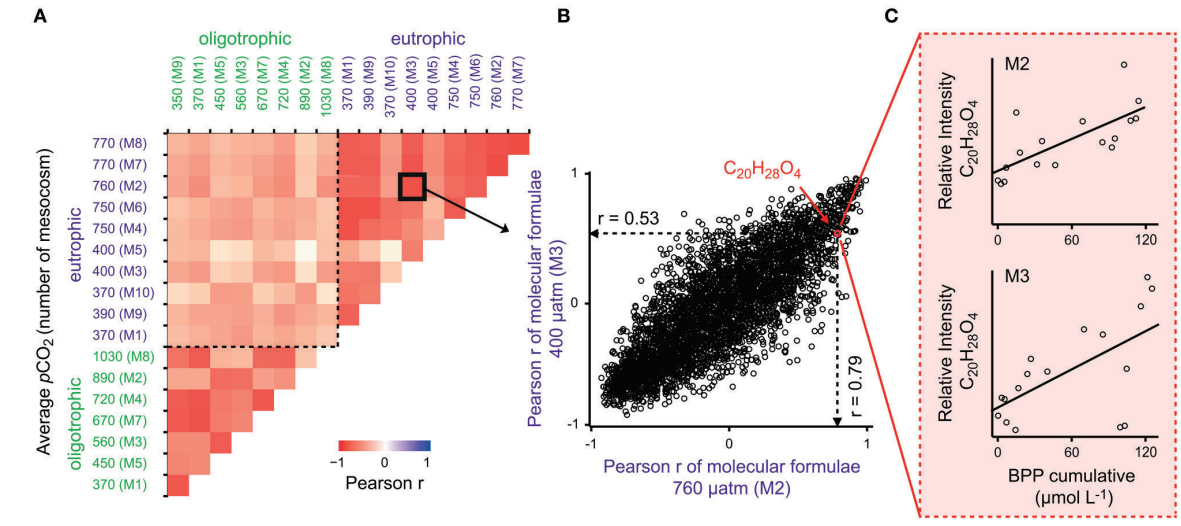

FIGURE 4 | Production of similar compounds in all mesocosms. **(A)** Pearson's product-moment correlation between individual mesocosms in a coastal mesocosm study in a Swedish Fjord (Zark et al., 2015a) and in the presented oligotrophic mesocosm experiment. The calculation is based on **(B)** Pearson product-moment correlation coefficients (r) from **(C)** correlation of relative signal intensities of molecular formulae with cumulative BPP. This statistical analysis illustrates the similarities in succession of molecular compounds between the experiments. The color scale displays the Pearson correlation coefficient (r) with values between −1 (negative linear relation) and 1 (positive linear relation). Similar compounds correlate with cumulative BPP in all mesocosms with an overall highly significant correlation of r = 0.45 ($p < 0.0001$, n = 3,972).

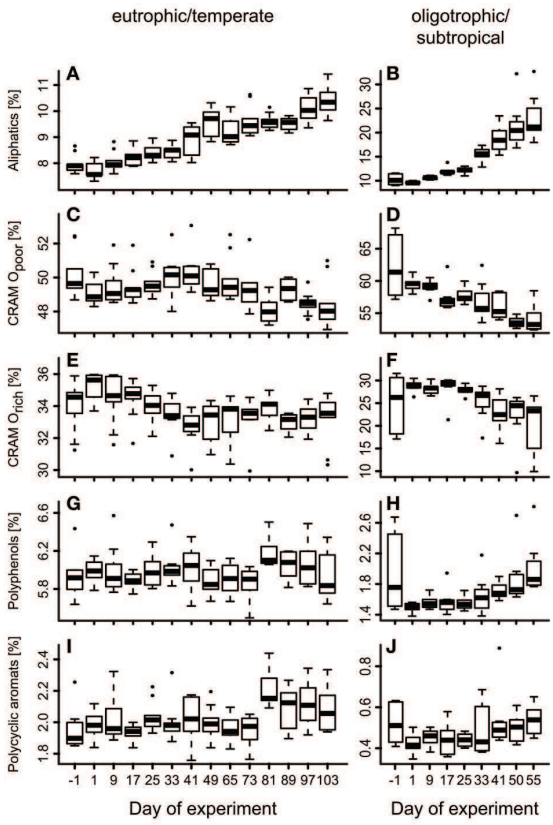

FIGURE 5 | Succession of different compound groups over experiment time. Box-Whisker plots display the different compound groups as defined in the Materials and Methods section in **(A)**,**(C)**,**(E)**,**(G)**,**(I)** a eutrophic/temperate mesocosm experiment in a Swedish Fjord (Zark et al., 2015a) and **(B)**,**(D)**,**(F)**,**(H)**,**(J)** the oligotrophic/subtropical mesocosm experiment presented in this paper as percentage of cumulative signal intensities from FT-ICR-MS analysis.

lack of replicates, and the fact that only a short time period was monitored compared to the time scales typically used for projections. Nevertheless, they are consistent with previous mesocosm experiments, for example with studies conducted in Finland (Paul et al., 2015) and in the Arctic (Czerny et al., 2013; Engel et al., 2013) where higher DOC accumulation was observed under strongly elevated pCO_2 levels of up to 1,420 µatm. In agreement to the proposed threshold, it was reported that lower maximum target levels of ~700–800 µatm pCO_2 showed no significant effect on DOC concentration (MacGilchrist et al., 2014; Zark et al., 2015a). These studies, however, were all conducted in coastal areas under eutrophic conditions. Studies conducted under oligotrophic conditions in the Mediterranean Sea without artificial addition of nutrients showed no effect on chlorophyll *a* and DOC accumulation under higher pCO_2 levels of up to ~1,000 µatm (Maugendre et al., 2017). Incubation studies using water from the oligotrophic Okhotsk Sea even show higher DOC removal under enhanced CO_2 (Yoshimura et al., 2010). Conclusively, the effect of pCO_2 on DOM quantity appears to be ambiguous in the literature, most likely because it may strongly depend on the environmental settings, particularly the respective location, nutritional status and organismic community composition.

Production of a Fraction of Compounds with Similar Molecular Formulae in All Mesocosms

In a previous mesocosm experiment in a Swedish Fjord with elevated pCO_2 levels of 760 µatm, we observed no effects of pCO_2 on DOM compounds being consumed or produced over time (Zark et al., 2015a; Bach et al., 2016). The same was true for this study in the subtropical North Atlantic Ocean. Despite indications for DOC accumulation, the overall effect of pCO_2 on DOM bulk molecular composition, if present, is smaller than the variance between control replicates toward the end of the experiment. Nevertheless, it is possible that some DOM compounds are produced by phytoplankton and quickly recycled by bacteria as a response to elevated CO_2 levels. Such enhanced cycle would not necessarily leave detectable imprints in the DOM molecular composition of our samples, because our sampling frequency did not resolve the relevant time scales and possibly also because of rapid aggregation of biopolymers to particles (Engel et al., 2004, 2014; Taucher et al., 2015). Furthermore, CO_2 may have a strong impact on specific DOM degradation processes which become not apparent in bulk analyses (Allgaier et al., 2008; Bergen et al., 2016).

To improve our current understanding of the underlying DOM dynamics, cumulative BPP was used as proxy to assess in more detail the pCO_2-induced differences in the accumulating DOM fraction over time. It is important to differentiate between DOM reactivity fractions because DOM with short turnover times does not significantly contribute to oceanic carbon export, unless it aggregates to larger particles which sink to the bottom and get buried in the sediment. On the other hand, longer-lived DOM compounds may contribute to carbon sequestration into the oceans interior. Due to the sampling frequency and duration, we covered mainly two operationally-defined reactivity fractions of DOM in our study, i.e., labile and semi-labile DOM. A major fate of photosynthetically produced labile DOM is quick turnover within the microbial loop on timescales of hours to days (Ducklow et al., 2001; Hansell, 2013), whereas semi-labile DOM resists microbial degradation in the surface ocean and accumulates over months and years before it is transported to depths of >100 m (Hansell et al., 2012). We assumed that semi-labile DOM compounds accumulate as a result of bacterial activity and thus correlate with cumulative BPP. It has to be noted, that other cumulative data may be also used as proxy for the accumulating DOM, but may not be environmentally meaningful. Refractory and ultra-refractory DOM may also have been produced by microbial transformation or other processes during our study, but cannot be separated from semi-labile DOM, since the lifetime of both reactivity fractions exceeds by far the duration of our experiment. However, it should be noted that

due to our sampling frequency (every second day) highly labile DOM was not resolved as well.

We found that half of the detected molecular formulae showed significant ($p < 0.05$) correlation with cumulative BPP similar for all mesocosms over time. This finding is remarkable, given the fact that the plankton community composition inside the mesocosms differed in relation to the pCO_2 level (Taucher et al., 2017). Whereas, freshly produced DOM from different phytoplankton species is clearly distinct in its individual chemical composition (Landa et al., 2014), the accumulating DOM fraction in our experiment, which remains after an initially rapid remineralization and microbial degradation of the highly labile compounds, was not. This notion may be explained by functional redundancy either in plankton communities regarding production of similarly stable compounds, or in degradation processes. Our results from a natural system support previous small-scale mesocosm experiments indicating production of similar compounds over long timescales despite variability in phytoplankton composition (Osterholz et al., 2015).

Applying the same approach to the molecular DOM data from our experiment in a Swedish Fjord (Zark et al., 2015a,b), we found a similar fraction of molecular formulae in both, the oligotrophic North Atlantic Ocean and the eutrophic fjord system. In both experiments, they significantly correlated with cumulative BPP in a similar manner. These findings suggest that compounds with the same elemental composition also show the same spatial and temporal dynamics in production and degradation. The formation of similar molecular compounds following the breakdown of the phytoplankton bloom, independent of environmental conditions such as phytoplankton community structure and acidification, indicates a rather universal microbial DOM transformation in different ecosystems. This finding points toward a high resilience of processes shaping the molecular DOM signature in complex pelagic communities.

CONCLUSION

DOM concentration and composition in our large-scale mesocosm experiments showed the same succession independent of pCO_2 treatment. OA induced effects became only apparent at the two highest CO_2, i.e., levels $>890\,\mu atm$, through elevated DOC concentrations during the last experimental phase. However, molecular DOM pool composition remained the same. Regarding climate scenarios, the obtained pCO_2 threshold level will be reached under the "business as usual emission" scenario until the end of the century (IPCC, 2014; Gattuso et al., 2015). However, the observed trends were not pronounced and can only serve as an indicator. If excess DOC was available in a future high CO_2 ocean, it could function as nutrient for new production. Alternatively, it could be sequestered and may thereby cause a negative feedback to the climate system. pCO_2 levels below $\sim 890\,\mu atm$ did not reveal significant differences in DOM quality and molecular compound groups show similar dynamics over the succession of phytoplankton blooms in two highly contrasting environments, i.e., a temperate eutrophic vs. a subtropical oligotrophic system. This finding indicates a high resilience of microbial DOM transformation processes independent of any environmental variable leading to generally very similar temporal dynamics of DOM groups following phytoplankton blooms. Comparing different large-scale OA mesocosm experiments, thus, provides valuable insights into the biogeochemical dynamics of DOM compounds.

AUTHOR CONTRIBUTIONS

All authors were involved in conceiving the study. MZ, UR, TH, and NB took the samples. MZ and NB conducted solid-phase extractions. FT-ICR-MS analysis was performed by MZ. TH and HG analyzed BPP rates. Statistical analyses were done by MZ and TD. MZ wrote the manuscript with comments from all other authors.

FUNDING

Financial support for this study was provided by the German Ministry of Education and Research (BMBF, FKZ 03F06550 and FKZ 03F07280) through the BIOACID (Biological Impacts of Ocean ACIDification) project. UR received additional funding from the Leibniz Award 2012 by the German Research Foundation (DFG).

ACKNOWLEDGMENTS

We thank the team of the Gran Canaria mesocosm experiment in 2014, in particular A. Ludwig for the logistical organization and coordination. We also thank the staff of the Plataforma Oceánica de Canarias (PLOCAN) for hosting our team, sharing their research facilities, and providing technical assistance. We thank the captain and crew of RV *Hesperides* for deploying and recovering the mesocosms (cruise 29HE20140924) and RV *Poseidon* for transporting the mesocosms and providing support in testing the deep water collector during cruise POS463. The authors furthermore thank K. Klaproth, M. Friebe, and I. Ulber for technical support with FT-ICR-MS and DOC/TDN analysis. We acknowledge A. Nauendorf for the analysis of Chl *a* concentrations, J. Meyer for carbonate chemistry measurements, and Eliesabeth Walter for support of BPP measurements. Nutrient concentrations were kindly provided by E. Achterberg and M. Esposito. All DOM data is archived at the PANGAEA data library (pangaea.de/10.1594/PANGAEA.869453) and will be made available upon request.

SUPPLEMENTARY MATERIAL

The Supplementary Material for this article can be found online at: http://journal.frontiersin.org/article/10.3389/fmars.2017.00271/full#supplementary-material

REFERENCES

Allgaier, M., Vogt, M., Thyrhaug, R., Riebesell, U., and Grossart, H.-P. (2008). Coupling of heterotrophic bacteria to phytoplankton bloom development at different pCO_2 levels: a mesocosm study. *Biogeosciences* 5, 317–359. doi: 10.5194/bg-5-1007-2008

Aristeguí, J., Barton, E. D., Álvarez-Salgado, X. A., Santos, A. M. P., Figueiras, F. G., Kifani, S., et al. (2009). Sub-regional ecosystem variability in the Canary Current upwelling. *Prog. Oceanogr.* 83, 33–48. doi: 10.1016/j.pocean.2009.07.031

Azam, F., Fenchel, T., Field, J. G., Gray, J. S., Meyer-Reil, L. A., and Thingstad, F. (1983). The ecological role of water-column microbes in the sea. *Mar. Ecol. Prog. Ser.* 10, 257–263. doi: 10.3354/meps010257

Bach, L. T., Taucher, J., Boxhammer, T., Ludwig, A., The Kristineberg, KOSMOS Consortium, Achterberg, E. P., et al. (2016). Influence of ocean acidification on a natural winter-to-summer plankton succession: first insights from a long-term mesocosm study draw attention to periods of low nutrient concentrations. *PLoS ONE* 11:e0159068. doi: 10.1371/journal.pone.0159068

Bergen, B., Endres, S., Engel, A., Zark, M., Dittmar, T., Sommer, U., et al. (2016). Acidification and warming affect prominent bacteria in two seasonal phytoplankton blooms. *Environ. Microbiol.* 18, 4579–4595. doi: 10.1111/1462-2920.13549

Bray, J. R., and Curtis, J. T. (1957). An ordination of the upland forest communities of Southern Wisconsin. *Ecol. Monogr.* 27, 325–349. doi: 10.2307/1942268

Carlson, C. A., Del Giorgio, P. A., and Herndl, G. J. (2007). Microbes and the dissipation of energy and respiration: from cells to ecosystems. *Oceanography* 20, 89–100. doi: 10.5670/oceanog.2007.52

Czerny, J., Schulz, K. G., Boxhammer, T., Bellerby, R. G. J., Büdenbender, J., Engel, A., et al. (2013). Implications of elevated CO_2 on pelagic carbon fluxes in an Arctic mesocosm study - an elemental mass balance approach. *Biogeosciences* 10, 3109–3125. doi: 10.5194/bg-10-3109-2013

Dickson, A. G., Afghan, J. D., and Anderson, G. C. (2003). Reference materials for oceanic CO_2 analysis: a method for the certification of total alkalinity. *Mar. Chem.* 80, 185–197. doi: 10.1016/S0304-4203(02)00133-0

Dittmar, T., Koch, B., Hertkorn, N., and Kattner, G. (2008). A simple and efficient method for the solid-phase extraction of dissolved organic matter (SPE-DOM) from seawater. *Limnol. Oceanogr. Methods* 6, 230–235. doi: 10.4319/lom.2008.6.230

Ducklow, H. W., Steinberg, D. K., and Buesseler, K. O. (2001). Upper ocean carbon export and the biological pump. *Oceanography* 14, 50–58. doi: 10.5670/oceanog.2001.06

Dutkiewicz, S., Morris, J. J., Follows, M. J., Scott, J., Levitan, O., Dyhrman, S. T., et al. (2015). Impact of ocean acidification on the structure of future phytoplankton communities. *Nat. Clim. Change* 5, 1002–1006. doi: 10.1038/nclimate2722

Eberlein, T., Wohlrab, S., Rost, B., John, U., Bach, L. T., Riebesell, U., et al. (2017). Effects of ocean acidification on primary production in a coastal North Sea phytoplankton community. *PLoS ONE* 12:e0172594. doi: 10.1371/journal.pone.0172594

Engel, A., Borchard, C., Piontek, J., Schulz, K. G., Riebesell, U., and Bellerby, R. (2013). CO_2 increases ^{14}C primary production in an Arctic plankton community. *Biogeosciences* 10, 1291–1308. doi: 10.5194/bg-10-1291-2013

Engel, A., Piontek, J., Grossart, H.-P., Riebesell, U., Schulz, K. G., and Sperling, M. (2014). Impact of CO_2 enrichment on organic matter dynamics during nutrient induced coastal phytoplankton blooms. *J. Plankton Res.* 36, 641–657. doi: 10.1093/plankt/fbt125

Engel, A., Thoms, S., Riebesell, U., Rochelle-Newall, E., and Zondervan, I. (2004). Polysaccharide aggregation: a sink of marine dissolved organic carbon. *Nature* 428, 929–932. doi: 10.1038/nature02453

Gattuso, J.-P., Magnan, A., Billé, R., Cheung, W. W. L., Howes, E. L., Joos, F., et al. (2015). Contrasting futures for ocean and society from different anthropogenic CO_2 emissions scenarios. *Science* 349, aac4722. doi: 10.1126/science.aac4722

Green, N. W., Perdue, E. M., Aiken, G. R., Butler, K. D., Chen, H., Dittmar, T., et al. (2014). An intercomparison of three methods for the large-scale isolation of oceanic dissolved organic matter. *Mar. Chem.* 161, 14–19. doi: 10.1016/j.marchem.2014.01.012

Grossart, H.-P., Allgaier, M., Passow, U., and Riebesell, U. (2006). Testing the effect of CO_2 concentration on the dynamics of marine heterotrophic bacterioplankton. *Limnol. Oceanogr.* 51, 1–11. doi: 10.4319/lo.2006.51.1.0001

Hansell, D. A. (2013). Recalcitrant dissolved organic carbon fractions. *Annu. Rev. Mar. Sci.* 5, 421–445. doi: 10.1146/annurev-marine-120710-100757

Hansell, D. A., Carlson, C. A., and Schlitzer, R. (2012). Net removal of major marine dissolved organic carbon fractions in the subsurface ocean. *Global Biogeochem. Cycles* 26:GB1016. doi: 10.1029/2011GB004069

Hedges, J. I. (1992). Global biogeochemical cycles: progress and problems. *Mar. Chem.* 39, 67–93. doi: 10.1016/0304-4203(92)90096-S

Hertkorn, N., Benner, R., Frommberger, M., Schmitt-Kopplin, P., Witt, M., Kaiser, K., et al. (2006). Characterization of a major refractory component of marine dissolved organic matter. *Geochim. Cosmochim. Acta* 70, 2990–3010. doi: 10.1016/j.gca.2006.03.021

Hofmann, G. E., Smith, J. E., Johnson, K. S., Send, U., Levin, L. A., et al. (2011). High-frequency dynamics of ocean pH: a multi-ecosystem comparison. *PLoS ONE* 6:e28983. doi: 10.1371/journal.pone,.0028983

IPCC (2014). "Climate Change 2014: impacts, adaptation, and vulnerability. Part A: global and sectoral aspects," in *Contribution of Working Group II to the Fifth Assessment Report of the Intergovernmental Panel on Climate Change* (Cambridge; New York, NY: Cambridge University Press).

Joint, I., Doney, S. C., and Karl, D. M. (2011). Will ocean acidification affect marine microbes? *ISME J.* 5, 1–7. doi: 10.1038/ismej.2010.79

Kirchman, D. L. (1993). "Leucine incorporation as a measure of biomass production by heterotrophic bacteria," in *Handbook of Methods in Aquatic Microbial Ecology*, eds P. F. Kemp, B. F. Sherr, E. B. Sherr, and J. J. Cole (Boca Raton, FL: Lewis), 509–512.

Koch, B. P., and Dittmar, T. (2006). From mass to structure: an aromaticity index for high-resolution mass data of natural organic matter. *Rapid Commun. Mass Spectrom.* 20, 926–932. doi: 10.1002/rcm.2386

Koch, B. P., Dittmar, T., Witt, M., and Kattner, G. (2007). Fundamentals of molecular formula assignment to ultrahigh resolution mass data of natural organic matter. *Anal. Chem.* 79, 1758–1763. doi: 10.1021/ac061949s

Kroeker, K. J., Kordas, R. L., Crim, R. N., and Singh, G. G. (2010). Meta-analysis reveals negative yet variable effects of ocean acidification on marine organisms. *Ecol. Lett.* 13, 1419–1434. doi: 10.1111/j.1461-0248.2010.01518.x

Landa, M., Cottrell, M. T., Kirchman, D. L., Kaiser, K., Medeiros, P. M., Tremblay, L., et al. (2014). Phylogenetic and structural response of heterotrophic bacteria to dissolved organic matter of different chemical composition in a continuous culture study. *Environ. Microbiol.* 16, 1668–1681. doi: 10.1111/1462-2920.12242

Le Queré, C., Peters, G. P., Andres, R. J., Andrew, R. M., Boden, T., and Ciais, P. (2013). Global carbon budget 2013. *Earth Syst. Sci. Data* 6, 689–760. doi: 10.5194/essdd-6-689-2013

Longhurst, A., Sathyendranath, S., Platt, T., and Caverhill, C. (1995). An estimate of global primary production in the ocean from satellite radiometer data. *J. Plankt. Res.* 17, 1245–1271. doi: 10.1093/plankt/17.6.1245

Lueker, T. J., Dickson, A. G., and Keeling, C. D. (2000). Ocean pCO_2 calculated from dissolved inorganic carbon, alkalinity, and equations for K1 and K2: validation based on laboratory measurements of CO_2 in gas and seawater at equilibrium. *Mar. Chem.* 70, 105–119. doi: 10.1016/S0304-4203(00)00022-0

MacGilchrist, G. A., Shi, T., Tyrell, T., Richier, S., Moore, C. M., Dumousseaud, C., et al. (2014). Effects of enhanced pCO_2 levels on the production of dissolved organic carbon and transparent exopolymer particles in short-term bioassay experiments. *Biogeosciences* 11, 3695–3706. doi: 10.5194/bg-11-3695-2014

Maugendre, L., Gattuso, J.-P., Poulton, A. J., Dellisanti, W., Gaubert, M., Guieu, C., et al. (2017). No detectable effect of ocean acidification on plankton metabolism in the NW oligotrophic Mediterranean Sea: results from two mesocosm studies. *Estuar. Coast. Shelf Sci.* 186, 89–99. doi: 10.1016/j.ecss.2015.03.009

Mopper, K., Stubbins, A., Ritchie, J. D., Bialk, H. M., and Hatcher, P. G. (2007). Advanced instrumental approaches for characterization of marine dissolved organic matter: extraction techniques, mass spectrometry, and nuclear magnetic resonance. *Chem. Rev.* 107, 419–442. doi: 10.1021/cr050359b

Moran, M. A., Kujawinski, E. B., Stubbins, A., Fatland, R., Aluwihare, L. I., Buchan, A., et al. (2016). Deciphering ocean carbon in a changing world. *Proc. Natl. Acad. Sci. U.S.A.* 113, 3143–3151. doi: 10.1073/pnas.1514645113

Neuer, S., Cianca, A., Helmke, P., Freudenthal, T., Davenport, R., Meggers, H., et al. (2007). Biogeochemistry and hydrography in the eastern subtropical North

Atlantic gyre. Results from the European time-series station ESTOC. *Prog. Oceanogr.* 72, 1−29. doi: 10.1016/j.pocean.2006.08.001

Oksanen, J., Blanchet, F. G., Kindt, R., Legendre, P., Minchin, P. R., O'Hara, R. B., et al. (2013). *Vegan: Community Ecology Package.* R package version 2.0-10. Available online at: http://CRAN.R-project.org/package=vegan

Osterholz, H., Niggemann, J., Giebel, H.-A., Simon, M., and Dittmar, T. (2015). Inefficient microbial production of refractory dissolved organic matter in the ocean. *Nat. Commun.* 6, 7422. doi: 10.1038/ncomms8422

Paul, A. J., Bach, L. T., Schulz, K.-G., Boxhammer, T., Czerny, J., Achterberg, E. P., et al. (2015). Effect of elevated CO_2 on organic matter pools and fluxes in a summer Baltic Sea plankton community. *Biogeosciences* 12, 6181−6203. doi: 10.5194/bg-12-6181-2015

Pierrot, D. E., Lewis, E., and Wallace, D. W. R. (2006). *MS Excel Program Developed for CO_2 System Calculations*. ORNL/CDIAC-105a, Carbon Dioxide Information Analysis Center, Oak Ridge National Laboratory, U.S. Department of Energy, Oak Ridge, TN.

Piontek, J., Lunau, M., Händel, N., Borchard, C., Wurst, M., and Engel, A. (2010). Acidification increases microbial polysaccharide degradation in the ocean. *Biogeosciences* 7, 1615−1624. doi: 10.5194/bg-7-1615-2010

Qian, J., and Mopper, K. (1996). Automated high-performance, high-temperature combustion total organic carbon analyzer. *Anal. Chem.* 68, 3090−3097. doi: 10.1021/ac960370z

Riebesell, U. (2000). Carbon fix for a diatom. *Nature* 407, 959−960. doi: 10.1038/35039665

Riebesell, U., Bach, L. T., Bellerby, R. G. J., Bermúdez Monsalve, J. R., Boxhammer, T., Czerny, J., et al. (2017). Competitive fitness of a predominant pelagic calcifier impaired by ocean acidification. *Nat Geosci.* 10, 19−23. doi: 10.1038/ngeo2854

Riebesell, U., Czerny, J., von Bröckel, K., Boxhammer, T., Büdenbender, J., Deckelnick, M., et al. (2013). Technical note: a mobile sea-going mesocosm system - new opportunities for ocean change research. *Biogeosciences* 10, 1835−1847. doi: 10.5194/bg-10-1835-2013

Riebesell, U., Schulz, K. G., Bellerby, R. G. J., Botros, M., Fritsche, P., Meyerhöfer, M., et al. (2007). Enhanced biological carbon consumption in a high CO_2 ocean. *Nature* 450, 545−549. doi: 10.1038/nature06267

Riedel, T., and Dittmar, T. (2014). A method detection limit for the analysis of natural organic matter via Fourier transform ion cyclotron resonance mass spectrometry. *Anal. Chem.* 86, 8876−8382. doi: 10.1021/ac501946m

Riedel, T., Zark, M., Vähätalo, A. V., Niggemann, J., Spencer, R. G. M., Hernes, P. J., et al. (2016). Molecular signatures of biogeochemical transformations in dissolved organic matter from ten world rivers. *Front. Earth Sci.* 4:85. doi: 10.3389/feart.2016.00085

Romera-Castillo, C., Letscher, R. T., and Hansell, D. A. (2016). New nutrients exert fundamental control on dissolved organic carbon accumulation in the surface Atlantic Ocean. *Proc. Natl. Acad. Sci. U.S.A.* 113, 10497−10502. doi: 10.1073/pnas.1605344113

Rossel, P. E., Vähätalo, A. V., Witt, M., and Dittmar, T. (2013). Molecular composition of dissolved organic matter from a wetland plant (*Juncus effusus*) after photochemical and microbial decomposition (1.25 yr): common features with deep sea dissolved organic matter. *Org. Geochem.* 60, 62–71. doi: 10.1016/j.orggeochem.2013.04.013

Salisbury, J., Green, M., Hunt, C., and Campbell, J. (2008). Coastal acidification by rivers: a threat to shellfish? *Eos* 89, 513. doi: 10.1029/2008EO500001

Šantl-Temkiv, T., Finster, K., Dittmar, T., Hansen, B. M., Thyrhaug, R., and Nielsen, N. W. (2013). Hailstones: a window into the microbial and chemical inventory of a storm cloud. *PLoS ONE* 8:e53550. doi: 10.1371/journal.pone.0053550

Schulz, K. G., Bellerby, R. G. J., Brussaard, C. P. D., Büdenbender, J., Czerny, J., Engel, A., et al. (2013). Temporal biomass dynamics of an Arctic plankton bloom in response to increasing levels of atmospheric carbon dioxide. *Biogeosciences* 10, 161−180. doi: 10.5194/bg-10-161-2013

Simon, M., and Azam, F. (1989). Protein content and protein synthesis rates of planktonic marine bacteria. *Mar. Ecol. Prog. Ser.* 51, 201−213. doi: 10.3354/meps051201

Stubbins, A., and Dittmar, T. (2012). Low volume quantification of dissolved organic carbon and dissolved nitrogen. *Limnol. Oceanogr. Methods* 10, 347–352. doi: 10.4319/lom.2012.10.347

Taucher, J., Bach, L. T., Boxhammer, T., Achterberg, E. P., Algueró-Muñiz, M., Arístegui, J., et al. (2017). Influence of ocean acidification and deep water upwelling on oligotrophic plankton communities in the subtropical North Atlantic: insights from an *in situ* mesocosm study. *Front. Earth. Sci.* 4:85. doi: 10.3389/fmars.2017.00085

Taucher, J., Jones, J., James, A., Brzezinski, M. A., Carlson, C. A., Riebesell, U., et al. (2015). Combined effects of CO_2 and temperature on carbon uptake and partitioning by the marine diatoms *Thalassiosira weissflogii* and *Dactyliosolen fragilissimus*. *Limnol. Oceanogr.* 60, 901−919. doi: 10.1002/lno.10063

Yoshimura, T., Nishioka, J., Suzuki, K., Hattori, H., Kiyosawa, H., and Watanabe, Y. W. (2010). Impacts of elevated CO_2 on organic carbon dynamics in nutrient depleted Okhotsk Sea surface waters. *J. Exp. Mar. Biol. Ecol.* 395, 191−198. doi: 10.1016/j.jembe.2010.09.001

Zark, M., Riebesell, U., and Dittmar, T. (2015a). Effects of ocean acidification on marine dissolved organic matter are not detectable over the succession of phytoplankton blooms. *Sci. Adv.* 1:e1500531. doi: 10.1126/sciadv.1500531

Zark, M., Riebesell, U., and Dittmar, T. (2015b). Dissolved organic matter molecular composition and concentrations from a large scale mesocosm study KOSMOS 2013 Kristineberg) on ocean acidification. *PANGAEA*. doi: 10.1594/PANGAEA.846137

Zhai, W., and Zhao, H. (2016). Quantifying air–sea re-equilibration-implied ocean surface CO_2 accumulation against recent atmospheric CO_2 rise. *J. Oceanogr.* 72, 651. doi: 10.1007/s10872-016-0350-8

Conflict of Interest Statement: The authors declare that the research was conducted in the absence of any commercial or financial relationships that could be construed as a potential conflict of interest.

frontiers

Supplementary Material

Ocean Acidification Experiments in Large-Scale Mesocosms Reveal Similar Dynamics of Dissolved Organic Matter Production and Biotransformation

Maren Zark[1*], Nadine K. Broda[1], Thomas Hornick[2], Hans-Peter Grossart[2,3], Ulf Riebesell[4], Thorsten Dittmar[1]

*** Correspondence:** Dr. Maren Zark: maren.zark@uol.de

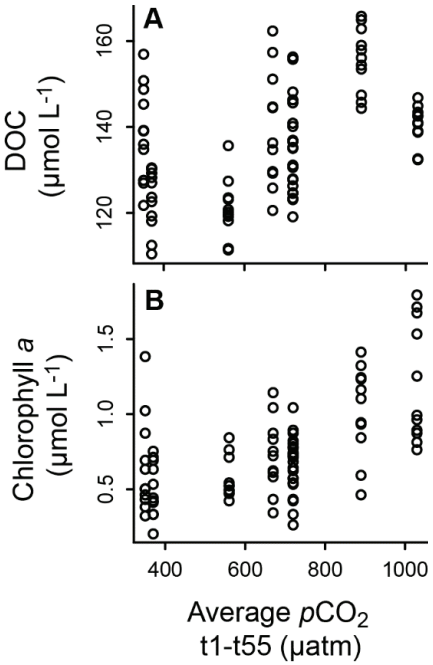

Supplementary Figure 1. Carbon dioxide concentrations as driver for trends in bulk data during phase III. (**A**) DOC and (**B**) chlorophyll *a* plotted for increasing average pCO_2 values of experiment days 35-55 (post-bloom).

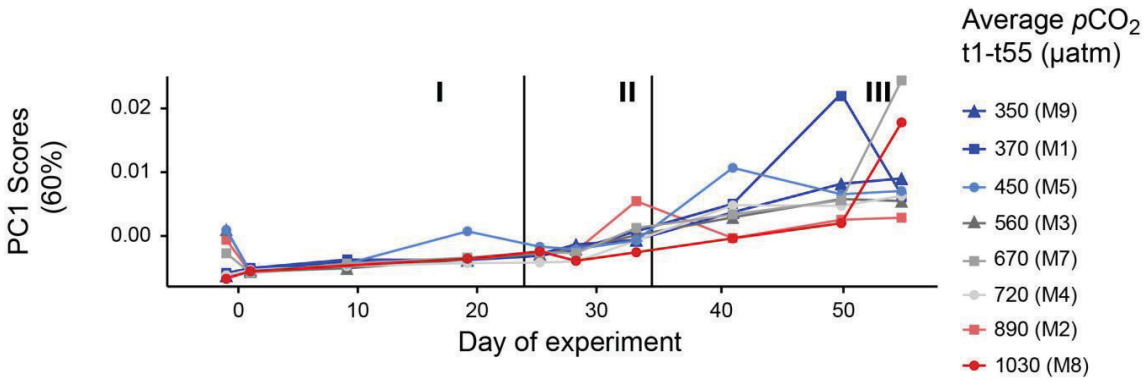

Supplementary Figure 2. Time series of molecular DOM composition inside the mesocosms. Results from the PCA (PC1) of 7212 molecular formulae and their MS signal intensities.

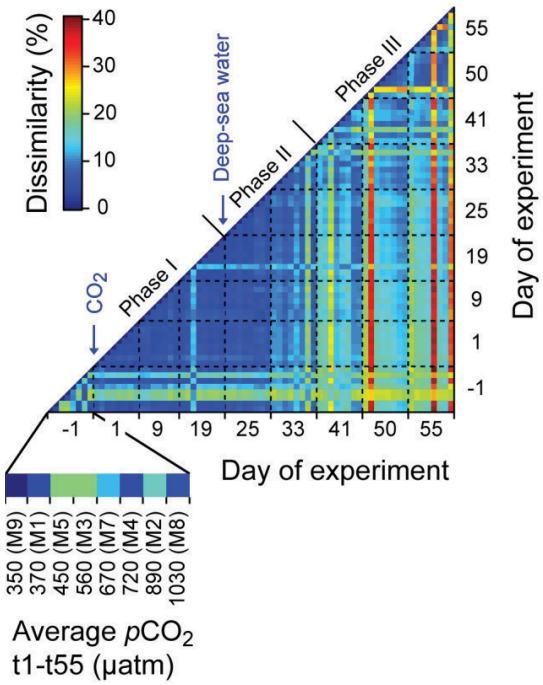

Supplementary Figure 3. Molecular dissimilarity between mesocosms. For dissimilarity analysis, the 5,205 most intense molecular formulae from each sample were considered. The dissimilarity on a Bray-Cutis level may reach values between 0 (the two mesocosms share all molecular formulae in similar abundances) and 1 (the mesocosms share no molecular formulae), which were transferred to percentages (from 0 to 100% dissimilarity). The color scale was cut at 40% dissimilarity level as no mesocosms showed higher dissimilarity in DOM composition. Samples were first ordered by average pCO_2 values from day 1 to day 55 and second by the respective day of the experiment.

5. Chapter 5 - Manuscript 4

Experimental summer storm induces changes in bacterial community structure with lasting biogeochemical consequences

Thomas Hornick[1]*, Lars Ganzert[1], Stella A. Berger[1], Mark O. Gessner[1,2], Darren P. Giling[1,3,4], Jens C. Nejstgaard[1], Jason N. Woodhouse[1], Hans-Peter Grossart[1,5]*

To be submitted**

[1] Experimental Limnology, Leibniz-Institute of Freshwater Ecology and Inland Fisheries, Stechlin, Germany

[2] Department of Ecology, Berlin Institute of Technology (TU Berlin), Ernst-Reuter-Platz 1, 10623 Berlin, Germany

[3] German Centre for Integrative Biodiversity Research (iDiv) Halle-Jena-Leipzig, Deutscher Platz 5e, 04103 Leipzig, Germany

[4] Institute of Biology, Leipzig University, Johannisallee 21, 04103 Leipzig

[5] Potsdam University, Institute for Biochemistry and Biology, Maulbeerallee 2, 14469 Potsdam, Germany

*corresponding authors: H.-P. Grossart (hgrossart@igb-berlin.de) and T. Hornick (hornick@igb-berlin.de)

** manuscript formatted in style of this thesis

Abstract

Climate change is projected to increase frequency and severity of episodic weather events. In particular, heavy summer storms can disrupt the thermal stratification and associated vertical gradients of temperate lakes. We conducted a large-volume (~1300 m^3) enclosure experiment in oligotrophic-mesotrophic Lake Stechlin and simulated a summer storm by mixing over a four-hour period in early August. Entrainment of colder and nutrient-enriched metalimnic water into the surface mixed layer lead to pronounced physical-chemical changes that significantly affected bacterial community assembly. Network analyses of the relation between environmental variables and differential abundant OTUs in control and mixed enclosures revealed multiple driving factors that impacted on the abundance of microbial taxa up to six weeks after the mixing. The decay of a cyanobacterial bloom that developed in response to mixing significantly increased bacterial protein production and respiration of heterotrophic bacteria, reflecting high organic matter turnover on suspended particles that largely determined C-sequestration to the sediment. The results highlight effects on bacterial community assembly and heterotrophic bacterial metabolism that are associated to entrainment of deep water into the mixed layer and assess consequences of an episodic disturbance event for the coupling between bacterial metabolism and autochthonous DOM production in large volume clear-water lakes.

Key words

Lake mixing, short-term disturbance, large-volume mesocosm, microbial community composition, extreme weather events, deep chlorophyll maximum (DCM), bacterial production, interaction network, cyanobacteria

1. Introduction

Recorded increases in atmospheric moisture and sea surface temperature will provide a warmer and wetter climate, raising the occurrence and severity of global weather extremes (Trenberth, 2012; IPCC, 2013). Consequently, more intense summer storms can be expected (Rahmstorf and Coumou, 2011; Coumou and Rahmstorf, 2012; Trenberth, 2012; IPCC, 2013) with potentially far reaching consequences for stratified lake ecosystems. Our current understanding, however, on how such exceptional disturbance events might alter biodiversity, community assembly and functioning of stratified lake ecosystems is still limited (e.g. Jennings et al., 2012; Jones et al., 2008; Weithoff et al., 2000; Shade et al., 2010; Kasprzak et al., 2017) and may fundamentally differ from concepts gained in terrestrial ecosystem research. Disturbances in terrestrial ecosystems, such as droughts or warming mostly decrease both resource availability and net productivity (e.g, Tilman and Downing, 1994; Ives and Carpenter, 2007; Vogel et al., 2012). Aquatic ecosystems, in contrast, usually experience resource enrichment (e.g. introduction of organic matter and nutrients from

terrestrial environments or other water layers) with a subsequent increase in ecosystem productivity (e.g. Jones et al., 2008; Giling et al., 2017).

Summer storms, in particular, have the potential to perturb thermal the stratification of lakes, potentially disrupting the thermocline and deepening the mixed layer. Thereby, physical properties of the water column can be changed for several days with potential long-term effects on spatial distribution, composition and functionality of organisms (e.g. Jennings et al., 2012; Kasprzak et al., 2017). Summer storms often lead to an intrusion of colder metalimnic water into the surface layer, which (i) decreases surface layer water temperature and increases epilimnion thickness, (ii) redistributes metalimnic organisms throughout the whole mixed layer, thus exposing them to higher levels of photosynthetic active radiation (PAR), and (iii) mixes nutrient- (P, N) and carbon dioxide (CO_2)-rich water into the upper eutrophic layer. All of these processes in combination fuel phytoplankton production in the phototrophic zone by releasing organisms from nutrient and light limitation (Weithoff et al., 2000; Jennings et al., 2012; Giling et al., 2017).

To better understand the ecological mechanisms of storm-induced short-term disturbances in stratified lakes, we experimentally assessed the effect of water-column mixing in summer 2014 by using the world's largest enclosure facility in the oligo-mesotrophic Lake Stechlin (www.lake-lab.de). Lake Stechlin has a pronounced deep chlorophyll maximum (DCM), and thus summer storms have a high potential to redistribute metalimnic phytoplankton biomass into the upper mixed layer (Kasprzak et al., 2017). As such, storm "Otto", in July 2011 caused a pronounced deepening of the thermocline and stimulated a substantial cyanobacterial bloom in Lake Stechlin, triggering a cascade of processes towards extremes of turbidity never observed before in three decades of lake monitoring (Kasprzak et al., 2017). We successfully reproduced key physical, chemical and biological responses of such an extreme storm event similar to *in situ* observations following summer storm "Otto" (Kasprzak et al., 2017). Changes in water chemistry and physics by entrainment of metalimnic water with associated organisms from a DCM into the upper mixed layer stimulated phytoplankton growth and caused predictable lake ecosystem consequences at the level of primary producers as described earlier by Giling et al. (2017).

Although consequences on bacterial community processes following storm-induced disturbance events have been tested (e.g. Jones et al., 2008; Shade et al., 2010), yet, little mechanistic knowledge on changes in their functionality in deep and clear stratified lakes exist. This is surprising since heterotrophic processes are vital in order to understand how summer storms might change lake carbon budgets and feedback to the global CO_2 budget (Tranvik et al., 2009; Raymond et al., 2013). Here, we highlight effects on community assembly and heterotrophic bacterial metabolism that are associated to entrainment of deep water into the mixed water layer and assess consequences of an episodic disturbance event for the coupling between bacterial metabolism and autochthonous DOM production in large volume clear-water lakes. Based on measurements of bacterial protein production (BPP), metabolic modelling and by applying DNA-based amplicon sequencing we were able

to follow temporal changes in bacterial community composition and heterotrophic processes after such an extreme disturbance event in a replicated manner. We tested the hypotheses that storm-induced lake mixing (i) restructures bacterial communities, (ii) increases metabolic heterotrophic processes due to enhanced autotrophic productivity, and (iii) subsequently alters carbon-sequestration to the sediment.

2. Materials and Methods

2.1 Experimental system and sampling

The experiment was conducted in large-volume enclosures (~1300 m^3) installed in Lake Stechlin, north-eastern Germany (53°08036”N, 13°01041”E; www.lake-lab.de). Epilimion and hypolimnion water masses were exchanged by simultaneously pumping lake water in and out of the enclosures using submersible impeller pumps that cause minimum plankton disturbance, as successfully used at other enclosure facilities (e.g. Nejstgaard et al., 1997, 2006). A DCM which was present in the metalimnion of Lake Stechlin at this time was subsequent inserted into the metalimnion of each enclosure by identical water replacement. A summer storm was simulated in four randomly selected enclosures on 6th August 2014 without sediment disturbance to deepen the thermocline from 9 to 14 m by mixing for 4 hours (Giling et al., 2017). Water samples were collected from the well-mixed epilimnion at 2.5 m and from the hypolimnion at 16 m. Determination of water physical-chemical variables was performed following standard protocols (see SUPPLEMENT-Materials and Methods).

2.2 Metabolic variables

Rates of bacterial protein production (BPP) were determined by incorporation of ^{14}C-leucine (Simon and Azam, 1989). Triplicates and a formol-killed control (5 ml) were incubated in situ with ^{14}C-Leu (Hartmann Analytic GmbH, Germany) at a final concentration of 80 nM for 1 h in dark, water permeable containers mounted at 2 m and 14 m. After fixation with 2 % formalin, samples were filtered onto 3.0 µm (PA bacteria) and subsequent the filtrate on 0.2 µm (FL bacteria) nitrocellulose filters (Sartorius AG, Göttingen, Germany) and processed according Attermeyer et al. (2013). The incorporated leucine was measured as disintegrations per minute (dpm) on a liquid scintillation analyzer (TriCarb 2810 TR, Perkin Elmer Inc., Illinois, USA) and converted into BPP-C by applying an intracellular isotope dilution factor of 2 (Kirchman, 1993) and a factor of 0.86 to convert the produced protein to carbon (Simon and Azam, 1989).

Bacterial Respiration (BR) was determined indirectly, based on the assumption that ecosystem respiration (ER) is the sum of BR + phytoplankton respiration (PR) + zooplankton respiration (ZR) by assuming a PR of 30% GPP and a fixed ratio of BR to ZR of 1.5 as described in Berman et al. (2010). Gross primary production (GPP) and ecosystem respiration (ER)

were derived from Giling et al. (2017), which used a diel oxygen (O_2) model to partition the changes in dissolved oxygen concentration into the contribution by biological processes and physical processes following Grace et al. (2015) and Song et al. (2016) and using a photosynthetic quotient of 1.2 and a respiratory quotient of 1.0 to express metabolic rates in carbon units (Wetzel and Likens, 2000).

2.3 Prokaryote abundance

Abundance of heterotrophic FL prokaryotes was determined by flow cytometry (BD Accuri™ C6), from 0.5 % glutaraldehyde fixed and flash-frozen samples (-80°C), after staining with SYBR© green I (Life Technologies Inc.). Identification was based on gating of SYBR© green I fluorescence against the side scatter signal and phycoerythrin orange fluorescence (Marie et al., 1999). Particle-associated (PA) prokaryotes were enumerated by epifluorescence-microscopy on a Leica Leitz DMRB fluorescence microscope with UV- and blue light excitation filters (Leica Microsystems, Wetzlar, Germany) as described in (Hornick et al., 2017). We subsequently refer to heterotrophic bacteria, since bacteria account for the majority of non-photosynthetic prokaryotes in surface waters.

2.4 DNA sampling, extraction and sequencing

Water samples (1L) for molecular analyses were filtered onto 3.0 µm and subsequently on 0.2 µm polycarbonate membrane filters (Whatman, Dassel, Germany) to size-separate between particle-associated (PA) and free-living (FL) organisms. Filters were stored at -20 °C. DNA was extracted from the filters with chloroform-phenol-isoamylalcohol (25:24:1; Carl Roth, Karlsruhe, Germany), CTAB (SERVA, Heidelberg, Germany) and zirconium beads (Carl Roth, Karlsruhe, Germany) according to (Nercessian et al., 2005).

2.5 Sequencing and bioinformatics analyses

PCR, library preparation and sequencing were performed at LGC Genomics (Berlin, Germany). Briefly, the V3-V4 region was amplified using primers 341F-785R (Klindworth et al., 2013), followed by library preparation and sequencing on a MiSeq Illumina platform.

Sequences were quality checked and analysed using Mothur v1.37.6 (Schloss et al., 2009). Sequences shorter than 300 bp or with ambiguities and homopolymer stretches of more than 8 bases were excluded from further analysis. Chimera check was performed using UCHIME (Edgar et al., 2011) and global singleton sequences were removed. Sequences were clustered into operational taxonomic units (OTU) using VSEARCH (Rognes et al., 2016; as implemented in Mothur) with a minimum sequence similarity value of 97 %. Taxonomy assignment of the OTUs was based on the naïve Bayesian RDP classifier (Wang et al., 2007) using the SILVA reference database v123 with a confidence threshold of 80 %. For further analyses, reads that were less abundant than five in the whole dataset were removed.

2.6 Statistical analyses

We tested for the effect of the treatment (mixing) across periods of time and modeled the response variable as a function of treatment by using linear mixed effect models (LME). To account for the dependency amongst observations of the same enclosure, we used enclosure as a random intercept. Additionally, we corrected for residual autocorrelation by incorporating a temporal autocorrelation structure (AR1). Data were transformed when appropriate. Visual inspection of residual plots did not reveal any obvious deviations from homoscedasticity or normality. LME were performed using R (R Core Team, 2016) and package 'nlme'(Pinheiro et al., 2017).

Bacterial community composition (BCC) was analysed using Principal Coordinate Analyses (PCoA) and R-function 'pcoa' with a correction for negative eigenvalues (Paradis et al., 2004) based on the Bray-Curtis measure (Bray and Curtis, 1957). We used permutational multivariate analysis of variance (PERMANOVA, perm=999) to test for significant ($p < 0.05$) differences (McArdle and Anderson, 2001; Anderson et al., 2008). Distance-based linear modeling (DistLM) was performed to relate physical/chemical predictor variables to the multivariate community assemblage (Legendre and Anderson, 1999; McArdle and Anderson, 2001; Anderson et al., 2008). Environmental data and microbial data were normalized or square root-transformed, respectively (Anderson et al., 2008). Distance based redundancy analysis (dbRDA) was used for visual interpretation of the DistLM in multi-dimensional space (Anderson et al., 2008). For downstream analyses on α-diversity measures all samples were rarefied to an equal sequence number per sample to avoid heterogeneity in sequencing depth. Analyses were performed with R 3.2.5 (R Core Team, 2016) using packages 'vegan' (Oksanen et al., 2017) and 'ggplot2' (Wickham, 2009) as well as PERMANOVA + for Primer (Anderson et al., 2008; Clarke and Gorley, 2006). Differential abundance of single OTUs between mixed and control enclosures across time based on the negative binomial distribution was determined using R-package 'DESeq2' (Love et al., 2014).

2.7 Network analyses

Absolute abundances of OTUs were approximated from relative abundances for heterotrophic prokaryotes and cyanobacteria by using flow cytometry (FL) and microscopy (PA) cell counts. We made an initial reduction of this dataset by including only OTUs which occurred at least in ten samples and/or were among the 450 most abundant OTUs in FL or PA bacterial communities. For this reduced list, we calculated the pairwise maximal information coefficient (MIC; Reshef et al., 2011) between the approximated absolute abundances of these OTUs across the entire data set. Following false discovery rate correction the results were visualized as network (NET1) using Cytoscape v. 3.3.0 (Shannon, 2003; Smoot et al., 2011). For each OTU we calculated the betweenness centrality (proportion of passes through a variable for each shortest path between any two variables) (Doncheva et al., 2012), which was highlighted as potential proxy for identifying key species

(Eldridge et al., 2015; Guidi et al., 2016). We then calculated the MIC values between environmental variables and only OTUs that were previously shown to be differentially abundant between control and mixed enclosures using DESeq2 (described above) and visualized this as a network (NET2). Betweeness centrality values from NET1 were overlayed onto OTUs in NET2 and visualized as a proportion of node size. We subsequently divided this into three subnetworks, with the first containing OTUs differentially abundant directly after mixing (t1, NET2-I), after six days (t6, NET2-II) and thereafter (t21-42, NET2-III).

3. Results

3.1 Epilimnic responses in water physical-chemical variables and phytoplankton development

PERMANOVA of a multivariate assemblage of epilimnic water physical-chemical variables revealed a strong temporal variation (Time-$F_{8,54}$ = 68.3, p < 0.001) and significant differences between mixed and control enclosures (Treatment-$F_{1,54}$ = 25.86, p < 0.001), however, not consistent through time (Treatment x Time-$F_{8,54}$ = 3.98, p < 0.001) (Table S1). Control and mixed enclosures separated directly after mixing until t3 on the first and second principal component (PC, explaining together 53.4 % of variation, Table S2) of a PCA (Figure 1), which describes well the disruption of water chemistry and physics by mixing colder metalimnic water with higher concentrations of dissolved and particulate matter into the epilimnion. After one day, thus, mixing resulted in an 2.4-fold and 2-fold increase in TDN and SRP, respectively, relative to the control enclosures (exact one-tailed Mann-Whitney U; mixed > control; n_{mixed} = 4; $n_{control}$ = 4; TDN: p = 0.01, SRP: p = 0.03). Within three days, extra dissolved nutrients were transferred into particulate matter given as the percentage total particulate phosphorous (TPP) of total phosphorous (TP), and resulted in Chl *a* concentrations 1.8-fold higher than in the control (exact one-tailed Mann-Whitney U; mixed > control; N_{mixed} = 4; $N_{control}$ = 4; %TPP of TP: p = 0.01, Chl *a*: p = 0.01) (Figure 1). The increase in Chl *a* concentration persisted over 4 weeks ($LME_{t3\text{-}t27}$: $F_{1,6}$ = 8.0, p = 0.03) (Figure 1).

3.2 Epilimnic bacterial community composition

Epilimnic FL and PA bacteria comprised different bacterial community compositions (BCC) throughout the experiment (PERMANOVA; fraction-$F_{1,67}$ = 61.92, p < 0.001; time-$F_{4,67}$ = 6.30, p < 0.001) (Figure S1). Thereby size-fraction (FL vs. PA) explained about 2.5-times more variation in BCC than time. Subsequent, FL and PA BCC were analyzed separately for effects of mixing and temporal development.

3.2.1 Effects on diversity and community composition

Mixing significantly increased richness (^0D) in epilimnic FL and PA bacterial communities at t1, however, no significant effect on richness can be observed at later time points anymore (Figure S2). Hill numbers ^1D and ^2D were only significantly affected by mixing at t1 in case of

PA BCC. Nonetheless ^{2}D was generally decreased in case of FL BCC in mixed enclosures between t1 and t21. Six weeks post mixing we could not observe any effects of the treatment on bacterial α-diversity measures anymore. Irrespective of mixing, PA BCC showed generally decreased Pielou´s eveness (J) during phytoplankton bloom conditions (Figure S2).

Most chemical variables revealed a significant relationship with both FL and PA bacterial β-diversity by distance-based linear modeling (DISTLM) ("marginal tests"; Table S3-I). Temperature was the strongest predictor of community structure, explaining ~12 % and ~15 % of variance in FL and PA BCC, respectively. However, also concentration of ammonia, particulate organic matter (POM), Chl *a* and dissolved silica (DSi) explained comparable high amounts of variation (~10-13 %). The best model fits of a DISTLM, allowing for parameter interactions, explained ~35 % and 19 % of variation in FL and PA BCC, respectively (Table S4-II). An ordination of the DISTLM by distance-based redundancy analysis (dbRDA) reflects direct and indirect effects of mixing on FL and PA BCC by changes in temperature, nutrient concentration and phytoplankton biomass (Figure S3). Decreased epilimnic temperature and increased nutrient concentration (TDN) separated both bacterial communities between mixed and control enclosures on t1 on the first three dbRDA axes. Increased phytoplankton biomass (POC, Chl *a*) in the three mixed enclosures with enhanced concentrations of Chl *a* resulted in the separation between mixed and control enclosures of both FL and PA bacterial communities at t21 (Figure 3). However, no effects of mixing on BCC could be observed after six weeks post mixing (t42) in constrained (dbRDA) or unconstrained analyses (PCoA) (Figures S3 & S4).

Mixing significantly affected 131 OTUs during the experiment (Table S5) from which 21 OTUs contributed >1 % in either control or mixed enclosures at one particular time point (Table 1). Directly after mixing (t1), 17 FL and 53 PA OTUs revealed a significantly different relative abundance between mixed and control enclosures, contributing in average to ~4 % (FL) and ~11 % (PA) to BCC in all mixed enclosures. Relative to control enclosures, the relative abundance of mixing-sensitive OTUs decreased on average by ~11 % in case of FL bacteria, but increased by ~7 % in case of PA bacteria, respectively. Thus, mixing affected directly more PA bacteria positively, from which OTU002, taxonomically identified as *Dolichospermum* sp., increased its relative abundance ~3.8-fold up to ~61 ± 6 % in all mixed enclosures within one week (t6) relative to the controls (Table 1). Interestingly, another *Cyanobacteria*-OTU (OUT004, *SubsectionI_FamilyI*) was the most negatively affected bacterial OTU which was present in both FL and PA bacterial communities. During the bloom breakdown of *Dolichospermum* sp. several PA *Proteobacteria*-OTUs increased in mixed enclosures (Table 1). At the same time a relative increase in *FukuN18* (*Verrucomicrobia*) and *Sporichtyaceae* (*Actinobacteria*) can be observed in the FL BCC (Figure 2; Figure S5).

3.2.2 Interaction network between affected OTUs and environmental variables

We explored the dependence between all pairs of environmental variables and approximated absolute abundances of significantly different OTUs, between mixed and control enclosures across the entire data set, using the maximal information coefficient (MIC). Subnetworks were constructed by visualizing only correlations between environmental variables and OTUs, whose abundance was significantly impacted. These subnetworks are primarily a representation of which variables drove the differences in abundance of single OTUs between control and mixed enclosures over a particular time period (Figure 3). The majority of OTUs impacted in the short term (t1) resulted in an increased abundance, and were positively correlated with the concentration of dissolved nutrients (Figure 3-I (A,B)) and negatively correlated with water temperature (Figure 3-I (B)). In contrast, the few OTUs negatively impacted, exhibited a strong positive correlation to water temperature (Figure 3-I (C)). Over the short term only two significantly affected OTUs were significantly correlated with particulate nutrient concentrations alone.

Over the medium term (t6-t42), multiple driving factors emerged with distinct settings, which impacted on the abundance of microbial taxa. (i) After one week (t6) a number of OTUs belonging mainly to *Bacteroidetes* (Figure 3-II (D)) and other bacterial groups (Figure 3-II (E) increased with mixing, associated with the variation in temperature, proton and DOM concentrations. This increase exhibited no relation to Chl *a* (>3 µm) or POM. (ii) In addition, at t6 a set of cyanobacterial OTUs revealed an increased abundance in mixed relative to control mesocosms (Figure 3-II (F). These OTUs were taxonomically assigned to *Dolichospermum* sp. (OTU002), *Planktothrix* sp. (OTU073) and one unknown cyanobacteria (OTU010). During the course of the experiment *Dolichospermum* sp. largely drove the increase in Chl *a,* as assessed by microscopic and FlowCAM analysis, thus revealing a strong positive correlation to Chl *a.* In contrast, *Planktothrix* sp. did not reveal any correlation to Chl *a* or POM, potentially being among organisms that were mixed in from the metalimnion. (iii) At t21, differences in OTU abundance (*Verrucomicrobia*, *Betaproteobacteria*) between mixed and control enclosures were mainly associated to concentrations of POM and Chl *a* (>3 µm) (Figure 3-III (G)). (iv) At t42 a group of *Bacteroidetes* was negatively affected in the mixed enclosures during post-bloom conditions (Figure 3-III (H)).

3.3 Epilimnic heterotrophic activity and bacterial abundance

Within two days, mixing increased BR-C in mixed relative to control enclosures, an observation which persisted throughout the experiment (LME $_{t1\text{-}t42}$, BR-C: $F_{1,54} = 9.084$, $p < 0.024$) (Figure 4). In particular, unproportional high BR in relation to the present nutrient conditions could be observed at t21 associated to the decline in Chl *a* concentration in three mixed enclosure that developed a bloom of *Dolichospermum* sp. In contrast, differences in BPP-C between control and mixed enclosures could not be observed during the first three

weeks ($LME_{t1\text{-}t14}$, $p > 0.05$). However, effects of mixing resulted in a ca. 1.6-fold higher BPP-C than in the control on day 21 (exact two-tailed Mann-Whitney U; $n_{mixed} = 4$; $n_{control} = 4$; $p = 0.02$), mainly driven by PA bacteria that colonized senescent cells of *Dolichospermum* sp. during the bloom decay (Figure 4, Figure S5). Subsequently, in the three mixed enclosures, which formed a bloom of *Dolichospermum* sp. PA and FL bacterial BPP-C was stimulated ($LME_{t21\text{-}t42}$; PA: $F_{1,19} = 13.69$, $p = 0.014$; FL: $F_{1,19} = 7.129$, $p = 0.044$). Bacterial abundances and csBPP-C do not reveal consistent differences of mixing relative to control enclosures. However, higher bacterial abundances in mixed enclosures can be observed, when FL bacteria yielded their maximum abundance during the experiment at t14 and when PA bacteria colonized colonies of *Dolichospermum* sp. during the bloom breakdown at t21 (Figure S5).

3.4 Heterotrophic processes in the hypolimnion during and after the *Dolichospermum* sp. bloom

Following the epilimnic breakdown of Chl *a* in the three enclosures which developed a pronounced bloom of *Dolichospermum* sp., hypolimnic BPP-C did not increase. Between t10 and t35 we observed a decrease in BPP-C and BGE at enhanced rates of BR in the mixed enclosures relative to the controls ($LME_{t10\text{-}t35}$: ER-C: $F_{1,32} = 15.134$, $p = 0.0081$; log2(BPP-C+1): $F_{1,16} = 12.524$, $p = 0.0122$; BGE: $F_{1,16} = 54.8754$, $p = 0.0003$; Figure 5).

4. Discussion

4.1 Impact of mixing on community assembly

It is often hypothesized that ecological disturbances alter community assembly process (Myers et al., 2015). The entrainment of deep water into the epilimnion increased the physico-chemical variability between mixed enclosures compared to the controls. However, at the same time (t1) we observed lowest β-diversities between all mixed enclosures compared to controls in FL and PA bacterial communities (Figure 6), suggesting that the disturbance creates communities that are more similar to one another by imposing a consistent selective pressure. Thus, the disturbance itself might act as a strong selection factor reducing stochasticity (Zhou et al., 2014). The majority of OTUs, for which mixing significantly increased abundance were likely introduced from a deep water community into the epilimnion as indicted by the presence of specific OTUs and their relation to decreased water temperatures and increased dissolved nutrients (Figure 3). The increase in bacterial richness (Figure S2) after mixing diminished rapidly within one week, suggesting that most of the introduced metalimnic community was not able to persist. However, network analysis suggested that other members of the microbial community were also favored during the re-stratification of the water column and the degradation of organic matter (Figure 3-II). We identified several increased OTUs belonging to *Bacteroidetes* which were co-correlated to increased abundances of *Planktothtrix* sp. with mixing at t6. *Planktothtrix* sp. was potentially

mixed in from the metalimnion, but did not further increase in abundance in the mixed layer after one week. It is thus likely that *Bactroidetes* were favored from the degradation of organic matter mixed into the epilimnion or dead organisms not able to cope with the new environmental conditions. Also, we observed a pronounced increase in the proportion of filamentous cyanobacteria of the genus *Dolichospermum* sp. contributing to and structuring PA BCC within one week. This strong increase occurred across all mixed enclosures, irrespectively that only three out of four enclosures continued to finally form a bloom of *Dolichospermum* sp. with up to ~7 µg of total Chl *a* L^{-1} ca. 2.5 weeks after the mixing event. The collapse of *Dolichospermum* sp. in one of the mixed enclosures after one week (mesososm #13) was likely caused by an infection with parasites (Kagami et al., 2014; Frenken et al., 2017) or cyanophages (Šulčius and Holmfeldt, 2016; Šulčius et al., 2017). Although the precise reason remains unclear, the rapid decrease of *Dolichospermum* sp. cells in this particular enclosure points to an unexceptional lysis event, which was not directly related to mixing. Nonetheless, mixing also altered PA BCC in this particular enclosure and a different community developed compared to all controls was observed. After ca. 6 weeks after the disturbance, all bacterial communities converged towards the control structure showing a high degree of resilience. This agrees with several studies examining the resilience of lake microbial communities to different types of disturbances including perturbations by typhoons (Jones et al., 2008), nutrient addition (Shade et al., 2011) or mixing as well as whole-ecosystem mixing (Shade et al., 2012b).

4.2 Implications for carbon cycling

Induced mixing of the water column had the direct effect of stimulating the growth of autotrophic microorganisms with a particularly high affinity for nutrient uptake. In natural lakes, summer storm events have typically resulted in large blooms of diazotrophic cyanobacteria such as *Dolichospermum* sp. (Jennings et al., 2012; Kasprzak et al., 2017), a trend we were able to reproduce in this study. The competitive advantage of these organisms, following mixing events, is due to a combination of different traits including the storage of phosphorous and nitrogen in large organic macromolecules (Klemke et al., 2014), fixation of atmospheric nitrogen (Karlson et al., 2015; Klawonn et al., 2016) regulation of buoyancy (Reynolds et al., 1987; Klemer et al., 1996) as well as the possibility to clog the feeding apparatus of herbivorous zooplankton (Lampert, 1987). Such environmental filtering not only impacts adjacent microbial communities but also has implications for both heterotrophic and autotrophic contributions to carbon cycling (Shade et al., 2012a). Under stable stratified conditions the proliferation of cyanobacteria within the epilimnion is limited by the availability of nutrients. Within deep stratified lakes, the formation of a DCM reflects a balance between the nutrient limitation of epilimnic waters and light limitation at deeper depths. Summer storms disrupt this balance by redistributing large amounts of nutrients into the photic epilimnion where they can be rapidly assimilated into phytoplankton biomass (e.g., *Dolichospermum* sp.). This additional input of nutrients relaxes phytoplankton

from nutrient limitation allowing for a much broader distribution of phytoplankton cells across the whole epilimnion. There self-shading may shift the system from nutrient towards light and hence carbon limitation. Under these conditions decomposition of the nutrient enriched POM selects for organisms with an increased propensity for complex carbohydrate utilisation, in this case particle-associated *Betaproteobacteria* (*Burkholderiales*, *Comamonadaceae*), and free-living *Verrucomicrobia* (*Fuku_N18*) (Martinez-Garcia et al., 2012; Cardman et al., 2014; He et al., 2017). The colonization and decomposition of senescent cells of *Dolichospermum* sp. during bloom decay strongly elevated BPP mainly on particles, and explains an unproportional high BR in relation to the present nutrient conditions at t21 (Figure 4), presumably with consequences for gas fluxes between lake and atmosphere and deposition of nutrients and carbon to the sediments. Interestingly, during increase and breakdown of *Dolichospermum* sp. we observed a significant decreased hypolimnic BPP and BGE in mixed enclosures. We argue that the high bacterial organic matter turnover on cells of *Dolichospermum* in the epilimnion enhanced the recalcitrance of exported particles, thus increasing efficient nutrient recycling in the epilimnion but decreasing POM and nutrient availability in the hypolimnion.

Surprisingly, we did not detect a contemporaneous change in BPP or abundance of heterotrophic prokaryotes (HP) due to mixing until the breakdown of Chl *a* ca. 3 weeks post mixing. Weithoff et al. (2000) performed a similar enclosure experiment in Lake Flakensee but applying two mixing events with a delay of eight days. Thereby bacterial abundance almost doubled within one day after the first mixing but remained unchanged compared to the control after the second mixing. This observation coincided with different local phytoplankton and zooplankton communities during and after both mixing events. Although Weithoff et al. (2000) report that the nutrient supply was even larger during the second mixing event, cladoceran grazing was likely an important factor in controlling bacterial abundance (Weithoff et al., 2000). In Lake Stechlin, a generally high proportion of Cryptophytes and other potential mixotrophs are contributing to phytoplankton community composition. Also, bacterivorous mixotrophs such as *Cryptomonas* species commonly dominate late summer plankton communities (Mitra et al., 2014; Grujcic et al., 2018) and are abundant during the formation of a DCM (Tittel et al., 2003), that was disrupted by mixing. Although we did not determine grazing rates, it is thus likely that effects on bacterial biomass production, in particular during the first three weeks, were masked through enhanced bacterial grazing by mixotrophs or zooplankton, rather than assuming that bacteria were not stimulated by the supply of bioavailable nutrients.

4.3 Conclusion

Our results highlight effects on community assembly and heterotrophic bacterial metabolism that are associated to entrainment of deep water into the mixed water layer and assess consequences for the coupling between bacterial metabolism and autochthonous DOM production in large volume clear-water lakes. We identified settings

of environmental conditions after the mixing event which impacted microbial populations, changing their relative as well as absolute abundance. Thereby, water column disturbance of a summer storm with its associated canalizing ecological drivers may act as a deterministic rather than a stochastic force greatly influencing bacterial dynamics and functions. Our investigation of post-mixing environmental conditions and biotic interactions clearly demonstrate that changes in physical-chemical gradients by mixing impact bacterial community assembly and may further exacerbate warming related increases in cyanobacterial blooms (Posch et al., 2012; Elliott, 2012; Paerl and Paul, 2012). In the long-term run, a potential selection for heterotrophic bacteria with an increased propensity for remineralisation of more complex carbohydrate pools due to mixing related shifts in phytoplankton communities and nutrient content of the organic matter is likely to increase internal eutrophication of freshwater environments.

5. Acknowledgements

We are grateful to the entire TemBi and LakeLab teams for the preparation of the experiment, assistance with sampling, advice and provision of data. These teams include M. Arias, S. Beeske, P. Casper, M. Degebrodt, W. Eckert, C. Engelhardt, A. Fuchs, S. Hamadouche, P. Kasprzak, T. Kettner, G. Kirillin, B. Laube, M. Lentz, E. Mach, U. Mallok, K.C. Martinez-Cruz, J. Padisak, M. Papke, A. Penske, R. Roßberg, M. Sachtleben, J. Sareyka, G. Santaolalla, M. Schnittger, G. Selmeczy and A. Sepulveda-Jauregui. Additionally, we thank K. Pohlmann for advice on statistical analyses. This study was supported by a Leibniz Competition grant to P. Casper and HPG (project 'Climate driven changes in biodiversity of microbiota' – TemBi; SAW-2011-IGB-2), funding received by MOG from the German Federal Ministry of Education and Research (BMBF) for constructing the enclosure facility (no. 033L041B), and a Core Facility grant to MOG from the German Research Foundation (DFG) to operate the facility (no. GE 1775/2-1).

6. Conflict of Interest

The authors declare no conflict of interest.

7. Tables

Table 1: Differentially abundant bacterial OTUs in artificial mixed and control enclosures with taxonomic affiliation. Only OTUs contributing >1% to mean relative read abundance in either control or mixed enclosures are listed. The full list of significantly affected OTUs by mixing can be obtained from Table S5. Testing for differentially abundant taxa was achieved using the DESeq function in the DESeq2 package (Love et al., 2014) with multiple-inference correction (Benjamini and Hochberg, 1995) and a significance level of $p < 0.01$. One artificial mixed enclosure (#E13), which did not develop a bloom of *Dolichospermum* sp., was

excluded from calculations after t6. OTUs present in both FL and PA bacterial size-fractions are marked in bold.

8. Figures

Figure 1: I) First and second principal component (PC) of a principal component analysis (PCA) of water physical-chemical variables comprising dissolved and particulate organic matter, measures of carbonate chemistry, photosynthetically active radiation (PAR) and temperature (see Table S2). Box and whisker plots of **II-A)** Chl *a* concentration and **II-B)** percentage total particulate phosphorus (TPP) of total phosphorus (TP). One mixed enclosure (#13), which did not develop a bloom of *Dolichospermum* sp. after t6 is indicated by an open triangle. The lower and upper hinges correspond to the first and third quantiles (25^{th} and 75^{th} percentiles). Upper and lower whiskers extend from the hinges at maximum 1.5 times the inter-quantile range. Data beyond the end of whiskers are plotted individually.

Figure 2: Stacked bar plot of **A)** free-living (FL) and **B)** particle associated (PA) bacterial community composition during the course of the experiment. Only the most abundant taxonomic bacterial groups are shown. A more detailed phylogenetic resolution can be obtained from Figure S5.

Figure 3: Network representation of the dependence between environmental variables and approximated absolute abundances of significantly different OTUs between mixed and control enclosures across the entire data set, using the maximal information coefficient (MIC). NET2-subnetworks (I-III) were constructed by visualizing only correlations between environmental variables and OTUs, whose abundance was significantly impacted at **I)** t1, **II)** t6 as well as **III)** t21 and t42 (t42 marked with white numbers) (see Text). These subnetworks are primarily a representation of which variables drove the differences in abundance of single OTUs between control and mixed enclosures over a particular time period.

Figure 4: Box and whisker plots of **I-A)** bacterial protein production (BPP-C) and **I-B)** bacterial respiration (BR-C) in the epilimnion during the course of the experiment. **II)** Relation between bacterial respiration (BR-C) and carbon-to-phosphorous ratio (C:P) of particulate organic matter. Filaments of *Dolichospermum* sp. were heavily colonized by bacterial cells during the breakdown of a bloom of *Dolichospermum* sp., which developed in three out of four artificial mixed mesocosms. One mixed enclosure (#13) which did not develop a *Dolichospermum* sp. bloom after t6 is indicated by an open triangle. Symbols refer to mixed and control enclosures, respectively. Colors indicate the time point during the course of the experiment (legend upper right). The lower and upper hinges correspond to the first and third quantiles (25^{th} and 75^{th} percentiles). Upper and lower whiskers extend from the hinges at maximum 1.5 times the inter-quantile range. Data beyond the end of whiskers are plotted individually.

Figure 5: I) Heterotrophic processes in hypolimnion: **A)** Bacterial protein production (BPP-C), **B)** bacterial respiration (BR-C) and **C)** bacterial growth efficiency (BGE). BGE, calculated as BPP-C/(BPP-C + BR-C), denotes how much carbon is transferred into biomass and can be used as an approximation for bacterial fitness and efficiency of carbon usage (del Giorgio and Cole, 1998). One mixed enclosure (#13) which did not develop a *Dolichospermum* sp. bloom after t6 is indicated by an open triangle.

Figure 6: Dissimilarities in community composition of **A)** particle-associated (PA) and **B)** free-living (FL) bacteria (Bray-Curtis distance) and **C)** differences in water physical-chemical properties (Euclidean distance). Physical and chemical variables (Table S2) were log(x+1)-transformed, centered and scaled. Bray-Curtis similarity index was calculated based on square-root-transformed compositional community data. One mixed enclosure (#13) which revealed different Chl *a* dynamics is indicated by an open triangle. The lower and upper hinges correspond to the first and third quantiles (25^{th} and 75^{th} percentiles). Upper and lower whiskers extend from the hinges at maximum 1.5 times the inter-quantile range. Data beyond the end of whiskers are plotted individually. Significance is indicated by asterisks (Dunn´s test of multiple comparisons following a significant Kruskal-Wallis test with correction according (Benjamini and Hochberg, 1995) to control the experimental error rate (Ogle, 2017)). Dissimilarities with one mixed enclosure (#13) which did not develop a *Dolichospermum* sp. bloom after t6 is indicated by an open triangle.

9. References

Anderson MJ, Gorley RN, Clarke KR. (2008). PERMANOVA + for PRIMER: Guide to Software and Statistical Methods. PRIMER-E: Plymouth, UK.

Attermeyer K, Premke K, Hornick T, Hilt S, Grossart H-P. (2013). Ecosystem-level studies of terrestrial carbon reveal contrasting bacterial metabolism in different aquatic habitats. *Ecology* **94**: 2754–2766.

Benjamini Y, Hochberg Y. (1995). Controlling the False Discovery Rate: a Practical and Powerful Approach to Multiple Testing. *J R Stat Soc* **57**: 289–300.

Berman T, Yacobi YZ, Parparov A, Gal G. (2010). Estimation of long-term bacterial respiration and growth efficiency in Lake Kinneret. *FEMS Microbiol Ecol* **71**: 351–363.

Bray JR, Curtis JT. (1957). An Ordination of the Upland Forest Communities of Southern Wisconsin. *Ecol Monogr* **27**: 325–349.

Cardman Z, Arnosti C, Durbin A, Ziervogel K, Cox C, Steen AD, et al. (2014). *Verrucomicrobia* are candidates for polysaccharide-degrading bacterioplankton in an Arctic fjord of Svalbard. *Appl Environ Microbiol* **80**: 3749–3756.

Clarke KR, Gorley RN. (2006). PRIMER v6: User manual/Tutorial. PRIMER-E: Plymouth, UK.

Coumou D, Rahmstorf S. (2012). A decade of weather extremes. *Nat Clim Chang* **2**. e-pub ahead of print, doi: 10.1038/nclimate1452.

del Giorgio PA, Cole JJ. (1998). Bacterial Growth Efficiency In Natural Aquatic Systems. *Annu Rev Ecol Syst* **29**: 503–541.

Doncheva NT, Assenov Y, Domingues FS, Albrecht M. (2012). Topological analysis and interactive visualization of biological networks and protein structures. *Nat Protoc* **7**: 670–685.

Edgar RC, Haas BJ, Clemente JC, Quince C, Knight R. (2011). UCHIME improves sensitivity and speed of chimera detection. *Bioinformatics* **27**: 2194–2200.

Eldridge DJ, Woodhouse JN, Curlevski NJA, Hayward M, Brown M V, Neilan BA. (2015). Soil-foraging animals alter the composition and co-occurrence of microbial communities in a desert shrubland. *ISME J* **9**: 2671–2681.

Elliott JA. (2012). Is the future blue-green? A review of the current model predictions of how climate change could affect pelagic freshwater cyanobacteria. *Water Res* **46**: 1364–1371.

Frenken T, Alacid E, Berger SA, Bourne EC, Gerphagnon M, Grossart H-P, et al. (2017). Integrating chytrid fungal parasites into plankton ecology: research gaps and needs. *Environ Microbiol* **19**: 3802–3822.

Giling DP, Nejstgaard JC, Berger SA, Grossart H-P, Kirillin G, Penske A, et al. (2017). Thermocline deepening boosts ecosystem metabolism: evidence from a large-scale lake enclosure experiment simulating a summer storm. *Glob Chang Biol* **23**: 1448–1462.

Grace MR, Giling DP, Hladyz S, Caron V, Thompson RM, Mac Nally R. (2015). Fast processing of diel oxygen curves: Estimating stream metabolism with BASE (BAyesian Single-station Estimation). *Limnol Oceanogr Methods* **13**: e10011.

Grujcic V, Nuy JK, Salcher MM, Shabarova T, Kasalicky V, Boenigk J, et al. (2018). Cryptophyta as major bacterivores in freshwater summer plankton. *ISME J* **12**: 1668–1681.

Guidi L, Chaffron S, Bittner L, Eveillard D, Larhlimi A, Roux S, et al. (2016). Plankton networks driving carbon export in the oligotrophic ocean. *Nature* **532**: 465–470.

He S, Stevens SLR, Chan L-K, Bertilsson S, Glavina del Rio T, Tringe SG, et al. (2017). Ecophysiology of Freshwater Verrucomicrobia Inferred from Metagenome-Assembled Genomes. *mSphere* **2**: e00277-17.

Hornick T, Bach LT, Crawfurd KJ, Spilling K, Achterberg EP, Woodhouse JN, et al. (2017). Ocean acidification impacts bacteria–phytoplankton coupling at low-nutrient conditions. *Biogeosciences* **14**: 1–15.

IPCC (2013). *Climate Change 2013: The Physical Science Basis. Contribution of Working Group I to the Fifth Assessment Report of the Intergovernmental Panel on Climate Change* [Stocker, T.F., D. Qin, G.-K. Plattner, M. Tignor, S.K. Allen, J. Boschung, A. Nauels, Y. Xia, V. Bex and P.M. Midgley (eds.)]. Cambridge University Press, Cambridge, United Kingdom and New York, NY, USA, 1535 pp, doi:10.1017/CBO9781107415324.

Ives AR, Carpenter SR. (2007). Stability and Diversity of Ecosystems. *Science (80-)* **317**: 58–62.

Jennings E, Jones S, Arvola L, Staehr PA, Gaiser E, Jones ID, et al. (2012). Effects of weather-related episodic events in lakes: an analysis based on high-frequency data. *Freshw Biol* **57**: 589–601.

Jones SE, Chiu C-Y, Kratz TK, Wu J-T, Shade A, McMahon KD. (2008). Typhoons initiate predictable change in aquatic bacterial communities. *Limnol Oceanogr* **53**: 1319–1326.

Kagami M, Miki T, Takimoto G. (2014). Mycoloop: chytrids in aquatic food webs. *Front Microbiol* **5**: 1–9.

Karlson AML, Duberg J, Motwani NH, Hogfors H, Klawonn I, Ploug H, et al. (2015). Nitrogen

fixation by cyanobacteria stimulates production in Baltic food webs. *Ambio* **44**: 413–426.

Kasprzak P, Shatwell T, Gessner MO, Gonsiorczyk T, Kirillin G, Selmeczy G, et al. (2017). Extreme Weather Event Triggers Cascade Towards Extreme Turbidity in a Clear-water Lake. *Ecosystems*. e-pub ahead of print, doi: 10.1007/s10021-017-0121-4.

Kirchman DL. (1993). Leucine incorporation as a measure of biomass production by heterotrophic bacteria. In: Kemp P, Sherr BF, Sherr EB, Cole JJ (eds). *Current methods in aquatic microbial ecology*. Lewis Publishers: New York, USA, pp 509–512.

Klawonn I, Nahar N, Walve J, Andersson B, Olofsson M, Svedén JB, et al. (2016). Cell-specific nitrogen- and carbon-fixation of cyanobacteria in a temperate marine system (Baltic Sea). *Environ Microbiol* **18**: 4596–4609.

Klemer AR, Cullen JJ, Mageau MT, Hanson KM, Sundell R a. (1996). Cyanobacterial Buoyancy regulation: The Paradoxical Roles of Carbon. *J Phycol* **32**: 47–53.

Klemke F, Beyer G, Sawade L, Saitov A, Korte T, Maldener I, et al. (2014). All1371 is a polyphosphate-dependent glucokinase in Anabaena sp. PCC 7120. *Microbiology* **160**: 2807–2819.

Klindworth A, Pruesse E, Schweer T, Peplies J, Quast C, Horn M, et al. (2013). Evaluation of general 16S ribosomal RNA gene PCR primers for classical and next-generation sequencing-based diversity studies. *Nucleic Acids Res* **41**: e1.

Lampert W. (1987). Laboratory studies on zooplankton-cyanobacteria interactions. *New Zeal J Mar Freshw Res* **21**: 483–490.

Legendre P, Anderson MJ. (1999). Distance-Based Redundancy Analysis: Testing Multispecies Responses in Multifactorial Ecological Experiments. *Ecol Monogr* **69**: 1–24.

Love MI, Huber W, Anders S. (2014). Moderated estimation of fold change and dispersion for RNA-seq data with DESeq2. *Genome Biol* **15**: 550.

Marie D, Brussaard CPD, Thyrhaug R, Bratbak G, Vaulot D. (1999). Enumeration of Marine Viruses in Culture and Natural Samples by Flow Cytometry Enumeration of Marine Viruses in Culture and Natural Samples by Flow Cytometry. *Appl Environ Microbiol* **65**: 45–52.

Martinez-Garcia M, Brazel DM, Swan BK, Arnosti C, Chain PSG, Reitenga KG, et al. (2012). Capturing single cell genomes of active polysaccharide degraders: An unexpected contribution of *Verrucomicrobia*. *PLoS One* **7**: 1–11.

McArdle BH, Anderson MJ. (2001). Fitting Multivariate Models to Community Data : A Comment on Distance-Based Redundancy Analysis. *Ecology* **82**: 290–297.

Mitra A, Flynn KJ, Burkholder JM, Berge T, Calbet A, Raven JA, et al. (2014). The role of mixotrophic protists in the biological carbon pump. *Biogeosciences* **11**: 995–1005.

Myers JA, Chase JM, Crandall RM, Jiménez I. (2015). Disturbance alters beta-diversity but not the relative importance of community assembly mechanisms. *J Ecol* **103**: 1291–1299.

Nejstgaard J, Gismervik I, Solberg P. (1997). Feeding and reproduction by *Calanus finmarchicus*, and microzooplankton grazing during mesocosm blooms of diatoms and the coccolithophore *Emiliania huxleyi*. *Mar Ecol Prog Ser* **147**: 197–217.

Nejstgaard J, Frischer M, Verity P, Anderson J, Jacobsen A, Zirbel M, et al. (2006). Plankton development and trophic transfer in seawater enclosures with nutrients and *Phaeocystis pouchetii* added. *Mar Ecol Prog Ser* **321**: 99–121.

Nercessian O, Noyes E, Kalyuzhnaya MG, Lidstrom ME, Chistoserdova L. (2005). Bacterial Populations Active in Metabolism of C1 Compounds in the Sediment of Lake Washington, a Freshwater Lake. *Appl Environ Microbiol* **71**: 6885–6899.

Ogle DH. (2017). FSA: Fisheries Stock Analysis. R package version 0.8.17.

Oksanen J, Blanchet FG, Friendly M, Kindt R, Legendre P, McGlinn D, et al. (2017). vegan: Community Ecology Package. R package version 2.4-2. https://CRAN.R-project.org/package=vegan.

Paerl HW, Paul VJ. (2012). Climate change: Links to global expansion of harmful cyanobacteria. *Water Res* **46**: 1349–1363.

Paradis E, Claude J, Strimmer K. (2004). APE: Analyses of Phylogenetics and Evolution in R language. *Bioinformatics* **20**: 289–290.

Pinheiro J, Bates D, DebRoy S, Sarkar D, Team RC. (2017). nlme: Linear and Nonlinear Mixed Effects Models. R package version 3.1-131, https://CRAN.R-project.org/package=nlme.

Posch T, Köster O, Salcher MM, Pernthaler J. (2012). Harmful filamentous cyanobacteria favoured by reduced water turnover with lake warming. *Nat Clim Chang* **2**: 809–813.

R Core Team. (2016). R: A language and environment for statistical computing. R Foundation for Statistical Computing, Vienna, Austria. URL https://www.R-project.org/.

Rahmstorf S, Coumou D. (2011). Increase of extreme events in a warming world. *Proc Natl Acad Sci* **108**: 17905–17909.

Raymond PA, Hartmann J, Lauerwald R, Sobek S, McDonald C, Hoover M, et al. (2013). Global carbon dioxide emissions from inland waters. *Nature* **503**: 355–359.

Reshef DN, Reshef YA, Finucane HK, Grossman SR, McVean G, Turnbaugh PJ, et al. (2011). Detecting Novel Associations in Large Data Sets. *Science* **334**: 1518–1524.

Reynolds CS, Oliver RL, Walsby AE. (1987). Cyanobacterial dominance: The role of buoyancy regulation in dynamic lake environments. *New Zeal J Mar Freshw Res* **21**: 379–390.

Rognes T, Flouri T, Nichols B, Quince C, Mahé F. (2016). VSEARCH: a versatile open source tool for metagenomics. *PeerJ* **4**: e2584.

Schloss PD, Westcott SL, Ryabin T, Hall JR, Hartmann M, Hollister EB, et al. (2009). Introducing mothur: Open-Source, Platform-Independent, Community-Supported Software for Describing and Comparing Microbial Communities. *Appl Environ Microbiol* **75**: 7537–7541.

Shade A, Chiu C, McMahon KD. (2010). Seasonal and Episodic Lake Mixing Stimulate Differential Planktonic Bacterial Dynamics. *Microb Ecol* **59**: 546–554.

Shade A, Read JS, Welkie DG, Kratz TK, Wu CH, McMahon KD. (2011). Resistance, resilience and recovery: aquatic bacterial dynamics after water column disturbance. *Environ Microbiol* **13**: 2752–2767.

Shade A, Peter H, Allison SD, Baho DL, Berga M, Bürgmann H, et al. (2012a). Fundamentals of Microbial Community Resistance and Resilience. *Front Microbiol* **3**: 1–19.

Shade A, Read JS, Youngblut ND, Fierer N, Knight R, Kratz TK, et al. (2012b). Lake microbial communities are resilient after a whole-ecosystem disturbance. *ISME J* **6**: 2153–2167.

Shannon P. (2003). Cytoscape: A Software Environment for Integrated Models of Biomolecular Interaction Networks. *Genome Res* **13**: 2498–2504.

Simon M, Azam F. (1989). Protein content and protein synthesis rates of planktonic marine bacteria. *Mar Ecol Prog Ser* **51**: 201–213.

Smoot ME, Ono K, Ruscheinski J, Wang P-L, Ideker T. (2011). Cytoscape 2.8: new features for data integration and network visualization. *Bioinformatics* **27**: 431–432.

Song C, Dodds WK, Trentman MT, Rüegg J, Ballantyne F. (2016). Methods of approximation influence aquatic ecosystem metabolism estimates. *Limnol Oceanogr Methods* **14**: 557–569.

Šulčius S, Slavuckytė K, Paškauskas R. (2017). The predation paradox: Synergistic and antagonistic interactions between grazing by crustacean predator and infection by cyanophages promotes bloom formation in filamentous cyanobacteria. *Limnol Oceanogr* **62**: 2189–2199.

Šulčius S, Holmfeldt K. (2016). Viruses of microorganisms in the Baltic Sea: current state of research and perspectives. *Mar Biol Res* **12**: 115–124.

Tilman D, Downing JA. (1994). Biodiversity and stability in grasslands. *Nature* **367**: 363–365.

Tittel J, Bissinger V, Zippel B, Gaedke U, Bell E, Lorke A, et al. (2003). Mixotrophs combine resource use to outcompete specialists: Implications for aquatic food webs. *Proc Natl Acad Sci* **100**: 12776–12781.

Tranvik LJ, Downing JA, Cotner JB, Loiselle SA, Striegl RG, Ballatore TJ, et al. (2009). Lakes and reservoirs as regulators of carbon cycling and climate. *Limnol Oceanogr* **54**: 2298–2314.

Trenberth KE. (2012). Framing the way to relate climate extremes to climate change. *Clim Change* **115**: 283–290.

Vogel A, Scherer-Lorenzen M, Weigelt A. (2012). Grassland Resistance and Resilience after Drought Depends on Management Intensity and Species Richness. *PLoS One* **7**: e36992.

Wang Q, Garrity GM, Tiedje JM, Cole JR. (2007). Naive Bayesian Classifier for Rapid Assignment of rRNA Sequences into the New Bacterial Taxonomy. *Appl Environ Microbiol* **73**: 5261–5267.

Weithoff G, Lorke A, Walz N. (2000). Effects of water-column mixing on bacteria, phytoplankton, and rotifers under different levels of herbivory in a shallow eutrophic lake. *Oecologia* **125**: 91–100.

Wetzel RG, Likens GE. (2000). Limnological Analyses. Springer New York: New York, NY.

Wickham H. (2009). ggplot2: Elegant Graphics for Data Analysis. Springer-Verlag: New York.

Zhou J, Deng Y, Zhang P, Xue K, Liang Y, Van Nostrand JD, et al. (2014). Stochasticity, succession, and environmental perturbations in a fluidic ecosystem. *Proc Natl Acad Sci* **111**: e836–e845.

Table 1:

OTU	taxonomic affiliation	fraction	DOE	log2-fold change	mean control (1SD)	mean mixed (1SD)	n control	n mixed
OTU021	*Bacteroidetes; Algoriphagus*	FL	1	-2.88	2.12 (1.17)	0.27 (0.12)	3	3
OTU174	*Proteobacteria; Limnohabitans*	FL	1	6.77	0.01 (0.01)	1.02 (0.97)	3	3
OTU103	*Tenericutes; Mycoplasma*	FL	1	-9.7	3.41 (4.12)	0 (0)	3	3
OTU028	*Verrucomicrobia; Candidatus_Methylacidiphilum*	FL	1	-4.44	3.58 (3.14)	0.17 (0.08)	3	3
OTU048	*Verrucomicrobia; Opitutae*_vadinHA64_unclassified	FL	1	-4.25	5.49 (5.85)	0.25 (0.19)	3	3
OTU004	*Cyanobacteria; FamilyI*_unclassified	FL	6	-3.11	11.13 (2.42)	1.38 (1.08)	4	4
		FL	21	-5.1	8.09 (6.53)	0.16 (0.23)	4	3
OTU006	*Actinobacteria; Sporichthyaceae*_unclassified	FL	21	1.98	2.6 (0.86)	6.99 (2.15)	4	3
OTU040	*Cyanobacteria; Synechococcus*	FL	21	-3.81	1 (0.91)	0.05 (0.07)	4	3
OTU011	*Verrucomicrobia;* FukuN18_freshwater_group_unclassified	FL	21	8.34	0.09 (0.06)	24.06 (7.67)	4	3
OTU027	*Verrucomicrobia;* FukuN18_freshwater_group_unclassified	FL	21	4.62	0.13 (0.1)	2.24 (0.98)	4	3
OTU005	*Verrucomicrobia; Opitutae*_vadinHA64_unclassified	FL	21	-2.09	11.59 (1.09)	1.77 (0.4)	4	3
OTU136	*Bacteroidetes; Fluviicola*	FL	42	-2.68	1.07 (0.26)	0.16 (0.12)	4	3
OTU019	*Proteobacteria; Gammaproteobacteria*_unclassified	PA	1	-4.91	1.2 (1.87)	0.04 (0.05)	3	3
OTU027	*Verrucomicrobia;* FukuN18_freshwater_group_unclassified	PA	1	1.91	0.26 (0.2)	1.07 (0.14)	3	3
OTU002	*Cyanobacteria; Dolichospermum* (*sensu Anabaena*)	PA	6	2.77	16.04 (14.31)	60.92 (6.21)	4	4
OTU004	*Cyanobacteria; FamilyI*_unclassified	PA	6	-3.65	23.1 (13.61)	0.96 (0.57)	4	4
OTU014	*Proteobacteria; Burkholderiales*_unclassified	PA	6	3.53	0.29 (0.25)	1.92 (1.23)	4	4
		PA	21	8.72	0.06 (0.05)	17.67 (13.68)	3	3
OTU193	*Bacteria_unclassified; Bacteria*_unclassified	PA	21	-6.46	1.14 (0.81)	0.01 (0.01)	3	3
OTU077	*Proteobacteria; Cellvibrio*	PA	21	5.79	0.09 (0.07)	3.19 (4.67)	3	3
OTU029	*Proteobacteria; Comamonadaceae*_unclassified	PA	21	6.22	0.18 (0.07)	7.93 (7.63)	3	3
OTU116	*Proteobacteria; Rhizobacter*	PA	21	4.42	0.1 (0.08)	1.22 (1.31)	3	3
OTU081	*Bacteroidetes; Flavobacterium*	PA	42	-4.6	2.81 (3.59)	0.07 (0.02)	4	3
OTU109	*Proteobacteria; Burkholderiales*_unclassified	PA	42	-7.57	3.52 (5.71)	0 (0)	4	3

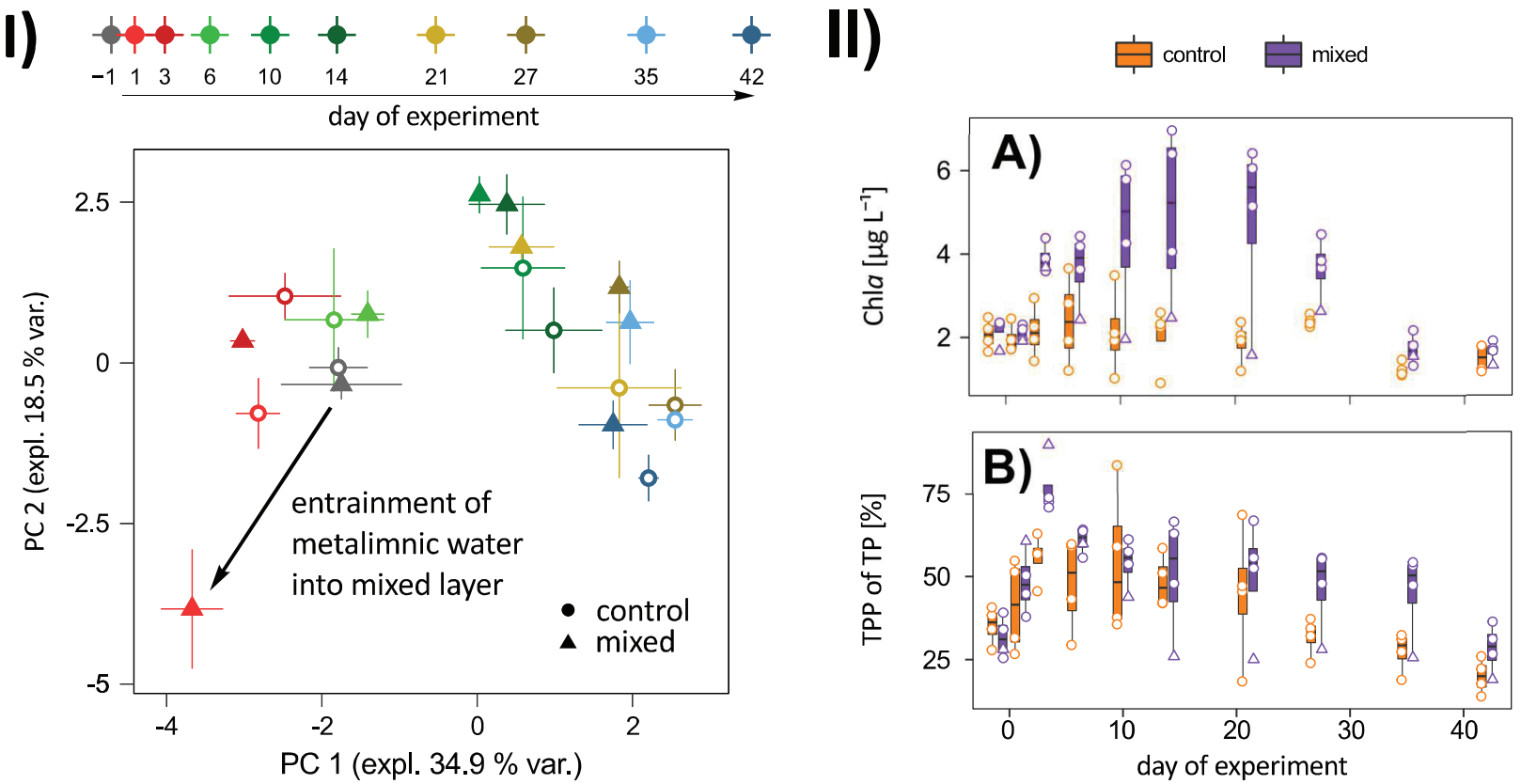
I)
−1 1 3 6 10 14 21 27 35 42
day of experiment
2.5
0
-2.5
-5
PC 2 (expl. 18.5 % var.)
-4 -2 0 2
PC 1 (expl. 34.9 % var.)
entrainment of
metalimnic water
into mixed layer
control
mixed
II)
control
mixed
A)
Chl*a* [µg L^{-1}]
6
4
2
B)
TPP of TP [%]
75
50
25
0 10 20 30 40
day of experiment

Figure 1:

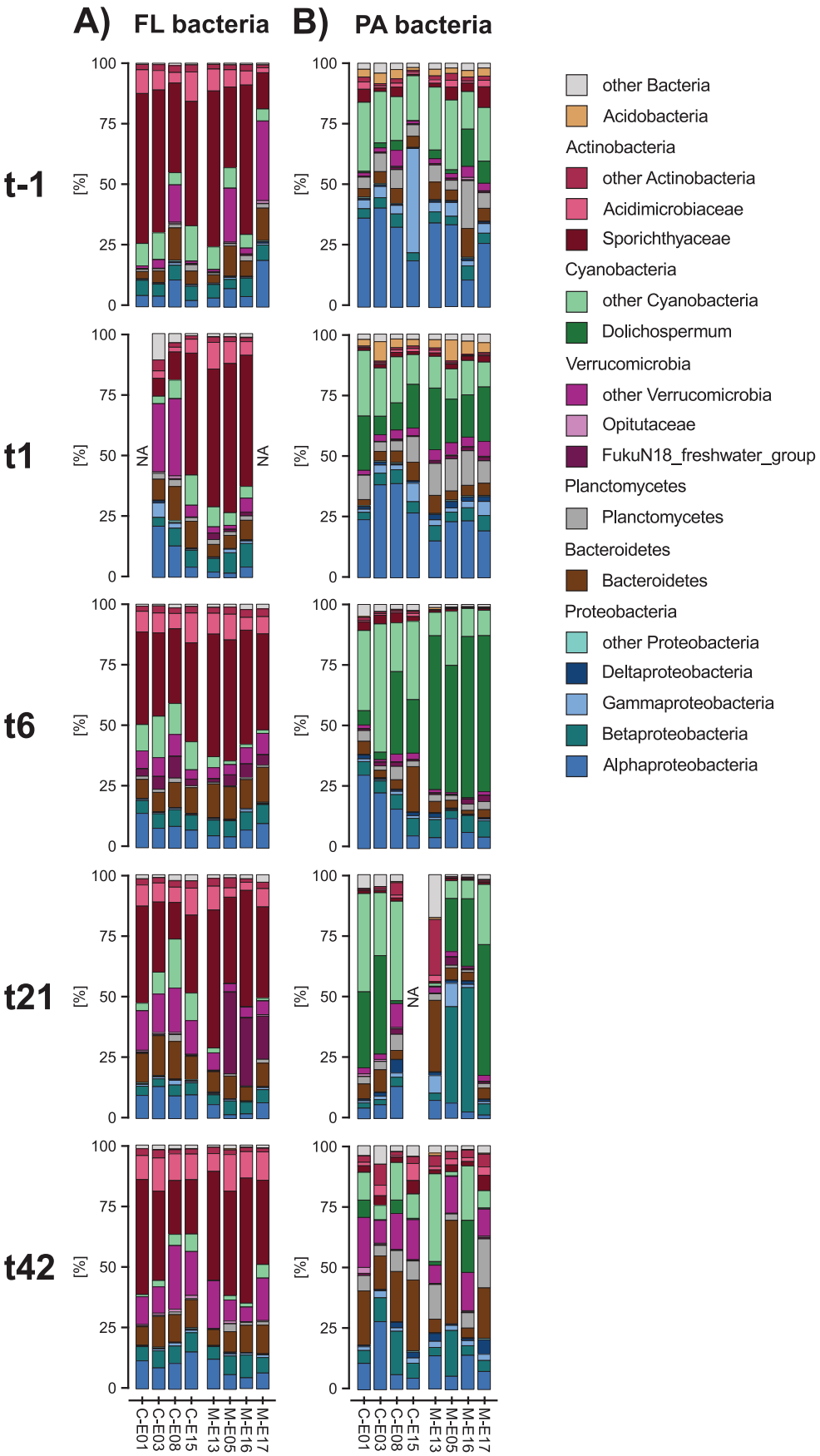
A) FL bacteria
B) PA bacteria
t-1
t1
t6
t21
t42
[%]
100
75
50
25
0
NA
C-E01
C-E03
C-E08
C-E15
M-E13
M-E05
M-E16
M-E17
other Bacteria
Acidobacteria
Actinobacteria
other Actinobacteria
Acidimicrobiaceae
Sporichthyaceae
Cyanobacteria
other Cyanobacteria
Dolichospermum
Verrucomicrobia
other Verrucomicrobia
Opitutaceae
FukuN18_freshwater_group
Planctomycetes
Planctomycetes
Bacteroidetes
Bacteroidetes
Proteobacteria
other Proteobacteria
Deltaproteobacteria
Gammaproteobacteria
Betaproteobacteria
Alphaproteobacteria

Figure 2:

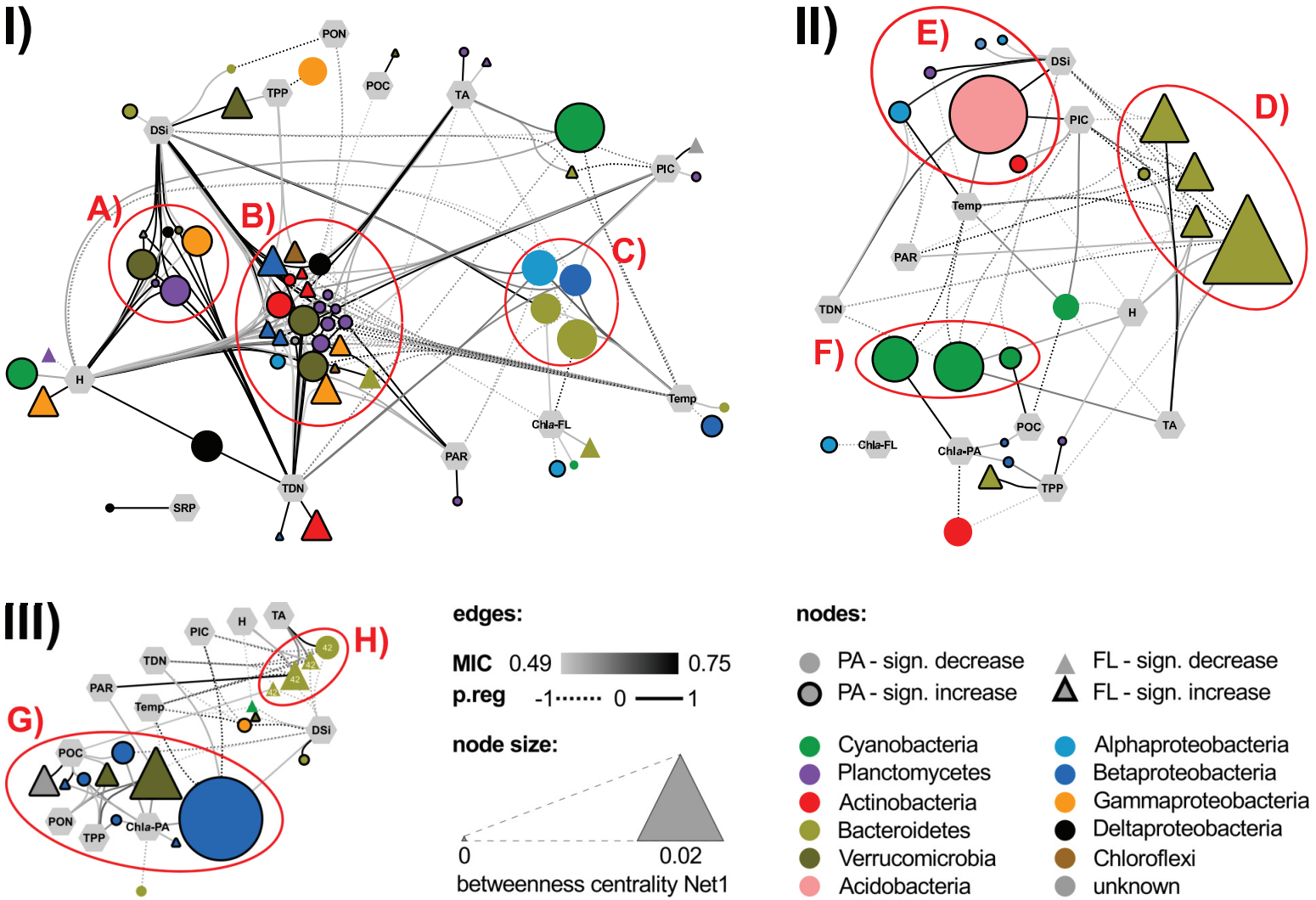
I)
II)
III)
A)
B)
C)
D)
E)
F)
G)
H)
PON
TPP
POC
TA
DSi
PIC
H
Temp
Chla-FL
PAR
TDN
SRP
Chla-PA
edges:
MIC 0.49 0.75
p.reg -1 0 1
node size:
0
0.02
betweenness centrality Net1
nodes:
PA - sign. decrease
PA - sign. increase
FL - sign. decrease
FL - sign. increase
Cyanobacteria
Planctomycetes
Actinobacteria
Bacteroidetes
Verrucomicrobia
Acidobacteria
Alphaproteobacteria
Betaproteobacteria
Gammaproteobacteria
Deltaproteobacteria
Chloroflexi
unknown

Figure 3:

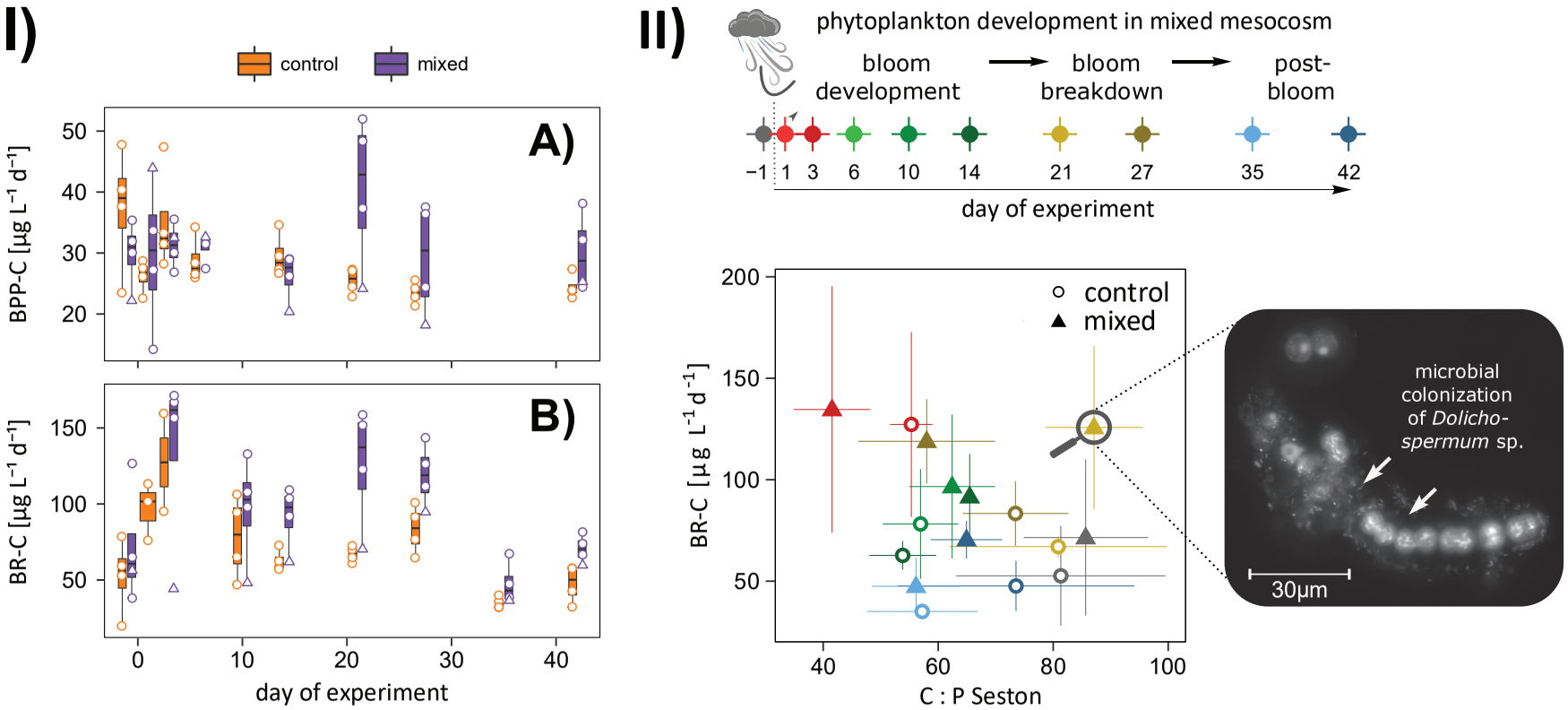
I)
control
mixed
A)
BPP-C [µg L⁻¹ d⁻¹]
50
40
30
20
B)
BR-C [µg L⁻¹ d⁻¹]
150
100
50
0
10
20
30
40
day of experiment
II)
phytoplankton development in mixed mesocosm
bloom development
bloom breakdown
post-bloom
−1 1 3 6 10 14 21 27 35 42
day of experiment
BR-C [µg L⁻¹ d⁻¹]
200
150
100
50
control
mixed
40
60
80
100
C : P Seston
microbial colonization of Dolicho-spermum sp.
30µm

Figure 4:

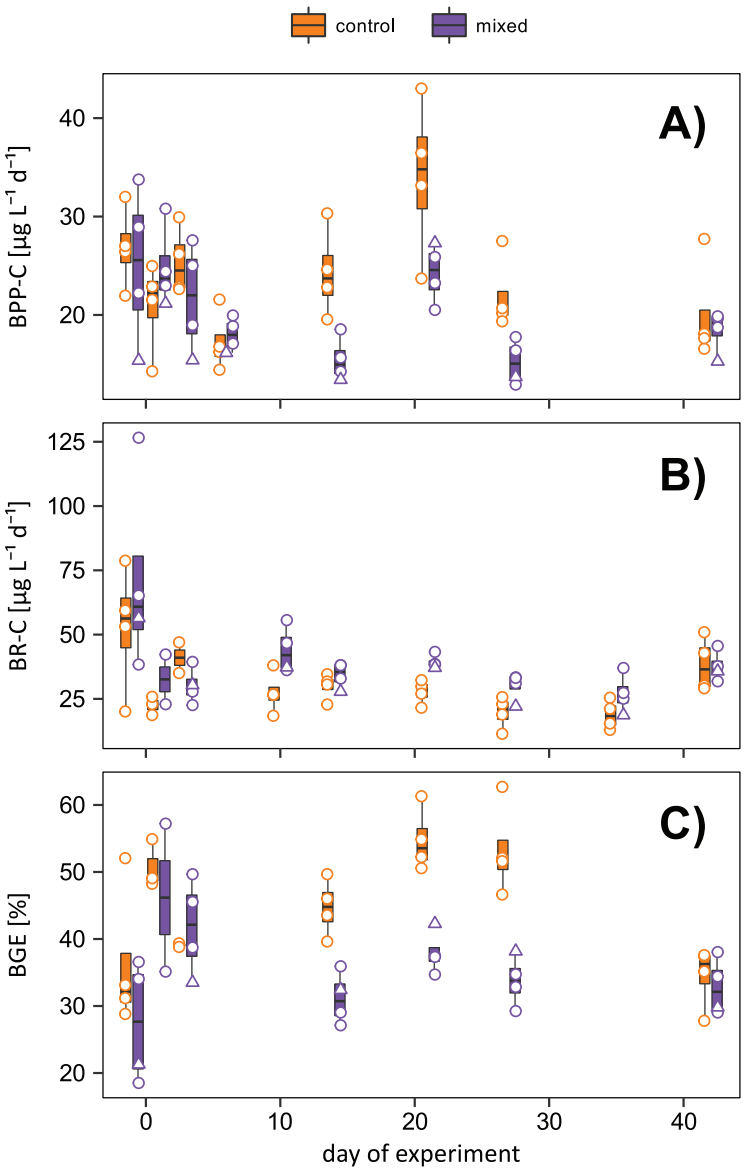
control
mixed
A)
B)
C)
BPP-C [µg L^{-1} d^{-1}]
BR-C [µg L^{-1} d^{-1}]
BGE [%]
day of experiment

Figure 5:

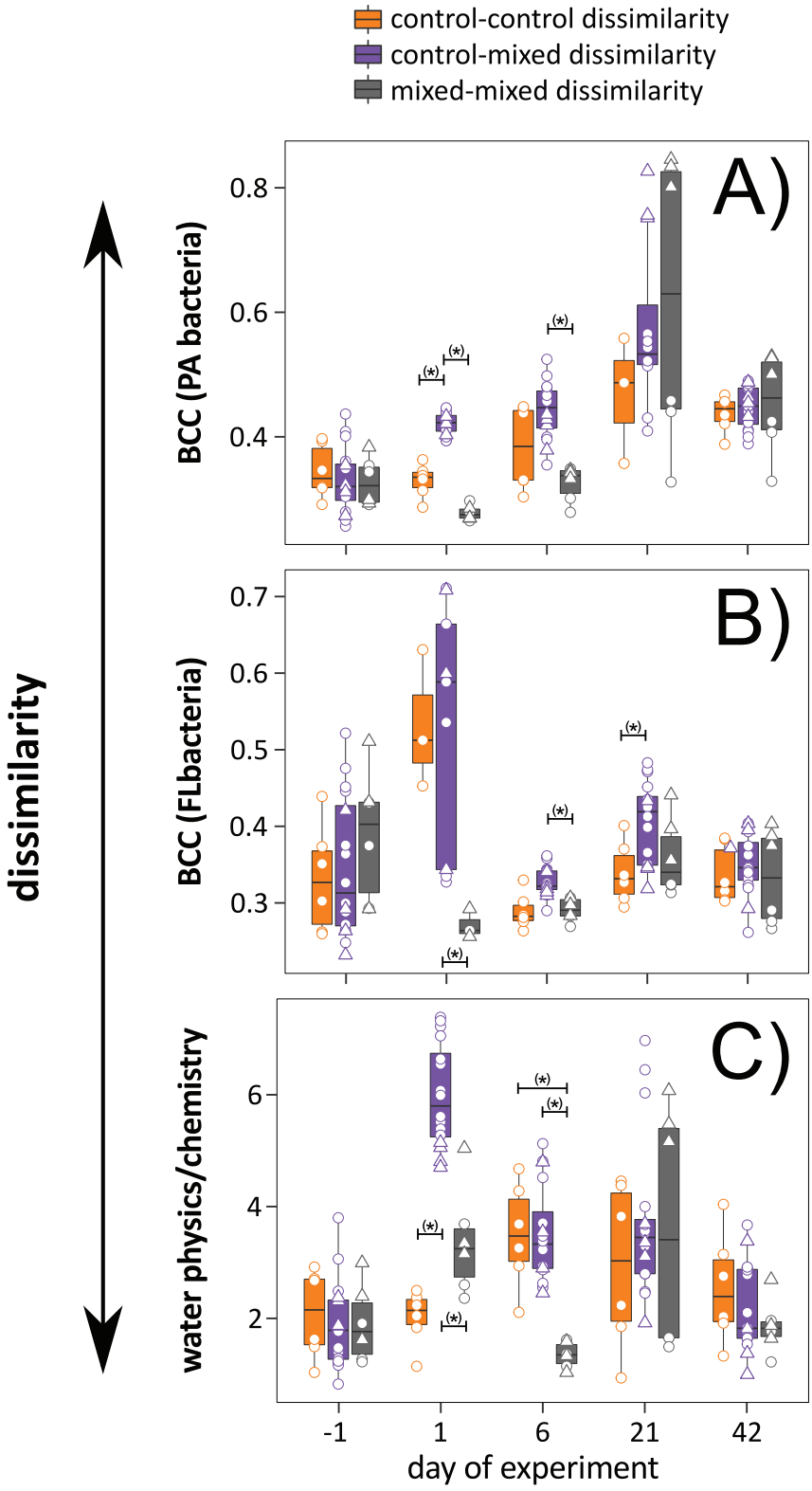
control-control dissimilarity
control-mixed dissimilarity
mixed-mixed dissimilarity
dissimilarity
BCC (PA bacteria)
BCC (FLbacteria)
water physics/chemistry
A)
B)
C)
0.8
0.6
0.4
0.7
0.5
0.3
6
4
2
(*)
-1
1
6
21
42
day of experiment

Figure 6:

Supplement - Materials and Methods

Experimental manipulation and sampling

The experiment was conducted in large-volume enclosures (~1300 m^3) installed in Lake Stechlin, north-eastern Germany (53°08036”N, 13°01041”E; www.lake-lab.de). Periphyton on the curtains was removed and fish excluded prior to the experiment. The water column in eight enclosures was prepared for the experiment by first exchanging the hypolimnic (8–16 m) and thereafter epilimnic (0–8 m) water masses with water from the respective layers in the surrounding lake, during the two last weeks of July 2014. Water was exchanged by simultaneously pumping lake water in and out of the enclosures using submersible impeller pumps that cause minimum plankton disturbance, as successfully used at other enclosure facilities (Nejstgaard *et al.*, 1997, 2006). A DCM was present in the metalimnion of Lake Stechlin at this time. This plankton community was inserted into the metalimnion of each enclosure by exchanging the water between 7 m and 8 m after the water replacement. After complete water exchange with the lake, the enclosures were monitored for three days (August 3rd–5th) prior to applying the experimental treatment. A summer storm was simulated in four randomly selected enclosures on 6th August 2014 without sediment disturbance. This was achieved using the same pumps used for filling the enclosures to deepen the thermocline from 9 to 14 m (mixing for 4 h, from 03:00 to 07:00 hours). Water samples were collected with two-L water samplers (Limnos, Turku, Finland) from the well-mixed epilimnion at 2.5 m, from the metalimnion between 7.5 and 10 m, as the upper mixed layer deepened later in the season, and from the hypolimnion at 16 m.

Chemical variables

Samples for dissolved organic carbon (DOC), total dissolved nitrogen (TDN) and soluble reactive phosphorus (SRP) were filtered through precombusted (450°C, 6 h) GF-75 filters (Sterlitech, nominal pore size of 0.3 µm) and immediately analyzed for TDN and SRP concentrations on a flow injection analyzer (FIA, MLE Dresden, Germany) according to the manufacturer’s instructions. DOC concentration was determined with a TOC-V Analyzer (Shimadzu, Kyoto, Japan). Samples for dissolved silicate (DSi) were injected into a carrier stream with an ammonium molybdate reagend at pH 1.2 and adding oxalic adic using a FIASTAR 5000 (Foss Analytical AB, Höganäs, Sweden). The molybdate-reactive silica was measured at 720 nm.

Seston was filtered on precombusted GF-75 filters (Sterlitech, nominal pore size of 0.3 µm), dried at 60°C and stored in a desiccator upon analyses. Subsamples of 1 cm diameter were taken from one filter with a rotary cutter for measuring total particulate carbon (TPC), particulate inorganic carbon (PIC) and simultaneous particulate organic nitrogen (PON) and total particulate phosphorous (TPP). TPC was determined with an Eltra SC-800 Surface Carbon Determinator (Eltra GmbH, Haan, Germany) according the manufacturer´s instructions. PIC was measured using infrared gas analysis of CO_2 subsequently to the reaction of calcite in a 10% HCl solution (Infralyt 50 SAXON Junkalor GmbH, Dessau, Germany). Concentration of particulate organic carbon (POC) was calculated by

subtracting PIC from TPC. PON and TPP were determined simultaneous using peroxodisulfate oxidation according (Ebina *et al.*, 1983). Thereby samples were autoclaved and both the concentrations of oxidation products nitrates and orthophosphates measured on a flow injection analyzer (FIA, MLE Dresden, Germany) according to the manufacturer's instructions.

Chlorophyll a was determined by filtering 200–800 mL of water onto polycarbonate membrane filters (0.2 µm; Whatman, Dassel, Germany), followed by extraction in 90% acetone at 4°C overnight and analysis with a fluorescence spectrophotometer (Hitachi F-7000, Tokyo, Japan).

Ebina J, Tsutsui T, Shirai T. (1983). Simultaneous determination of total nitrogen and total phosphorus in water using peroxodisulfate oxidation. *Water Res* **17**: 1721–1726.

Nejstgaard J, Frischer M, Verity P, Anderson J, Jacobsen A, Zirbel M, *et al.* (2006). Plankton development and trophic transfer in seawater enclosures with nutrients and Phaeocystis pouchetii added. *Mar Ecol Prog Ser* **321**: 99–121.

Nejstgaard J, Gismervik I, Solberg P. (1997). Feeding and reproduction by *Calanus finmarchicus*, and microzooplankton grazing during mesocosm blooms of diatoms and the coccolithophore *Emiliania huxleyi*. *Mar Ecol Prog Ser* **147**: 197–217.

Supplement - Tables and Figures

Table S1: Results of a two-factorial permutational multivariate analysis of variance (PERMANOVA) on a resemblance matrix (Euclidian distance) of centered and scaled chemical and physical variables. PERMANOVA (9999 permutations) is based on a multivariate assemblage of particulate inorganic carbon (PIC), particulate organic carbon (POC), particulate organic nitrogen (PON), total particulate phosphorous (TPP), dissolved organic carbon (DOC), dissolved silica (DSi), total dissolved nitrogen (TDN), soluble reactive phosphorous (SRP), proton concentration (H^+), total alkalinity (TA), ammonia concentration (NH_4^+), surface photosynthetic active radiation (PAR) and water temperature (Temp). Degree of freedom (d*f*); sum of squares (SS). No differences in dispersion within the same geometric framework could be detected ($p > 0.6$) (Anderson, 2001). Prior to the analysis data were log(x+1)-transformed and normalized according to (Clarke and Gorley, 2006). The initial conditions between control and later mixed enclosures one day prior the treatment revealed no differences in water chemistry (PERMANOVA: $F_{1,6} = 0.5664$; $p > 0.7$).

Table S2: Eigenvectors and explained variation of the first axis of a principal component analysis (PCA) on centered and scaled chemical and physical variables. Most of the chemical and physical variables load with sizable importance on PC 1, thus depicting an overall combination of chemical variables for explaining the variation in environmental variables. PC 2 is largely explained by concentrations of particulate organic matter (POC, PON, TPP), reflecting the variation in Chl *a* (spearman´s correlation: $r_s = 0.67$, $p < 0.001$). PC 3 represents measurements of the carbonate system. According the broken stick model (Jackson 1993) only components 1-3 should be used to interpret the PCA. PIC-particulate inorganic carbon, POC-particulate organic carbon, PON-particulate organic nitrogen, TPP-total particulate phosphorous, DOC-dissolved organic carbon, DSi-dissolved silica, TDN-total dissolved nitrogen, SRP-soluble reactive phosphorous, H^+-proton concentration, TA-total alkalinity, ammonia concentration (NH_4^+), surface photosynthetically active radiation (PAR) and water temperature (Temp). Prior to the analysis data were log(x+1)-transformed and normalized according to (Clarke and Gorley, 2006).

Table S3: Collinearity among predictor variables using Pearsons´s coefficient ρ. Only significant correlation coefficients are reported. Combinations of variables with $\rho > 0.7$ were excluded from DistLM (Table S4). Particulate inorganic carbon (PIC), particulate organic carbon (POC), particulate organic nitrogen (PON), total particulate phosphorous (TPP), dissolved organic carbon (DOC), dissolved silica (DSi), total dissolved nitrogen (TDN), soluble reactive phosphorous (SRP), proton concentration (H^+), total alkalinity (TA), ammonia concentration (NH_4^+), concentration of chlorophyll *a* (Chl *a*) and temperature (Temp).

Table S4: Relation between water physical-chemical variables and bacterial β-diversity using DistLM (distance-based linear modelling). The marginal test **(I)** examines the

relation between β-diversity and each predictor variable individually, whereas the conditional test **(II)** examines the relationship by fitting all predictors into the most parsimonious model. To determine the suitability of predictor variables for use in a linear model, collinearity of the predictor variables was tested by calculating pairwise Pearson`s correlation coefficients ρ (Table S3). Variables with a ρ > 0.7 were not used in combination for modelling (e.g. PON and POC, TA and H^+) the relationship between the resemblance matrix and predictor variables, since such variables contain effectively the same information and are redundant for purposes of the analysis. E.g., in case of Chl *a* and POC (with a comparatively low ρ = 0.72), both variables are related to phytoplankton development and have a similar ecological meaning. Thus, including both variables in DistLM would not help gaining further information which of both factors structured the bacterial community. The overall best model solution was chosen based on Akaike´s information criterion (AIC) with a second-order bias correction applied (AICc) (Hurvich and Tsai, 1989). Thereby models with AICc differences of 1 were considered as equal and a model with equal AICc but less fitted variables was generally preferred. Therefore, coupled with the before mentioned preliminary diagnostics to assess multi-collinearity (Table S3) among predictor variables, several potentially relevant models are reported **(II)**. Significance was determined by 9999 permutations of residuals under a reduced model. DistLM is based on a resemblance matrix (Bray-curtis similariy) on the basis of multivariate species abundance data from free-living and particle-associated bacteria. Prior analyses abundance data were standardized to the total read abundance per sample (percentage) and square-root-transformed (Anderson et al. 2008). Visualization of the best model fit in multi-dimensional space was performed using the dbRDA routine (Legendre and Anderson, 1999; McArdle *et al.*, 2001) (Figure S3). Values in the table represent the estimation of the variance component (VC), the level of significance (*p*) and the sum of squares (SS).

Table S5: Differentially abundant bacterial OTUs in artificial mixed and control mesocosms with taxonomic affiliation. Testing for differentially abundant taxa was achieved using the DESeq function in the DESeq2 package (Love *et al.*, 2014) with multiple-inference correction (Benjamini and Hochberg, 1995) and a significance level of p < 0.01. One artificial mixed enclosure (#E13), which did not develop a bloom of *Dolichospermum* sp. after t6, was excluded from calculations at t21 and t42.

Figure S1: Principal Coordinate Analysis (PCoA) of epilimnic bacterial community composition (BCC) during the course of the experiment. Water samples were size-fractionated for revealing free-living (FL; 0.2-5.0 µm) and particle-associated (PA; >5.0 µm)) BCC. Prior analysis samples were standardized to the total read abundance per sample (%) and square-root-transformed. FL and PA bacteria comprise a significantly different BCC throughout the experiment (PERMANOVA; fraction-$F_{1,67}$ = 61.92, p < 0.001; time-$F_{4,67}$ = 6.30, p < 0.001; fraction x time-$F_{4,67}$ = 2.53, p < 0.001; dispersion of both size-fractions was not significantly different at each level of time; $SS_{fraction}$ = 5.44, SS_{time} = 2.22).

Figure S2: Three orders of diversity (Hill numbers ^{q}D with q = 0,1 and 2) and Pielou´s eveness (J) between mixed and control enclosures during the experiment (Chao *et al.*, 2014; Pielou, 1975; Lucas *et al.*, 2017). Thereby ^{0}D equals species richness, ^{1}D equals exponential of Shannon´s entropy index and ^{2}D equals the inverse of Simpson´s concentration index, respectively (Chao *et al.*, 2014). Calculations were made after rarefying to an equal number of 3904 reads per sample to control for unequal sampling effort. Significance is indicated by asterisks (two-tailed Mann-Whitney U; $p \leq 0.05$). One mixed enclosure (#13), which did not develop a bloom of *Dolichospermum* sp. after t6 is indicated by an open triangle. The lower and upper hinges correspond to the first and third quantiles (25^{th} and 75^{th} percentiles). Upper and lower whiskers extend from the hinges at maximum 1.5 times the inter-quantile range. Data beyond the end of whiskers are plotted individually.

Figure S3: dbRDA-ordination (distance-based redundancy analysis) of fitted values from the most parsimonious model (Table S4-II) revealed by distance-based linear modelling (DISTLM). DISTLM was used to model the relationship between the bacterial community composition and physical-chemical predictor variables in the epilimnion (Table S3, Table S4-I) of **A,B)** particle-associated (PA) and **C)** free-living (FL) bacteria. Arrows indicate the relationship between dbRDA coordinate axes and orthonormal variables in the final DISTLM (multiple partial correlations). These vectors can be interpreted as the effect of a given predictor variable on the construction of the constrained ordination (note: vectors are scaled to axis). One mixed enclosure (#13), which did not develop a bloom of *Dolichospermum* sp. after t6 is indicated by an open triangle and was excluded from the calculation of the 95 %- confidence interval after t6. Small numbers indicate enclosure number.

Figure S4: Principal Coordinate Analysis (PCoA) of epilimnic **A, B)** free-living (FL) and **B, C)** particle-associated (PA) bacterial community composition. The first three axes explain cumulatively ca. 53.3 % (FL) and 54.7 % (PA) of variance, respectively, and represent the number of "meaningful" components according to the broken-stick model (Jackson, 1993). One mixed enclosure (#13), which did not develop a bloom of *Dolichospermum* sp. after t6 is indicated by an open triangle and was excluded from the calculation of the 95 %-confidence interval after t6. Small numbers indicate enclosure number.

Figure S5: I) Proportion and taxonomic affiliation at phylum level of free-living (FL) and particle-associated (PA) bacterial 16s rRNA sequences of metalimnic samples from t-1 and epilimnic samples during the course of the experiment. **II-VI)** Proportion and taxonomic affiliation of *Actinobacteria*, *Bacteroidetes*, *Cyanobacteria*, *Proteobacteria* and *Verruco-microbia*. Genera contributing less than 1% to total reads in one sample were grouped as "Others". C-control; M-mixed (e.g. C-E15 refers to control - epilimnion of mesocosm Nr. 15 or M-M16 refers to mixed - metalimnion of mesocosm Nr. 16, respectively). Three samples were excluded from further analysis due to low read abundance (< 1000, indicated by "NA").

During the entire experiment FL bacterial communities consisted mainly of the phyla *Actinobacteria* (following indicated as: min-max; mean ± 1SD; 15-75 %; 51 ± 16 %), *Proteobacteria* (7-31 %; 14 ± 5 %), *Verrucomicrobia* (1-37 %; 14 ± 10 %), *Bacteroidetes* (3-16 %; 10 ± 3 %) and *Cyanobacteria* (0-20 %; 6 ± 5 %). Thereby, the most abundant OTUs across all epilimnic samples (grouped at the highest taxonomic resolution) belonged to *hgcI_clade* (6-49 %; 30 ± 10 %), *Sporichthyaceae* (2-23 %; 11 ± 6 %), and *CL500-29-marine_group* (2-15 %; 8 ± 3 %) (*Actinobacteria*); *LD12_freshwater_group* (1-18 %; 7 ± 5 %) (*Proteobacteria*); *SubsectionI_FamilyI* (0-18 %; 6 ± 5 %) (*Cyanobacteria*) and *Opitutae_vadinHA64* (9-24 %; 8 ± 6 %) as well as *FukuN18_freshwater_group* (0-34 %; 3 ± 7 %) (*Verrucomicrobia*).

PA bacterial communities consisted mainly of the phyla *Cyanobacteria* (2-78 %; 38 ± 22 %), *Proteobacteria* (8-65 %; 30 ± 15 %), *Bacteroidetes* (2-43 %; 9 ± 9 %), *Planktomycetes* (1-20 %; 7 ± 5 %), *Verrucomicrobia* (1-24 %; 6 ± 5 %) and *Actinobacteria* (0-26 %; 6 ± 5 %). The most abundant OTUs across all epilimnic samples (grouped at the highest taxonomic resolution) comprising PA bacterial communities belonged to *Dolichospermum* (0-66 %; 18 ± 20 %), *SubsectionI_FamilyI* (0-41 %; 8 ± 9 %) and *Snowella* (0-32 %; 7 ± 7 %) (*Cyanobacteria*) as well as *Roseomonas* (0-31 %; 12 ± 10 %) (*Proteobacteria*).

Figure S6: Box and whisker plots of **A,B)** bacterial abundance, **C,D)** bacterial protein production (BPP-C) and **(E,F)** cell-specific BPP-C in the epilimnion of **I)** free-living and **II)** particle associated bacteria during the course of the experiment. One mixed enclosure (#13), which did not develop a bloom of *Dolichospermum* sp. after t6 is indicated by an open triangle. The lower and upper hinges correspond to the first and third quantiles (25^{th} and 75^{th} percentiles). Upper and lower whiskers extend from the hinges at maximum 1.5 times the inter-quantile range. Data beyond the end of whiskers are plotted individually.

Anderson MJ. (2001). A new method for non-parametric multivariate analysis of variance. *Austral Ecol* **26**: 32–46.

Benjamini Y, Hochberg Y. (1995). Controlling the False Discovery Rate: a Practical and Powerful Approach to Multiple Testing. *J R Stat Soc* **57**: 289–300.

Chao A, Gotelli NJ, Hsieh TC, Sander EL, Ma KH, Colwell RK, *et al.* (2014). Rarefaction and extrapolation with Hill numbers: a framework for sampling and estimation in species diversity studies. *Ecol Monogr* **84**: 45–67.

Clarke KR, Gorley RN. (2006). PRIMER v6: User manual/Tutorial. PRIMER-E Ltd: Plymouth, UK.

Hurvich CM, Tsai C-L. (1989). Regression and time series model selection in small samples. *Biometrika* **76**: 297–307.

Jackson DA. (1993). Stopping Rules in Principal Components Analysis: A Comparison of Heuristical and Statistical Approaches. *Ecology* **74**: 2204–2214.

Legendre P, Anderson MJ. (1999). Distance-Based Redundancy Analysis: Testing

Multispecies Responses in Multifactorial Ecological Experiments. *Ecol Monogr* **69**: 1–24.

Love MI, Huber W, Anders S. (2014). Moderated estimation of fold change and dispersion for RNA-seq data with DESeq2. *Genome Biol* **15**: 550.

Lucas R, Groeneveld J, Harms H, Johst K, Frank K, Kleinsteuber S. (2017). A critical evaluation of ecological indices for the comparative analysis of microbial communities based on molecular datasets. *FEMS Microbiol Ecol* **93**: fiw209.

McArdle BH, Anderson MJ. (2001). Fitting Multivariate Models to Community Data : A Comment on Distance-Based Redundancy Analysis. *Ecology* **82**: 290–297.

Pielou EC. (1975). Ecological diversity. Wiley: New York.

Table S1:

Source of variation	d*f*	SS	Pseudo-*F*	*p* (perm)
Treatment	1	0.07482	25.8615	0.000999 (***)
Time (day of experiment)	8	1.58088	68.3042	0.000999 (***)
Time x Treatment	8	0.09211	3.9798	0.000999 (***)
Residuals	54	0.15623		

Table S2:

	Variable	**PC1**	**PC2**	**PC3**
	PIC	-0.31		0.2
	POC	-0.22	0.46	-0.24
	PON	-0.18	0.47	-0.3
	TPP	-0.31	0.34	-0.3
	DOC			0.13
	DSi	-0.38	-0.17	
	TDN	-0.41	-0.19	
	SRP	-0.18	-0.32	-0.27
	H+	-0.11	-0.41	-0.42
	TA	0.16		-0.51
	NH_4^+	-0.43	-0.14	0.15
	PAR	-0.27	-0.16	-0.16
	Temp	-0.3	0.25	0.38
% variation		**34.9**	**18.5**	**16.7**
cum % variation		**34.9**	**53.4**	**70.1**

Table S3:

	PIC	POC	PON	TPP	DOC	DSi	TDN	SRP	H+	TA	Chl *a*	Temp	PAR
POC													
PON		**0.77**											
TPP	0.18	0.62	**0.74**										
DOC				-0.14									
DSi	0.56			0.39	-0.39								
TDN	0.62	-0.16	-0.14	0.22	-0.32	**0.79**							
SRP	0.23	-0.3	-0.26		-0.28	0.66	**0.88**						
H^+		-0.3	-0.27		-0.34	**0.73**	**0.87**	**0.92**					
TA	-0.26	-0.27	-0.18		-0.42	0.59	0.64	0.67	**0.75**				
Chl *a*		**0.72**	0.66	0.42	0.2	-0.26	-0.45	-0.5	-0.52	-0.38			
Temp	0.52	0.12	0.1		0.02	0.08	0.1	-0.02	0.03	0.01	-0.1		
PAR	0.23	0.27		-0.11									
NH_4^+	0.67	0.08		0.39		**0.78**	**0.95**	0.36	0.33	-0.45	-0.13	0.62	0.4

Table S4:

I) relationship between β-diversity and each individual predictor variable (marginal test)

variable	PA bacteria				FL bacteria			
	SS	pseudo-*F*	$p^{(*)}$	VC (%)	SS	pseudo-*F*	$p^{(*)}$	VC (%)
Temp	8019	6.498	**0.0001**	14.93	3973.2	4.8795	**0.0001**	11.94
PAR	3129.3	2.2905	0.0088	0.06	1957.3	2.2491	0.0079	0.06
Chl *a*	6478.5	5.0783	**0.0001**	12.07	2456.6	2.8685	**0.0019**	0.07
POC	6844.9	5.4075	**0.0001**	12.75	2312.4	2.6876	**0.0017**	0.07
PON	5433.6	4.147	**0.0001**	10.12	1911.6	2.1933	0.0096	0.06
TPP	6950.6	5.5035	**0.0001**	12.95	2366.5	2.7553	**0.0012**	0.07
DSi	5496.8	4.221	**0.0001**	10.24	2887.8	3.4199	**0.0001**	0.09
DOC	2246.4	1.616	0.0683	0.04	972.21	1.0831	0.3246	0.03
TDN	5139.4	3.9175	**0.0001**	0.1	2955.4	3.5077	**0.0007**	0.09
SRP	1992.1	1.426	0.1133	0.04	1176.8	1.3193	0.1377	0.04
pH	4317.1	3.2358	**0.0002**	0.08	2340.5	2.7227	**0.0015**	0.07
TA	4406.9	3.3092	**0.0004**	0.08	2345.2	2.7286	**0.0022**	0.07
NH_4^+	6096.2	4.7403	**0.001**	11.4	3371.1	4.0567	**0.001**	10.1

$^{(*)}$ Bold numbers indicate significance after Bonferroni-correction to account for multiple testing.

II) best model fits of DistLM (conditional test) based on AICc and number of used variable

PA bacteria			FL bacteria		
AICc	**VC (%)**	**variables**	**AICc**	**VC (%)**	**variables**
273.91	35.5	POC, TDN,Temp	256.01	19.3	Chl *a*, Temp
273.98	35.4	POC, DSi, Temp			
274.04	35.3	Chl *a*, TDN, Temp			
274.17	35.1	Chl *a*, DSi, Temp			
274.3	34.9	TPP, TDN, Temp			

Table S5:

fraction	DOE	OTU	mean control	mean mixed	SD control	SD mixed	baseMean	log2FoldChange	lfcSE	stat	padj	Phylum	Family	Genus
FL	1	OTU048	5.49	0.25	5.85	0.19	498.85	-4.25	1.20	-3.55521	0.00913	Verrucomicrobia	Opitutae_vadinHA64_unclassified	Opitutae_vadinHA64_unclassified
FL	1	OTU028	3.58	0.17	3.14	0.08	409.09	-4.44	1.26	-3.53828	0.00913	Verrucomicrobia	Unknown_Family	Candidatus_Methylacidiphilum
FL	1	OTU103	3.41	0.00	4.12	0.00	405.82	-9.70	2.57	-3.77752	0.00727	Tenericutes	Mycoplasmataceae	Mycoplasma
FL	1	OTU021	2.12	0.27	1.17	0.12	205.86	-2.88	0.74	-3.87163	0.00611	Bacteroidetes	Cyclobacteriaceae	Algoriphagus
FL	1	OTU174	0.01	1.02	0.01	0.97	91.44	6.77	1.62	4.17766	0.00374	Proteobacteria	Comamonadaceae	Limnohabitans
FL	1	OTU044	0.74	0.05	0.52	0.03	69.45	-3.87	0.91	-4.26187	0.00374	Planctomycetes	Phycisphaeraceae	Phycisphaeraceae_unclassified
FL	1	OTU100	0.04	0.49	0.03	0.10	47.00	3.97	0.99	4.00947	0.00580	Chloroflexi	SL56_marine_group_unclassified	SL56_marine_group_unclassified
FL	1	OTU213	0.00	0.37	0.00	0.52	34.69	8.40	2.37	3.55176	0.00913	Proteobacteria	CABC2E06	CABC2E06_unclassified
FL	1	OTU167	0.00	0.24	0.00	0.19	21.74	8.35	2.15	3.87668	0.00611	Proteobacteria	Methylococcaceae	Methylobacter
FL	1	OTU239	0.00	0.20	0.00	0.15	18.13	8.05	2.20	3.65966	0.00875	Proteobacteria	Methylophilaceae	Methylophilaceae_unclassified
FL	1	OTU372	0.00	0.18	0.00	0.07	16.29	6.36	1.52	4.18270	0.00374	Proteobacteria	Nitrosomonadaceae	Nitrosomonadaceae_unclassified
FL	1	OTU397	0.00	0.15	0.00	0.04	13.35	7.87	2.10	3.74299	0.00727	Actinobacteria	Sporichthyaceae	hgcI_clade
FL	1	OTU393	0.00	0.14	0.00	0.06	12.93	6.03	1.56	3.86237	0.00611	Planctomycetes	Planctomycetaceae	Planctomycetaceae_unclassified
FL	1	OTU290	0.00	0.14	0.00	0.03	12.70	7.82	2.10	3.73098	0.00727	Chlorobi	OPB56	OPB56_unclassified
FL	1	OTU468	0.00	0.14	0.00	0.08	12.56	7.68	2.17	3.53528	0.00913	Proteobacteria	Gallionellaceae	Candidatus_Nitrotoga
FL	1	OTU374	0.00	0.12	0.00	0.06	11.26	7.61	2.13	3.57246	0.00913	Actinobacteria	TM146	TM146_unclassified
FL	1	OTU560	0.00	0.11	0.00	0.01	9.96	7.52	2.10	3.57410	0.00913	Actinobacteria	Acidimicrobiaceae	CL500-29_marine_group
FL	6	OTU004	11.13	1.38	2.42	1.08	1075.10	-3.11	0.46	-6.70556	0.00000	Cyanobacteria	FamilyI	FamilyI_unclassified
FL	6	OTU123	0.14	0.62	0.10	0.19	60.06	1.95	0.52	3.73820	0.00547	Bacteroidetes	Chitinophagaceae	Filimonas
FL	6	OTU085	0.03	0.34	0.02	0.13	29.19	3.05	0.54	5.60592	0.00000	Bacteroidetes	Flavobacteriaceae	Flavobacterium
FL	6	OTU131	0.05	0.30	0.03	0.06	28.18	2.26	0.50	4.53715	0.00027	Proteobacteria	Proteobacteria_unclassified	Proteobacteria_unclassified
FL	6	OTU149	0.28	0.08	0.03	0.06	30.71	-1.97	0.52	-3.81098	0.00467	Cyanobacteria	FamilyI	FamilyI_unclassified
FL	6	OTU207	0.01	0.21	0.02	0.13	17.07	3.26	0.76	4.29733	0.00068	Bacteroidetes	Cryomorphaceae	Fluviicola
FL	6	OTU165	0.01	0.16	0.01	0.08	13.04	4.26	0.87	4.86761	0.00009	Bacteroidetes	Cryomorphaceae	Fluviicola
FL	6	OTU114	0.01	0.14	0.01	0.06	11.46	3.61	0.79	4.56512	0.00027	Bacteroidetes	env.OPS_17	env.OPS_17_unclassified
FL	6	OTU087	0.01	0.08	0.01	0.03	6.94	2.97	0.83	3.58563	0.00882	Bacteroidetes	NS11-12_marine_group	NS11-12_marine_group_unclassified
FL	21	OTU011	0.09	24.06	0.06	7.67	2529.91	8.34	0.72	11.61595	0.00000	Verrucomicrobia	FukuN18_freshwater_group	FukuN18_freshwater_group_unclassified
FL	21	OTU005	11.59	1.77	1.09	0.40	1293.65	-2.09	0.53	-3.96422	0.00311	Verrucomicrobia	Opitutae_vadinHA64_unclassified	Opitutae_vadinHA64_unclassified
FL	21	OTU004	8.09	0.16	6.53	0.23	807.66	-5.10	0.95	-5.39882	0.00001	Cyanobacteria	FamilyI	FamilyI_unclassified
FL	21	OTU006	2.60	6.99	0.86	2.15	977.30	1.98	0.54	3.64559	0.00769	Actinobacteria	Sporichthyaceae	Sporichthyaceae_unclassified
FL	21	OTU027	0.13	2.24	0.10	0.98	262.96	4.62	0.72	6.43222	0.00000	Verrucomicrobia	FukuN18_freshwater_group	FukuN18_freshwater_group_unclassified
FL	21	OTU040	1.00	0.05	0.91	0.07	99.63	-3.81	0.97	-3.94165	0.00311	Cyanobacteria	FamilyI	Synechococcus
FL	21	OTU149	0.20	0.01	0.07	0.01	20.59	-3.51	0.83	-4.20612	0.00128	Cyanobacteria	FamilyI	FamilyI_unclassified
FL	21	OTU014	0.00	0.19	0.00	0.12	20.30	6.92	1.32	5.23692	0.00001	Proteobacteria	Burkholderiales_unclassified	Burkholderiales_unclassified
FL	21	OTU033	0.00	0.17	0.00	0.16	16.74	6.51	1.29	5.04272	0.00003	Proteobacteria	Comamonadaceae	Comamonadaceae_unclassified
FL	21	OTU276	0.00	0.17	0.00	0.09	15.77	5.88	1.10	5.32762	0.00001	Verrucomicrobia	Chthoniobacteraceae	Chthoniobacter
FL	21	OTU353	0.16	0.00	0.24	0.00	15.35	-6.53	1.77	-3.69891	0.00681	Proteobacteria	Rhodobacteraceae	Paracocccus
FL	21	OTU378	0.09	0.00	0.04	0.00	8.17	-6.19	1.74	-3.56557	0.00966	Cyanobacteria	FamilyI	Synechococcus

FL	21	OTU398	0.00	0.06	0.00	0.01	5.49	6.53	1.71	3.82165	0.00459	Bacteria_unclassified	Bacteria_unclassified	Bacteria_unclassified
FL	42	OTU136	1.07	0.16	0.26	0.12	98.92	-2.68	0.68	-3.96572	0.00498	Bacteroidetes	Cryomorphaceae	Fluviicola
FL	42	OTU094	0.58	0.06	0.48	0.03	49.40	-3.12	0.68	-4.58235	0.00125	Bacteroidetes	Cryomorphaceae	Fluviicola
FL	42	OTU196	0.11	0.00	0.09	0.00	8.99	-5.07	1.16	-4.38329	0.00159	Chloroflexi	Roseiflexaceae	Roseiflexus
FL	42	OTU337	0.08	0.00	0.07	0.00	6.20	-5.50	1.33	-4.14846	0.00303	Bacteroidetes	Cryomorphaceae	Fluviicola
PA	1	OTU019	1.20	0.04	1.87	0.05	92.98	-4.91	1.03	-4.75966	0.00009	Proteobacteria	Gammaproteobacteria_unclassified	Gammaproteobacteria_unclassified
PA	1	OTU027	0.26	1.07	0.20	0.14	100.69	1.91	0.57	3.35646	0.00836	Verrucomicrobia	FukuN18_freshwater_group	FukuN18_freshwater_group_unclassified
PA	1	OTU084	0.15	0.95	0.05	0.16	83.60	2.61	0.44	5.88886	0.00000	Proteobacteria	Caulobacteraceae	Brevundimonas
PA	1	OTU167	0.00	0.77	0.00	0.73	58.78	9.63	1.82	5.30231	0.00002	Proteobacteria	Methylococcaceae	Methylobacter
PA	1	OTU111	0.61	0.07	0.78	0.05	50.95	-3.18	0.86	-3.70768	0.00353	Bacteroidetes	Flavobacteriaceae	Flavobacterium
PA	1	OTU026	0.15	0.60	0.05	0.22	57.38	1.92	0.51	3.76031	0.00296	Verrucomicrobia	OPB35_soil_group_unclassified	OPB35_soil_group_unclassified
PA	1	OTU093	0.58	0.15	0.16	0.01	57.16	-2.04	0.42	-4.86064	0.00006	Proteobacteria	Betaproteobacteria_unclassified	Betaproteobacteria_unclassified
PA	1	OTU242	0.00	0.50	0.00	0.27	37.50	7.52	1.28	5.85042	0.00000	Planctomycetes	Phycisphaeraceae	CL500-3
PA	1	OTU224	0.00	0.48	0.00	0.33	35.78	9.03	1.84	4.90349	0.00006	Proteobacteria	Comamonadaceae	Comamonadaceae_unclassified
PA	1	OTU071	0.12	0.44	0.04	0.13	43.03	1.77	0.49	3.60922	0.00472	Cyanobacteria	FamilyI	Anabaena
PA	1	OTU200	0.03	0.40	0.03	0.19	32.18	3.51	0.72	4.87260	0.00006	Planctomycetes	Planctomycetaceae	Schlesneria
PA	1	OTU213	0.00	0.30	0.00	0.32	23.30	6.83	1.34	5.08256	0.00003	Proteobacteria	CABC2E06	CABC2E06_unclassified
PA	1	OTU197	0.29	0.06	0.10	0.01	27.11	-2.21	0.50	-4.44854	0.00029	Proteobacteria	Bradyrhizobiaceae	Bosea
PA	1	OTU128	0.02	0.28	0.02	0.17	22.99	3.45	0.76	4.51731	0.00024	Bacteroidetes	Porphyromonadaceae	Paludibacter
PA	1	OTU239	0.00	0.26	0.00	0.27	19.37	8.23	1.89	4.35258	0.00038	Proteobacteria	Methylophilaceae	Methylophilaceae_unclassified
PA	1	OTU228	0.03	0.26	0.02	0.04	21.44	3.22	0.61	5.27286	0.00002	Bacteroidetes	Chitinophagaceae	Sediminibacterium
PA	1	OTU114	0.01	0.25	0.00	0.13	19.39	4.08	0.78	5.25130	0.00002	Bacteroidetes	env.OPS_17	env.OPS_17_unclassified
PA	1	OTU351	0.00	0.24	0.00	0.16	18.02	8.17	1.88	4.35404	0.00038	Planctomycetes	Planctomycetaceae	Planctomyces
PA	1	OTU262	0.03	0.20	0.03	0.08	17.10	2.75	0.75	3.65023	0.00429	Planctomycetes	vadinHA49_unclassified	vadinHA49_unclassified
PA	1	OTU011	0.01	0.20	0.01	0.11	15.97	3.95	0.89	4.42243	0.00031	Verrucomicrobia	FukuN18_freshwater_group	FukuN18_freshwater_group_unclassified
PA	1	OTU334	0.00	0.19	0.00	0.09	14.75	5.61	1.12	5.02842	0.00003	Planctomycetes	Phycisphaeraceae	CL500-3
PA	1	OTU073	0.01	0.19	0.01	0.06	15.11	4.33	0.83	5.20053	0.00002	Cyanobacteria	FamilyI	Planktothrix
PA	1	OTU290	0.00	0.19	0.00	0.04	14.18	7.93	1.86	4.26076	0.00055	Chlorobi	OPB56	OPB56_unclassified
PA	1	OTU172	0.00	0.17	0.00	0.10	12.65	6.13	1.36	4.50810	0.00024	Planctomycetes	Planctomycetaceae	Planctomyces
PA	1	OTU226	0.01	0.17	0.00	0.07	13.33	3.74	0.79	4.71784	0.00010	Planctomycetes	vadinHA49_unclassified	vadinHA49_unclassified
PA	1	OTU470	0.00	0.15	0.00	0.03	11.24	7.64	1.87	4.07502	0.00108	Proteobacteria	GR-WP33-58	GR-WP33-58_unclassified
PA	1	OTU086	0.15	0.01	0.11	0.01	12.40	-3.31	0.85	-3.89516	0.00204	Bacteroidetes	Bacteroidetes_unclassified	Bacteroidetes_unclassified
PA	1	OTU245	0.01	0.15	0.02	0.12	12.39	3.40	0.99	3.42852	0.00728	Cyanobacteria	FamilyI	Pseudanabaena
PA	1	OTU493	0.00	0.15	0.00	0.06	11.09	7.60	1.89	4.02918	0.00126	Planctomycetes	OM190_unclassified	OM190_unclassified
PA	1	OTU349	0.00	0.13	0.00	0.05	9.91	7.45	1.89	3.94798	0.00170	Planctomycetes	Phycisphaeraceae	CL500-3
PA	1	OTU377	0.00	0.13	0.01	0.08	9.56	5.59	1.33	4.19643	0.00070	Proteobacteria	Sandaracinaceae	Sandaracinus
PA	1	OTU235	0.02	0.13	0.01	0.09	10.97	2.77	0.80	3.46369	0.00669	Proteobacteria	Comamonadaceae	Comamonadaceae_unclassified
PA	1	OTU500	0.00	0.12	0.00	0.05	9.00	7.34	1.89	3.88186	0.00207	Planctomycetes	Phycisphaeraceae	CL500-3
PA	1	OTU253	0.12	0.00	0.17	0.00	9.23	-5.87	1.43	-4.09036	0.00106	Bacteroidetes	Flavobacteriaceae	Flavobacterium
PA	1	OTU356	0.01	0.11	0.01	0.05	9.39	3.09	0.88	3.51043	0.00604	Proteobacteria	Rhodospirillaceae	Roseospirillum
PA	1	OTU370	0.00	0.10	0.00	0.03	7.76	7.16	1.90	3.77791	0.00285	Actinobacteria	Actinobacteria_unclassified	Actinobacteria_unclassified
PA	1	OTU567	0.00	0.10	0.00	0.01	7.69	7.16	1.89	3.78252	0.00285	Proteobacteria	Blfdi19	Blfdi19_unclassified

PA	1	OTU283	0.10	0.01	0.07	0.01	8.79	-2.82	0.84	-3.36832	0.00836	Bacteroidetes	Flavobacteriaceae	Flavobacterium
PA	1	OTU511	0.00	0.09	0.00	0.07	6.83	6.96	1.94	3.59485	0.00474	Proteobacteria	CABC2E06	CABC2E06_unclassified
PA	1	OTU529	0.00	0.08	0.00	0.03	6.50	5.23	1.37	3.80674	0.00272	Planctomycetes	OM190_unclassified	OM190_unclassified
PA	1	OTU254	0.00	0.08	0.00	0.04	6.20	5.02	1.38	3.63193	0.00447	Verrucomicrobia	Opitutaceae	Opitutus
PA	1	OTU436	0.08	0.01	0.04	0.01	6.67	-3.18	0.89	-3.57658	0.00495	Cyanobacteria	Cyanobacteria_unclassified	Cyanobacteria_unclassified
PA	1	OTU630	0.00	0.08	0.00	0.05	5.78	6.74	1.93	3.48543	0.00632	Proteobacteria	Deltaproteobacteria_unclassified	Deltaproteobacteria_unclassified
PA	1	OTU440	0.00	0.08	0.00	0.02	5.59	6.74	1.91	3.52032	0.00597	Bacteria_unclassified	Bacteria_unclassified	Bacteria_unclassified
PA	1	OTU369	0.00	0.07	0.01	0.04	5.71	4.02	1.20	3.36508	0.00836	Planctomycetes	Planctomycetaceae	Planctomyces
PA	1	OTU642	0.00	0.07	0.00	0.05	5.52	6.68	1.94	3.43939	0.00716	Verrucomicrobia	Verrucomicrobia_unclassified	Verrucomicrobia_unclassified
PA	1	OTU100	0.00	0.07	0.00	0.02	5.53	4.90	1.36	3.60315	0.00472	Chloroflexi	SL56_marine_group_unclassified	SL56_marine_group_unclassified
PA	1	OTU584	0.00	0.06	0.00	0.00	4.99	4.76	1.36	3.49919	0.00615	Proteobacteria	mle1-27	mle1-27_unclassified
PA	1	OTU632	0.00	0.06	0.00	0.04	4.87	4.82	1.43	3.37563	0.00836	Proteobacteria	Proteobacteria_unclassified	Proteobacteria_unclassified
PA	1	OTU180	0.00	0.06	0.00	0.02	4.76	4.69	1.38	3.38943	0.00822	Actinobacteria	Sporichthyaceae	Sporichthya
PA	1	OTU094	0.00	0.06	0.01	0.02	4.67	4.59	1.37	3.35704	0.00836	Bacteroidetes	Cryomorphaceae	Fluviicola
PA	1	OTU705	0.00	0.06	0.00	0.02	4.49	6.47	1.93	3.34274	0.00861	Verrucomicrobia	OPB35_soil_group_unclassified	OPB35_soil_group_unclassified
PA	1	OTU484	0.00	0.06	0.00	0.02	4.44	6.45	1.93	3.33572	0.00867	Verrucomicrobia	Unknown_Family	Candidatus_Methylacidiphilum
PA	6	OTU002	16.04	60.92	14.31	6.21	12401.06	2.77	0.76	3.66319	0.00668	Cyanobacteria	FamilyI	Dolichospermum (sensu Anabaena)
PA	6	OTU004	23.10	0.96	13.61	0.57	2459.48	-3.65	0.71	-5.12834	0.00008	Cyanobacteria	FamilyI	FamilyI_unclassified
PA	6	OTU014	0.29	1.92	0.25	1.23	369.00	3.53	0.82	4.28292	0.00141	Proteobacteria	Burkholderiales_unclassified	Burkholderiales_unclassified
PA	6	OTU006	0.47	0.08	0.17	0.03	57.03	-1.65	0.45	-3.64563	0.00681	Actinobacteria	Sporichthyaceae	Sporichthyaceae_unclassified
PA	6	OTU017	0.22	0.46	0.06	0.24	98.97	1.89	0.47	4.06067	0.00291	Acidobacteria	SJA-149	SJA-149_unclassified
PA	6	OTU042	0.40	0.02	0.32	0.01	37.29	-3.62	0.79	-4.58988	0.00048	Actinobacteria	Acidimicrobiales_Incertae_Sedis	Candidatus_Microthrix
PA	6	OTU134	0.07	0.14	0.03	0.04	30.56	1.87	0.50	3.77303	0.00512	Proteobacteria	Alphaproteobacteria_unclassified	Alphaproteobacteria_unclassified
PA	6	OTU301	0.01	0.13	0.01	0.03	23.84	4.62	0.95	4.83637	0.00018	Planctomycetes	vadinHA49_unclassified	vadinHA49_unclassified
PA	6	OTU084	0.09	0.13	0.02	0.03	30.70	1.37	0.36	3.79667	0.00512	Proteobacteria	Caulobacteraceae	Brevundimonas
PA	6	OTU226	0.01	0.12	0.01	0.07	21.17	4.06	0.95	4.28441	0.00141	Planctomycetes	vadinHA49_unclassified	vadinHA49_unclassified
PA	6	OTU073	0.01	0.10	0.01	0.05	17.87	4.55	0.73	6.26145	0.00000	Cyanobacteria	FamilyI	Planktothrix
PA	6	OTU114	0.03	0.10	0.02	0.08	18.68	2.84	0.77	3.71583	0.00603	Bacteroidetes	env.OPS_17	env.OPS_17_unclassified
PA	6	OTU165	0.00	0.09	0.00	0.09	14.58	5.48	1.13	4.85504	0.00018	Bacteroidetes	Cryomorphaceae	Fluviicola
PA	6	OTU429	0.00	0.06	0.00	0.07	10.95	4.87	1.24	3.94064	0.00396	Bacteria_unclassified	Bacteria_unclassified	Bacteria_unclassified
PA	6	OTU350	0.06	0.00	0.03	0.00	5.63	-3.99	1.02	-3.91980	0.00396	Bacteroidetes	LiUU-11-161	LiUU-11-161_unclassified
PA	6	OTU390	0.01	0.06	0.01	0.04	9.69	3.81	1.08	3.53058	0.00966	Proteobacteria	Hot_Creek_32_unclassified	Hot_Creek_32_unclassified
PA	6	OTU613	0.00	0.03	0.00	0.03	7.15	4.43	1.18	3.77140	0.00512	Cyanobacteria	FamilyI	Anabaena
PA	6	OTU270	0.00	0.03	0.00	0.03	5.19	4.50	1.16	3.86821	0.00420	Proteobacteria	Holosporaceae	Holosporaceae_unclassified
PA	6	OTU489	0.00	0.03	0.00	0.02	6.09	4.24	1.07	3.96483	0.00394	Proteobacteria	Blfdi19	Blfdi19_unclassified
PA	6	OTU574	0.00	0.03	0.00	0.02	4.56	6.11	1.47	4.14121	0.00231	Proteobacteria	Proteobacteria_unclassified	Proteobacteria_unclassified
PA	6	OTU596	0.00	0.03	0.00	0.02	4.57	4.04	1.10	3.66513	0.00668	Planctomycetes	vadinHA49_unclassified	vadinHA49_unclassified
PA	6	OTU821	0.00	0.02	0.00	0.01	4.08	5.86	1.51	3.87631	0.00420	Cyanobacteria	FamilyI	Snowella
PA	6	OTU010	0.00	0.01	0.00	0.00	2.48	5.38	1.52	3.53387	0.00966	Cyanobacteria	FamilyI	FamilyI_unclassified
PA	21	OTU014	0.06	17.67	0.05	13.68	2437.70	8.72	1.19	7.32751	0.00000	Proteobacteria	Burkholderiales_unclassified	Burkholderiales_unclassified
PA	21	OTU029	0.18	7.93	0.07	7.63	1130.72	6.22	1.17	5.32188	0.00002	Proteobacteria	Comamonadaceae	Comamonadaceae_unclassified
PA	21	OTU077	0.09	3.19	0.07	4.67	414.40	5.79	1.29	4.48539	0.00059	Proteobacteria	Cellvibrionaceae	Cellvibrio

PA	21	OTU116	0.10	1.22	0.08	1.31	166.16	4.42	1.21	3.66195	0.00933	Proteobacteria	Comamonadaceae	Rhizobacter
PA	21	OTU193	1.14	0.01	0.81	0.01	72.75	-6.46	1.28	-5.06214	0.00004	Bacteria_unclassified	Bacteria_unclassified	Bacteria_unclassified
PA	21	OTU125	0.02	0.50	0.02	0.48	68.13	5.05	1.38	3.65131	0.00933	Proteobacteria	Comamonadaceae	Comamonadaceae_unclassified
PA	21	OTU115	0.29	0.00	0.38	0.00	17.76	-6.06	1.59	-3.81060	0.00638	Bacteroidetes	Bacteroidetes_unclassified	Bacteroidetes_unclassified
PA	21	OTU248	0.00	0.20	0.00	0.13	26.53	6.48	1.54	4.21519	0.00161	Bacteroidetes	env.OPS_17	env.OPS_17_unclassified
PA	21	OTU398	0.00	0.19	0.00	0.13	20.50	6.18	1.51	4.08264	0.00239	Bacteria_unclassified	Bacteria_unclassified	Bacteria_unclassified
PA	42	OTU109	3.52	0.00	5.71	0.00	386.63	-7.57	1.56	-4.84130	0.00053	Proteobacteria	Burkholderiales_unclassified	Burkholderiales_unclassified
PA	42	OTU081	2.81	0.07	3.59	0.02	312.85	-4.60	1.15	-4.00191	0.00857	Bacteroidetes	Flavobacteriaceae	Flavobacterium
PA	42	OTU422	0.24	0.00	0.32	0.00	25.94	-6.68	1.66	-4.01824	0.00857	Bacteroidetes	Flavobacteriaceae	Elizabethkingia

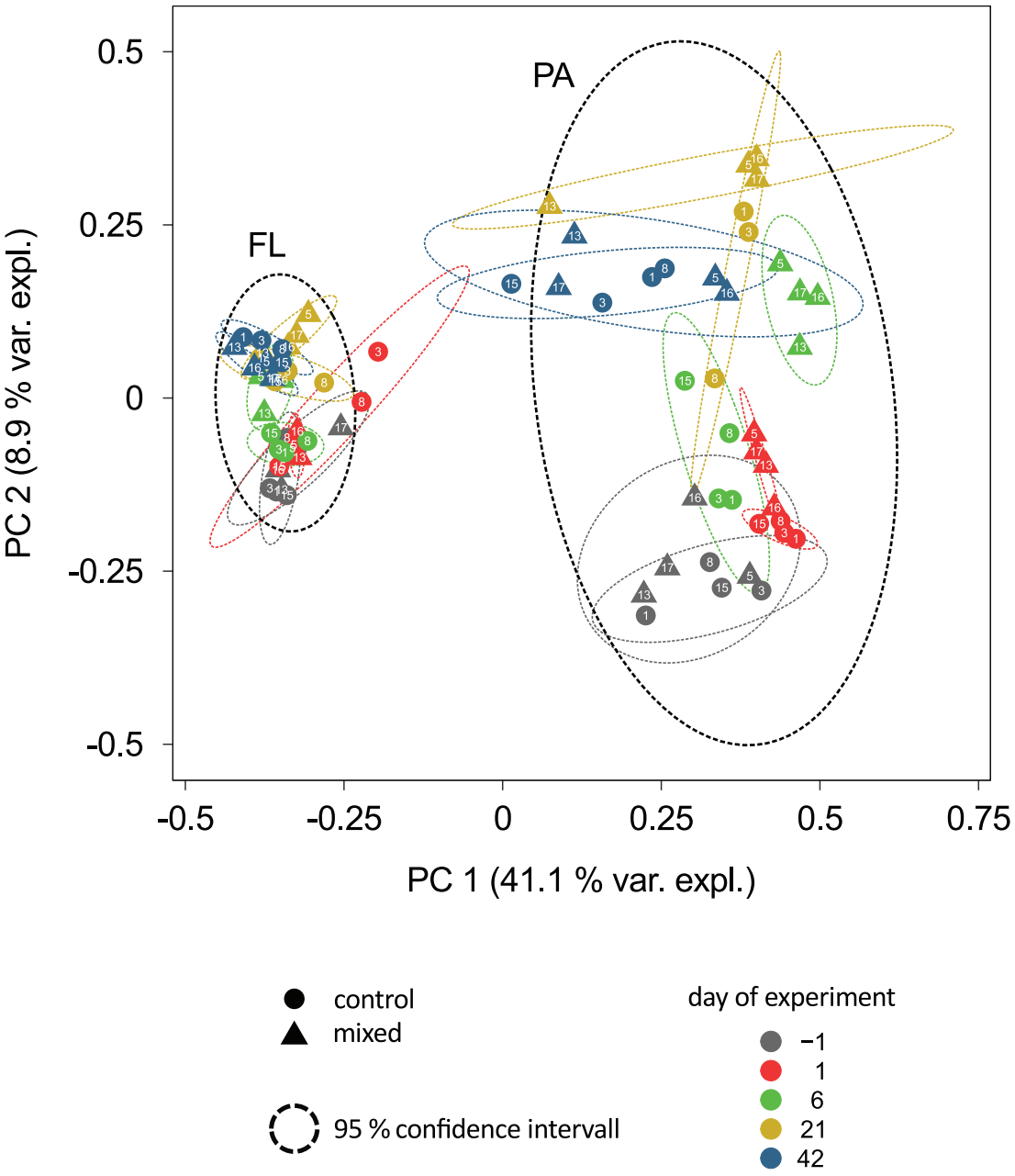
PA
FL
0.5
0.25
0
-0.25
-0.5
-0.5
-0.25
0
0.25
0.5
0.75
PC 2 (8.9 % var. expl.)
PC 1 (41.1 % var. expl.)
control
mixed
95 % confidence intervall
day of experiment
−1
1
6
21
42

Figure S1:

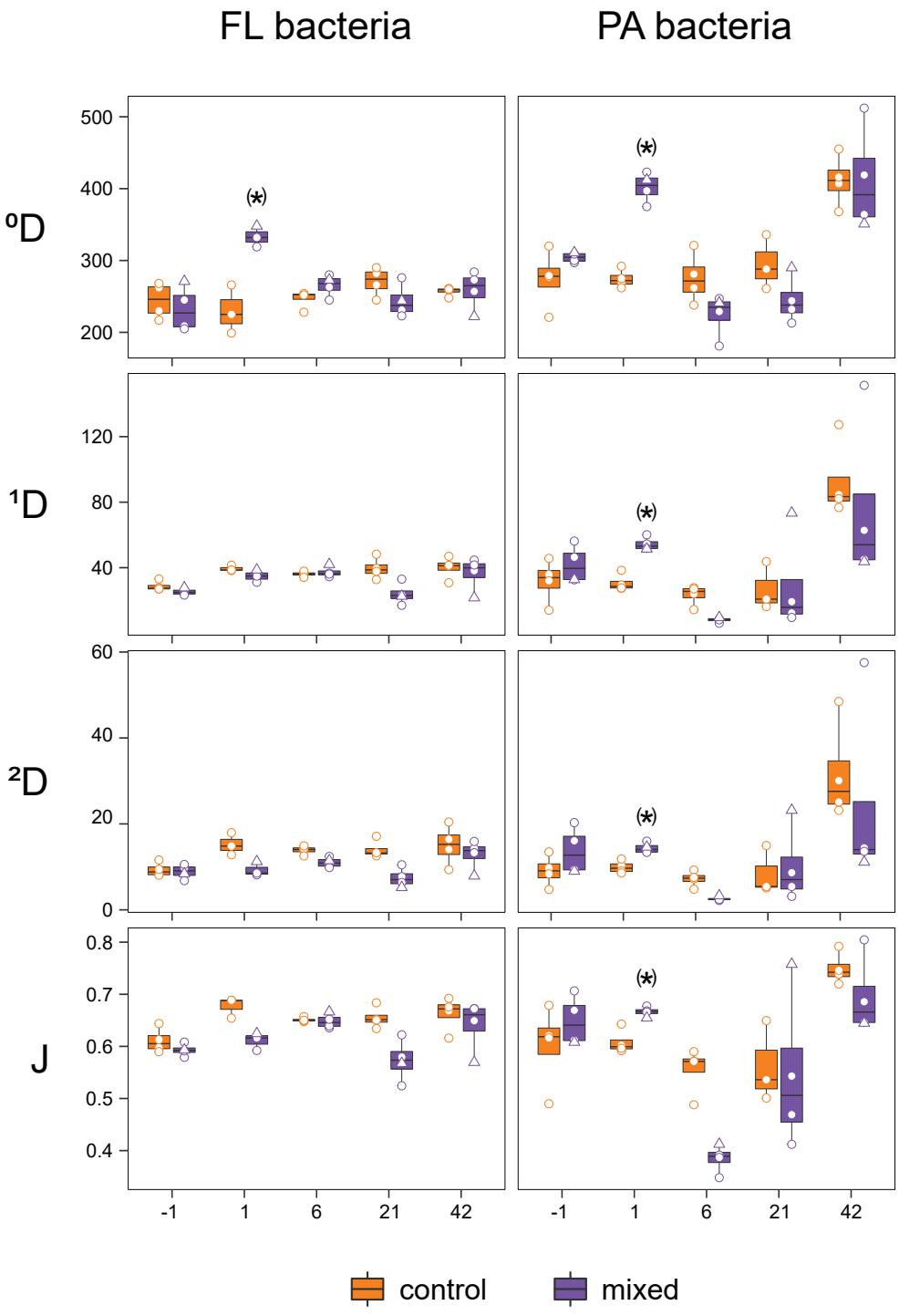
FL bacteria
PA bacteria
⁰D
¹D
²D
J
(*)
500
400
300
200
120
80
40
60
20
0
0.8
0.7
0.6
0.5
0.4
-1
1
6
21
42
control
mixed

Figure S2:

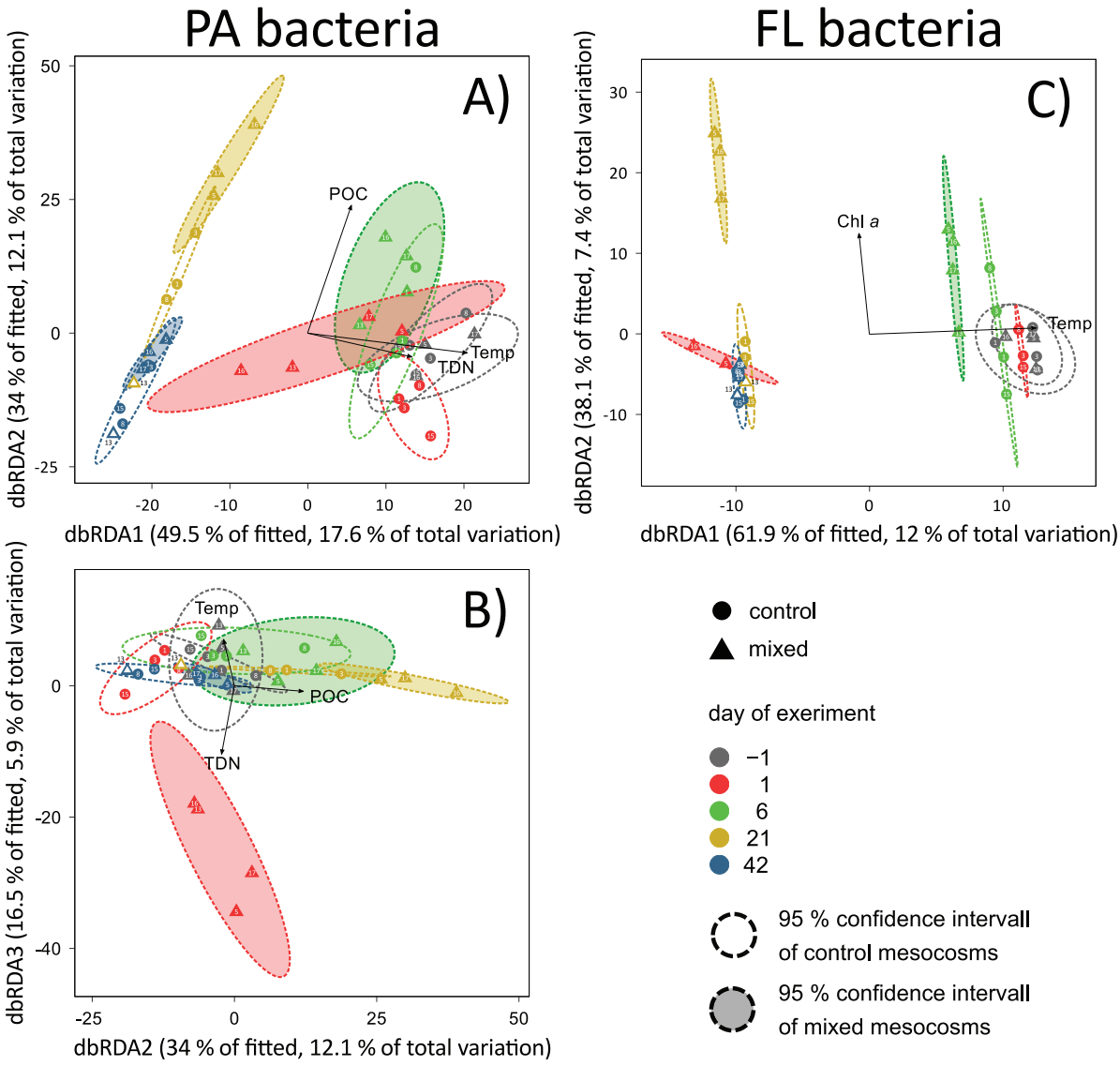
PA bacteria
A)
POC
Temp
TDN
dbRDA2 (34 % of fitted, 12.1 % of total variation)
dbRDA1 (49.5 % of fitted, 17.6 % of total variation)
FL bacteria
C)
Chl a
Temp
dbRDA2 (38.1 % of fitted, 7.4 % of total variation)
dbRDA1 (61.9 % of fitted, 12 % of total variation)
B)
Temp
POC
TDN
dbRDA3 (16.5 % of fitted, 5.9 % of total variation)
dbRDA2 (34 % of fitted, 12.1 % of total variation)
control
mixed
day of exeriment
−1
1
6
21
42
95 % confidence intervall of control mesocosms
95 % confidence intervall of mixed mesocosms

Figure S3:

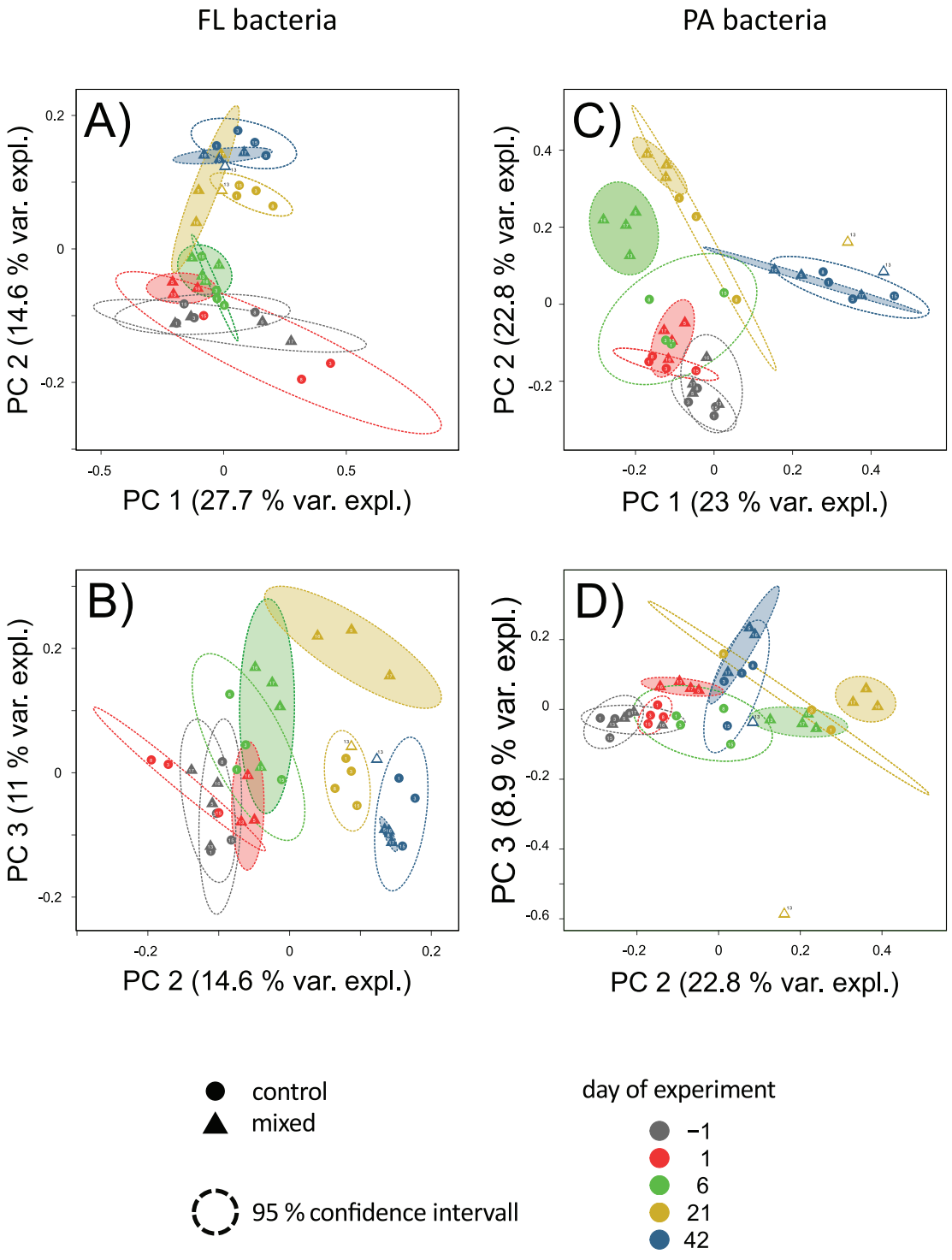
FL bacteria
PA bacteria
A)
B)
C)
D)
PC 2 (14.6 % var. expl.)
PC 1 (27.7 % var. expl.)
PC 3 (11 % var. expl.)
PC 2 (14.6 % var. expl.)
PC 2 (22.8 % var. expl.)
PC 1 (23 % var. expl.)
PC 3 (8.9 % var. expl.)
PC 2 (22.8 % var. expl.)
control
mixed
95 % confidence intervall
day of experiment
−1
1
6
21
42

Figure S4:

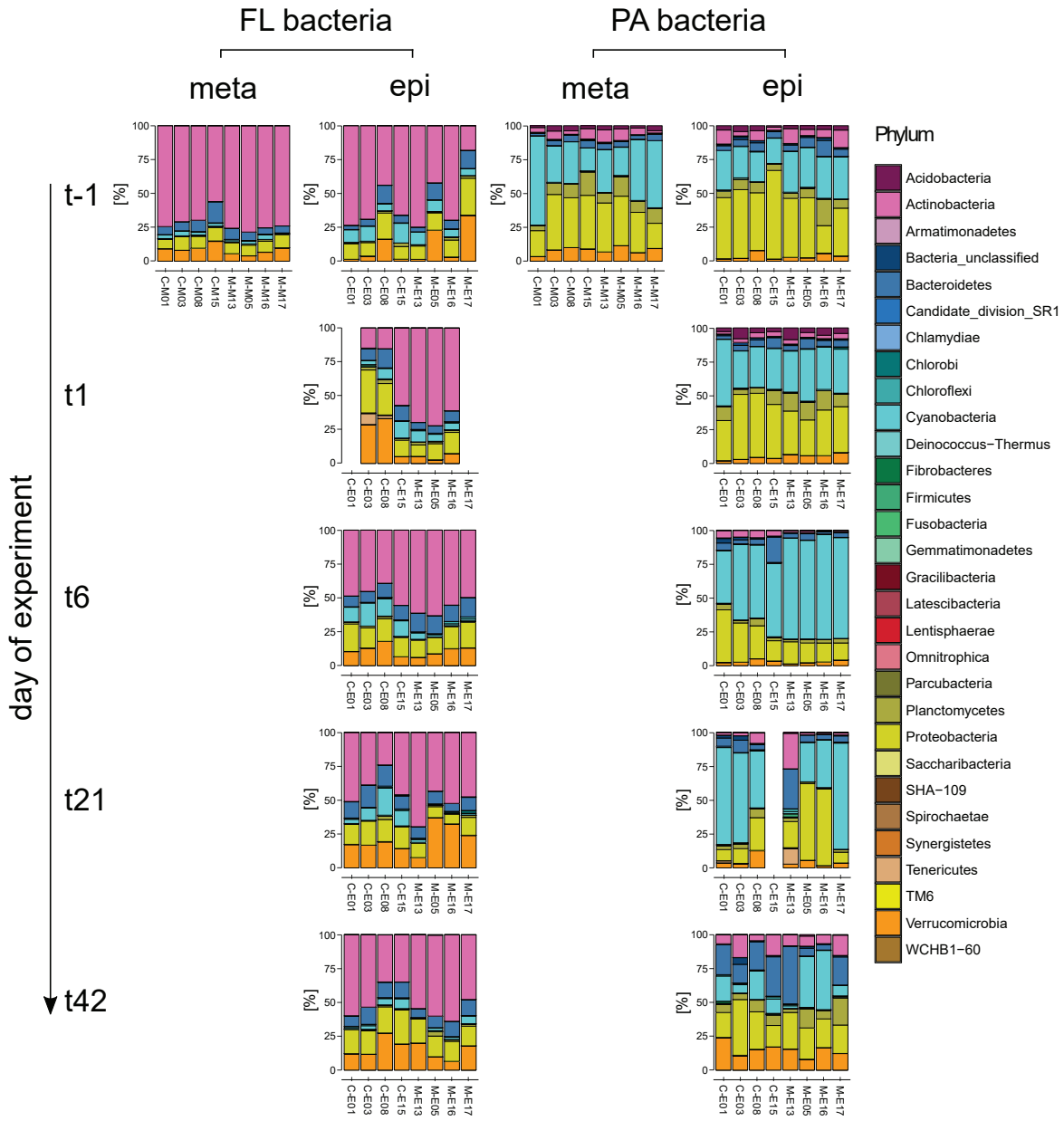
FL bacteria
PA bacteria
meta
epi
meta
epi
day of experiment
t-1
t1
t6
t21
t42
[%]
Phylum
Acidobacteria
Actinobacteria
Armatimonadetes
Bacteria_unclassified
Bacteroidetes
Candidate_division_SR1
Chlamydiae
Chlorobi
Chloroflexi
Cyanobacteria
Deinococcus−Thermus
Fibrobacteres
Firmicutes
Fusobacteria
Gemmatimonadetes
Gracilibacteria
Latescibacteria
Lentisphaerae
Omnitrophica
Parcubacteria
Planctomycetes
Proteobacteria
Saccharibacteria
SHA−109
Spirochaetae
Synergistetes
Tenericutes
TM6
Verrucomicrobia
WCHB1−60

Figure S5-I:

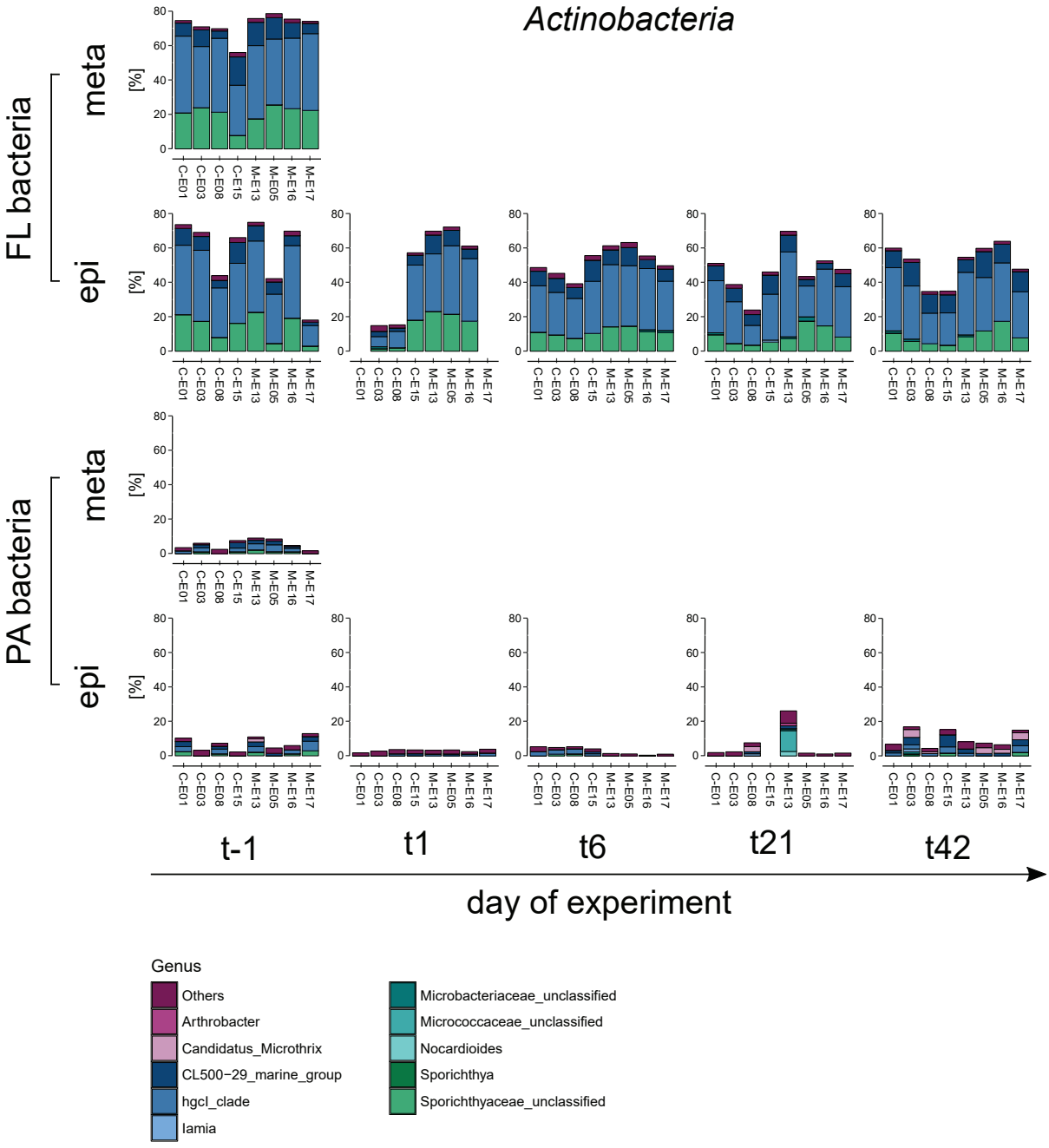
Actinobacteria
FL bacteria
PA bacteria
meta
epi
[%]
C-E01
C-E03
C-E08
C-E15
M-E13
M-E05
M-E16
M-E17
t-1
t1
t6
t21
t42
day of experiment
Genus
Others
Arthrobacter
Candidatus_Microthrix
CL500−29_marine_group
hgcI_clade
Iamia
Microbacteriaceae_unclassified
Micrococcaceae_unclassified
Nocardioides
Sporichthya
Sporichthyaceae_unclassified

Figure S5-II:

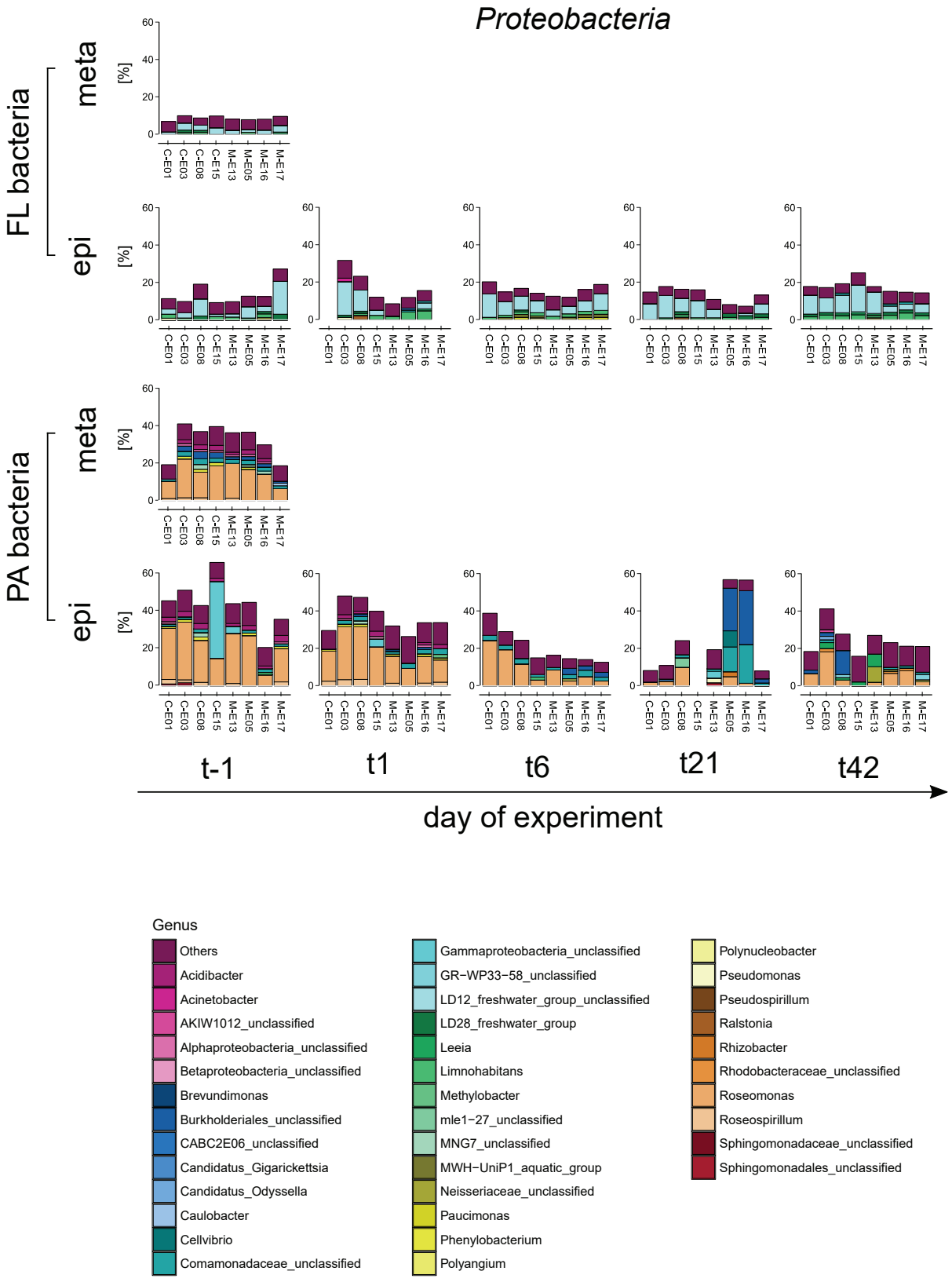

Figure S5-III:

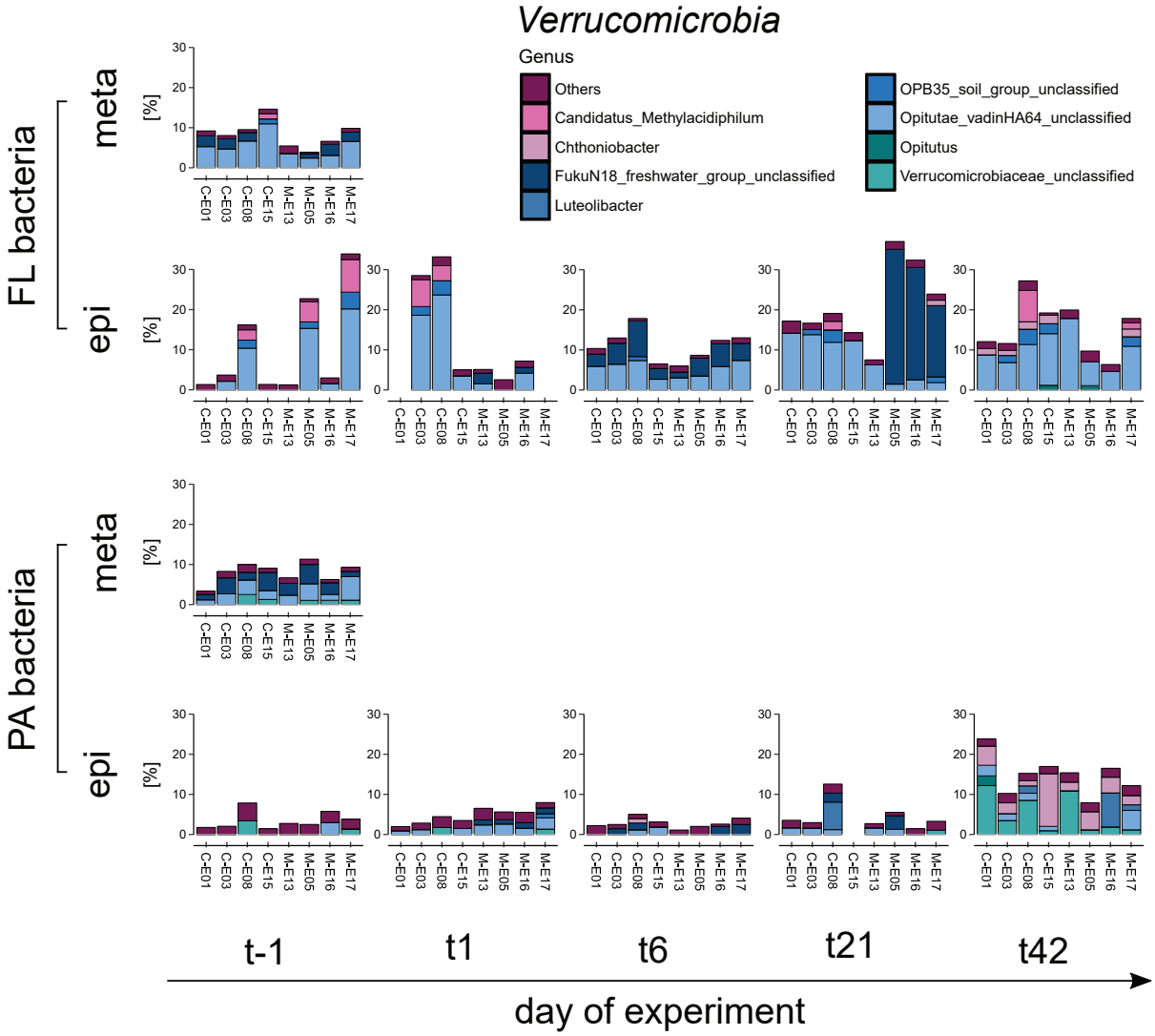
Verrucomicrobia
Genus
Others
Candidatus_Methylacidiphilum
Chthoniobacter
FukuN18_freshwater_group_unclassified
Luteolibacter
OPB35_soil_group_unclassified
Opitutae_vadinHA64_unclassified
Opitutus
Verrucomicrobiaceae_unclassified
FL bacteria
PA bacteria
meta
epi
[%]
C-E01
C-E03
C-E08
C-E15
M-E13
M-E05
M-E16
M-E17
t-1
t1
t6
t21
t42
day of experiment

Figure S5-IV:

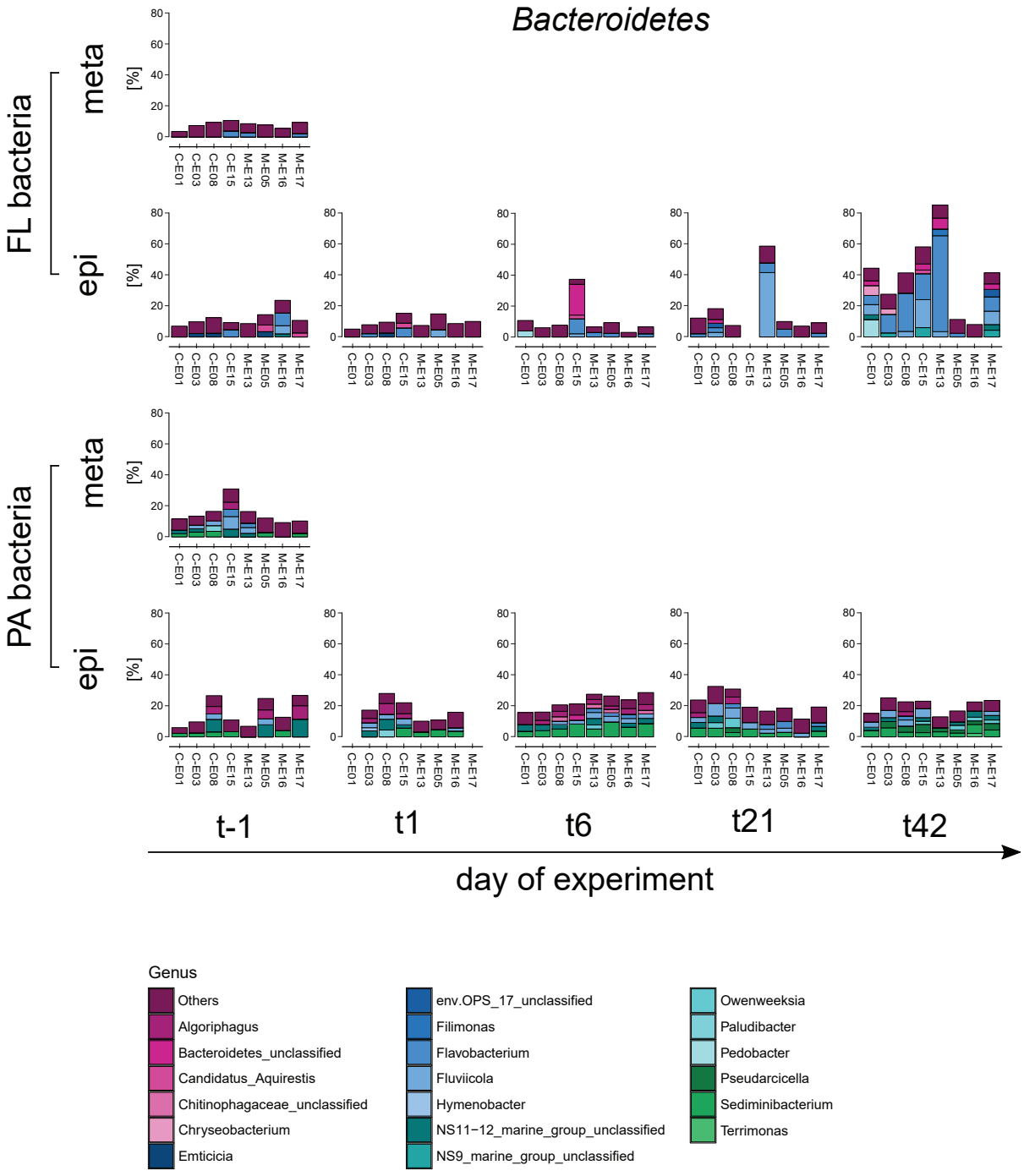
Bacteroidetes
FL bacteria
PA bacteria
meta
epi
[%]
C-E01
C-E03
C-E08
C-E15
M-E13
M-E05
M-E16
M-E17
t-1
t1
t6
t21
t42
day of experiment
Genus
Others
Algoriphagus
Bacteroidetes_unclassified
Candidatus_Aquirestis
Chitinophagaceae_unclassified
Chryseobacterium
Emticicia
env.OPS_17_unclassified
Filimonas
Flavobacterium
Fluviicola
Hymenobacter
NS11−12_marine_group_unclassified
NS9_marine_group_unclassified
Owenweeksia
Paludibacter
Pedobacter
Pseudarcicella
Sediminibacterium
Terrimonas

Figure S5-V:

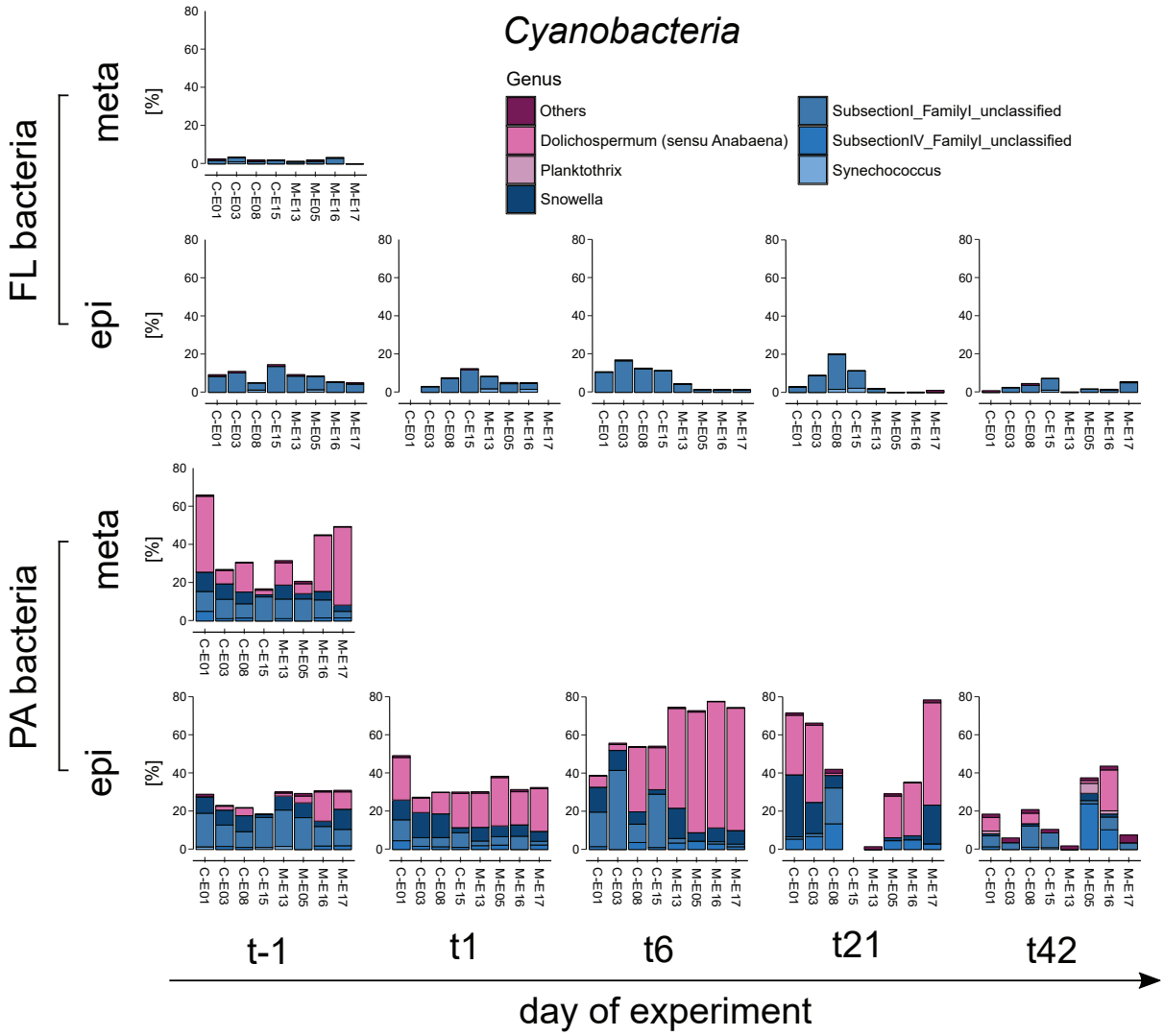
Cyanobacteria
Genus
Others
Dolichospermum (sensu Anabaena)
Planktothrix
Snowella
SubsectionI_FamilyI_unclassified
SubsectionIV_FamilyI_unclassified
Synechococcus
FL bacteria
PA bacteria
meta
epi
[%]
C-E01
C-E03
C-E08
C-E15
M-E13
M-E05
M-E16
M-E17
t-1
t1
t6
t21
t42
day of experiment

Figure S5-VI:

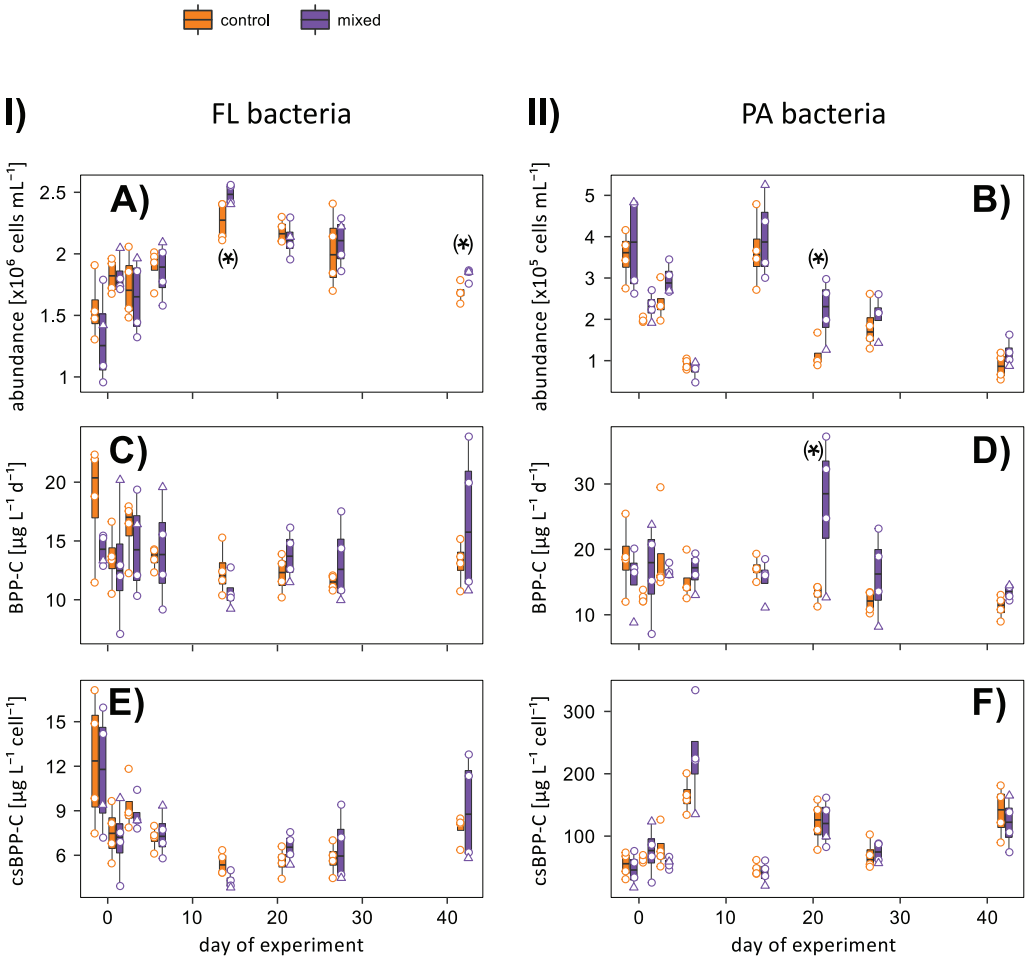
control
mixed
I)
FL bacteria
II)
PA bacteria
A)
B)
C)
D)
E)
F)
abundance [x10^6 cells mL^-1]
abundance [x10^5 cells mL^-1]
BPP-C [µg L^-1 d^-1]
csBPP-C [µg L^-1 cell^-1]
day of experiment
day of experiment

Figure S6:

6. Chapter 6 - Synthesis

This thesis intends to achieve a better understanding of how and to what extend ongoing ocean acidification and projected climate-change related alterations in weather patterns and climate extremes might impact heterotrophic bacteria in different aquatic ecosystems in the future. In this chapter, I synthesize important aspects presented in **Chapters 2 to 5** and summarize the major knowledge and mechanistic insights gained from several mesocosm experiments during my doctoral thesis, which have been performed at different marine locations and in Lake Stechlin. Based on this, I draw attention to and suggest research gaps where future research efforts should be made.

6.1 Will ocean acidification affect marine microbes?

Already in 2011, Joint et al., (2011) addressed this question in their review article, summarizing current knowledge on potential effects of OA on marine microbes after more than one decade of extensive OA research. They concluded that major biogeochemical processes in the oceans except of calcification will not be fundamentally different under future higher CO_2/lower pH conditions, until evidence is obtained to the contrary. Based on comparisons made with microbes in other aquatic environments, that readily accommodate very large and rapid seasonal and spatial pH changes that are orders of magnitude greater than those projected for the twenty second century oceans, Joint et al., (2011) expected a high functional resilience of microbial communities to OA. Seven years later, I thus will ask the question again: Do we have now evidence to the contrary?

During the past years, several *in situ* experiments on OA effects have been performed to investigate potential OA-induced changes in natural plankton communities across seasons and different locations (see **APPENDIX Table 1**). The results have been evaluated within prominent projects like BIOACID ('Biological Impacts of Ocean Acidification') or MedSeA ('Mediterranean Sea Acidification under changing climate') that intended to discover how the local and seasonal differences in observations influence potential OA effects and aimed to disentangle general patterns of plankton metabolic and community shifts in response to OA (Riebesell and Gattuso, 2015; Maugendre et al., 2017; Schulz et al., 2017; Alvarez-Fernandez et al., 2018). **Chapters 2 to 4** of this doctoral thesis present results from mesocosm studies performed in the freshwater part of the Baltic Sea (Tvärminne) (**Chapter 2 and 3**), the more saline Kattegat (Gullmarsfjord) (**Chapter 4**), and the subtropical Atlantic (Gando Bay, Gran Canaria) (**Chapter 4**) addressing specific seasonal and regional conditions that cover a wide range of estuarine and marine ecosystem characteristics. All three studies, however, were performed without inorganic nutrient additions to focus solely on OA effects during periods of low-nutrient concentrations in temperate regions or oligotrophic subtropical conditions (Paul et al., 2015; Bach et al., 2016; Taucher et al., 2017a). Such conditions are representative for most parts of the oceans for extended periods throughout the year (Moore et al., 2013) and were not well represented in former studies that have

been performed mostly at high phytoplankton biomass conditions, partly provoked by nutrient amendments (see **APPENDIX Table 1**). The results from **Chapters 2 to 4** thus fill a current knowledge gap in OA research addressing metabolic responses of heterotrophic bacteria within plankton communities at low-nutrient concentrations to OA.

Chapter 2 and 3 evaluate OA effects in a brackish coastal ecosystem during low-nutrient summer months. Indications that OA effects are greater under nutrient limitation (de Kluijver et al., 2010) and, in particular, the limited number of OA studies in brackish waters motivated this mesocosm study to be performed in the Baltic Sea. Although, the results from **Chapter 2** do not suggest a consistent pCO_2-induced effect on bulk or cell-specific rates of protein production or biovolume of heterotrophic bacteria, when considered as individual components, our multivariate analyses revealed a significant effect of the pCO_2 treatment on the entire assemblages of dissolved and particulate nutrients, metabolic variables and the microbial community composition. Thereby, the impact of pCO_2 on community metabolism occurred indirectly, potentially through varying physicochemical parameters and feedback mechanisms in the food web leading to changes in the microbial community composition, particularly in small-sized phytoplankton. Also a C budget examining major C pools and fluxes revealed a clear effect of increasing pCO_2 concentration (**Chapter 3**). Lower C loss processes by heterotrophic bacterial respiration and mineralization at elevated pCO_2 levels resulted in higher TPC and DOC pools compared to the ambient pCO_2 concentration. The difference in organic carbon at elevated pCO_2 levels remained fixed in the DOC pool as well as an increasing biomass of small-sized phytoplankton. Although there was an overall increase in community production, this did not stimulate heterotrophic bacterial metabolism or affect C export. **Our results suggest that during extended periods at low-nutrient concentrations increasing pCO_2 levels indirectly impact the growth balance of heterotrophic bacteria and shift the ecosystem to a more autotrophic system.**

Chapter 4 evaluates how potential OA-induced changes in bacterial biotransformation of DOM relate to qualitative changes in DOM. At this, it is important to differentiate between DOM reactivity fractions because DOM with short turnover times does not contribute significantly to oceanic carbon export, unless it aggregates to larger particles sinking to the bottom and being buried in the sediment (Hansell et al., 2009; Dittmar and Stubbins, 2014; Moran et al., 2016). Here, we specifically focussed on DOM that is transformed by microbes and accumulates on timescales of weeks or longer (i.e. semilabile DOM). Such semilabile DOM accounts for approximately one fifth of the global export production and describes an important transitional form to refractory carbon resisting further degradation and hence is stored for hundreds to thousands of years in the ocean's interior (Hansell et al., 2009; Hansell and Carlson, 2002; Ogawa and Tanoue, 2003; Dittmar and Stubbins, 2014). About 50% of the molecular formulae detected by Fourier-transform ion cyclotron resonance mass spectrometry (FT-ICR-MS) throughout the experiment correlated significantly in mass spectrometric signal intensity with cumulative BPP and were likely a product of microbial transformation. It has to be noted that not all DOM can be analysed by FT-ICR-MS due to

limitations of current extraction protocols (Dittmar et al., 2008), however, in particular a good coverage of semilabile and refractory compounds is warranted, whilst the method is limited in the detection of labile DOM compounds (e.g. small sugars, amino acids) (Mopper et al., 2007; Dittmar et al., 2008). Surprisingly, we observed similar succession patterns for individual compound pools during a phytoplankton bloom and subsequent accumulation of these compounds in mesocosm studies performed at different nutrient conditions irrespective of the pCO_2 treatment. **The similar dynamics in DOM production and transformation during and subsequent to a phytoplankton bloom reveal that OA-induced changes in the dynamics of bacterial DOM transformation are unlikely to impact DOM quality.** In addition, there have been no indications that in dependence of nutrient conditions, different amounts of photosynthetic organic matter are channelled into the more recalcitrant DOM pool via the microbial loop. This provides novel insights into the general dynamics of the marine DOM pool.

The results of **Chapters 2 to 4**, embedded within current knowledge on OA research, identify the following research directions where future research efforts should be invested.

6.1.1 Impact of OA on natural microbial communities - Drawing attention to low-nutrient conditions and food web interactions

The net productivity and carbon sequestration in the oceans are determined by a balance between autotrophic and heterotrophic processes. Both processes have been determined to be sensitive to OA, however, responses are variable across plankton communities and further modulated by specific environmental factors. A recent meta-analysis by Alvarez-Fernandez et al. (2018) reveals an overall increase in phytoplankton standing stock in response to OA by analysing potential OA-induced changes in natural plankton communities across various *in situ* mesocosm studies targeting OA effects. Thereby, the authors identified nutrient conditions as a particularly important factor for the reactions of plankton communities to OA. Depending on the inorganic nutrient availability, the effect on primary producers was channelled differently into heterotrophic consumers (Alvarez-Fernandez et al., 2018). In particular, at N-depleted conditions changes in bacterial biomass standing stocks evolved in response to OA, while bacterial abundances were not affected during N-replete periods (Alvarez-Fernandez et al., 2018). Although the authors explained the different responses to emerge from food web effects and particularly by the increase in small-sized phytoplankton, yet, specific mechanisms remain unresolved.

Nutrient modulated OA effects on the bacterial metabolism

Chapter 2 addresses specifically potential OA effects on the coupling of heterotrophic bacteria to phytoplankton during nutrient depleted periods. Bacteria-phytoplankton interactions are complex and change throughout the development of a phytoplankton bloom and associated nutrient conditions. At nutrient-replete conditions, phytoplankton exudates are rapidly used by planktonic bacteria (Iturriaga and Hoppe, 1977; Obernosterer

and Herndl, 1995) which often are able to take up inorganic nutrients more efficiently than phytoplankton (Azam et al., 1983). During periods of nutrient limitation, phytoplankton exudation of carbon would lead to an apparently paradoxical situation in which phytoplankton stimulate heterotrophic bacteria actively to support growth of phytoplankton via recycling of nutrients, but at the same time compete with phytoplankton for essential nutrients (Azam et al., 1983; Bratbak and Thingstad, 1985; Suttle et al., 1990; Drakare et al., 2003; Grossart and Simon, 2007; Buchan et al., 2014). Impacts of OA on physiology and growth balance of phytoplankton or heterotrophic organisms might particularly evolve during periods when such a strong nutrient-derived phytoplankton-bacteria relation is present. This will also impact the ratio between autotrophic and heterotrophic processes affecting net ecosystem productivity and C sequestration. In **Chapter 2**, this is indicated by a decrease in the ratio between heterotrophic bacterial biovolume and the concentration of Chl *a* (BV_{het}:Chl *a*) with increasing pCO_2 during post-bloom conditions. Further, it is affirmed by a C budget approach in **Chapter 3** that revealed an ecosystem shifts to a more autotrophic system under OA conditions when nutrients were depleted. An impact of OA on the bacterial growth balance was also observed by Motegi et al. (2013) during a CO_2 enrichment experiment in an Arctic fjord. Although this mesocosm study was performed with nutrient enrichment and no clear effects of pCO_2 on bacterial respiration, bacterial carbon demand (BCD) or bacterial growth efficiency (BGE) were reported, Motegi et al. (2013) observed an enhanced leucine to thymidine ratio with increasing pCO_2 at the end of the experiment when nutrient concentrations were low, suggesting that changes in pCO_2 potentially influenced bacterial production, growth rate and growth balance. Furthermore, two pelagic mesocosm experiments performed within the MedSeA project in the Mediterranean Sea at oligotrophic summer and mesotrophic winter conditions revealed nutrient modulated OA effects on the bacterial metabolism. A mean deviation approach highlighted negative relations of enzyme activities as well as bacterial carbon production to pCO_2 (Celussi et al., 2017). Such observations of negative impacts on the bacterial growth balance are also supported by metatranscriptome analyses showing differential gene expression patterns as a response to elevated pCO_2 (Bunse et al., 2016). Thereby, Bunse et al. (2016) report on an increase in genes encoding proton pumps with elevated pCO_2 including respiration complexes, proteorhodopsin and membrane transporters that might negatively impact on bacterial homeostasis. These responses were substantial for numerous pH homeostasis genes but only at low-chlorophyll conditions (Chl *a* < 2.5 µg L^{-1}) (Bunse et al., 2016). During our experiment in the Baltic Sea (**Chapter2**), Spilling et al. (2016a) reported on consistently lower community respiration rates in CO_2-enriched treatments with up to 40 % difference between controls and the highest pCO_2 treatment. The lower respiration rates agree with observations of Teira et al. (2012) studying two bacterial isolates belonging to *Rhodobacteriaceae* and *Flavobacteriaceae*. However, in their study pCO_2 did not negatively affect bacterial growth and further increased BGE. Other studies with natural plankton communities have pointed to no effect or increased respiration rates at elevated CO_2 concentration (Tanaka et al., 2013).

OA effects on heterotrophic bacteria-phytoplankton interactions

Although there are indications, that the physiology of heterotrophic bacteria might be affected directly by OA, the special food web relation between phytoplankton and heterotrophic bacteria when nutrients are low is likely to be the key to understand the different responses of heterotrophic bacteria to OA at nutrient replete versus depleted conditions. Both food web components may interact indirectly if the behaviour of one component modifies the environment and thus affects the behaviour of the other component. Low nutrient conditions benefit generally small-sized plankton, which, due to their high volume-to-surface ratio as well as a small boundary layer surrounding these cells, are favoured compared to larger cells in terms of resource acquisition (Raven, 1998; Moore et al., 2013). Thus, in a small-sized plankton community, phytoplankton and bacterioplankton might be restricted to comparable uptake kinetics in terms of nutrient acquisition. Here, physiological effects caused by OA on small-sized phytoplankton could increase autotrophy by releasing such phytoplankton from physiological constrains in carbon and nutrient uptake and featuring them to a superior nutrient competitor in a small-sized plankton community (Bach et al., 2017). Indeed, there is consistency in results from several OA experiments that suggest picoeukaryotes as winners in a future ocean (Brussaard et al., 2013; Bermúdez et al., 2016; Sala et al., 2016; Bach et al., 2017; Crawfurd et al., 2017; Schulz et al., 2017; Alvarez-Fernandez et al., 2018). In addition to advantages associated to the size-related difference in nutrient and carbon uptake across the cell and potentially positive OA effects on the carbon concentration mechanism, the photosynthetic activity that counteracts OA within the microenvironment surrounding phytoplankton cells could represent a mechanism that favour small-sized phytoplankton (e.g. Hendriks et al., 2010). Photosynthesis might deplete pCO_2 and raise pH within the boundary layer around phytoplankton cells, so that pH actually experienced by organisms may differ from that in the bulk water phase (Sand-Jensen et al., 1985; Kühl et al., 1995; Hendriks et al., 2010). In contrast, heterotrophic bacteria most likely respire carbon-rich compounds when nutrients are low that lead to an enhanced pCO_2 and a reduction of pH around the cells. Hence, the actual pH experienced within the boundary layer of organisms does not necessarily correspond to the pH that occurs in the bulk water phase, as pH within the boundary layer is strongly affected by the metabolism of organisms themselves (Hendriks et al., 2010). Biological processes, thus, can affect specific food-web components differently, providing homeostasis against changes in pH in bulk waters or even increasing the effects of OA on water chemistry expected during the 21st century.

Considerations for future experiments to assess nutrient modulated OA effects

Models that aim at predicting the impacts of OA on microbial processes have to extend beyond predictions of the pH in bulk waters to consider boundary layer effects and nutrient

uptake kinetics. Also, experiments have to address more specifically interactions between food web components, organism traits and species, as discussed above. Although results gained from single species experiments might not be transferable directly to natural plankton communities, where complex species interactions between autotrophic and heterotrophic processes across several trophic levels occur, more small-scale, targeted approaches on species interactions between bacteria and phytoplankton are needed to link species physiological traits to species interactions and their feedback with the environment. In the past, this was done primarily for interactions between different phytoplankton (Dutkiewicz et al., 2015). Results emphasize that the different responses to elevated pCO_2 caused sufficient changes in the competitive fitness between phytoplankton types to alter community structure significantly (Dutkiewicz et al., 2015). However, targeted experiments that disentangle physiological constraints of OA on the metabolism of heterotrophic bacteria or go even beyond the cellular level are scarce (e.g. Teira et al., 2012; Bunse et al., 2016) and should be promoted in the future. Only the incorporation of results from targeted, small-scale experiments can lead to a mechanism-based interpretation of large-scale experiments assessing whole plankton communities. Also, carbon and nutrient uptake representations in models should be more focused on individual plankton functional types and their interaction with heterotrophic bacteria with regard to OA effect and other environmental factors such as nutrient conditions (Silyakova et al., 2013). Thus, variability in stoichiometry and community production may be better understood if pCO_2 sensitivities of the plankton´s functional type in biogeochemical uptake kinetics and trophic interactions are better constrained (Silyakova et al., 2013). Also, the transfer of bacterial biomass to higher trophic levels and loss of bacterial biomass to viral lyses has to be better assessed under future ocean conditions. In particular, studies that address rates of bacterial grazing and viral lysis in response to OA are scarce (Larsen et al., 2008; Brussaard et al., 2013; Crawfurd et al., 2017; Tsiola et al., 2017). Here, animals including flagellates, ciliates and zooplankton, are known to select for high-quality food resources in proportions greater than would be predicted based on food quantity, suggesting that low-flux, high-quality subsidies may be selected that may disproportionately affect food web and ecosystem processes (Marcarelli et al., 2011). Thus, selective grazing might lead to adaptations in bacterial communities, e.g. increasing aggregation processes (Pernthaler et al., 1997; Jürgens et al., 1999). Also the role of viruses in transferring organic carbon from bacterial biomass back to the DOM pool via the lysis of cells is largely unknown. Particularly, host-virus relations between specific bacteria and viruses have to be disentangled in more detail (Larsen et al., 2008; Danovaro et al., 2011; Brum et al., 2015). Taken together, the results presented in this thesis instigate OA-related changes in heterotrophic bacteria´s physiology, affecting nutrient pools and the fluxes between them. How these changes balance out in multi-trophic communities and how these alterations impact nutrient reservoirs and carbon sequestration in a future ocean should be focus of ongoing research.

6.1.2 Impact of OA on natural microbial communities - Drawing attention to bacterial community composition

The results presented in **Chapters 2 to 4** do not report on changes in bacterial community composition (BCC) in response to OA. However, there are indications that BCC might be impacted by OA (Arnosti et al., 2011; Allgaier et al., 2008; Krause et al., 2012). Findings by Krause et al. (2012) suggest that already moderate pH changes have the potential to cause compositional shifts in BCC. In their experiment performed in the North Sea, bacteria susceptible to changes in pH consisted of different members of *Gammaproteobacteria*, *Flavobacteriaceae*, *Rhodobacteracea*, *Campylobacteracea* and further less abundant groups (Krause et al., 2012). Also Allgaier et al. (2008) reported on changes of BCC with pCO_2, but only for FL bacteria, whereas the dynamics of attached bacteria seemed to be independent of pCO_2 and tightly coupled to phytoplankton development. However, there are also studies that identified only weak, negligible or no impact of pCO_2 on BCC (Roy et al., 2013; Newbold et al., 2012; Oliver et al., 2014; Bergen et al., 2016) or assessed OA impacts in combination with other environmental factors, such as temperature (Lindh et al., 2013; Bergen et al., 2016). In order to advance our understanding of carbon and nutrient cycling of DOM in a future ocean, upcoming research should integrate the relationship between microbial community composition and DOM cycling to account for specific metabolic interactions between microorganisms and substrate compounds (Romano et al., 2014; Shabarova et al., 2014; Osterholz et al., 2016). Although we could not determine OA effects on bacterial biotransformation in **Chapter 4** by relating cumulative BPP to dynamics of DOM compounds, OA might impact specific bacterial groups and their metabolic capacity which in turn might influence specific organic matter degradation processes and DOM characteristics. In particular, studies that target metabolic processes at the subcellular level are needed (e.g. Bunse et al., 2016).

6.1.3 Impact of OA on natural microbial communities – Is there a tipping point?

In **Chapter 2**, our gradient design simulating different CO_2 concentrations extending from present to future conditions aimed specifically for revealing a threshold concentration beyond OA-induced changes propels a system to a new state. **Chapter 2** reveals a significant impact of OA on the correlation-based relation between different autotrophic phytoplankton and heterotrophic bacteria above about 820 µatm fCO_2. In most measured variables, the lowest OA treatment (ca. 500 µatm fCO_2) showed comparable dynamics and responses than the controls (ca. 360 µatm fCO_2), differing from the three highest CO_2-treatments above 820 µatm fCO_2. This indicates that plankton communities might be resistant to OA impacts up to a certain threshold. Unfortunately, three mesocosms failed during the experiment as a consequence of welding faults that captured a gradient of fCO_2 between 500 µatm and 820 µatm fCO_2. It is thus not possible to conclude on a more detailed

CO_2 concentration above impacts on plankton communities might be expected. However, this information is of utmost importance for policymakers, intergovernmental agreements and actions to reduce CO_2 emissions. Future research should thus focus on threshold concentrations to close this knowledge gap. Therefore, highly replicated gradient designs are needed to have sufficient statistical power.

6.2 Do summer storms impact bacterial dynamics in lakes?

There is increasing evidence that the influence of human-caused climate change would become sufficiently strong as to push certain weather events beyond the bounds of natural variability (Herring et al., 2018). This phenomenon was first assessed for heat events where the influence of climate change is most pronounced, however, also impacts on other weather patterns such as storm events are likely to occur (Herring et al., 2018). Therefore, it is just a matter of time until retrospective analysis will reveal a clear signal of climate change (Herring et al., 2018). It is of utmost importance to assess already now, how such storm events impact lake ecosystems. In combination with projections on future climate scenarios it is essential to evaluate to what challenges mankind will be faced if frequency and magnitude of storms might change in the future to maintain certain ecosystem services provided by lakes such as the provision of water quality, food security and recreational values.

Particularly in summer, lentic systems are impacted by storms due to disturbances of the stratified water column with its associated vertical physical-chemical gradients and patterns in organism distributions. The experiment, reported in **Chapter 5**, reproduced key physical, chemical and biological responses of a severe summer storm event in large-volume mesocosms (http://www.lake-lab.de/) based on observations of the summer storm `Otto´ hitting Lake Stechlin in July 2011 (Kasprzak et al., 2017; Giling et al., 2017a). The artificial mixing mimicked realistically the disruption of the existing water thermal stratification and extension of the upper mixed water layer within naturally observed bounds during storm events by about 5 m (Giling et al., 2017a). Although it has to be admitted, that mesocosms are limited in their horizontal dimensions and might not be capable to reproduce all physical mechanism associated with a storm event (e.g. internal seiches) (Kasprzak et al., 2017), they allow for realistic studies on specific mechanisms that are associated with storm events at the ecosystem level. Here, the experiment specifically aimed for revealing a mechanistic understanding how the entrainment of deep water into the mixed layer of a deep clear-water lake impacts vertical environmental gradients as well as the spatial distribution and temporal development of organisms up to six weeks after the artificial mixing event. The artificial mixing increased concentrations of dissolved nutrients and inorganic carbon as well as the availability of light in the mixed layer that stimulated phytoplankton development and whole lake ecosystem metabolism as reported by Giling et al. (2017a) and assessed by more detailed multivariate analyses of water physico-chemical variables in **Chapter 5**. As such, entrainment of deep water into the mixed layer was assessed to cause important and

predictable lake ecosystem consequences at the level of primary producers in deep clear-water lakes (Giling et al., 2017a).

In **Chapter 5**, I focus on the impact of mixing on heterotrophic bacterial metabolism as well as associated changes in bacterial abundance and community composition. To my knowledge, this has not been assessed in such a consistent manner for deep clear-water lakes before. Although several studies have already evaluated effects of episodic mixing events including storms, typhoons or hurricanes on bacterial processes and community dynamics, these studies, however, have mostly been performed in shallow or small lentic systems where resuspension of sediments or the input of terrestrial matter might decrease light penetration into the water column and changes in C availability for plankton organism causes different ecosystem responses compared to deep clear-water lakes (Jennings et al., 2012; de Eyto et al., 2016; Perga et al., 2018; Vidon et al., 2018). Recently, Perga et al. (2018) assessed the effect of storms associated with high turbidity input due to inorganic minerals from the watershed in the high-altitude Lake Muzelle. Notwithstanding their intensity, the storms did not trigger long-lasting consequences to the lake characteristics when light penetration into the lake was not modified, whereas storms decreased autotrophic production and increased heterotrophic processes for the rest of the open-water season when light penetration was reduced by an increase in turbidity input from the watershed (Perga et al., 2018). However, large volume, clear-water lakes have been shown to be internally regulated even after intense precipitation events (Rantakari and Kortelainen, 2005; Ojala et al., 2011; Vachon and del Giorgio, 2014). Here, heterotrophic processes are largely determined by the availability of autochthonous, phytoplankton-derived organic matter, which production has been found to be stimulated after natural as well as artificial storm events for this particular lake type (Jennings et al., 2012; Kasprzak et al., 2017; Giling et al., 2017a). **My results highlight effects on community assembly and heterotrophic bacterial metabolism that are associated to entrainment of deep water into the mixed water layer and assess consequences of an episodic disturbance event for the coupling between bacterial metabolism and autochthonous DOM production in large-volume, clear-water lakes.**

Mixing clearly affected bacterial community assembly as assessed by relative differences in abundance of specific bacterial OTUs and in α- and β-diversity measures across time. Mixing increased the bacterial richness in the mixed layer, most likely by introducing a deep water layer community. Although this short term response diminished rapidly within one week, mixing impacted community dynamics for about one month. About 6 weeks after the disturbance, all bacterial communities converged towards the non-treated control indicating a high degree of resilience. This agrees well with several previous studies examining the resilience of lake microbial communities to different types of disturbances including perturbations by typhoons (Jones et al., 2008), nutrient addition (Shade et al., 2011) or mixing as well as a whole-ecosystem manipulation by mixing (Shade et al., 2012b). For certain OTUs, however, a significant signal of mixing could still be detected after six

weeks, indicating potential consequences for long-term community assembly across seasons. Though, such speculative long-term impacts were not in the scope of this 42-days study, they might be focus of future research. Across the period of this study, changes in temperature, PAR and concentrations of dissolved nutrients associated to mixing caused direct responses in bacterial community assembly for about one week. Thereafter, mixing impacted indirectly bacterial communities due to a differential phytoplankton development and its associated consequences for nutrient dynamics and carbonate chemistry when compared to control mesocosms. **As such, entrainment of deep water into the mixed layer caused significant responses in the bacterial community development for a prolonged period during summer stratification.**

Artificial mixing strongly stimulated the development of filamentous cyanobacteria (mainly *Dolichospermum* sp.) that drove gross primary production (Giling et al., 2017a) and thus impacted heterotrophic bacterial metabolism and community assembly. Based on the analysis of sequencing data, the relative abundance of OTUs that could be assigned to *Dolichospermum* sp. increased and structured the PA BCC in all four mesocosms within one week after mixing. Irrespectively of the fact that only three mesocosms formed a bloom of *Dolichospermum* sp., our mixing treatments suggest that filamentous cyanobacteria might be favoured by disturbance events during summer thermal stratification, further exacerbating warming related increases in cyanobacterial blooms (Posch et al., 2012; Elliott, 2012; Paerl and Paul, 2012). Under stable stratified conditions the proliferation of cyanobacteria within the epilimnion is limited by the availability of nutrients. Within deep stratified lakes, the formation of a DCM reflects a balance between nutrient limitation in epilimnic waters and light limitation at greater depths. Summer storms disrupt this balance by redistributing large amounts of nutrients into the photic epilimnion where they can be assimilated rapidly into phytoplankton biomass (e.g. *Dolichospermum* sp.). This additional input of nutrients relaxes phytoplankton from nutrient limitation allowing for a much broader distribution of phytoplankton cells across the whole epilimnion. There self-shading may shift the system from nutrient towards light and hence carbon limitation. Under these conditions decomposition of the nutrient enriched POM selects for organisms with an increased propensity for complex carbohydrate utilisation, in this case *Betaproteobacteria* and *Verrucomicrobia* (Martinez-Garcia et al., 2012; Cardman et al., 2014; He et al., 2017). This was reflected in increased bacterial respiration rates resulting in a higher POC remineralization, presumably with consequences for gas fluxes between lake and atmosphere and deposition of nutrients and carbon to the sediments. In the long-term run, these shifts in nutrient content of the organic matter pool as well as heterotrophic bacteria with an increased propensity for remineralization of the more complex carbohydrate pools may likely increase eutrophication of these freshwater environments.

Our experimental data on mixing-induced responses of a deep, nutrient-poor lake are of utmost importance to realistically implement the natural variation of different lake types into global models predicting ecological consequences of global climate change. The

presented results highlight important features of such lakes and draw attention to large and intermediate-sized lakes that dominate the total lake surface area but are not well represented in current literature compared to small lakes, basically due to their low abundance (Verpoorter et al., 2014). In times of an increasing availability of satellite and high-resolution observatory data that allow for better predictions of environmental parameters, ecosystem-studies, as here reported, are needed to advance our knowledge on bacterial community assembly, metabolic processes and biotic interactions of heterotrophic bacteria with other components of the aquatic food web. This will allow us to better assess impacts of climate change on inland waters and their feedback mechanisms.

6.2.1 Impact of storms on natural microbial communities – Drawing attention to microbial community assembly

Ecological disturbances are hypothesized to alter the relative abundance distribution and diversity-productivity relationship by processes of selection, drift, speciation/diversification and dispersal (Vellend, 2010; Nemergut et al., 2013). Thereby, habitat filtering across environmental gradients changes the relative fitness of individual biological units (e.g. OTUs, phylogenetic groups, functional groups) that vary genetically and in expressed functional traits (Krause et al., 2014). Functional traits characterize morpho-physio-phenological characteristics which impact fitness indirectly via their effects on growth, reproduction and survival (Violle et al., 2007). Trait-based models are an emerging tool in ecology with the potential to link together species interactions, community dynamics, environmental responses, ecosystem processes and consequently ecosystem functioning (Violle et al., 2007; Allison, 2012). Whereas functional trait approaches are regularly used for higher organisms (e.g. in plant ecosystems), their application in microbial ecology is often restricted by an appropriate trait characterization of microbes and in particular heterotrophic bacteria (Krause et al., 2014). Here, the simulated summer storm disturbance imposed a strong selective pressure that reduced β-diversity of bacterial communities between mixed mesocosms, thus acting as a deterministic rather than a stochastic force that greatly influenced bacterial dynamics and functions. The combination of different traits including the capacity to store phosphorous in poly-phosphate granules (Klemke et al., 2014), the ability to fix nitrogen (Karlson et al., 2015; Klawonn et al., 2016) and to regulate buoyancy (Reynolds et al., 1987; Klemer et al., 1996) as well as mechanisms to resist grazing by herbivorous zooplankton (Lampert, 1987) likely caused the proliferation of filamentous cyanobacteria (i.e. *Dolichospermum* sp.) after the mixing disturbance. In this case, reasonable well constrained functional traits can be used for explaining *Dolichospermum* sp. development and ecosystem processes. However, in contrast to diazotrophic cyanobacteria or other autotrophic microbes, functional traits driving dynamics of most heterotrophic microbes are not well defined (Krause et al., 2014). Thus, future research should foster experimental approaches that specifically target the definition of functional traits of particular heterotrophic microbes (e.g. enzymatic capacities and genes involved in

degradation of particular compounds). In particular, a combination of eco-physiological studies with contemporary molecular tools in a trait-based framework could reinforce our ability to link microbial diversity to ecosystem processes (Krause et al., 2014). As such, eco-physiological traits of *Verrucomicrobia* could be inferred from metagenome-assembled genomes that identified their propensities for complex carbohydrate utilisation, ammonia uptake and survival at low-P conditions (He et al., 2017). These traits agree with the observations from **Chapter 5**, identifying *Verrucomicrobia* as one of the key mineralizers of cyanobacteria-derived organic matter. Irrespective of this particular exception, the majority of OTUs did not have a cultured representative, could not be assigned phylogenetically or did not allow for further trait characterization due to the lack of literature. Although the development of certain OTUs could be assigned by network analysis to particular abiotic and biotic variables, further physiological characterization and predictions were restricted by current phylogenetic resolution and trait characterization. However, such information is essential to understand abundance changes in biological units for better predicting how community changes affect ecosystem functions.

6.2.2 Impact of storms on natural microbial communities – Drawing attention to particle-associated processes and C-sequestration

Research during the past decades has demonstrated that the role of inland waters in C cycling is disproportionately more important than their surface area would suggest (Cole et al., 2007; Tranvik et al., 2009, 2018). Thus, impacts of climate change on inland waters have the potential to give significant climate feedbacks on a regional or even global scale. Although pristine and nutrient-poor lakes have been assumed to be less affected by climate change, our results in accordance with several other studies (Jennings et al., 2012; Kasprzak et al., 2017; Giling et al., 2017a) indicate that even nutrient-poor clear-water lake ecosystems bear the risk to face internal eutrophication and hence more pronounced phytoplankton blooms. Transformation and mineralization of phytoplankton biomass by heterotrophic bacteria might have a subsequent impact on C-sequestration and greenhouse gas exchange with the atmosphere.

Chapter 5 focuses on the mineralization of phytoplankton-derived organic matter by heterotrophic bacteria after an artificial mixing event and draws attention to bacterial mineralization processes on phytoplankton aggregates. Here, senescent cells of *Dolichospermum* sp. were identified as `hotspots´ of heterotrophic bacterial transformation and mineralization processes that affected not only PA but also FL bacterial communities and largely drove differences in BPP and BR between mixed and control mesocosms. Thereby, bacterial colonization appeared to be dependent on population dynamics and the physiological state of *Dolichospermum* sp. Highest PA bacterial abundances and activities were observed on senescent phytoplankton cells. A few studies that have reported high colonization on actively growing cells (e.g. Smith et al., 1995). However, we reported here the bacterial colonization of phytoplankton cells in the late course of the bloom cycle which

agrees with most studies examining bacterial colonization of phytoplankton in response to phytoplankton physiology and community structure (Middelboe et al., 1995; Riemann and Winding, 2001; Grossart et al., 2005; Mayali et al., 2011; Znachor et al., 2012; Bižić-Ionescu et al., 2014). My results indicate that potential physiological interactions among heterotrophic bacteria and cyanobacteria change over the course of the algal bloom cycle, suggesting temporal patterns of bacterial colonization that impact on processes of C transformation (**Fig. 4**).

Aggregates with their associated microorganisms largely contribute to the `biological carbon pump´ by transporting C to deep waters and the sediment (Alldredge and Silver, 1988; Grossart and Simon, 1998; Volkman and Tanoue, 2002). Thereby, the processes of aggregation, particle OM transformation and sedimentation are closely linked to interactions between phytoplankton and the associated microbial communities (Azam and Long, 2001; Simon et al., 2002). As such, the presence of PA bacteria has been reported to be a prerequisite for aggregation of certain phytoplankton species and can enhance aggregate formation by e.g. the production of TEP (Decho, 1990; Heissenberger and Herndl, 1994) or gluing single algal cells through bacterial micro-colonies (Grossart et al., 2006b). In contrast, aggregate breakdown by hydrolytic enzyme activity of heterotrophic bacteria may reduce the vertical flux of OM (Smith et al., 1992; Grossart and Ploug, 2001; Bižić-Ionescu et al., 2014). During this experiment, concentrations of TEP were not determined and thus it is not possible to draw conclusions on how PA bacteria influenced the phytoplankton aggregation process by microbial exopolymer formation. However, epifluorescence microscopy revealed huge numbers of PA bacteria that were associated to a microlayer surrounding cells of *Dolichospermum* sp. when disproportional high rates of epilimnic BR were observed (**Chapter 5**). These observations suggest an effective mineralization by complex heterotrophic bacterial networks on *Dolichospermum* sp. cells in the epilimnion that counteracts the sedimentation flux and potentially increased the flux of CO_2 at the water-atmosphere interface. In that context, filamentous cyanobacteria have been reported to create their own microenvironment with steep gradients of dissolved gases and substrates that might impact growth conditions of associated bacteria compared to the surrounding water (Eichner et al., 2017). In addition, features (e.g. buoyancy regulation, low content of ballast material (Klemer et al., 1996)) that prevent them from sinking through the water column render filamentous cyanobacteria susceptible to colonization, creating `hotspots´ of bacterial C transformation in the epilimnion. Interestingly, in our experiment, an increase and peak of *Bacillariophyceae* biomass was observed associated with the breakdown of filamentous cyanobacteria (Grossart et al., in prep.). This observation further suggests that *Bacillariophyceae* profited from heterotrophic bacterial transformation of cyanobacterial biomass and the release of DOM and CO_2 into the surrounding water. Although speculative, stimulation and death of *Bacillariophyceae* likely prolonged and controlled sedimentation following the bloom breakdown of the filamentous cyanobacteria, greatly impacting C sequestration in mixed mesocosms.

Future experimental approaches, thus, should consider more specifically causes and mechanisms that drive heterotrophic bacterial colonization on phytoplankton cells depending on phytoplankton species and their specific physiology (e.g. Yawata et al., 2014). Direct measurements of small-scale physical-chemical characteristics and biogeochemical processes associated with large phytoplankton, but also aggregates in general, are crucial in order to understand the overall role of PA heterotrophic bacteria in C transformation, C export and ecosystem respiration in aquatic systems (Datta et al., 2016). Since the overall C-sequestration and gas fluxes at the water-atmosphere interface are finally determined as a sum of all processes happening at different microhabitats within the aquatic continuum, the presented results should stimulate research that allows for a better resolution of spatial scales within the aquatic system.

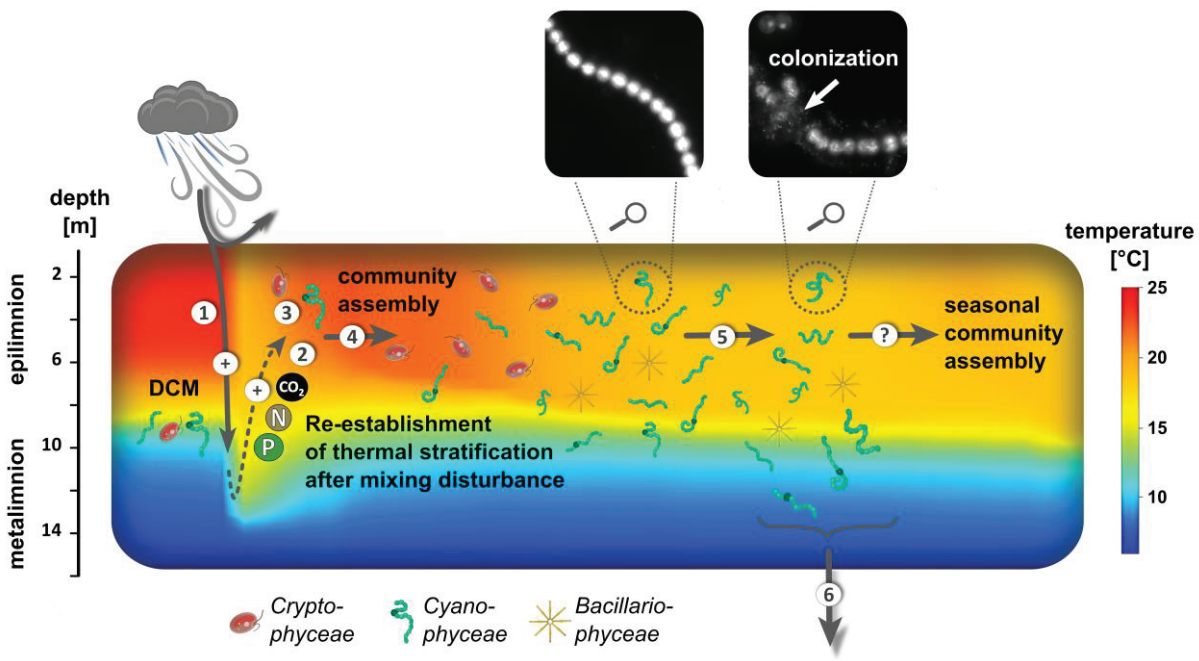

Figure 4: Conceptual graph summarizing the effects of a summer storm perturbation on stratified clear-water lake ecosystems. (1) Wind energy of summer storms perturbs the stable summer stratification, extending the mixed layer and deepening the thermocline. (2) Mixing introduces nutrient- (P, N, Si) and CO_2-rich water with (3) organisms from the metalimnion into the epilimnion. (4) The increase in nutrients, PAR and C-availability impacts plankton community assembly. Likely, organisms with a high P storage capacity and grazing resistance will be favoured (e.g. filamentous cyanobacteria such as *Dolichospermum* sp. and large diatoms) following the development of organisms with a high P and N scavenging potential. (5) Nutrient-limitation and self-shading of phytoplankton will restrict phytoplankton growth. Finally, colonization and mineralization of senescent phytoplankton cells by heterotrophic bacteria largely determines C-sequestration to the sediment (6).

6.3 Remarks and perspectives

6.3.1 Methodological considerations

Due to the complexity of natural ecosystems not all components within the aquatic food web or an elemental cycle can be monitored routinely to better assess impacts of changing environmental conditions (e.g. change in pH/pCO_2) on ecosystem processes. Thus, ecologists regularly monitor either single species, groups of organisms, biochemical pools or fluxes (i.e. biomasses or metabolic processes) and infer from observed differences in these parameters to impacts at the ecosystem level. Can we indeed infer from the measurement of a single pool or flux within a complex ecosystem that this particular pool or flux is impacted without taking into account the complexity of the whole ecosystem?

The following three examples highlight important C pools and fluxes in aquatic microbial ecology that interact dynamically with other biomass pools and metabolic processes within the aquatic food web. Their determination, however, is often impaired by certain methodological restrictions. One pool with a high turnover is bacterial biomass that might not alter significantly in size, although organic matter can be exchanged to a high extent between bacterial biomass and other components of the aquatic food web influencing the flow of chemical elements and energy within the ecosystem (**Fig. 5**) (e.g. Ducklow, 1983). In particular, grazing of bacterial biomass is often not assessed, thus, restricting an estimation of bacterial biomass turnover. Another pool, whose determination might be restricted to methodological considerations, is DOM. DOM usually has an operational definition as any material that passes through a glass fibre filter with a nominal pore size (e.g. GF/F or GF-75). We need to be aware that this methodological restriction does not exactly indicate the true `dissolved phase´ of organic matter. Lee et al. (1995) assessed that, for example, 22-38 % of the total bacterial biomass can pass through a filter with a nominal pore size of 0.7 µm causing problems in separation between pools of DOM and bacteria. Also, it is well established to separate between PA and FL bacterial communities and processes driving differential microbial processes on particles, including phytoplankton, and the surrounding water, based on a size-fractionation during water sample analysis. However, bacteria attach and detach continuously from particles and there is evolving consideration to question a strict separation between PA and FL bacteria (Grossart et al., 2003; Grossart and Tang, 2010; Grossart, 2010).

These examples highlight how challenging it can be to trace certain components within the aquatic food web and to account for interactions with other components, either methodologically or statistically (**Fig.5**). To account - at least partly - for trophic interactions and methodological uncertainties that could not be assessed in the present studies, primarily multivariate statistics had been used considering simultaneously multiple variables in one analysis and accounting for these uncertainties by the portion of unexplained variance. In addition to statistical considerations, however, also improvements

of the currently used methods are needed. The next step should be to extend size-fractionated approaches, which are to date the method of choice due to experimental and methodological limitations, from the level of bulk measurements to the scale of microenvironmental measurements for better tracing species-species and species-environment interactions (e.g. Stocker, 2012). This could either be performed by linking targeted small-scale laboratory experiments with field observations or using targeted single-cell/micro-environmental approaches during ecosystem-level and field experiments. In that context, recent developments in single-cell genomics (Walker and Parkhill, 2008; Kalisky and Quake, 2011), transcriptomics (Sandberg, 2014) and proteomics (Irish et al., 2006; Newman et al., 2006) as well as biogeochemical measurements (e.g. nanoscale secondary ion mass spectrometry (Nano-SIMS; Braun et al., 2018; Eichner et al., 2017) and *in situ* high-resolution measurements at the cell-level (e.g. *in situ* cameras; Taucher et al., 2018) are promising tools that should also be used more frequently to answer targeted research question in aquatic microbial ecology.

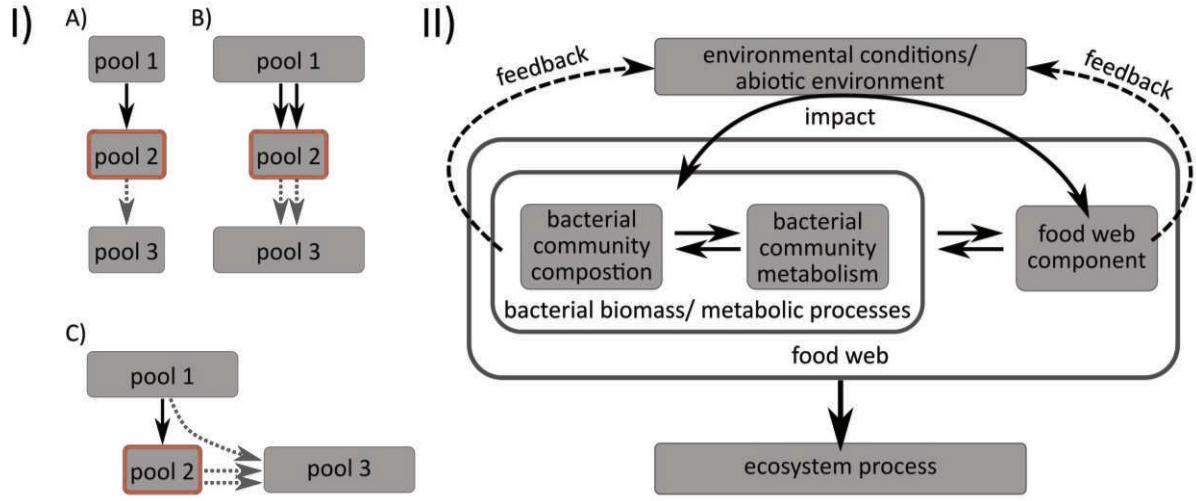

Figure 5: I) Conceptual graph summarizing the relationship between pool size and fluxes of any measured variable. Sizes of rectangles and arrows represent the corresponding sizes of pools and fluxes, respectively. Although the size of pool 2 remains equal in all three cases (A-C), the fluxes between pool 1, pool 2 and pool 3 (arrows) may be different. **II) Conceptual relationship between the abiotic environment, bacterial biomass and metabolic processes (e.g. bacterial production, respiration) as well as ecosystem processes (e.g. C-sequestration).** Bacterial biomass and metabolic processes interact with other biomass pools and metabolic processes in the aquatic food web. The sum of all processes and biomass components finally determines certain ecosystem processes and functions.

6.3.2 Need for experiments assessing multi-stressors

Humans impact ecosystems directly or indirectly in multiple ways along the aquatic continuum from terrestrial ecosystems and inland waters to the ocean (Vitousek, 1997;

Allan, 2004; Adrian et al., 2009; Hoegh-Guldberg and Bruno, 2010; Woodward et al., 2010; Bauer et al., 2013; Regnier et al., 2013; Reichstein et al., 2013). As such, anthropogenic changes in atmospheric GHG concentrations, food-production (e.g. overfishing), land-use patterns, freshwater use, nitrogen and phosphorus deposition or use of chemical pollutants (e.g. antibiotics, toxins, micro-plastics, etc.), just to name a few, might cause changes that perturb climate, biogeochemical cycles and biotic variables (Allan, 2004; Steffen et al., 2004; Heino et al., 2009; Rockström et al., 2009; Hoegh-Guldberg and Bruno, 2010; Steffen et al., 2015). Particularly, the increase in water temperature (Adrian et al., 2009; Hoegh-Guldberg and Bruno, 2010) and water-column stratification (Capotondi et al., 2012; Taucher et al., 2014), the impacts of eutrophication (Bennett et al., 2001; Flanagan et al., 2003), deoxygenation/hypoxia (Keeling et al., 2010; Conley et al., 2011; Rabalais et al., 2014) and invasive species (Stachowicz et al., 2002; Rahel and Olden, 2008; Heino et al., 2009) as well as the increase in terrestrial organic matter due to sea-level rise, permafrost melting or surface-runoff (Labat et al., 2004; Gedney et al., 2006; Vermeer and Rahmstorf, 2009; Schuur and Abbott, 2011; Schuur et al., 2015) may act in concert with OA and episodic weather-related disturbances. Thus, aquatic organisms are often exposed to several stressors simultaneouslly. While ecological research documents regularly the individual effect of one of these various stressors on species and ecosystems, research on the cumulative and interactive impacts of multiple stressors is less frequent (Crain et al., 2008). However, cumulative effects might act in an additive, synergistic or antagonistic manner (Folt et al., 1999; Coors and De Meester, 2008; Crain et al., 2008). To reduce uncertainties in climate-change projections, thus, ecosystem-manipulation studies have to address also the interactions of multiple ecosystem stressors (Gruber and Galloway, 2008). In addition to an understanding of how stressors and in particular multi-stressor interactions will affect populations, we also require a better understanding of how species might respond via acclimation and adaptive evolutionary processes (Sunday et al., 2014; Schlüter et al., 2016; Monroe et al., 2018; Tong et al., 2018).

6.4 Epilogue

With the Paris Agreement of the 21st UNFCCC Conference of Parties (COP21), a historic climatic agreement was reached in 2015 after some 20 years of negotiations (UNFCCC, 2015; Schellnhuber et al., 2016). The Paris Agreement aims to "[…] holding the increase in the global average temperature to well below 2 °C above pre-industrial levels and to pursue efforts to limit the temperature increase to 1.5 °C above pre-industrial levels […]" (UNFCCC, 2015). If the current mitigation efforts and future commitments are adequate to accomplish the goals of the Agreement is still under debate (Williamson, 2016; Rogelj et al., 2017; Millar et al., 2017; Lawrence et al., 2018). Especially, the withdrawal of the United States of America (USA) from the Paris Agreement in June 2017 as one of the most important industrial nations and second largest producer of GHG emissions in the world (Janssens-Maenhout et al., 2017) makes it hard to reach the goals of the Agreement. However, climate

change is clearly an intergenerational problem and major political, societal and economic decisions need to be undertaken urgently to make provisions for the needs of successor generations (Hansen et al., 2013; Wunsch et al., 2013). Therefore, it is the task of the scientific community to assess risks for ecosystems and their provided services, to evaluate and forecast climate-relevant feedbacks and to give possible solutions for preventing climate change.

VI. List of References

Adrian R, O'Reilly CM, Zagarese H, Baines SB, Hessen DO, Keller W, et al. (2009). Lakes as sentinels of climate change. *Limnol Oceanogr* **54**: 2283–2297.

Aeschbach-Hertig W, Holzner CP, Hofer M, Simona M, Barbieri A, Kipfer R. (2007). A time series of environmental tracer data from deep meromictic Lake Lugano, Switzerland. *Limnol Oceanogr* **52**: 257–273.

Allan JD. (2004). Landscapes and Riverscapes: The Influence of Land Use on Stream Ecosystems. *Annu Rev Ecol Evol Syst* **35**: 257–284.

Alldredge AL, Silver MW. (1988). Characteristics, Dynamics and Significance of Marine Snow. *Prog Oceanogr* **20**: 41–82.

Allgaier M, Grossart H. (2006). Seasonal dynamics and phylogenetic diversity of free-living and particle-associated bacterial communities in four lakes in northeastern Germany. *Aquat Microb Ecol* **45**: 115–128.

Allgaier M, Riebesell U, Vogt M, Thyrhaug R, Grossart H-P. (2008). Coupling of heterotrophic bacteria to phytoplankton bloom development at different pCO_2 levels: a mesocosm study. *Biogeosciences* **5**: 1007–1022.

Allison SD. (2012). A trait-based approach for modelling microbial litter decomposition. *Ecol Lett* **15**: 1058–1070.

Allison SD, Martiny JBH. (2008). Resistance, resilience, and redundancy in microbial communities. *Proc Natl Acad Sci* **105**: 11512–11519.

Alvarez-Fernandez S, Bach LT, Taucher J, Riebesell U, Sommer U, Aberle N, et al. (2018). Plankton responses to ocean acidification: The role of nutrient limitation. *Prog Oceanogr* **165**: 11–18.

Amon RMW, Benner R. (1994). Rapid cycling of high-molecular-weight dissolved organic matter in the ocean. *Nature* **369**: 549–552.

Arnosti C. (2011). Microbial Extracellular Enzymes and the Marine Carbon Cycle. *Ann Rev Mar Sci* **3**: 401–425.

Arnosti C, Grossart H, Mühling M, Joint I, Passow U. (2011). Dynamics of extracellular enzyme activities in seawater under changed atmospheric pCO_2: a mesocosm investigation. *Aquat Microb Ecol* **64**: 285–298.

Arvola L, Järvinen M, Hakala I. (2006). Nutrient export from small boreal catchment areas: the influence of annual and seasonal hydrology. *SIL Proceedings, 1922-2010* **29**: 2031–2034.

Attermeyer K, Hornick T, Kayler ZE, Bahr A, Zwirnmann E, Grossart H-P, et al. (2014). Enhanced bacterial decomposition with increasing addition of autochthonous to allochthonous carbon without any effect on bacterial community composition. *Biogeosciences* **11**: 1479–1489.

Azam F. (1998). Microbial Control of Oceanic Carbon Flux: The Plot Thickens. *Science* **280**: 694–696.

Azam F, Fenchel T, Field J, Gray J, Meyer-Reil L, Thingstad F. (1983). The Ecological Role of Water-Column Microbes in the Sea. *Mar Ecol Prog Ser* **10**: 257–263.

Azam F, Long RA. (2001). Sea snow microcosms. *Nature* **414**: 495–498.

Azam F, Malfatti F. (2007). Microbial structuring of marine ecosystems. *Nat Rev Microbiol* **5**: 782–791.

Bach LT, Riebesell U, Schulz KG. (2011). Distinguishing between the effects of ocean acidification and ocean carbonation in the coccolithophore Emiliania huxleyi. *Limnol Oceanogr* **56**: 2040–2050.

Bach LT, Mackinder LCM, Schulz KG, Wheeler G, Schroeder DC, Brownlee C, et al. (2013). Dissecting the impact of CO_2 and pH on the mechanisms of photosynthesis and calcification in the coccolithophore *Emiliania huxleyi*. *New Phytol* **199**: 121–134.

Bach LT, Taucher J, Boxhammer T, Ludwig A, Achterberg EP, Algueró-Muñiz M, et al. (2016). Influence of Ocean Acidification on a Natural Winter-to-Summer Plankton Succession: First Insights from a Long-Term Mesocosm Study Draw Attention to Periods of Low Nutrient Concentrations. *PLoS One* **11**: e0159068, doi:10.1371/journal.pone.0159068.

Bach LT, Alvarez-Fernandez S, Hornick T, Stuhr A, Riebesell U. (2017). Simulated ocean acidification reveals winners and losers in coastal phytoplankton. *PLoS One* **12**: e0188198, doi:10.1371/journal.pone.0188198.

Banse K. (1995). Zooplankton: Pivotal role in the control of ocean production. *ICES J Mar Sci* **52**: 265–277.

Bastviken D, Cole J, Pace M, Tranvik L. (2004). Methane emissions from lakes: Dependence of lake characteristics, two regional assessments, and a global estimate. *Global Biogeochem Cycles* **18**: GB4009, doi:10.1029/2004GB002238.

Bastviken D, Tranvik LJ, Downing JA, Crill PM, Enrich-Prast A. (2011). Freshwater Methane Emissions Offset the Continental Carbon Sink. *Science* **331**: 50–50.

Battin TJ, Kaplan LA, Findlay S, Hopkinson CS, Marti E, Packman AI, et al. (2008). Biophysical controls on organic carbon fluxes in fluvial networks. *Nat Geosci* **1**: 95–100.

Battin TJ, Luyssaert S, Kaplan LA, Aufdenkampe AK, Richter A, Tranvik LJ. (2009). The boundless carbon cycle. *Nat Geosci* **2**: 598–600.

Battoe LE. (1985). Changes in Vertical Phytoplankton Distribution in Response to Natural Disturbances in a Temperate and a Subtropical Lake. *J Freshw Ecol* **3**: 167–174.

Bauer JE, Cai W-J, Raymond PA, Bianchi TS, Hopkinson CS, Regnier PAG. (2013). The changing carbon cycle of the coastal ocean. *Nature* **504**: 61–70.

Bennett EM, Carpenter SR, Caraco NF. (2001). Human Impact on Erodable Phosphorus and Eutrophication: A Global Perspective. *Bioscience* **51**: 227.

Bergen B, Endres S, Engel A, Zark M, Dittmar T, Sommer U, et al. (2016). Acidification and warming affect prominent bacteria in two seasonal phytoplankton bloom mesocosms. *Environ Microbiol* **18**: 4579–4595.

Berggren M, Laudon H, Jonsson A, Jansson M. (2010). Nutrient Constraints on Metabolism Affect the Temperature Regulation of Aquatic Bacterial Growth Efficiency. *Microb Ecol* **60**: 894–902.

Bermúdez JR, Riebesell U, Larsen A, Winder M. (2016). Ocean acidification reduces transfer

of essential biomolecules in a natural plankton community. *Sci Rep* **6**: 27749, doi:10.1038/srep27749.

Biddanda, BA. (2017). Global significance of the changing freshwater carbon cycle. *Eos* 98, https://doi.org/10.1029/2017EO069751. Published on 21 March 2017.

Biddanda B, Benner R. (1997). Carbon, nitrogen, and carbohydrate fluxes during the production of particulate and dissolved organic matter by marine phytoplankton. *Limnol Oceanogr* **42**: 506–518.

Bižić-Ionescu M, Amann R, Grossart H-P. (2014). Massive Regime Shifts and High Activity of Heterotrophic Bacteria in an Ice-Covered Lake. *PLoS One* **9**: e113611, doi:10.1371/journal.pone.0113611.

Bjørnsen PK. (1988). Phytoplankton exudation of organic matter: Why do healthy cells do it? *Limnol Oceanogr* **33**: 151–154.

Blottière L, Jaffar-Bandjee M, Jacquet S, Millot A, Hulot FD. (2017). Effects of mixing on the pelagic food web in shallow lakes. *Freshw Biol* **62**: 161–177.

Bosselmann S, Riemann B. (1986). Zooplankton. In: Riemann B, Sndergaard M (eds). *Carbon Dynamics in eutrophic, temperate Lakes*. Elsevier: New York, USA, pp. 199–236.

Boxhammer T, Bach LT, Czerny J, Riebesell U. (2016). Technical note: Sampling and processing of mesocosm sediment trap material for quantitative biogeochemical analysis. *Biogeosciences* **13**: 2849–2858.

Boxhammer T, Taucher J, Bach LT, Achterberg EP, Algueró-Muñiz M, Bellworthy J, et al. (2018). Enhanced transfer of organic matter to higher trophic levels caused by ocean acidification and its implications for export production: A mass balance approach. *PLoS One* **13**: e0197502, doi:10.1371/journal.pone.0197502.

Bratbak G, Thingstad T. (1985). Phytoplankton-bacteria interactions: an apparant paradox? Analysis of a model system with both competition and commensalism. *Mar Ecol Prog Ser* **25**: 23–30.

Braun PD, Schulz-Vogt HN, Vogts A, Nausch M. (2018). Differences in the accumulation of phosphorus between vegetative cells and heterocysts in the cyanobacterium *Nodularia spumigena*. *Sci Rep* **8**: 6–11.

Brum JR, Ignacio-Espinoza JC, Roux S, Doulcier G, Acinas SG, Alberti A, et al. (2015). Patterns and ecological drivers of ocean viral communities. *Science* **348**: 1261498, doi:10.1126/science.1261498.

Brussaard CPD, Noordeloos AAM, Witte H, Collenteur MCJ, Schulz K, Ludwig A, et al. (2013). Arctic microbial community dynamics influenced by elevated CO_2 levels. *Biogeosciences* **10**: 719–731.

Buchan A, LeCleir GR, Gulvik CA, González JM. (2014). Master recyclers: features and functions of bacteria associated with phytoplankton blooms. *Nat Rev Microbiol* **12**: 686–698.

Bunse C, Lundin D, Karlsson CMG, Akram N, Vila-Costa M, Palovaara J, et al. (2016). Response of marine bacterioplankton pH homeostasis gene expression to elevated CO_2. *Nat Clim Chang* **6**: 483–487.

Caldeira K, Wickett ME. (2005). Ocean model predictions of chemistry changes from

carbon dioxide emissions to the atmosphere and ocean. *J Geophys Res* **110**: 1–12.

Cantin A, Beisner BE, Gunn JM, Prairie YT, Winter JG. (2011). Effects of thermocline deepening on lake plankton communities. *Can J Fish Aquat Sci* **68**: 260–276.

Capotondi A, Alexander MA, Bond NA, Curchitser EN, Scott JD. (2012). Enhanced upper ocean stratification with climate change in the CMIP3 models. *J Geophys Res* **117**: C04031, doi:10.1029/2011JC007409.

Cardman Z, Arnosti C, Durbin A, Ziervogel K, Cox C, Steen AD, et al. (2014). *Verrucomicrobia* are candidates for polysaccharide-degrading bacterioplankton in an Arctic fjord of Svalbard. *Appl Environ Microbiol* **80**: 3749–3756.

Carlson AC. (2002). Production and removal processes. In: Hansell DA, Carlson CA (eds). *Biogeochemistry of Marine Dissolved Organic Matter*. Academic Press: Boston, MA, USA.

Carlson C, del Giorgio P, Herndl G. (2007). Microbes and the Dissipation of Energy and Respiration: From Cells to Ecosystems. *Oceanography* **20**: 89–100.

Carpenter SR, Cole JJ, Kitchell JF, Pace ML. (1998). Impact of dissolved organic carbon, phosphorus, and grazing on plankton biomass and production in experimental lakes. *Limnol Oceanogr* **43**: 73–80.

Carpenter SR, Cole JJ, Pace ML, Van de Bogert M, Bade DL, Bastviken D, et al. (2005). Ecosystem Subsidies: Terrestrial Support of Aquatic Food Webs from ^{13}C Addition to Contrasting Lakes. *Ecology* **86**: 2737–2750.

Cauwet G. (1978). Organic chemistry of sea water particulates. Concepts and developments. *Ocean Acta* **1**: 99–105.

Celussi M, Malfatti F, Annalisa F, Gazeau F, Giannakourou A, Pitta P, et al. (2017). Ocean acidification effect on prokaryotic metabolism tested in two diverse trophic regimes in the Mediterranean Sea. *Estuar Coast Shelf Sci* **186**: 125–138.

Chrost R, Riemann B. (1994). Storm-stimulated enzymatic decomposition of organic matter in benthic/pelagic coastal mesocosms. *Mar Ecol Prog Ser* **108**: 185–192.

Ciais P, Sabine C, Bala G, Bopp L, Brovkin V, Canadell J, et al. (2013). Carbon and Other Biogeochemical Cycles. In: Stocker TF, Qin D, Plattner G-K, Tignor M, Allen SK, Boschung J, Nauels A, Xia Y, Bex V and Midgley PM (eds). *Climate Change 2013: The Physical Science Basis. Contribution of Working Group I to the Fifth Assessment Report of the Intergovernmental Panel on Climate Change*. Cambridge University Press: Cambridge, United Kingdom and New York, NY, USA, pp. 465-570, doi:10.1017/CBO9781107415324.015.

Cole J, Findlay S, Pace M. (1988). Bacterial production in fresh and saltwater ecosystems: a cross-system overview. *Mar Ecol Prog Ser* **43**: 1–10.

Cole JJ, Pace ML, Carpenter SR, Kitchell JF. (2000). Persistence of net heterotrophy in lakes during nutrient addition and food web manipulations. *Limnol Oceanogr* **45**: 1718–1730.

Cole JJ, Prairie YT, Caraco NF, McDowell WH, Tranvik LJ, Striegl RG, et al. (2007). Plumbing the Global Carbon Cycle: Integrating Inland Waters into the Terrestrial Carbon Budget. *Ecosystems* **10**: 172–185.

Collins M, Knutti R, Arblaster J, Dufresne J-L, Fichefet T, Friedlingstein P, et al. (2013): Long-

term Climate Change: Projections, Commitments and Irreversibility. In: Stocker TF, Qin D, Plattner G-K, Tignor M, Allen SK, Boschung J, Nauels A, Xia Y, Bex V and Midgley PM (eds). *Climate Change 2013: The Physical Science Basis. Contribution of Working Group I to the Fifth Assessment Report of the Intergovernmental Panel on Climate Change*. Cambridge University Press: Cambridge, United Kingdom and New York, NY, USA, pp. 1029–1136, doi:10.1017/CBO9781107415324.024.

Conley DJ, Carstensen J, Aigars J, Axe P, Bonsdorff E, Eremina T, et al. (2011). Hypoxia Is Increasing in the Coastal Zone of the Baltic Sea. *Environ Sci Technol* **45**: 6777–6783.

Coors A, De Meester L. (2008). Synergistic, antagonistic and additive effects of multiple stressors: predation threat, parasitism and pesticide exposure in Daphnia magna. *J Appl Ecol* **45**: 1820–1828.

Coumou D, Rahmstorf S. (2012). A decade of weather extremes. *Nat Clim Chang* **2**: 491–496.

Covert J, Moran M. (2001). Molecular characterization of estuarine bacterial communities that use high- and low-molecular weight fractions of dissolved organic carbon. *Aquat Microb Ecol* **25**: 127–139.

Crain CM, Kroeker K, Halpern BS. (2008). Interactive and cumulative effects of multiple human stressors in marine systems. *Ecol Lett* **11**: 1304–1315.

Crawfurd KJ, Alvarez-Fernandez S, Mojica KDA, Riebesell U, Brussaard CPD. (2017). Alterations in microbial community composition with increasing fCO_2: a mesocosm study in the eastern Baltic Sea. *Biogeosciences* **14**: 3831–3849.

Crutzen PJ. (2002). Geology of mankind. *Nature* **415**: 23–23.

Czerny J, Schulz KG, Boxhammer T, Bellerby RGJ, Büdenbender J, Engel A, et al. (2013a). Implications of elevated CO_2 on pelagic carbon fluxes in an Arctic mesocosm study – an elemental mass balance approach. *Biogeosciences* **10**: 3109–3125.

Czerny J, Schulz KG, Krug SA, Ludwig A, Riebesell U. (2013b). Technical Note: The determination of enclosed water volume in large flexible-wall mesocosms 'KOSMOS'. *Biogeosciences* **10**: 1937–1941.

Czerny J, Schulz KG, Ludwig A, Riebesell U. (2013c). Technical Note: A simple method for air–sea gas exchange measurements in mesocosms and its application in carbon budgeting. *Biogeosciences* **10**: 1379–1390.

Danovaro R, Corinaldesi C, Dell'Anno A, Fuhrman JA, Middelburg JJ, Noble RT, et al. (2011). Marine viruses and global climate change. *FEMS Microbiol Rev* **35**: 993–1034.

Datta MS, Sliwerska E, Gore J, Polz MF, Cordero OX. (2016). Microbial interactions lead to rapid micro-scale successions on model marine particles. *Nat Commun* **7**: 11965, doi:10.1038/ncomms11965.

Dean WE, Gorham E. (1998). Magnitude and significance of carbon burial in lakes, reservoirs, and peatlands. *Geology* **26**: 535–538.

Decho A. (1990). Microbial exopolymer secretions in ocean environments: Their role(s) in food webs and marine processes. *Ocean Mar Biol Annu Rev* **28**: 73–153.

de Eyto E, Jennings E, Ryder E, Sparber K, Dillane M, Dalton C, et al. (2016). Response of a humic lake ecosystem to an extreme precipitation event: physical, chemical, and biological implications. *Inl Waters* **6**: 483–498.

de Kluijver A, Soetaert K, Schulz KG, Riebesell U, Bellerby RGJ, Middelburg JJ. (2010). Phytoplankton-bacteria coupling under elevated CO_2 levels: a stable isotope labelling study. *Biogeosciences* **7**: 3783–3797.

De La Rocha CL, Passow U. (2007). Factors influencing the sinking of POC and the efficiency of the biological carbon pump. *Deep Sea Res Part II* **54**: 639–658.

del Giorgio PA, Cole JJ. (1998). Bacterial Growth Efficiency In Natural Aquatic Systems. *Annu Rev Ecol Syst* **29**: 503–541.

Diehl S. (2002). Phytoplankton, Light, and Nutrients in a Gradient of Mixing Depths: Theory. *Ecology* **83**: 386–398.

Dittmar T, Koch B, Hertkorn N, Kattner G. (2008). A simple and efficient method for the solid-phase extraction of dissolved organic matter (SPE-DOM) from seawater. *Limnol Oceanogr Methods* **6**: 230–235.

Dittmar T, Stubbins A. (2014). Dissolved Organic Matter in Aquatic Systems. In: Birrer B, Falkowski P, Freeman K (eds) *Treatise on Geochemistry*. 2nd edition, Volume 12, Elsevier, pp. 125–156.

Doney SC, Fabry VJ, Feely RA, Kleypas JA. (2009). Ocean Acidification: The Other CO_2 Problem. *Ann Rev Mar Sci* **1**: 169–192.

Drakare S, Blomqvist P, Bergström A-K, Jansson M. (2003). Relationships between picophytoplankton and environmental variables in lakes along a gradient of water colour and nutrient content. *Freshw Biol* **48**: 729–740.

Druffel ERM, Williams PM, Bauer JE, Ertel JR. (1992). Cycling of dissolved and particulate organic matter in the open ocean. *J Geophys Res* **97**: 15639, doi:10.1029/92JC01511.

Ducklow H. (2008). Microbial services: challenges for microbial ecologists in a changing world. *Aquat Microb Ecol* **53**: 13–19.

Ducklow HW. (1983). Production and Fate of Bacteria in the Oceans. *Bioscience* **33**: 494–501.

Ducklow HW, Carlson CA. (1992). Oceanic Bacterial Production. In: Marshall KC (ed). *Advances in Microbial Ecology*. Springer: Boston, MA, USA, pp. 113–181.

Ducklow HW, Kirchman DL, Quinby HL, Carlson CA, Dam HG. (1993). Stocks and dynamics of bacterioplankton carbon during the spring bloom in the eastern North Atlantic Ocean. *Deep-Sea Res Part II* **40**: 245–263.

Dutkiewicz S, Morris JJ, Follows MJ, Scott J, Levitan O, Dyhrman ST, et al. (2015). Impact of ocean acidification on the structure of future phytoplankton communities. *Nat Clim Chang* **5**: 1002–1006.

Easterling DR. (2000). Climate Extremes: Observations, Modeling, and Impacts. *Science* **289**: 2068–2074.

Egge JK, Thingstad TF, Larsen A, Engel A, Wohlers J, Bellerby RGJ, et al. (2009). Primary production during nutrient-induced blooms at elevated CO_2 concentrations. *Biogeosciences* **6**: 877–885.

Eichner M, Rost B, Kranz SA. (2014). Diversity of ocean acidification effects on marine N2 fixers. *J Exp Mar Bio Ecol* **457**: 199–207.

Eichner MJ, Klawonn I, Wilson ST, Littmann S, Whitehouse MJ, Church MJ, et al. (2017).

Chemical microenvironments and single-cell carbon and nitrogen uptake in field-collected colonies of Trichodesmium under different pCO_2. *ISME J* **11**: 1305–1317.

Elliott JA. (2012). Is the future blue-green? A review of the current model predictions of how climate change could affect pelagic freshwater cyanobacteria. *Water Res* **46**: 1364–1371.

Endres S, Galgani L, Riebesell U, Schulz K-G, Engel A. (2014). Stimulated Bacterial Growth under Elevated pCO_2: Results from an Off-Shore Mesocosm Study. *PLoS One* **9**: e99228, doi:10.1371/journal.pone.0099228.

Engel A. (2002). Direct relationship between CO_2 uptake and transparent exopolymer particles production in natural phytoplankton. *J Plankton Res* **24**: 49–53.

Engel A, Borchard C, Piontek J, Schulz KG, Riebesell U, Bellerby R. (2013). CO_2 increases ^{14}C primary production in an Arctic plankton community. *Biogeosciences* **10**: 1291–1308.

Engel A, Delille B, Jacquet S, Riebesell U, Rochelle-Newall E, Terbrüggen A, et al. (2004). Transparent exopolymer particles and dissolved organic carbon production by Emiliania huxleyi exposed to different CO_2 concentrations: a mesocosm experiment. *Aquat Microb Ecol* **34**: 93–104.

Engel A, Zondervan I, Aerts K, Beaufort L, Benthien A, Chou L, et al. (2005). Testing the direct effect of CO_2 concentration on a bloom of the coccolithophorid *Emiliania huxleyi* in mesocosm experiments. *Limnol Oceanogr* **50**: 493–507.

Evans MR. (2012). Modelling ecological systems in a changing world. *Philos Trans R Soc B* **367**: 181–190.

Fabry VJ, Seibel BA, Feely RA, Orr JC. (2008). Impacts of ocean acidification on marine fauna and ecosystem processes. *ICES J Mar Sci* **65**: 414–432.

Falkowski P. (2000). The Global Carbon Cycle: A Test of Our Knowledge of Earth as a System. *Science* **290**: 291–296.

Falkowski PG, Raven JA. (2007). Aquatic photosynthesis. Princeton University Press: Princeton, NJ, USA.

Fee EJ. (1976). The vertical and seasonal distribution of chlorophyll in lakes of the Experimental Lakes Area, northwestern Ontario: Implications for primary production estimates. *Limnol Oceanogr* **21**: 767–783.

Field CB. (1998). Primary Production of the Biosphere: Integrating Terrestrial and Oceanic Components. *Science* **281**: 237–240.

Flanagan KM, McCauley E, Wrona F, Prowse T. (2003). Climate change: the potential for latitudinal effects on algal biomass in aquatic ecosystems. *Can J Fish Aquat Sci* **60**: 635–639.

Fogg GE. (1983). The Ecological Significance of Extracellular Products of Phytoplankton Photosynthesis. *Bot Mar* **26**: 3–14.

Folt CL, Chen CY, Moore M V., Burnaford J. (1999). Synergism and antagonism among multiple stressors. *Limnol Oceanogr* **44**: 864–877.

Fuhrman J, Suttle C. (1993). Viruses in Marine Planktonic Systems. *Oceanography* **6**: 51–63.

Fuhrman JA. (1999). Marine viruses and their biogeochemical and ecological effects. *Nature* **399**: 541–548.

Gedney N, Cox PM, Betts RA, Boucher O, Huntingford C, Stott PA. (2006). Detection of a direct carbon dioxide effect in continental river runoff records. *Nature* **439**: 835–838.

Gervais F, Padisák J, Koschel R. (1997). Do light quality and low nutrient concentration favour picocyanobacteria below the thermocline of the oligotrophic Lake Stechlin? *J Plankton Res* **19**: 771–781.

Giling DP, Nejstgaard JC, Berger SA, Grossart H-P, Kirillin G, Penske A, et al. (2017a). Thermocline deepening boosts ecosystem metabolism: evidence from a large-scale lake enclosure experiment simulating a summer storm. *Glob Chang Biol* **23**: 1448–1462.

Giling DP, Staehr PA, Grossart HP, Andersen MR, Boehrer B, Escot C, et al. (2017b). Delving deeper: Metabolic processes in the metalimnion of stratified lakes. *Limnol Oceanogr* **62**: 1288–1306.

Glasby TM, Underwood AJ. (1996). Sampling to differentiate between pulse and press perturbations. *Environ Monit Assess* **42**: 241–252.

Gobler CJ, Hutchins DA, Fisher NS, Cosper EM, Saňudo-Wilhelmy SA. (1997). Release and bioavailability of C, N, P Se, and Fe following viral lysis of a marine chrysophyte. *Limnol Oceanogr* **42**: 1492–1504.

Gogou A, Repeta DJ. (2010). Particulate-dissolved transformations as a sink for semi-labile dissolved organic matter: Chemical characterization of high molecular weight dissolved and surface-active organic matter in seawater and in diatom cultures. *Mar Chem* **121**: 215–223.

Goldman CR, Kumagai M, Robarts RD (eds). (2012). Climatic Change and Global Warming of Inland Waters: Impacts and Mitigation for Ecosystems and Societies. John Wiley & Sons, Ltd: Chichester, UK, pp. 472.

Gorham E, Boyce FM. (1989). Influence of Lake Surface Area and Depth Upon Thermal Stratification and the Depth of the Summer Thermocline. *J Great Lakes Res* **15**: 233–245.

Graham EB, Knelman JE, Schindlbacher A, Siciliano S, Breulmann M, Yannarell A, et al. (2016). Microbes as Engines of Ecosystem Function: When Does Community Structure Enhance Predictions of Ecosystem Processes? *Front Microbiol* **7**: 1–10.

Grossart H-P. (2010). Ecological consequences of bacterioplankton lifestyles: changes in concepts are needed. *Environ Microbiol Rep* **2**: 706–714.

Grossart H, Simon M. (1998). Significance of limnetic organic aggregates (lake snow) for the sinking flux of particulate organic matter in a large lake. *Aquat Microb Ecol* **15**: 115–125.

Grossart HP, Ploug H. (2001). Microbial degradation of organic carbon and nitrogen on diatom aggregates. *Limnol Oceanogr* **46**: 267–277.

Grossart H-P, Kiørboe T, Tang K, Ploug H. (2003). Bacterial Colonization of Particles: Growth and Interactions. *Appl Environ Microbiol* **69**: 3500–3509.

Grossart HP, Levold F, Allgaier M, Simon M, Brinkhoff T. (2005). Marine diatom species harbour distinct bacterial communities. *Environ Microbiol* **7**: 860–873.

Grossart H-P, Allgaier M, Passow U, Riebesell U. (2006a). Testing the effect of CO_2 concentration on the dynamics of marine heterotrophic bacterioplankton. *Limnol*

Oceanogr **51**: 1–11.

Grossart H, Kiørboe T, Tang K, Allgaier M, Yam E, Ploug H. (2006b). Interactions between marine snow and heterotrophic bacteria: aggregate formation and microbial dynamics. *Aquat Microb Ecol* **42**: 19–26.

Grossart H, Simon M. (2007). Interactions of planktonic algae and bacteria: effects on algal growth and organic matter dynamics. *Aquat Microb Ecol* **47**: 163–176.

Grossart H-P, Tang KW. (2010). www.aquaticmicrobial.net. *Commun Integr Biol* **3**: 491–494.

Gruber N, Galloway JN. (2008). An Earth-system perspective of the global nitrogen cycle. *Nature* **451**: 293–296.

Gruber N, Gloor M, Mikaloff Fletcher SE, Doney SC, Dutkiewicz S, Follows MJ, et al. (2009). Oceanic sources, sinks, and transport of atmospheric CO_2. *Global Biogeochem Cycles* **23**: GB1005, doi:10.1029/2008GB003349.

Guan LL, Kamino K. (2001). Bacterial response to siderophore and quorum-sensing chemical signals in the seawater microbial community. *BMC Microbiol* **1**: 1–11.

Hansell D, Carlson C, Repeta D, Schlitzer R. (2009). Dissolved Organic Matter in the Ocean: A Controversy Stimulates New Insights. *Oceanography* **22**: 202–211.

Hansell DA, Carlson CA (eds). (2002). Biogeochemistry of Marine Dissolved Organic Matter. Academic Press: Boston, MA, USA.

Hansen J, Kharecha P, Sato M, Masson-Delmotte V, Ackerman F, Beerling DJ, et al. (2013). Assessing "Dangerous Climate Change": Required Reduction of Carbon Emissions to Protect Young People, Future Generations and Nature. *PLoS One* **8**: e81648, 10.1371/journal.pone.0081648.

Hartmann DL, Klein Tank AMG, Rusticucci M, Alexander LV, Brönnimann S, Charabi Y, et al. (2013). Observations: Atmosphere and Surface. In: Stocker TF, Qin D, Plattner G-K, Tignor M, Allen SK, Boschung J, Nauels A, Xia Y, Bex V and Midgley PM (eds): *Climate Change 2013: The Physical Science Basis. Contribution of Working Group I to the Fifth Assessment Report of the Intergovernmental Panel on Climate Change*. Cambridge University Press: Cambridge, United Kingdom and New York, NY, USA, pp. 159–254, doi:10.1017/CBO9781107415324.008.

He S, Stevens SLR, Chan L-K, Bertilsson S, Glavina del Rio T, Tringe SG, et al. (2017). Ecophysiology of Freshwater *Verrucomicrobia* Inferred from Metagenome-Assembled Genomes. *mSphere* **2**: e00277-17, doi:10.1128/mSphere .00277-17.

Hedges JI. (1992). Global biogeochemical cycles: progress and problems. *Mar Chem* **39**: 67–93.

Hein M, Sand-Jensen K. (1997). CO_2 increases oceanic primary production. *Nature* **388**: 526–527.

Heino J, Virkkala R, Toivonen H. (2009). Climate change and freshwater biodiversity: detected patterns, future trends and adaptations in northern regions. *Biol Rev* **84**: 39–54.

Heissenberger A, Herndl GJ. (1994). Formation of high molecular weight material by free-living marine bacteria. *Mar Ecol Prog Ser* **111**: 129–135.

Heissenberger A, Leppard GG, Herndl GJ. (1996). Relationship between the Intracellular Integrity and the Morphology of the Capsular Envelope in Attached and Free-Living Marine Bacteria. *Appl Environ Microbiol* **62**: 4521–4528.

Hendriks IE, Duarte CM, Álvarez M. (2010). Vulnerability of marine biodiversity to ocean acidification: A meta-analysis. *Estuar Coast Shelf Sci* **86**: 157–164.

Hennon GMM, Hernández Limón MD, Haley ST, Juhl AR, Dyhrman ST. (2017). Diverse CO_2-Induced Responses in Physiology and Gene Expression among Eukaryotic Phytoplankton. *Front Microbiol* **8**: 2547. doi: 10.3389/fmicb.2017.02547

Herring SC, Christidis N, Hoell A, Kossin JP, Schreck III CJ, and Stott PA. (eds). (2018). Explaining Extreme Events of 2016 from a Climate Perspective. *Bull. Amer. Meteor. Soc.* **99** (1): S1-S157.

Hessen DO, Tranvik LJ (eds). (1998). Aquatic Humic Substances. Springer: Berlin and Heidelberg, Germany.

Hobbie JE. (1988). A comparison of the ecology of planktonic bacteria in fresh and salt water. *Limnol Oceanogr* **33**: 750–764.

Hoegh-Guldberg O, Bruno JF. (2010). The Impact of Climate Change on the World's Marine Ecosystems. *Science* **328**: 1523–1528.

Houser JN. (2006). Water color affects the stratification, surface temperature, heat content, and mean epilimnetic irradiance of small lakes. *Can J Fish Aquat Sci* **63**: 2447–2455.

Huisman J, Weissing FJ. (1994). Light-Limited Growth and Competition for Light in Well-Mixed Aquatic Environments: An Elementary Model. *Ecology* **75**: 507–520.

Huisman J, Weissing FJ. (1995). Competition for Nutrients and Light in a Mixed Water Column: A Theoretical Analysis. *Am Nat* **146**: 536–564.

Huisman J, van Oostveen P, Weissing FJ. (1999). Critical depth and critical turbulence: Two different mechanisms for the development of phytoplankton blooms. *Limnol Oceanogr* **44**: 1781–1787.

Huisman J, Sharples J, Stroom JM, Visser PM, Kardinaal WEA, Verspagen JMH, et al. (2004). Changes In Turbulent Mixing Shift Competition For Light Between Phytoplankton Species. *Ecology* **85**: 2960–2970.

Hutchins D, Mulholland M, Fu F. (2009). Nutrient Cycles and Marine Microbes in a CO_2-Enriched Ocean. *Oceanography* **22**: 128–145.

Hutchinson GE. (1975). A Treatise on Limnology, Vol. 1, Geography, physics and chemistry. John Wiley & Sons Inc.: New York, NY, USA, pp. 672.

Idso SB. (1973). On the concept of lake stability. *Limnol Oceanogr* **18**: 681–683.

Imberger J. (1985). The diurnal mixed layer. *Limnol Oceanogr* **30**: 737–770.

Imberger J, Patternson JC. (1990). Physical limnology. *Adv Appl Mech* **27**: 303–475.

IPCC (2013a). Summary for Policymakers. In: Stocker TF, Qin D, Plattner G-K, Tignor M, Allen SK, Boschung J, Nauels A, Xia Y, Bex V and Midgley PM (eds). *Climate Change 2013: The Physical Science Basis. Contribution of Working Group I to the Fifth Assessment Report of the Intergovernmental Panel on Climate Change*. Cambridge University Press: Cambridge, United Kingdom and New York, NY, USA, pp. 1–30,

doi:10.1017/CBO9781107415324.004.

IPCC (2013b). Climate Change 2013: The Physical Science Basis. Contribution of Working Group I to the Fifth Assessment Report of the Intergovernmental Panel on Climate Change [Stocker TF, Qin D, Plattner G-K, Tignor M, Allen SK, Boschung J, Nauels A, Xia Y, Bex V and Midgley PM (eds)]. Cambridge University Press: Cambridge, United Kingdom and New York, NY, USA, pp. 1535, doi:10.1017/CBO9781107415324.

IPCC (2014). IPCC: Annex II: Glossary [Mach, K.J., S. Planton and C. von Stechow (eds)]. In: Core Writing Team, Pachauri RK and Meyer LA (eds): *Climate Change 2014: Synthesis Report. Contribution of Working Groups I, II and III to the Fifth Assessment Report of the Intergovernmental Panel on Climate Change*. IPCC: Geneva, Switzerland, pp. 117-130.

Irish JM, Kotecha N, Nolan GP. (2006). Mapping normal and cancer cell signalling networks: towards single-cell proteomics. *Nat Rev Cancer* **6**: 146–155.

Iturriaga R, Hoppe H-G. (1977). Observations of heterotrophic activity on photoassimilated organic matter. *Mar Biol* **40**: 101–108.

Jäger CG, Diehl S, Emans M. (2010). Physical Determinants of Phytoplankton Production, Algal Stoichiometry, and Vertical Nutrient Fluxes. *Am Nat* **175**: E91–E104, doi:10.1086/650728.

Janssens-Maenhout G, Crippa M, Guizzardi D, Muntean M, Schaaf E, Olivier JGJ, Peters JAHW, Schure KM. (2017). Fossil CO_2 and GHG emissions of all world countries, EUR 28766 EN, Publications Office of the European Union: Luxembourg, ISBN 978-92-79-73207-2, doi:10.2760/709792, JRC107877.

Jennings E, Jones S, Arvola L, Staehr PA, Gaiser E, Jones ID, et al. (2012). Effects of weather-related episodic events in lakes: an analysis based on high-frequency data. *Freshw Biol* **57**: 589–601.

Joint I, Doney SC, Karl DM. (2011). Will ocean acidification affect marine microbes? *ISME J* **5**: 1–7.

Jones AC, Liao TSV, Najar FZ, Roe BA, Hambright KD, Caron DA. (2013). Seasonality and disturbance: annual pattern and response of the bacterial and microbial eukaryotic assemblages in a freshwater ecosystem. *Environ Microbiol* **15**: 2557–2572.

Jones SE, Chiu C-Y, Kratz TK, Wu J-T, Shade A, McMahon KD. (2008). Typhoons initiate predictable change in aquatic bacterial communities. *Limnol Oceanogr* **53**: 1319–1326.

Jürgens K, Pernthaler J, Schalla S, Amann R. (1999). Morphological and Compositional Changes in a Planktonic Bacterial Community in Response to Enhanced Protozoan Grazing. *Appl Environ Microbiol* **65**: 1241–1250.

Kalisky T, Quake SR. (2011). Single-cell genomics. *Nat Methods* **8**: 311–314.

Karlson AML, Duberg J, Motwani NH, Hogfors H, Klawonn I, Ploug H, et al. (2015). Nitrogen fixation by cyanobacteria stimulates production in Baltic food webs. *Ambio* **44**: 413–426.

Kasprzak P, Shatwell T, Gessner MO, Gonsiorczyk T, Kirillin G, Selmeczy G, et al. (2017). Extreme Weather Event Triggers Cascade Towards Extreme Turbidity in a Clear-water Lake. *Ecosystems* **20**: 1207, doi:10.1007/s10021-017-0121-4.

Keeling RF, Körtzinger A, Gruber N. (2010). Ocean Deoxygenation in a Warming World. *Ann*

Rev Mar Sci **2**: 199–229.

Kirchman DL. (ed). (2008). Microbial Ecology of the Oceans. 2nd edition. Wiley-Liss: New York, NY, USA, pp. 620.

Kirchman DL, Malmstrom RR, Cottrell MT. (2005). Control of bacterial growth by temperature and organic matter in the Western Arctic. *Deep Sea Res Part II* **52**: 3386–3395.

Klausmeier CA, Litchman E. (2001). Algal games: The vertical distribution of phytoplankton in poorly mixed water columns. *Limnol Oceanogr* **46**: 1998–2007.

Klawonn I, Nahar N, Walve J, Andersson B, Olofsson M, Svedén JB, et al. (2016). Cell-specific nitrogen- and carbon-fixation of cyanobacteria in a temperate marine system (Baltic Sea). *Environ Microbiol* **18**: 4596–4609.

Klemer AR, Cullen JJ, Mageau MT, Hanson KM, Sundell R a. (1996). Cyanobacterial Buoyancy regulation: The Paradoxical Roles of Carbon. *J Phycol* **32**: 47–53.

Klemke F, Beyer G, Sawade L, Saitov A, Korte T, Maldener I, et al. (2014). All1371 is a polyphosphate-dependent glucokinase in *Anabaena* sp. PCC 7120. *Microbiology* **160**: 2807–2819.

Klug JL, Richardson DC, Ewing HA, Hargreaves BR, Samal NR, Vachon D, et al. (2012). Ecosystem Effects of a Tropical Cyclone on a Network of Lakes in Northeastern North America. *Environ Sci Technol* **46**: 11693–11701.

Krause E, Wichels A, Giménez L, Lunau M, Schilhabel MB, Gerdts G. (2012). Small Changes in pH Have Direct Effects on Marine Bacterial Community Composition: A Microcosm Approach. *PLoS One* **7**: e47035, doi:10.1371/journal.pone.0047035.

Krause S, Le Roux X, Niklaus PA, Van Bodegom PM, Lennon JT, Bertilsson S, et al. (2014). Trait-based approaches for understanding microbial biodiversity and ecosystem functioning. *Front Microbiol* **5**: 251, doi:10.3389/fmicb.2014.00251.

Kroeker KJ, Kordas RL, Crim RN, Singh GG. (2010). Meta-analysis reveals negative yet variable effects of ocean acidification on marine organisms. *Ecol Lett* **13**: 1419–1434.

Kroeker KJ, Kordas RL, Crim R, Hendriks IE, Ramajo L, Singh GS, et al. (2013). Impacts of ocean acidification on marine organisms: quantifying sensitivities and interaction with warming. *Glob Chang Biol* **19**: 1884–1896.

Kuha J, Arvola L, Hanson PC, Huotari J, Huttula T, Juntunen J, et al. (2016). Response of boreal lakes to episodic weather-induced events. *Inl Waters* **6**: 523–534.

Kühl M, Cohen Y, Dalsgaard T, Jørgensen B, Revsbech N. (1995). Microenvironment and photosynthesis of zooxanthellae in scleractinian corals studied with microsensors for O_2, pH and light. *Mar Ecol Prog Ser* **117**: 159–172.

Labat D, Goddéris Y, Probst JL, Guyot JL. (2004). Evidence for global runoff increase related to climate warming. *Adv Water Resour* **27**: 631–642.

Lampert W. (1987). Laboratory studies on zooplankton-cyanobacteria interactions. *New Zeal J Mar Freshw Res* **21**: 483–490.

Larsen JB, Larsen A, Thyrhaug R, Bratbak G, Sandaa R-A. (2008). Response of marine viral populations to a nutrient induced phytoplankton bloom at different pCO_2 levels. *Biogeosciences* **5**: 523–533.

Lawrence MG, Schäfer S, Muri H, Scott V, Oschlies A, Vaughan NE, et al. (2018). Evaluating climate geoengineering proposals in the context of the Paris Agreement temperature goals. *Nat Commun* **9**: 3734, doi:10.1038/s41467-018-05938-3.

Leach TH, Beisner BE, Carey CC, Pernica P, Rose KC, Huot Y, et al. (2017). Patterns and drivers of deep chlorophyll maxima structure in 100 lakes: The relative importance of light and thermal stratification. *Limnol Oceanogr*. **63**: 628-646.

Lee SH, Kang YC, Fuhrman JA. (1995). Imperfect retention of natural bacterioplakton cells by glass fibre filters. *Mar Ecol Prog Ser* **119**: 285–290.

Lewis SL, Maslin MA. (2015). Defining the Anthropocene. *Nature* **519**: 171–180.

Lima-Mendez G, Faust K, Henry N, Decelle J, Colin S, Carcillo F, et al. (2015). Determinants of community structure in the global plankton interactome. *Science* **348**: 1262073, 10.1126/science.1262073.

Lindh M V., Riemann L, Baltar F, Romero-Oliva C, Salomon PS, Granéli E, et al. (2013). Consequences of increased temperature and acidification on bacterioplankton community composition during a mesocosm spring bloom in the Baltic Sea. *Environ Microbiol Rep* **5**: 252–262.

Liu J, Weinbauer M, Maier C, Dai M, Gattuso J-P. (2010). Effect of ocean acidification on microbial diversity and on microbe-driven biogeochemistry and ecosystem functioning. *Aquat Microb Ecol* **61**: 291–305.

Logan BE, Passow U, Alldredge AL, Grossartt H-P, Simont M. (1995). Rapid formation and sedimentation of large aggregates is predictable from coagulation rates (half-lives) of transparent exopolymer particles (TEP). *Deep Sea Res Part II* **42**: 203–214.

Lüthi D, Le Floch M, Bereiter B, Blunier T, Barnola J, Siegenthaler U, et al. (2008). High-resolution carbon dioxide concentration record 650,000–800,000 years before present. *Nature* **453**: 379–382.

MacIntyre S, Flynn KM, Jellison R, Romero JR. (1999). Boundary mixing and nutrient fluxes in Mono Lake, California. *Limnol Oceanogr* **44**: 512–529.

Marcarelli AM, Baxter C V., Mineau MM, Hall RO. (2011). Quantity and quality: unifying food web and ecosystem perspectives on the role of resource subsidies in freshwaters. *Ecology* **92**: 1215–1225.

Mari X. (2008). Does ocean acidification induce an upward flux of marine aggregates? *Biogeosciences* **5**: 1023–1031.

Mari X, Rassoulzadegan F, Brussaard CPD, Wassmann P. (2005). Dynamics of transparent exopolymeric particles (TEP) production by Phaeocystis globosa under N- or P-limitation: a controlling factor of the retention/export balance. *Harmful Algae* **4**: 895–914.

Martinez-Garcia M, Brazel DM, Swan BK, Arnosti C, Chain PSG, Reitenga KG, et al. (2012). Capturing single cell genomes of active polysaccharide degraders: An unexpected contribution of *Verrucomicrobia*. *PLoS One* **7**: e35314. doi:10.1371/journal.pone.0035314.

Maugendre L, Guieu C, Gattuso J-P, Gazeau F. (2017). Ocean acidification in the Mediterranean Sea: Pelagic mesocosm experiments. A synthesis. *Estuar Coast Shelf Sci* **186**: 1–10.

Mayali X, Franks P, Burton R. (2011). Temporal attachment dynamics by distinct bacterial taxa during a dinoflagellate bloom. *Aquat Microb Ecol* **63**: 111–122.

Meinshausen M, Smith SJ, Calvin K, Daniel JS, Kainuma MLT, Lamarque J-F, et al. (2011). The RCP greenhouse gas concentrations and their extensions from 1765 to 2300. *Clim Change* **109**: 213–241.

Middelboe M, Jørgensen NOG. (2006). Viral lysis of bacteria: an important source of dissolved amino acids and cell wall compounds. *J Mar Biol Ass U.K.* **86**: 605-612.

Middelboe M, Søndergaard M, Letarte Y, Borch NH. (1995). Attached and free-living bacteria: Production and polymer hydrolysis during a diatom bloom. *Microb Ecol* **29**: 231–248.

Millar RJ, Fuglestvedt JS, Friedlingstein P, Rogelj J, Grubb MJ, Matthews HD, et al. (2017). Emission budgets and pathways consistent with limiting warming to 1.5 °C. *Nat Geosci* **10**: 741–747.

Moll RA, Stoermer EF. (1981). A hypothesis relating trophic status and subsurface chlorophyll maxima of lakes. *Arch Hydrobiol* **94**: 425–440.

Møller E, Thor P, Nielsen T. (2003). Production of DOC by *Calanus finmarchicus*, *C. glacialis* and *C. hyperboreus* through sloppy feeding and leakage from fecal pellets. *Mar Ecol Prog Ser* **262**: 185–191.

Monismith SG, MacIntyre S. (2009). The surface mixed layer in lakes and reservoirs. In: Likens GE (ed). *Encyclopedia of Inland Waters*. Elsevier: Amsterdam, Netherlands, pp. 568–582.

Monroe JG, Markman DW, Beck WS, Felton AJ, Vahsen ML, Pressler Y. (2018). Ecoevolutionary Dynamics of Carbon Cycling in the Anthropocene. *Trends Ecol Evol* **33**: 213–225.

Moore CM, Mills MM, Arrigo KR, Berman-Frank I, Bopp L, Boyd PW, et al. (2013). Processes and patterns of oceanic nutrient limitation. *Nat Geosci* **6**: 701–710.

Mopper K, Stubbins A, Ritchie JD, Bialk HM, Hatcher PG. (2007). Advanced instrumental approaches for characterization of marine dissolved organic matter: extraction techniques, mass spectrometry, and nuclear magnetic resonance spectroscopy. *Chem Rev* **107**: 419–442.

Moran MA, Kujawinski EB, Stubbins A, Fatland R, Aluwihare LI, Buchan A, et al. (2016). Deciphering ocean carbon in a changing world. *Proc Natl Acad Sci* **113**: 3143–3151.

Motegi C, Tanaka T, Piontek J, Brussaard CPD, Gattuso J-P, Weinbauer MG. (2013). Effect of CO_2 enrichment on bacterial metabolism in an Arctic fjord. *Biogeosciences* **10**: 3285–3296.

Nedwell D. (1999). Effect of low temperature on microbial growth: lowered affinity for substrates limits growth at low temperature. *FEMS Microbiol Ecol* **30**: 101–111.

Nelson CE, Wear EK. (2014). Microbial diversity and the lability of dissolved organic carbon. *Proc Natl Acad Sci* **111**: 7166–7167.

Nemergut DR, Schmidt SK, Fukami T, O'Neill SP, Bilinski TM, Stanish LF, et al. (2013). Patterns and Processes of Microbial Community Assembly. *Microbiol Mol Biol Rev* **77**: 342–356.

Newbold LK, Oliver AE, Booth T, Tiwari B, DeSantis T, Maguire M, et al. (2012). The response of marine picoplankton to ocean acidification. *Environ Microbiol* **14**: 2293–2307.

Newman JRS, Ghaemmaghami S, Ihmels J, Breslow DK, Noble M, DeRisi JL, et al. (2006). Single-cell proteomic analysis of *S. cerevisiae* reveals the architecture of biological noise. *Nature* **441**: 840–846.

Noble R, Fuhrman J. (1999). Breakdown and microbial uptake of marine viruses and other lysis products. *Aquat Microb Ecol* **20**: 1–11.

Obernosterer I, Herndl G. (1995). Phytoplankton extracellular release and bacterial growth: dependence on the inorganic N:P ratio. *Mar Ecol Prog Ser* **116**: 247–257.

Ogawa H, Tanoue E. (2003). Dissolved Organic Matter in Oceanic Waters. *J Oceanogr* **59**: 129–147.

Ojala A, Bellido JL, Tulonen T, Kankaala P, Huotari J. (2011). Carbon gas fluxes from a brown-water and a clear-water lake in the boreal zone during a summer with extreme rain events. *Limnol Oceanogr* **56**: 61–76.

Oliver AE, Newbold LK, Whiteley AS, van der Gast CJ. (2014). Marine bacterial communities are resistant to elevated carbon dioxide levels. *Environ Microbiol Rep* **6**: 574–582.

Osterholz H, Singer G, Wemheuer B, Daniel R, Simon M, Niggemann J, et al. (2016). Deciphering associations between dissolved organic molecules and bacterial communities in a pelagic marine system. *ISME J* **10**: 1717–1730.

Paerl HW, Paul VJ. (2012). Climate change: Links to global expansion of harmful cyanobacteria. *Water Res* **46**: 1349–1363.

Pardew J, Blanco Pimentel M, Low-Decarie E. (2018). Predictable ecological response to rising CO_2 of a community of marine phytoplankton. *Ecol Evol* **8**: 4292–4302.

Passow U. (2000). Formation of transparent exopolymer particles, TEP, from dissolved precursor material. *Mar Ecol Prog Ser* **192**: 1–11.

Passow U. (2002). Production of transparent exopolymer particles (TEP) by phyto- and bacterioplankton. *Mar Ecol Prog Ser* **236**: 1–12.

Passow U, Alldredge A. (1994). Distribution, size and bacterial colonization of transparent exopolymer particles (TEP) in the ocean. *Mar Ecol Prog Ser* **113**: 185–198.

Passow U, Shipe RF, Murray A, Pak DK, Brzezinski MA, Alldredge AL. (2001). The origin of transparent exopolymer particles (TEP) and their role in the sedimenatation of particulate matter. *Cont Shelf Res* **21**: 327–346.

Patalas K. (1984). Mid-summer mixing depths of lakes of different latitudes. *SIL Proceedings, 1922-2010* **22**: 97–102, doi:10.1080/03680770.1983.11897273

Paul AJ, Bach LT, Schulz K-G, Boxhammer T, Czerny J, Achterberg EP, et al. (2015). Effect of elevated CO_2 on organic matter pools and fluxes in a summer Baltic Sea plankton community. *Biogeosciences* **12**: 6181–6203.

Perga M-E, Bruel R, Rodriguez L, Guénand Y, Bouffard D. (2018). Storm impacts on alpine lakes: Antecedent weather conditions matter more than the event intensity. *Glob Chang Biol* **24**: 5004–5016.

Pernthaler J, Posch T, Šimek K, Vrba J, Amann R, Psenner R. (1997). Contrasting Bacterial

Strategies To Coexist with a Flagellate Predator in an Experimental Microbial Assemblage. *Appl Environ Microbiol* **63**: 596–601.

Petit JR, Jouzel J, Raynaud D, Barkov NI, Barnola J-M, Basile I, et al. (1999). Climate and atmospheric history of the past 420,000 years from the Vostok ice core, Antarctica. *Nature* **399**: 429–436.

Pimm SL. (1984). The complexity and stability of ecosystems. *Nature* **307**: 321–326.

Pinhassi J, Berman T. (2003). Differential Growth Response of Colony-Forming α- and γ-Proteobacteria in Dilution Culture and Nutrient Addition Experiments from Lake Kinneret (Israel), the Eastern Mediterranean Sea, and the Gulf of Eilat. *Appl Environ Microbiol* **69**: 199–211.

Pinhassi J, Sala MM, Havskum H, Peters F, Guadayol O s., Malits A, et al. (2004). Changes in Bacterioplankton Composition under Different Phytoplankton Regimens. *Appl Environ Microbiol* **70**: 6753–6766.

Piontek J, Lunau M, Händel N, Borchard C, Wurst M, Engel A. (2010). Acidification increases microbial polysaccharide degradation in the ocean. *Biogeosciences* **7**: 1615–1624.

Pomeroy LR. (1974). The Ocean's Food Web, A Changing Paradigm. *Bioscience* **24**: 499–504.

Pomeroy LR, Deibel D. (1986). Temperature Regulation of Bacterial Activity During the Spring Bloom in Newfoundland Coastal Waters. *Science* **233**: 359–361.

Porter KG, Sherr EB, Sherr BF, Pace M, Sanders RW. (1985). Protozoa in Planktonic Food Webs. *J Prozozool* **32**: 409–415.

Pörtner H-O. (2008). Ecosystem effects of ocean acidification in times of ocean warming: a physiologist's view. *Mar Ecol Prog Ser* **373**: 203–217.

Posch T, Köster O, Salcher MM, Pernthaler J. (2012). Harmful filamentous cyanobacteria favoured by reduced water turnover with lake warming. *Nat Clim Chang* **2**: 809–813.

Ptacnik R, Diehl S, Berger S. (2003). Performance of sinking and nonsinking phytoplankton taxa in a gradient of mixing depths. *Limnol Oceanogr* **48**: 1903–1912.

Rabalais N, Cai W-J, Carstensen J, Conley D, Fry B, Hu X, et al. (2014). Eutrophication-Driven Deoxygenation in the Coastal Ocean. *Oceanography* **27**: 172–183.

Rahel FJ, Olden JD. (2008). Assessing the Effects of Climate Change on Aquatic Invasive Species. *Conserv Biol* **22**: 521–533.

Rahmstorf S, Cazenave A, Church JA, Hansen JE, Keeling RF, Parker DE, et al. (2007). Recent Climate Observations Compared to Projections. *Science* **316**: 709–709.

Rahmstorf S, Coumou D. (2011) Increase of extreme events in a warming world. *Proc Natl Acad Sci* **108**: 17905-17909.

Randerson JT, Chapin FSI, Harden JW, Neff JC, Harmon ME. (2002). Net Ecosystem Production: A Comprehensive Measure of Net Carbon Accumulation by Ecosystems. *Ecol Appl* **12**: 937–947.

Rantakari M, Kortelainen P. (2005). Interannual variation and climatic regulation of the CO_2 emission from large boreal lakes. *Glob Chang Biol* **11**: 1368–1380.

Raven J, Caldeira K, Elderfield H, Hoegh-Guldberg O, Liss P, Riebesell, U., Shepherd, J., Turley, C. and Watson A. (2005). Ocean acidification due to increasing atmospheric carbon dioxide. The Royal Society: London, UK, pp. 68, ISBN 0-85403-617-2.

Raven JA. (1998). The twelfth Tansley Lecture. Small is beautiful: the picophytoplankton. *Funct Ecol* **12**: 503–513.

Raven JA, Falkowski PG. (1999). Oceanic sinks for atmospheric CO_2. *Plant, Cell Environ* **22**: 741–755.

Raymond PA, Hartmann J, Lauerwald R, Sobek S, McDonald C, Hoover M, et al. (2013). Global carbon dioxide emissions from inland waters. *Nature* **503**: 355–359.

Read JS, Hamilton DP, Jones ID, Muraoka K, Winslow LA, Kroiss R, et al. (2011). Derivation of lake mixing and stratification indices from high-resolution lake buoy data. *Environ Model Softw* **26**: 1325–1336.

Regnier P, Friedlingstein P, Ciais P, Mackenzie FT, Gruber N, Janssens IA, et al. (2013). Anthropogenic perturbation of the carbon fluxes from land to ocean. *Nat Geosci* **6**: 597–607.

Reichstein M, Bahn M, Ciais P, Frank D, Mahecha MD, Seneviratne SI, et al. (2013). Climate extremes and the carbon cycle. *Nature* **500**: 287–295.

Reynolds CS, Oliver RL, Walsby AE. (1987). Cyanobacterial dominance: The role of buoyancy regulation in dynamic lake environments. *New Zeal J Mar Freshw Res* **21**: 379–390.

Rhein M, Rintoul SR, Aoki S, Campos E, Chambers D, Feely RA, Gulev S, Johnson GC, Josey SA, Kostianoy A, Mauritzen C, Roemmich D, Talley LD and Wang F. (2013). Observations: Ocean. In: Stocker TF, Qin D, Plattner G-K, Tignor M, Allen SK, Boschung J, Nauels A, Xia Y, Bex V and Midgley PM (eds): *Climate Change 2013: The Physical Science Basis. Contribution of Working Group I to the Fifth Assessment Report of the Intergovernmental Panel on Climate Change*. Cambridge University Press: Cambridge, United Kingdom and New York, NY, USA, pp. 255–316, doi:10.1017/CBO9781107415324.010.

Riahi K, Grübler A, Nakicenovic N. (2007). Scenarios of long-term socio-economic and environmental development under climate stabilization. *Technol Forecast Soc Change* **74**: 887–935.

Riebesell U. (2004). Effects of CO_2 Enrichment on Marine Phytoplankton. *J Oceanogr* **60**: 719–729.

Riebesell U, Schulz KG, Bellerby RGJ, Botros M, Fritsche P, Meyerhöfer M, et al. (2007). Enhanced biological carbon consumption in a high CO_2 ocean. *Nature* **450**: 545–548.

Riebesell U, Kortzinger A, Oschlies A. (2009). Sensitivities of marine carbon fluxes to ocean change. *Proc Natl Acad Sci* **106**: 20602–20609.

Riebesell U, Lee K, Nejstgaard JC. (2010). Pelagic mesocosms. In: Riebesell U, Fabry VJ, Hansson L, Gattuso J-P (eds). *Guide to best practices for ocean acidification research and data reporting*. Publications Office of the European Union: Luxembourg, Luxembourg, pp. 95-112, doi:10.2777/58454.

Riebesell U, Tortell PD. (2011). Effects of Ocean Acidificaton on Pelagic Organisms and Ecosystems. In: Gattuse J-P, Hansson L (eds). *Ocean Acidification*. Oxford University

Press: Oxford, UK, pp. 99–121.

Riebesell U, Czerny J, von Bröckel K, Boxhammer T, Büdenbender J, Deckelnick M, et al. (2013). Technical Note: A mobile sea-going mesocosm system – new opportunities for ocean change research. *Biogeosciences* **10**: 1835–1847.

Riebesell U, Gattuso J-P. (2015). Lessons learned from ocean acidification research. *Nat Clim Chang* **5**: 12–14.

Riemann L, Winding A. (2001). Community Dynamics of Free-living and Particle-associated Bacterial Assemblages during a Freshwater Phytoplankton Bloom. *Microb Ecol* **42**: 274–285.

Robertson DM, Imberger J. (1994). Lake Number, a Quantitative Indicator of Mixing Used to Estimate Changes in Dissolved Oxygen. *Int Revue ges. Hydrobiol* **79**: 159–176.

Rockström J, Steffen W, Noone K, Persson Å, Chapin FS, Lambin EF, et al. (2009). A safe operating space for humanity. *Nature* **461**: 472–475.

Rogelj J, Schleussner C-F, Hare W. (2017). Getting It Right Matters: Temperature Goal Interpretations in Geoscience Research. *Geophys Res Lett* **44**: 10662-10665.

Roiha T, Tiirola M, Cazzanelli M, Rautio M. (2012). Carbon quantity defines productivity while its quality defines community composition of bacterioplankton in subarctic ponds. *Aquat Sci* **74**: 513–525.

Romano S, Dittmar T, Bondarev V, Weber RJM, Viant MR, Schulz-Vogt HN. (2014). Exo-Metabolome of *Pseudovibrio* sp. FO-BEG1 Analyzed by Ultra-High Resolution Mass Spectrometry and the Effect of Phosphate Limitation. *PLoS One* **9**: e96038, doi:10.1371/journal.pone.0096038.

Romme WH, Everham EH, Frelich LE, Moritz MA, Sparks RE. (1998). Are Large, Infrequent Disturbances Qualitatively Different from Small, Frequent Disturbances? *Ecosystems* **1**: 524–534.

Rösel S, Allgaier M, Grossart H-P. (2012). Long-Term Characterization of Free-Living and Particle-Associated Bacterial Communities in Lake Tiefwaren Reveals Distinct Seasonal Patterns. *Microb Ecol* **64**: 571–583.

Rösel S, Grossart H. (2012). Contrasting dynamics in activity and community composition of free-living and particle-associated bacteria in spring. *Aquat Microb Ecol* **66**: 169–181.

Roy A-S, Gibbons SM, Schunck H, Owens S, Caporaso JG, Sperling M, et al. (2013). Ocean acidification shows negligible impacts on high-latitude bacterial community structure in coastal pelagic mesocosms. *Biogeosciences* **10**: 555–566.

Sadro S, Melack JM. (2012). The Effect of an Extreme Rain Event on the Biogeochemistry and Ecosystem Metabolism of an Oligotrophic High-Elevation Lake. *Arctic, Antarct Alp Res* **44**: 222–231.

Sala MM, Aparicio FL, Balagué V, Boras JA, Borrull E, Cardelús C, et al. (2016). Contrasting effects of ocean acidification on the microbial food web under different trophic conditions. *ICES J Mar Sci* **73**: 670–679.

Sambrotto RN, Savidge G, Robinson C, Boyd P, Takahashi T, Karl DM, et al. (1993). Elevated consumption of carbon relative to nitrogen in the surface ocean. *Nature* **363**: 248–250.

Sand-Jensen K, Revsbech NP, Barker Jørgensen B. (1985). Microprofiles of oxygen in epiphyte communities on submerged macrophytes. *Mar Biol* **89**: 55–62.

Sandberg R. (2014). Entering the era of single-cell transcriptomics in biology and medicine. *Nat Methods* **11**: 22–24.

Sarmento H, Morana C, Gasol JM. (2016). Bacterioplankton niche partitioning in the use of phytoplankton-derived dissolved organic carbon: quantity is more important than quality. *ISME J* **10**: 2582–2592.

Sarmiento JL, Gruber N. (2002). Sinks for Anthropogenic Carbon. *Phys Today* **55**: 30–36, doi:10.1063/1.1510279.

Sarmiento JL, Slater R, Barber R, Bopp L, Doney SC, Hirst AC, et al. (2004). Response of ocean ecosystems to climate warming. *Global Biogeochem Cycles* **18**: GB3003, doi:10.1029/2003GB002134.

Sarnelle O. (2005). Daphnia as keystone predators: effects on phytoplankton diversity and grazing resistance. *J Plankton Res* **27**: 1229–1238.

Schellnhuber HJ, Rahmstorf S, Winkelmann R. (2016). Why the right climate target was agreed in Paris. *Nat Clim Chang* **6**: 649–653.

Schlüter L, Lohbeck KT, Gröger JP, Riebesell U, Reusch TBH. (2016). Long-term dynamics of adaptive evolution in a globally important phytoplankton species to ocean acidification. *Sci Adv* **2**: e1501660, doi:10.1126/sciadv.1501660.

Schmidt W. (1928). Über Temperatur und Stabilitätsverhältnisse von Seen. *Geogr Ann* **10**: 145–177.

Schulz KG, Bach LT, Bellerby RGJ, Bermúdez R, Büdenbender J, Boxhammer T, et al. (2017). Phytoplankton Blooms at Increasing Levels of Atmospheric Carbon Dioxide: Experimental Evidence for Negative Effects on Prymnesiophytes and Positive on Small Picoeukaryotes. *Front Mar Sci* **4**: 64, doi:10.3389/fmars.2017.00064.

Schuur EAG, Abbott B. (2011). High risk of permafrost thaw. *Nature* **480**: 32–33.

Schuur EAG, McGuire AD, Schädel C, Grosse G, Harden JW, Hayes DJ, et al. (2015). Climate change and the permafrost carbon feedback. *Nature* **520**: 171–179.

Schwoerbel J. (1999). Einführung in die Limnologie. 8. Auflage. Gustav Fischer Verlag: Stuttgart, Germany.

Shabarova T, Villiger J, Morenkov O, Niggemann J, Dittmar T, Pernthaler J. (2014). Bacterial community structure and dissolved organic matter in repeatedly flooded subsurface karst water pools. *FEMS Microbiol Ecol* **89**: 111–126.

Shade A, Kent AD, Jones SE, Newton RJ, Triplett EW, McMahon KD. (2007). Interannual dynamics and phenology of bacterial communities in a eutrophic lake. *Limnol Oceanogr* **52**: 487–494.

Shade A, Jones SE, McMahon KD. (2008). The influence of habitat heterogeneity on freshwater bacterial community composition and dynamics. *Environ Microbiol* **10**: 1057–1067.

Shade A, Chiu C-Y, McMahon KD. (2010a). Differential bacterial dynamics promote emergent community robustness to lake mixing: an epilimnion to hypolimnion transplant experiment. *Environ Microbiol* **12**: 455–466.

Shade A, Chiu C, McMahon KD. (2010b). Seasonal and Episodic Lake Mixing Stimulate Differential Planktonic Bacterial Dynamics. *Microb Ecol* **59**: 546–554.

Shade A, Read JS, Welkie DG, Kratz TK, Wu CH, McMahon KD. (2011). Resistance, resilience and recovery: aquatic bacterial dynamics after water column disturbance. *Environ Microbiol* **13**: 2752–2767.

Shade A, Peter H, Allison SD, Baho DL, Berga M, Bürgmann H, et al. (2012a). Fundamentals of Microbial Community Resistance and Resilience. *Front Microbiol* **3**: 417, doi:10.3389/fmicb.2012.00417

Shade A, Read JS, Youngblut ND, Fierer N, Knight R, Kratz TK, et al. (2012b). Lake microbial communities are resilient after a whole-ecosystem disturbance. *ISME J* **6**: 2153–2167.

Sherr EB, Sherr BF. (1994). Bacterivory and herbivory: Key roles of phagotrophic protists in pelagic food webs. *Microb Ecol* **28**: 223–235.

Shiah F, Ducklow H. (1994). Temperature and substrate regulation of bacterial abundance, production and specific growth rate in Chesapeake Bay, USA. *Mar Ecol Prog Ser* **103**: 297–308.

Sieburth JM, Davis PG. (1982). The role of heterotrophic nanoplankton in the grazing and nurturing of planktonic bacteria in the Sargasso and Caribbean seas. *Ann Inst Oceanogr* **58**: 285–296.

Siegenthaler U. (2005). Stable Carbon Cycle-Climate Relationship During the Late Pleistocene. *Science* **310**: 1313–1317.

Silyakova A, Bellerby RGJ, Schulz KG, Czerny J, Tanaka T, Nondal G, et al. (2013). Pelagic community production and carbon-nutrient stoichiometry under variable ocean acidification in an Arctic fjord. *Biogeosciences* **10**: 4847–4859.

Simon M, Grossart H-P, Schweitzer B, Ploug H. (2002). Microbial ecology of organic aggregates in aquatic ecosystems. *Aquat Microb Ecol* **28**: 175–211.

Skindersoe ME, Ettinger-Epstein P, Rasmussen TB, Bjarnsholt T, De Nys R, Givskov M. (2008). Quorum sensing antagonism from marine organisms. *Mar Biotechnol* **10**: 56–63.

Smith DC, Simon M, Alldredge AL, Azam F. (1992). Intense hydrolytic enzyme activity on marine aggregates and implications for rapid particle dissolution. *Nature* **359**: 139–142.

Smith DC, Steward GF, Long RA, Azam F. (1995). Bacterial mediation of carbon fluxes during a diatom bloom in a mesocosm. *Deep-Sea Res Part II* **42**: 75–97.

Sommer U. (1988). Phytoplankton succession in microcosm experiments under simultaneous grazing pressure and resource limitation. *Limnol Oceanogr* **33**: 1037–1054.

Sousa WP. (1984). The Role of Disturbance in Natural Communities. *Annu Rev Ecol Syst* **15**: 353–391.

Spilling K, Paul AJ, Virkkala N, Hastings T, Lischka S, Stuhr A, et al. (2016a). Ocean acidification decreases plankton respiration: evidence from a mesocosm experiment. *Biogeosciences* **13**: 4707–4719.

Spilling K, Schulz KG, Paul AJ, Boxhammer T, Achterberg EP, Hornick T, et al. (2016b).

Effects of ocean acidification on pelagic carbon fluxes in a mesocosm experiment. *Biogeosciences* **13**: 6081–6093.

Sswat M, Stiasny MH, Taucher J, Algueró-Muñiz M, Bach LT, Jutfelt F, et al. (2018). Food web changes under ocean acidification promote herring larvae survival. *Nat Ecol Evol* **2**: 836–840.

Stachowicz JJ, Terwin JR, Whitlatch RB, Osman RW. (2002). Linking climate change and biological invasions: Ocean warming facilitates nonindigenous species invasions. *Proc Natl Acad Sci* **99**: 15497–15500.

Steffen W, Richardson K, Rockstrom J, Cornell SE, Fetzer I, Bennett EM, et al. (2015). Planetary boundaries: Guiding human development on a changing planet. *Science* **347**: 1259855, doi:10.1126/science.1259855.

Steffen W, Sanderson A, Tyson PD, Jäger J, Matson PA, Moore III B, Oldfield F, Richardson K, Schellnhuber HJ, Turner BL, Wasson RJ. (2004). Global Change and the Earth System: A Planet Under Pressure. Springer-Verlag: Berlin and Heidelberg, Germany and New York, NY, USA, ISBN 3-540-40800-2.

Stewart RIA, Dossena M, Bohan DA, Jeppesen E, Kordas RL, Ledger ME, et al. (2013). Mesocosm Experiments as a Tool for Ecological Climate-Change Research. In: Woodward G, O'Gorman EJ (eds). *Advances in Ecological Research, Vol. 48, Global Change in Multispecies Systems: Part 3*. Academic Press: London, UK, Oxford, UK, Amsterdam, The Netherlands, Waltham, MA, USA, San Diego, CA, USA, pp. 71–181, ISBN: 978-0-12-417199-2.

Stocker R. (2012). Marine Microbes See a Sea of Gradients. *Science* **338**: 628–633.

Stoderegger K, Herndl GJ. (1998). Production and release of bacterial capsular material and its subsequent utilization by marine bacterioplankton. *Limnol Oceanogr* **43**: 877–884.

Strickland JDH. (1960). Measuring the Production of Marine Phytoplankton. In: Ricker WE, Carter NM (eds). Bulletin of the Fisheries Research Board of Canada, No. 122. Queen´s Printer: Ottawa, Canada, pp. 172.

Strickland JDH. (1965). Phytoplankton and Marine Primary Production. *Annu Rev Microbiol* **19**: 127–162.

Sulzberger B, Durisch-Kaiser E. (2009). Chemical characterization of dissolved organic matter (DOM): A prerequisite for understanding UV-induced changes of DOM absorption properties and bioavailability. *Aquat Sci* **71**: 104–126.

Sunagawa S, Coelho LP, Chaffron S, Kultima JR, Labadie K, Salazar G, et al. (2015). Structure and function of the global ocean microbiome. *Science* **348**: 1261359, doi:10.1126/science.1261359.

Sunday JM, Calosi P, Dupont S, Munday PL, Stillman JH, Reusch TBH. (2014). Evolution in an acidifying ocean. *Trends Ecol Evol* **29**: 117–125.

Suttle CA. (2007). Marine viruses — major players in the global ecosystem. *Nat Rev Microbiol* **5**: 801–812.

Suttle CA, Fuhrman JA, Capone DG. (1990). Rapid ammonium cycling and concentration-dependent partitioning of ammonium and phosphate: Implications for carbon transfer in planktonic communities. *Limnol Oceanogr* **35**: 424–433.

Tanaka T, Alliouane S, Bellerby RGB, Czerny J, de Kluijver A, Riebesell U, et al. (2013). Effect

of increased CO_2 on the planktonic metabolic balance during a mesocosm experiment in an Arctic fjord. *Biogeosciences* **10**: 315–325.

Tanaka T, Thingstad TF, Løvdal T, Grossart H-P, Larsen A, Allgaier M, et al. (2008). Availability of phosphate for phytoplankton and bacteria and of glucose for bacteria at different pCO_2 levels in a mesocosm study. *Biogeosciences* **5**: 669–678.

Tans P, Keeling C. (2015). NOAA/ESRL Global monitoring division. Available from www.esrl.noaa.gov/gmd/ccgg/trends/. [20.06.2018].

Taucher J, Bach LT, Riebesell U, Oschlies A. (2014). The viscosity effect on marine particle flux: A climate relevant feedback mechanism. *Global Biogeochem Cycles* **28**: 415–422.

Taucher J, Bach LT, Boxhammer T, Nauendorf A, Achterberg EP, Algueró-Muñiz M, et al. (2017a). Influence of Ocean Acidification and Deep Water Upwelling on Oligotrophic Plankton Communities in the Subtropical North Atlantic: Insights from an In situ Mesocosm Study. *Front Mar Sci* **4**. e-pub ahead of print, doi: 10.3389/fmars.2017.00085.

Taucher J, Haunost M, Boxhammer T, Bach LT, Algueró-Muñiz M, Riebesell U. (2017b). Influence of ocean acidification on plankton community structure during a winter-to-summer succession: An imaging approach indicates that copepods can benefit from elevated CO2 via indirect food web effects. *PLoS One* **12**: 85, doi:10.3389/fmars.2017.00085.

Taucher J, Stange P, Algueró-Muñiz M, Bach LT, Nauendorf A, Kolzenburg R, et al. (2018). In situ camera observations reveal major role of zooplankton in modulating marine snow formation during an upwelling-induced plankton bloom. *Prog Oceanogr* **164**: 75–88.

Teira E, Fernández A, Álvarez-Salgado X, García-Martín E, Serret P, Sobrino C. (2012). Response of two marine bacterial isolates to high CO_2 concentration. *Mar Ecol Prog Ser* **453**: 27–36.

Thompson ROR., Imberger J. (1980). Response of a numerical model of a stratified lake to wind stress. In: *Proc. 2nd Int. Symp. Stratified Flows, Trondheim, June 1980. Vol. 1*., pp. 562–570.

Tong S, Gao K, Hutchins DA. (2018). Adaptive evolution in the coccolithophore *Gephyrocapsa oceanica* following 1,000 generations of selection under elevated CO_2. *Glob Chang Biol* **24**: 3055–3064.

Tranvik LJ. (1988). Availability of dissolved organic carbon for planktonic bacteria in oligotrophic lakes of differing humic content. *Microb Ecol* **16**: 311–322.

Tranvik LJ. (1992). Allochthonous dissolved organic matter as an energy source for pelagic bacteria and the concept of the microbial loop. *Hydrobiologia* **229**: 107–114.

Tranvik LJ, Downing JA, Cotner JB, Loiselle SA, Striegl RG, Ballatore TJ, et al. (2009). Lakes and reservoirs as regulators of carbon cycling and climate. *Limnol Oceanogr* **54**: 2298–2314.

Tranvik LJ, Cole JJ, Prairie YT. (2018). The study of carbon in inland waters-from isolated ecosystems to players in the global carbon cycle. *Limnol Oceanogr Lett* **3**: 41–48.

Trenberth KE. (2012). Framing the way to relate climate extremes to climate change. *Clim Change* **115**: 283–290.

Trenberth KE, Fasullo JT, Shepherd TG. (2015a). Attribution of climate extreme events. *Nat Clim Chang* **5**: 725–730.

Trenberth KE, Zhang Y, Fasullo JT, Taguchi S. (2015b). Climate variability and relationships between top-of-atmosphere radiation and temperatures on Earth. *J Geophys Res Atmos* **120**: 3642–3659.

Tsai J-W, Kratz TK, Hanson PC, Wu J-T, Chang WYB, Artzberger PW, et al. (2008). Seasonal dynamics, typhoons and the regulation of lake metabolism in a subtropical humic lake. *Freshw Biol* **53**: 1929–1941.

Tsiola A, Pitta P, Giannakourou A, Bourdin G, Marro S, Maugendre L, et al. (2017). Ocean acidification and viral replication cycles: Frequency of lytically infected and lysogenic cells during a mesocosm experiment in the NW Mediterranean Sea. *Estuar Coast Shelf Sci* **186**: 139–151.

Turner MG, Baker WL, Peterson CJ, Peet RK. (1998). Factors Influencing Succession: Lessons from Large, Infrequent Natural Disturbances. *Ecosystems* **1**: 511–523.

Turner MG, Dale VH. (1998). Large, Infrequent Disturbances: Comparing Large, Infrequent Disturbances: What Have We Learned? *Ecosystems* **1**: 493–496.

UNFCCC. (2015). Adoption of the Paris Agreement FCCC/CP/2015/L.9/Rev.1, United Nations, New York, USA, Available from: https://unfccc.int/resource/docs/2015/cop21/eng/l09r01.pdf. [25.10.2018]

UNFCCC. (1992). United Nations Framework Convention on Climate Change. *United Nations*: New York, USA, Available from: http://unfccc.int/files/essential_background/convention/background/application/pdf/conveconve_text_with_annexes_english_for_posting.pdf [25.10.2018]

Vachon D, del Giorgio PA. (2014). Whole-Lake CO_2 Dynamics in Response to Storm Events in Two Morphologically Different Lakes. *Ecosystems* **17**: 1338–1353.

van Donk E, Hessen DO. (1993). Grazing resistance in nutrient-stressed phytoplankton. *Oecologia* **93**: 508–511.

Vellend M. (2010). Conceptual synthesis in community ecology. *Rev Biol* **85**: 183–206.

Verity P, Smetacek V. (1996). Organism life cycles, predation, and the structure of marine pelagic ecosystems. *Mar Ecol Prog Ser* **130**: 277–293.

Vermeer M, Rahmstorf S. (2009). Global sea level linked to global temperature. *Proc Natl Acad Sci* **106**: 21527–21532.

Verpoorter C, Kutser T, Seekell DA, Tranvik LJ. (2014). A global inventory of lakes based on high-resolution satellite imagery. *Geophys Res Lett* **41**: 6396–6402.

Vidon P, Karwan DL, Andres AS, Inamdar S, Kaushal S, Morrison J, et al. (2018). In the path of the Hurricane: impact of Hurricane Irene and Tropical Storm Lee on watershed hydrology and biogeochemistry from North Carolina to Maine, USA. *Biogeochemistry*. doi:10.1007/s10533-018-0423-4.

Violle C, Navas M-L, Vile D, Kazakou E, Fortunel C, Hummel I, et al. (2007). Let the concept of trait be functional! *Oikos* **116**: 882–892.

Vitousek PM. (1997). Human Domination of Earth's Ecosystems. *Science* **277**: 494–499.

Volk T, Hoffert MI. (1985). Ocean Carbon Pumps: Analysis of Relative Strengths and

Efficiencies in Ocean-Driven Atmospheric CO_2 Changes. In: Sundquist E, Broecker W (eds). *The Carbon Cycle and Atmospheric CO_2: Natural Variations Archaen to Present, Geophysical Monograph Series, Vol. 32*, American Geophysical Union: Washington, D.C., USA, pp. 99–110.

Volkman JK, Tanoue E. (2002). Chemical and Biological Studies of Particulate Organic Matter in the Ocean. *J Oceanogr* **58**: 265–279.

Walker A, Parkhill J. (2008). Single-cell genomics. *Nat Rev Microbiol* **6**: 176–177.

Walther G-R, Post E, Convey P, Menzel A, Parmesan C, Beebee TJC, et al. (2002). Ecological responses to recent climate change. *Nature* **416**: 389–395.

Wang G, Wang D, Trenberth KE, Erfanian A, Yu M, Bosilovich MG, et al. (2017a). The peak structure and future changes of the relationships between extreme precipitation and temperature. *Nat Clim Chang* **7**: 268–274.

Wang T, Tong S, Liu N, Li F, Wells ML, Gao K. (2017b). The fatty acid content of plankton is changing in subtropical coastal waters as a result of OA: Results from a mesocosm study. *Mar Environ Res* **132**: 51–62.

Weiss M, Abele U, Weckesser J, Welte W, Schiltz E, Schulz G. (1991). Molecular architecture and electrostatic properties of a bacterial porin. *Science* **254**: 1627–1630.

Weissing FJ, Huisman J. (1994). Growth and Competition in a Light Gradient. *J Theor Biol* **168**: 323–336.

Weithoff G, Lorke A, Walz N. (2000). Effects of water-column mixing on bacteria, phytoplankton, and rotifers under different levels of herbivory in a shallow eutrophic lake. *Oecologia* **125**: 91–100.

Weyhenmeyer GA, Willén E, Sonesten L. (2004). Effects of an extreme precipitation event on water chemistry and phytoplankton in the Swedish Lake Mälaren. *Boreal Environ Res* **9**: 409–420.

White PS, Jentsch A. (2001). The Search for Generality in Studies of Disturbance and Ecosystem Dynamics. In: Esser K, Lüttge U, Kadereit JW, Beyschlag W (eds). *Progress in Botany. Progress in Botany, Vol. 62*. Springer: Berlin, Germany, Heidelberg, Germany, pp. 399–450.

Wijtes T, McClure PJ, Zwietering MH, Roberts TA. (1993). Modelling bacterial growth of *Listeria monocytogenes* as a function of water activity, pH and temperature. *Int J Food Microbiol* **18**: 139–149.

Williams PJ leB. (1981). Microbial contribution to overall marine plankton metabolism: direct measurements of respiration. *Oceanol Acta* **4**: 359–364.

Williamson P. (2016). Emissions reduction: Scrutinize CO_2 removal methods. *Nature* **530**: 153-155.

Winslow LA, Zwart JA, Batt RD, Dugan HA, Iestyn Woolway R, Corman JR, et al. (2016). LakeMetabolizer: An R package for estimating lake metabolism from free-water oxygen using diverse statistical models. *Inl Waters* **6**: 622–636.

Wolf-Gladrow DA, Riebesell U, Burkhardt S, Bijma J. (1999). Direct effects of CO_2 concentration on growth and isotopic composition of marine plankton. *Tellus B* **51**: 461–476.

Woodward G, Perkins DM, Brown LE. (2010). Climate change and freshwater ecosystems: impacts across multiple levels of organization. *Philos Trans R Soc B* **365**: 2093–2106.

Wunsch C, Schmitt RW, Baker DJ. (2013). Climate change as an intergenerational problem. *Proc Natl Acad Sci* **110**: 4435–4436.

Yamada N, Suzumura M, Tsurushima N, Harada K. (2008). Impact on bacterial activities of ocean sequestration of carbon dioxide into bathypelagic layers. In: *OCEANS 2008 - MTS/IEEE Kobe Techno-Ocean*. *Proceedings of a meeting held 8-11 April 2008, Kobe, Japan.* IEEE: Hoes Lane, Piscataway, NJ, USA.

Yang Y, Hansson L, Gattuso J-P. (2016). Data compilation on the biological response to ocean acidification: an update. *Earth Syst Sci Data* **8**: 79–87.

Yannarell AC, Kent AD, Lauster GH, Kratz TK, Triplett EW. (2003). Temporal Patterns in Bacterial Communities in Three Temperate Lakes of Different Trophic Status. *Microb Ecol* **46**: 391–405.

Yannarell AC, Steppe TF, Paerl HW. (2007). Disturbance and recovery of microbial community structure and function following Hurricane Frances. *Environ Microbiol* **9**: 576–583.

Yawata Y, Cordero OX, Menolascina F, Hehemann J-H, Polz MF, Stocker R. (2014). Competition-dispersal tradeoff ecologically differentiates recently speciated marine bacterioplankton populations. *Proc Natl Acad Sci* **111**: 5622–5627.

Zeebe RE. (2012). History of Seawater Carbonate Chemistry, Atmospheric CO_2 , and Ocean Acidification. *Annu Rev Earth Planet Sci* **40**: 141–165.

Znachor P, Šimek K, Nedoma J. (2012). Bacterial colonization of the freshwater planktonic diatom *Fragilaria crotonensis*. *Aquat Microb Ecol* **66**: 87–94.

VII. Appendix

APPENDIX Table1: Summary of known published studies testing the effects of ocean acidification on heterotrophic bacteria within natural pelagic plankton communities. Only studies that present original data on heterotrophic bacterial processes, community composition and abundance/biomass development are represented. In addition, there are also studies on TEP production, enzyme activity and community metabolism (net community production, community respiration) listed, since this processes are largely determined by heterotrophic bacterial processes.

Allgaier M, Riebesell U, Vogt M, Thyrhaug R, Grossart H-P. (2008). Coupling of heterotrophic bacteria to phytoplankton bloom development at different pCO_2 levels: a mesocosm study. *Biogeosciences* **5**: 1007–1022.

Arnosti C, Grossart H, Mühling M, Joint I, Passow U. (2011). Dynamics of extracellular enzyme activities in seawater under changed atmospheric pCO_2: a mesocosm investigation. *Aquat Microb Ecol* **64**: 285–298.

Bach LT, Alvarez-Fernandez S, Hornick T, Stuhr A, Riebesell U. (2017). Simulated ocean acidification reveals winners and losers in coastal phytoplankton. *PLoS One* **12**: e0188198, doi:10.1371/journal.pone.0188.

Bellerby RGJ, Schulz KG, Riebesell U, Neill C, Nondal G, Heegaard E, et al. (2008). Marine ecosystem community carbon and nutrient uptake stoichiometry under varying ocean acidification during the PeECE III experiment. *Biogeosciences* **5**: 1517–1527.

Bergen B, Endres S, Engel A, Zark M, Dittmar T, Sommer U, et al. (2016). Acidification and warming affect prominent bacteria in two seasonal phytoplankton bloom mesocosms. *Environ Microbiol* **18**: 4579–4595.

Bourdin G, Gazeau F, Kerros M-E, Marro S, Pedrotti ML. (2017). Dynamics of transparent exopolymeric particles and their precursors during a mesocosm experiment: Impact of ocean acidification. *Estuar Coast Shelf Sci* **186**: 112–124.

Brussaard CPD, Noordeloos AAM, Witte H, Collenteur MCJ, Schulz K, Ludwig A, et al. (2013). Arctic microbial community dynamics influenced by elevated CO_2 levels. *Biogeosciences* **10**: 719–731.

Bunse C, Lundin D, Karlsson CMG, Akram N, Vila-Costa M, Palovaara J, et al. (2016). Response of marine bacterioplankton pH homeostasis gene expression to elevated CO_2. *Nat Clim Chang* **6**: 483–487.

Celussi M, Malfatti F, Annalisa F, Gazeau F, Giannakourou A, Pitta P, et al. (2017). Ocean acidification effect on prokaryotic metabolism tested in two diverse trophic regimes in the Mediterranean Sea. *Estuar Coast Shelf Sci* **186**: 125–138.

Chauhan A, Pathak A, Rodolfo-Metalpa R, Milazzo M, Green SJ, Hall-Spencer JM. (2015). Metagenomics Reveals Planktonic Bacterial Community Shifts across a Natural CO_2 Gradient in the Mediterranean Sea. *Genome Announc* **3**: e01543-14, doi:10.1128/genomeA.01543-14.

Crawfurd KJ, Alvarez-Fernandez S, Mojica KDA, Riebesell U, Brussaard CPD. (2017). Alterations in microbial community composition with increasing fCO_2: a mesocosm study in the eastern Baltic Sea. *Biogeosciences* **14**: 3831–3849.

Delille B, Harlay J, Zondervan I, Jacquet S, Chou L, Wollast R, et al. (2005). Response of primary production and calcification to changes of pCO_2 during experimental blooms of the coccolithophorid Emiliania huxleyi. *Global Biogeochem Cycles* **19**: GB2023, doi:10.1029/2004GB002318.

Deppeler S, Petrou K, Schulz KG, Westwood K, Pearce I, McKinlay J, and Davidson A. (2018). Ocean acidification of a coastal Antarctic marine microbial community reveals a critical threshold for CO_2 tolerance in phytoplankton productivity. *Biogeosciences* **15:** 209-231.

Egge JK, Thingstad TF, Larsen A, Engel A, Wohlers J, Bellerby RGJ, et al. (2009). Primary production during nutrient-induced blooms at elevated CO_2 concentrations. *Biogeosciences* **6**: 877–885.

Endres S, Galgani L, Riebesell U, Schulz K-G, Engel A. (2014). Stimulated Bacterial Growth under Elevated pCO_2: Results from an Off-Shore Mesocosm Study. *PLoS One* **9**: e99228, doi:10.1371/journal.pone.0099228.

Engel A. (2002). Direct relationship between CO_2 uptake and transparent exopolymer particles production in natural phytoplankton. *J Plankton Res* **24**: 49–53.

Engel A, Delille B, Jacquet S, Riebesell U, Rochelle-Newall E, Terbrüggen A, et al. (2004). Transparent exopolymer particles and dissolved organic carbon production by Emiliania huxleyi exposed to different CO_2 concentrations: a mesocosm experiment. *Aquat Microb Ecol* **34**: 93–104.

Grossart H-P, Allgaier M, Passow U, Riebesell U. (2006). Testing the effect of CO_2 concentration on the dynamics of marine heterotrophic bacterioplankton. *Limnol Oceanogr* **51**: 1–11.

Hornick T, Bach LT, Crawfurd KJ, Spilling K, Achterberg EP, Woodhouse JN, et al. (2017). Ocean acidification impacts bacteria–phytoplankton coupling at low-nutrient conditions. *Biogeosciences* **14**: 1–15.

Huang Y, Liu X, Laws EA, Chen B, Li Y, Xie Y, et al. (2018). Effects of increasing atmospheric CO_2 on the marine phytoplankton and bacterial metabolism during a bloom: A coastal mesocosm study. *Sci Total Environ* **633**: 618–629.

de Kluijver A, Soetaert K, Schulz KG, Riebesell U, Bellerby RGJ, Middelburg JJ. (2010). Phytoplankton-bacteria coupling under elevated CO_2 levels: a stable isotope labelling study. *Biogeosciences* **7**: 3783–3797.

Krause E, Wichels A, Giménez L, Lunau M, Schilhabel MB, Gerdts G. (2012). Small Changes in pH Have Direct Effects on Marine Bacterial Community Composition: A Microcosm Approach. *PLoS One* **7**: e47035.

Lee Y, Kumar KS, Lee K, Shin K, Park K-T, Yang EJ, et al. (2016). Effects of elevated CO_2 concentrations on the production and biodegradability of organic matter: An in-situ mesocosm experiment. *Mar Chem* **183**: 33–40.

Lin X, Huang R, Li Y, Li F, Wu Y, Hutchins DA, et al. (2018). Interactive network configuration maintains bacterioplankton community structure under elevated CO_2 in a eutrophic coastal mesocosm experiment. *Biogeosciences* **15**: 551–565.

Lindh M V., Riemann L, Baltar F, Romero-Oliva C, Salomon PS, Granéli E, et al. (2013). Consequences of increased temperature and acidification on bacterioplankton

community composition during a mesocosm spring bloom in the Baltic Sea. *Environ Microbiol Rep* **5**: 252–262.

Maas E, Law C, Hall J, Pickmere S, Currie K, Chang F, et al. (2013). Effect of ocean acidification on bacterial abundance, activity and diversity in the Ross Sea, Antarctica. *Aquat Microb Ecol* **70**: 1–15.

MacGilchrist GA, Shi T, Tyrrell T, Richier S, Moore CM, Dumousseaud C, et al. (2014). Effect of enhanced CO_2 levels on the production of dissolved organic carbon and transparent exopolymer particles in short-term bioassay experiments. *Biogeosciences* **11**: 3695–3706.

Maugendre L, Gattuso J-P, de Kluijver A, Soetaert K, van Oevelen D, Middelburg JJ, et al. (2017a). Carbon-13 labelling shows no effect of ocean acidification on carbon transfer in Mediterranean plankton communities. *Estuar Coast Shelf Sci* **186**: 100–111.

Maugendre L, Gattuso J-P, Louis J, de Kluijver A, Marro S, Soetaert K, et al. (2015). Effect of ocean warming and acidification on a plankton community in the NW Mediterranean Sea. *ICES J Mar Sci* **72**: 1744–1755.

Maugendre L, Gattuso J-P, Poulton AJ, Dellisanti W, Gaubert M, Guieu C, et al. (2017b). No detectable effect of ocean acidification on plankton metabolism in the NW oligotrophic Mediterranean Sea: Results from two mesocosm studies. *Estuar Coast Shelf Sci* **186**: 89–99.

Motegi C, Tanaka T, Piontek J, Brussaard CPD, Gattuso J-P, Weinbauer MG. (2013). Effect of CO_2 enrichment on bacterial metabolism in an Arctic fjord. *Biogeosciences* **10**: 3285–3296.

Newbold LK, Oliver AE, Booth T, Tiwari B, DeSantis T, Maguire M, et al. (2012). The response of marine picoplankton to ocean acidification. *Environ Microbiol* **14**: 2293–2307.

Oliver AE, Newbold LK, Whiteley AS, van der Gast CJ. (2014). Marine bacterial communities are resistant to elevated carbon dioxide levels. *Environ Microbiol Rep* **6**: 574–582.

Paulino AI, Egge JK, Larsen A. (2008). Effects of increased atmospheric CO_2 on small and intermediate sized osmotrophs during a nutrient induced phytoplankton bloom. *Biogeosciences* **5**: 739–748.

Piontek J, Borchard C, Sperling M, Schulz KG, Riebesell U, Engel A. (2013). Response of bacterioplankton activity in an Arctic fjord system to elevated CO_2: results from a mesocosm perturbation study. *Biogeosciences* **10**: 297–314.

Piontek J, Lunau M, Händel N, Borchard C, Wurst M, Engel A. (2010). Acidification increases microbial polysaccharide degradation in the ocean. *Biogeosciences* **7**: 1615–1624.

Ray JL, Töpper B, An S, Silyakova A, Spindelböck J, Thyrhaug R, et al. (2012). Effect of increased pCO_2 on bacterial assemblage shifts in response to glucose addition in Fram Strait seawater mesocosms. *FEMS Microbiol Ecol* **82**: 713–723.

Ren L, Jeppesen E, He D, Wang J, Liboriussen L, Xing P, et al. (2015). pH Influences the Importance of Niche-Related and Neutral Processes in Lacustrine Bacterioplankton Assembly. *Appl Environ Microbiol* **81**: 3104–3114.

Rochelle-Newall E, Delille B, Frankignoulle M, Gattuso J, Jacquet S, Riebesell U, et al. (2004). Chromophoric dissolved organic matter in experimental mesocosms maintained under different pCO_2 levels. *Mar Ecol Prog Ser* **272**: 25–31.

Roy A-S, Gibbons SM, Schunck H, Owens S, Caporaso JG, Sperling M, et al. (2013). Ocean acidification shows negligible impacts on high-latitude bacterial community structure in coastal pelagic mesocosms. *Biogeosciences* **10**: 555–566.

Sala MM, Aparicio FL, Balagué V, Boras JA, Borrull E, Cardelús C, et al. (2016). Contrasting effects of ocean acidification on the microbial food web under different trophic conditions. *ICES J Mar Sci* **73**: 670–679.

Silyakova A, Bellerby RGJ, Schulz KG, Czerny J, Tanaka T, Nondal G, et al. (2013). Pelagic community production and carbon-nutrient stoichiometry under variable ocean acidification in an Arctic fjord. *Biogeosciences* **10**: 4847–4859.

Spilling K, Paul AJ, Virkkala N, Hastings T, Lischka S, Stuhr A, et al. (2016). Ocean acidification decreases plankton respiration: evidence from a mesocosm experiment. *Biogeosciences* **13**: 4707–4719.

Tanaka T, Thingstad TF, Løvdal T, Grossart H-P, Larsen A, Allgaier M, et al. (2008). Availability of phosphate for phytoplankton and bacteria and of glucose for bacteria at different *p*CO**2** levels in a mesocosm study. *Biogeosciences* **5**: 669–678.

Yamada N, Suzumura M. (2010). Effects of seawater acidification on hydrolytic enzyme activities. *J Oceanogr* **66**: 233–241.

Yoshimura T, Nishioka J, Suzuki K, Hattori H, Kiyosawa H, Watanabe YW. (2010). Impacts of elevated CO_2 on organic carbon dynamics in nutrient depleted Okhotsk Sea surface waters. *J Exp Mar Bio Ecol* **395**: 191–198.

Zark M, Broda NK, Hornick T, Grossart H-P, Riebesell U, Dittmar T. (2017). Ocean Acidification Experiments in Large-Scale Mesocosms Reveal Similar Dynamics of Dissolved Organic Matter Production and Biotransformation. *Front Mar Sci* **4**: 317.

VIII. Danksagung

Der Weg zur finalen Fertigstellung dieser Arbeit war lang. Vielen Dank an alle, die mich dabei während der letzten Jahre begleitet haben!

Natürlich möchte ich zuerst Hans-Peter Großart für die Betreuung meiner wissenschaftlichen Arbeit seit Beginn der Diplomarbeit vor mehr als sieben Jahren danken. Danke für die vielen Ideen; das in mich gesetzte Vertrauen; die fachlichen aber auch privaten Gespräche; Möglichkeiten; Freiheiten; kritischen Kommentare und nicht zu vergessen, die vielen Jahre durchgängiger Finanzierung. Dank gilt auch allen Mentoren und wissenschaftlichen Wegbegleitern. Hier möchte ich mich im Besonderen bei Ulf Riebesell, Lennart Bach, Jason N. Woodhouse, Lars Ganzert und Kirsten Pohlmann bedanken, die während dieser Zeit immer ein offenes Ohr hatten und mit vielen guten Anregungen und Inspirationen, v.a. hinsichtlich der Datenauswertung, zum Gelingen dieser Arbeit beitrugen. Vielen Dank auch an Maren Voß und Karlheinz Altendorf, die sich die Zeit nahmen, diese Arbeit zu begutachten.

Desweiteren gilt mein Dank natürlich allen Mitstreitern, die mir während dieser Zeit im Büro, Labor, bei Experimenten, bei logistischen und bürokratischen Problemen oder bei der Datenauswertung beigestanden haben und auch ab- und zu mal für eine „Spätschicht“ zur Verfügung standen. Bei mittlerweile drei durchlebten Arbeitsgruppen-Zyklen am Stechlinsee, einschließlich der MIBI-AG und Abteilung III, sowie weiteren drei BIOACID-Experimenten in Finnland, Schweden und Gran Canaria mit den einzelnen KOSMOS-Teams ist diese Liste riesig und würde vermutlich vollkommen den Rahmen dieser Arbeit sprengen. Daher fühlt euch alle angesprochen: Vielen Dank! Mit einigen von euch teile ich besondere Erlebnisse aus dieser Zeit. Andere sind zu mehr als „nur“ Kollegen geworden. Vielen Dank auch an alle, die sich die Zeit nahmen mal über etwas anderes „abseits der Wissenschaft“ zu sprechen! Ohne viele von euch hätte die Arbeit definitiv niemals bewerkstelligt werden können! Besonders bedanken möchte ich mich an dieser Stelle bei: Allanah P., Andrea L., Armin P., Dana H., Darren G., Edith T., Eliesabeth W., Elke M., Georg E., H-P G., Jana M., Jan C., Jason W., Jens N., Jörg S., Kerstin S., Kirsten P., Kristian S., Lars G., Lennart B., Maren Z., Maria A. A., Mathias H., Matthias F., Michael S., Michael Ss., Monika D., Monika N., Nicola W., Rafael B., Reingard R., Solvig P., Stella B., Sylke W., Therese K., Tim B., Ulf R., Uta M und natürlich den restlichen MIBIs.

Mein ganz besonderer Dank jedoch gilt meiner Familie und meiner Freundin Anna, die mich immer unterstützten und mir den nötigen Rückhalt als auch dringende Auszeiten gaben. Auch wenn nicht immer klar war, was ich so den ganzen Tag getrieben habe, und ich auch keine Antwort auf die Frage „… und für was braucht man das?“ fand, vielen Dank Mama, Papa und Schwesterherz mit Familie! Vielen Dank Anna, dass du seit fünf Jahren an meiner Seite bist, für das Verständnis, dass die gemeinsame Zeit dabei vielmals knapp war und du oftmals meine Laune ertragen musstest. Vielen Dank für alles!

IX. Curriculum Vitae

Die Seiten 197-198 (Lebenslauf) enthalten persönliche Daten. Sie sind deshalb nicht Bestandteil der Online-Veröffentlichung.

X. Statement of originality

Erklärung gemäß §12 Abs. 7 der Promotionsordnung zur Erlangung des akademischen Grades eines Doktors der Naturwissenschaften an der Mathematisch-Naturwissenschaftlichen Fakultät der Universität Potsdam vom 18. September 2013:

Hiermit versichere ich, dass ich die vorliegende Dissertation selbstständig und ausschließlich mit den angegebenen Mitteln bzw. gekennzeichneten Quellen angefertigt habe und die Arbeit bisher an keiner anderen Hochschule eingereicht worden ist.

The work contained in this thesis has not been previously submitted for a degree at any other higher education institution. To the best of my knowledge and belief, the thesis contains no material previously published or written by another person except where due references are made.

Potsdam, 30. Oktober 2018 Thomas Hornick